Tier 2 Water Budget Analysis and Water Quantity Stress Assessment for the Oro North, Oro South, and Hawkestone Creeks Subwatersheds

Prepared For:

Lake Simcoe Region Conservation Authority
120 Bayview Parkway, Box 282
Newmarket, Ontario L3Y 4X1

May 2013

Prepared by:

3363 Yonge Street
Toronto, Ontario M4N 2M6

This project has received funding support from the Government of Ontario. Such support does not indicate endorsement by the Government of Ontario of the contents of this material.

May 17, 2013

Ms. Shelly Cuddy, Hydrogeologist
Lake Simcoe Region Conservation Authority
120 Bayview Parkway, Box 282
Newmarket, Ontario,
L3Y 4X1

RE: Tier 2 Water Budget Analysis and Water Quantity Stress Assessment for the Oro North, Oro South, and Hawkestone Creeks Subwatersheds.

Dear Ms. Cuddy:

We are pleased to provide a copy of our final report for the Tier 2 Water Budget Analysis and Water Quantity Stress Assessment for the Oro North, Oro South, and Hawkestone Creeks Subwatersheds. The report describes the development and calibration of an integrated surface water and groundwater flow for the entire Oro Moraine area and the application of the model to conduct a Tier 2 water budget analysis and stress assessment for the subwatersheds. The analysis of high volume and ecologically significant groundwater recharge areas (HVRAs and ESGRAs) will be the subject of a second report.

We trust this report meets with your satisfaction. Should you have any questions, please contact us. We thank you again for the opportunity to work with you on this important study for LSRCA.

Yours truly,

Earthfx Incorporated

Dirk Kassenaar, M.Sc., P.Eng.

E.J. Wexler, M.Sc., M.S.E., P.Eng.

Tier 2 Water Budget Analysis and Water Quantity Stress Assessment for Oro North, Oro South, and Hawkestone Creeks Subwatersheds

Table of Contents

LIST OF FIGURES

LIST OF TABLES

Tier 2 Water Budget Analysis and Water Quantity Stress Assessment for Oro North, Oro South, and Hawkestone Creeks Subwatersheds

1 Introduction

The Province of Ontario established the Lake Simcoe Protection Act (2008) and the Lake Simcoe Protection Plan (LSPP) in 2009 to "protect, improve or restore the ecological health of the Lake Simcoe Watershed including water quality, key natural heritage features and their functions, and key hydrologic features and their functions". The LSPP outlines a number of policies to support the maintenance of adequate flows required to maintain healthy aquatic ecosystems in the Lake Simcoe watershed. Specifically, Policy 5.2.SA requires that LSRCA complete a "Tier 2" water budget and stress assessment for all subwatersheds in the Lake Simcoe and Couchiching/Black River area that have not been assessed at that level under the Source Water Protection program established by the Clean Water Act (2006).

A "Tier 2" water budget is defined as: "a water budget developed using computer-based three-dimensional groundwater flow models and computer based continuous surface water flow models to assess groundwater flows and levels, surface water flows and levels, and the interactions between them" (Director's Technical Rules for the Clean Water Act, 2006).

1.1 Scope of Work

The Scope of Work for this project includes two main parts: (1) a Tier 2 water budget analysis and stress assessment; and (2) the identification and analysis of ecologically significant groundwater recharge areas (ESGRAs).

Part 1 of this study, the Tier 2 water budget and stress assessment, includes the following tasks:

- compile and assess available background information and data;
- assess available background information and data relative to the surface water flow/runoff model;
- analyze information and data gaps and define additional data requirements to enable the model to estimate hourly runoff and simulate the hydraulic behaviour of streams in the study area;
- develop and calibrate the integrated surface water and groundwater flow model:
    - apply techniques to enable the model to use hourly climate information as input;
    - calibrate the model to daily observed streamflow records concurrently with monthly and annual volumes to achieve the best overall fit;
    - simulate channel routing and wetland routing; and
    - simulate open-water (i.e., lake/wetland) evaporation and recharge
- estimate surface water/groundwater consumptive use;
- utilize the calibrated integrated surface water/groundwater model to assess water budget elements for each subwatershed; and

- apply the model for scenario analysis (existing and future water use conditions and drought conditions).

Part 2 of this study includes:

- conduct an assessment of HVRAS based on results of the water budget analysis;
- conduct an assessment of ESGRAs utilizing the calibrated model to identify the portions of the landscape that contribute discharge to cold water stream reaches and wetlands delineated by LSRCA; and
- assess data and knowledge gaps for future improvements.

Tasks common to both Part 1 and Part 2 include:

- prepare interim memoranda, meeting minutes, and draft and final reports;
- present various aspects of the project to LSRCA staff and Provincial staff;
- undertake all required project management; and
- transfer all digital information (including modelling files, GIS files, data files, etc.) to LSRCA staff. This will include model set up on LSRCA staff computers and basic instructions of how to run the model.

This report describes Part 1 of the project, including the development and calibration of the integrated groundwater/surface water model for the Oro Moraine area and the completion of the Tier 2 water budget assessment tasks.

1.2 Study Area Location

The Oro North, Oro South, and Hawkestone Creeks subwatersheds are located in the northwest portion of the Lake Simcoe watershed (Figure 1.1). The subwatersheds are contained within the Township of Oro-Medonte and the City of Orillia, both of which are within Simcoe County. Some general properties of the subwatersheds are provided in Table 1.1.

Table 1.1: Tier 2 subwatershed areas.

Subwatershed	Minimum Elevation (masl)	Maximum Elevation (masl)	Mean Elevation (masl)	Area (km^2)
Hawkestone Creek	218.0	380.4	291.5	47.8
Oro Creeks North	215.1	375.9	265.7	75.3
Oro Creeks South	218.5	312.4	261.7	57.4
Subtotal				180.5

The LSPP emphasizes a subwatershed assessment approach and, accordingly, the primary focus of this study is on the hydrology and hydrogeology of the three subwatersheds. It is important, however, to recognize that these subwatersheds are part of a larger physiographic and geologic feature; the Oro Moraine. The Oro Moraine is an area of high recharge and provides headwater flow to numerous streams that drain to Lake Simcoe, Minesing Swamp and Georgian Bay. A broader understanding of the hydrology and hydrogeology of the Oro Moraine is necessary to understand the three subwatersheds and, in particular, the lateral subwatershed inflows and outflows that must be quantified as part of this Tier 2 study. Accordingly, a larger Oro Moraine study area, labelled as “Model Boundary”, was defined as shown in Figure 1.1.

The Oro Moraine model boundary area, as shown in Figure 1.1, defines the extent of the integrated groundwater and surface water flow model developed for the purpose of this Tier 2 study. This larger study area contains portions of the City of Barrie and of Springwater, Tay, and Severn Townships and includes most or all of the catchments of Sturgeon River, Coldwater Creek, Silver Creek, Matheson Creek, and Willow Creek.

1.3 Previous Studies

The LSPP was developed to build on existing work such as the Source Water Protection Program (SWPP) studies completed under the Clean Water Act (2006). A SWPP Tier 1 water budget study was conducted by LSRCA for the Oro North, Oro South, and Hawkestone Creeks subwatersheds (LSRCA, 2004). The Tier 1 level assessment did not identify these subwatersheds as potentially "stressed", so no subsequent Tier 2 study was undertaken under the SWPP.

Tier 2 studies were completed for the Barrie Creeks watersheds to the south and the Coldwater Creek watersheds to the northwest (Golder, 2010). The Tier 2 study updated aspects of the Tier 1 study but did not significantly change the model or analysis of the Oro and Hawkestone watersheds. A complete summary of the SWPP work in the study area is included in the "Approved Assessment Report: Lake Simcoe and Couchiching-Black River Source Protection Area, Part 1 Lake Simcoe Watershed" (South Georgian Bay-Lake Simcoe Source Protection Committee., 2011).

Numerous gravel pit operations are located in the study area, particularly along the crest of the Oro Moraine. Dixon Hydrogeology Limited completed a study to assess "impacts of the combined existing and proposed extraction pits on the groundwater system, local surface water flows, and private wells" located on Oro Seventh Line Road (Dixon, 1992). This study summarized local well and aquifer testing and included basic estimates of water use by the gravel operations. The study provided some general guidance for the selection of aquifer parameters, but the monitoring data were too limited to be of specific use in the calibration of this model.

Beckers and Frind (2000 and 2001) conducted modelling studies of part of the Oro Moraine. They concluded that "…the flow simulations further show that near-surface heterogeneity has a profound impact on the sustainable capacity of a groundwater system and the location of sensitive recharge areas." The model developed in the Beckers and Frind study covered only a portion of the South Oro watershed.

An extensive study of the groundwater resources in the study area was completed by Golder Associates in 2004. The South Simcoe Municipal Groundwater Study (Golder, 2004) included the development of the Kempenfelt Bay WHPA Model. This model covered the southern part of the Oro Moraine area and used the topographic divide through the Oro Moraine as a model boundary.

Using data from an extensive high-quality drilling program, together with water well and other data, A. K. Burt of the Ontario Geological Survey (OGS) built a three-dimensional hydrostratigraphic model of the Oro Moraine area (Burt and Dodge, 2011). This model is discussed in detail in subsequent sections of this report and forms the basis for the integrated groundwater/surface water model developed for the Oro Moraine area as part of this study.

1.4 Study Approach

The study methodology was developed to address a number of key watershed issues. One consideration was weighing the benefit and limitations of using one of the existing numerical models. It was concluded that no existing model addressed all of the technical requirements without a considerable effort to expand or re-work the existing model. Accordingly, a new integrated surface water/groundwater model, specifically designed to incorporate the latest OGS Oro Moraine stratigraphy, was proposed for this study.

The technical approach centered on constructing a model using the U.S. Geological Survey (USGS) fully-integrated GSFLOW model. GSFLOW incorporates two submodels – the PRMS hydrologic model and the MODFLOW-NWT groundwater model. The PRMS model was already applied to the Oro North, Oro South, and Hawkestone Creek subwatersheds as part of a larger hydrological model development study for the entire Lake Simcoe basin (Earthfx, 2010a). The PRMS model was updated and extended to cover other subwatersheds outside the LSRCA that include portions of the Oro Moraine. The groundwater model built on the previous work by Beckers and Frind and the other Tier 2 SWPP numerical models and, most importantly, incorporated the complete OGS 2011 conceptual hydrostratigraphic model.

The advantages of the integrated modelling approach are manifold: foremost is (1) that the all headwater streams and provincially significant wetlands are represented properly in the model and (2) the relationships between the surface water bodies and their recharge areas are properly simulated. As noted, the model area was expanded to include Coldwater Creek, Willow Creek, and Silver Creek and, most importantly, the model calibration included data from the gauges on those streams. Beckers and Frind (2001) had concluded that additional data were needed to quantify the water budget for the Oro Moraine. By expanding the model study area to include these stream gauges and the additional PGMN wells in these subwatersheds, we have pursued a logical means of addressing that recommendation. An integrated model, developed with a focus on the shallow groundwater flow system, headwater streams, and wetlands, was also the best approach to address the finding of Beckers and Frind that near-surface heterogeneity is critical to the delineation of sensitive recharge areas.

Other key advantages of the GSFLOW code pertinent to this study include:

- Ability to refine the upper model layer to a finer mesh than the deeper groundwater system, so as to provide a better representation of recharge processes;
- Increased computational stability with the new MODFLOW-NWT solver, specifically designed for the simulation of shallow, complex, partially saturated layers;
- Advanced particle tracking, based on the industry-standard MODPATH code.

To conclude, the methodology followed ensured that, in addition to the Tier 2 objectives, the model best represented the ESGRA features and issues critical to the ecosystem protection aspects of the LSPP.

1.5 Figures

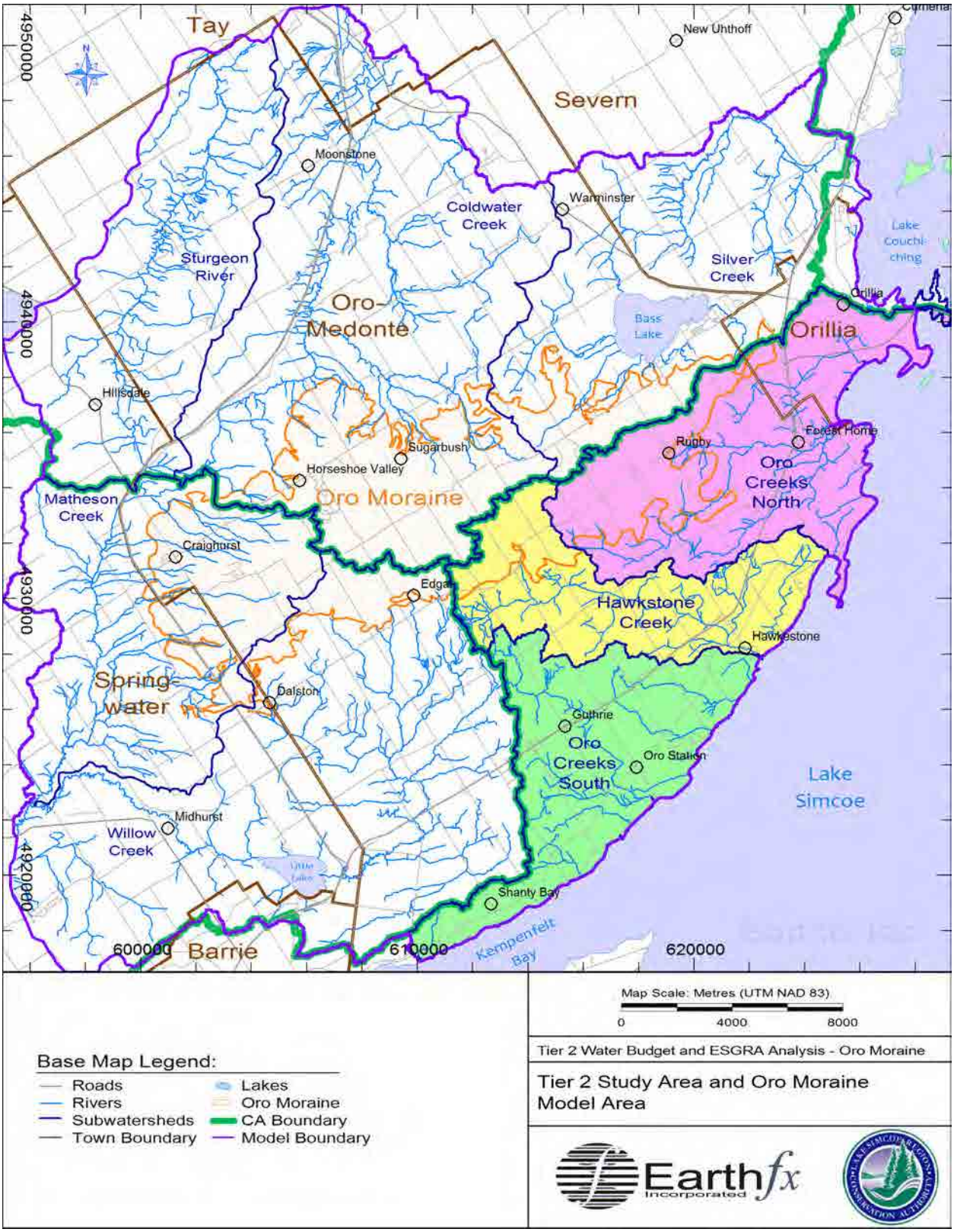

Figure 1.1 Tier 2 study area and model area.

2 Physical Setting

The physical setting, including topography, physiography, geology, climate, hydrology, and hydrogeology of the Oro Moraine model area are described briefly as they relate to the water balance for the study area as well as to the development and application of the integrated surface water/groundwater model.

2.1 Topography and Physiography

2.1.1 Topography

Land surface topography, based on the 5-m digital elevation model (DEM) produced by the Ontario Ministry of Natural Resources, is shown in Figure 2.1. Higher elevations occur along an east-west ridge formed by the Oro Moraine in the centre of the study area. The highest elevation is at about 405 metres above sea level (masl). Local relief ranges from 20 metres (m) to more than 150 m on the north side of the moraine. Areas of hummocky topography occur on top of the Oro Moraine and act to prevent surface runoff and focus infiltration. A second topographically high area is formed by a till upland near the Hamlet of Moonstone in the northwest part of the model area. Lowest elevations are associated with the stream valleys, in particular where Coldwater Creek (about 180 masl) and Willow Creek (about 185 masl) exit the model area. The larger streams are located within "tunnel channels" (discussed further on in Section 2.2.3) that separate the till uplands.

The watershed divide for the Oro North, Oro South, and Hawkestone Creeks subwatersheds occurs along the Oro Moraine. Lowest elevations in the subwatersheds occur along the Lake Simcoe shoreline (about 219 masl).

2.1.2 Physiography

The Oro Moraine model area lies mainly in Chapman and Putnam's (1984) Simcoe uplands physiographic region, which is fringed on the south, west and east by the Simcoe Lowlands and partly on the north by a segment of the Carden Plain (Figure 2.2). The Simcoe uplands are dominated by till plains and broad erosional valleys that contain either sand or clay plains. Chapman and Putnam (1984) classify the till plains in the uplands as drumlinized till plains but there are only a few drumlins mapped on the uplands in the model area. Lacustrine sand plains predominate in the low lying areas of the model area, but there is some clay plain in the northern part of the model area.

The Oro Moraine is a prominent feature that rests on the large till upland that dominates the model area. The moraine has an area of 165 km^2 and is composed mainly of sand and gravel. It is roughly wedge-shaped and trends east northeast-west southwest with the thinner end to the east. There are a number of abandoned beaches in the model area, which developed along the shorelines of postglacial lakes, in the low lying areas and on the flanks of the till uplands. The Oro Moraine model area is bounded on the east and south by Lake Simcoe and Lake Couchiching. There are two small lakes – Bass Lake and Little Lake – within the model area. Orr Lake lies just outside the western boundary. Numerous wetlands are found within the

model area on the flanks of the Oro Moraine and in the low-lying valleys. The Minesing Swamp is located southwest of the model area.

2.2 Geologic Setting

2.2.1 Precambrian Geology

Rocks of Middle Proterozoic age - 1.6 to 1.1 billion years before present (years BP) - outcrop or subcrop in the northern part of the model area and form the basement to the younger Ordovician sedimentary rocks throughout the rest of the area (see Easton and Carter, 1991; Easton, 1992). These rocks include felsic plutonic rocks and derived gneisses and migmatites, metasedimentary gneisses, and gneisses of uncertain protolith. They form part of the Go Home Domain of the Central Gneiss Belt, which is a major division of the Grenville Province of the Canadian Shield. Major structural trends, such as fold axes and foliation trajectories, are to the northwest. Following the major tectonic events which ended roughly 1 billion years BP (Easton, 1992) there was a long period of subaerial erosion preceding marine incursions during late Cambrian to Ordovician time. This erosional surface formed the substrate for sedimentation during the Ordovician Period. Regionally, the eroded 'Precambrian' surface dips gently to the south-southwest, and generally has subdued topography in the Precambrian outcrop area, but it has up to 100 m of relief under the Paleozoic cover rocks (Armstrong, 2000).

2.2.2 Paleozoic Geology

Most of the model area is underlain by a sequence of marine sedimentary rocks of middle Ordovician age (Figure 2.4) which represent sedimentation in a deepening (transgressing) epicontinental sea. The Paleozoic strata underlying the model area dip gently to the south or southwest. Bedrock surface topography is shown in Figure 2.5. The regional geology and the characteristics of these rocks are summarized in Johnson *et al.* (1992) and described in detail by Armstrong (2000). The following discussion is drawn mainly from this latter reference.

The oldest unit in the sequence is the Shadow Lake Formation, composed mainly of siliciclastic sediments that rest unconformably on the Precambrian surface. This formation consists of poorly-sorted argillaceous, arkosic sandstones and conglomerates, sandy shales and siltstones, and minor argillaceous dolostone and limestone. The rocks are non-fossiliferous and colour ranges from red to maroon to green. Average thickness is about 6 m. The various rock types are interbedded and have gradational contacts. The outcrop belt of this unit is very narrow and is largely limited to the low escarpment formed by the Paleozoic/Precambrian contact.

The Shadow Lake Formation is conformably overlain by the Gull River Formation, which consists of thin to medium beds of micritic to very fine-grained limestone, dolomitic limestone, and dolostone. The unit has two sparsely fossiliferous members: the lower member was deposited under mainly supratidal to intertidal conditions; the upper member was probably deposited in a tidal flat to very shallow subtidal environment. At the top of the lower member, there is a distinctive horizon about 1.5 m thick of light green, argillaceous dolostone or dolomitic limestone, known informally as the 'green marker bed', which is found throughout Armstrong's (2000) north Lake Simcoe study area. Overall thickness of the Gull River Formation is up to 25 m. Within the model area, the subcrop of this unit is limited to a three kilometre (km) wide re-entrant that extends to about five km south of Moonstone.

The Bobcaygeon Formation is the next unit in the sequence and is mainly limestone that is generally more fossiliferous and coarser grained than the underlying carbonates of the Gull River Formation. It is divided into three members. The rocks include fine- to coarse-grained packstones and grainstones in the lower and upper members, and interbedded shale and fine- to medium-grained limestone in the middle member. The upper member has shaly partings and some thin shale beds. The depositional environments were interpreted as shallow, carbonate shoal to inter-shoal and storm-influenced open marine shelf conditions. In terms of areal extent, this formation is the most significant Paleozoic unit subcropping in the model area (see Figure 2.4). Thickness is up to about 36 m.

The Verulam Formation is the youngest rock unit in the Oro Moraine model area and is divided into two informal members. The lower member consists of interbedded calcareous shale and limestone ranging from micritic mudstones to coarse-grained bioclastic packstones and grainstones. This member can be up to 40 m thick. Interpreted sedimentary environments include shoal and shelf settings with abundant evidence of storm influence. The upper member is up to 10 m of cross bedded, coarse-grained bioclastic limestone, indicative of shallowing shoal conditions. This member probably does not subcrop in the model area. The Verulam subcrops in a three to six km-wide band across the southern part of the model area.

Barnett (1988) has observed that there is visible karst - in the form of grikes and solution runnels and pipes - on Ordovician carbonate rocks where they outcrop north of the model area. Evidence of karst development in the subsurface has not been reported from any of the OGS boreholes in the model area.

2.2.3 Quaternary Geology

Like all of southern Ontario, the Oro Moraine model area was repeatedly glaciated during the Pleistocene Epoch, although locally there is only clear evidence for glacial activity during the Wisconsinan, the final major glacial episode. Regionally, sediments of Quaternary age form a complex blanket of unlithified deposits, up to 250 m thick, on the bedrock surface. Most of these sediments were deposited either directly from glacier ice, in meltwater streams, or in ice-marginal or ice-dammed lakes. The pattern of glaciation in the Great Lakes region was typically lobate, with relatively thin glacier ice flowing from the north filling the lake basins and then spreading out radially as the ice mass became thicker. With increasing ice thickness and coalescence of ice lobes, an overriding regional south to southwesterly flow was established near the time of the glacial maximum during the Nissouri Phase of the Late Wisconsinan (now called the Michigan Subepisode, as per Karrow *et al.*, 2000), approximately 20,000 years BP. The extent of ice recession during the Erie phase following the glacial maximum is not well understood. It is possible that glacier ice was continuously present within the model area until at least the end of the Port Bruce phase.

Early Wisconsinan (Ontario Subepisode) and Middle Wisconsinan (Elgin Subepisode) deposits in Southern Ontario have been well documented at sites such as the Scarborough Bluffs in Toronto (Karrow, 1967; Eyles and Eyles, 1983; Kelly and Martini, 1986; Hicock and Dreimanis, 1989; and Barnett, 1992) and the Woodbridge railway section (White, 1975; Kelly, 1994; Karrow et al., 2001). The Early Wisconsinan Scarborough Formation (lacustrine and deltaic sediments) and Sunnybrook Drift (fine-grained diamicton and lacustrine rhythmites) and the Middle Wisconsinan Thorncliffe Formation (lacustrine and subaqueous fan sediments) have been provisionally identified in logs for boreholes well north of Toronto in York and Durham regions

(see Earthfx (2013, in preparation)) and there are possibly equivalent units present in the model area (Burt and Dodge 2011).

The surficial geology of the area west of Lake Simcoe has been mapped by R.E. Deane (1950a, b), Burwasser and Boyd (1974), Finamore and Bajc (1984), P.J. Barnett (1997), and Barnett and Mate (1998). These maps have been incorporated in the Ontario Geological Survey (OGS) digital compilation map of southern Ontario Quaternary geology (OGS, 2010). Surficial geology for the Oro Moraine model area, based on the digital mapping, is shown in Figure 2.6.

The OGS also carried out two programs of subsurface investigation in the region, with eight fully cored boreholes drilled in 1990 (Barnett 1990, 1991) and 31 holes drilled between 2004 and 2006 (Burt and Dodge 2011). Borehole data from the more recent project were published as two separate OGS releases: Burt and Russell (2006) and Burt (2007). Using data from these boreholes, together with water well and other data, A. K. Burt of the OGS built a three-dimensional hydrostratigraphic model of the area (Burt and Dodge, 2011).

The lowlands within the project area are dominated by lacustrine sediments deposited in high level ice-marginal lakes and Glacial Lake Algonquin and its successor lakes following the last major episode of glaciation (Barnett 1988 and OGS 2010). These sediments are mainly sands, but there are scattered patches of fine-grained sediments - silt and clay - particularly in the northern part of the model area.

The surficial geology of the upland areas is more complex. According to Barnett (1989), the dominant surficial material is till or a unit dominated by till-like debris flows. These diamictons have sandy silt to silty sand matrices which, Barnett (1998) notes, contain mainly clasts of Precambrian rock types. The debris flows are thin and interbedded with sand, silt, and, less commonly, clay (Barnett, 1989). Barnett (1986) observed that there are three subglacial till units in the uplands, each associated with and separated by glaciolacustrine sediments. He noted in 1988 that there was no indication of the absolute age of any of these till units. Since then, the major surficial till sheet in the area has been correlated with the Newmarket Till (OGS, 2010 and Barnett, 1992). Barnett (1997) shows this till as having two mappable facies: a silt to sandy silt facies and a sand to silty facies.

The maps of Barnett (1997) and Barnett and Mate (1998) show an area of about 1.5 km^2 of clast-poor, silty to clayey silt diamicton east of Guthrie that is probably equivalent to the Kettleby Till of Port Huron phase age.

Glaciofluvial sediments and glaciolacustrine sediments are superimposed on the till in the uplands. Generally, these units are fairly thin and limited in areal extent but the Oro Moraine is a thick, extensive body of sand and gravel. Sedimentological analysis of the Oro Moraine by Slattery (2003) favours a predominantly subaqueous fan origin for the moraine sediments and he notes that the overall structure of the moraine is consistent with three stacked fan sequences. Measured paleocurrent directions are generally consistent with the southwesterly ice flow directions of the last regional ice movement and indicate a Lake Simcoe lobe source for the moraine sediments. Slattery (2003) states that the paleocurrent data, along with the morphology of the moraine and detailed sedimentological analysis, support the stacked fan sequence interpretation over the interlobate origin suggested by some earlier workers, such as Chapman and Putnam (1984), or a coalescing fan lobe hypothesis mentioned by Barnett (1986). Barnett (1989) states that the moraine appears to have been formed in three stages. One thing for certain is that the formation of this feature required a high level, ice-marginal lake.

The broad, U-shaped valleys that dissect the till uplands and form most of the Simcoe Lowlands are probably products of at least one major subglacial drainage event with an initial stage of vigorous erosion by a very large volume of water (Barnett, 1986, 1990a, 1990b; and Sharpe *et al*. 1999). Down cutting of these deeply incised 'tunnel valleys' was followed by sedimentation as the hydrodynamic conditions in the valley system changed with waning flow. Burt and Dodge (2011) have found evidence for three cycles of sedimentation within the tunnel valley system. An idealized sedimentary cycle for a tunnel valley starts with a coarse gravel base, which may contain lag deposits, fining upwards through finer fluvial gravels and sands to fine-grained deposits of silt or even clayey silt. This reflects the changing flow conditions from energetic flow to quiet, essentially lacustrine, conditions at the end of the cycle.

The timing of this event (or events) probably postdates the deposition of the Newmarket Till and predates or is contemporaneous with the formation of the Oak Ridges Moraine (Sharpe et al., 1999). Barnett (1986) observed that the two lower till units of the three subglacial tills mentioned above appear to have been truncated by tunnel valley erosion. The uppermost till drapes the landscape and the walls of the tunnel valleys and either is contemporaneous or postdates the formation of the valleys (Barnett, 1986). It is not clear if this till predates or postdates the Oro Moraine.

Following the withdrawal of the last major ice sheet, much of the area was affected by a series of ice marginal or ice-dammed lakes, including Glacial Lake Algonquin and its successor lakes (see Barnett 1992). Throughout the glacial history of the area, regional-scale glacial lakes or even local pondings were probably present in the area whenever it became at least partly ice free and there was no free drainage of glacial meltwater. There are abandoned beaches and spits, as well as erosional shore bluffs and terraces, present on the flanks of the till upland areas (Barnett, 1989 and 1997). Recent sediments include alluvial deposits along modern stream course and organic deposits in poorly-drained areas.

Drift in the model area is generally quite thick and ranges from 0 to 250 m (Figure 2.7). In the lowland areas it usually ranges from about 50 to 100 m but there are small areas with thin (<15 m thick) drift in the northern part of the model area, particularly east of Moonstone and between Lake Simcoe and Lake Couchiching. Overburden thickness in the till uplands is typically about 60 to 175 m but at the high point of the Oro Moraine it is about 250 m.

2.2.4 OGS Conceptual Hydrostratigraphic Model

The conceptual framework developed by Burt and Dodge (2011), summarized on Table 2.1, consists of 23 hydrostratigraphic units – 2 bedrock layers and 21 Quaternary (overburden) layers. Because it is a hydrostratigraphic model, it has alternating aquifer and aquitard layers. Many of these layers may contain parts of more than one lithostratigraphic unit that have been grouped together because of their hydrogeological properties and spatial relationships. Aquifers units typically contain mainly sand or sand and gravel but may contain beds of diamicton and fine-grained sediment. An aquitard unit commonly contains till and fine-grained water laid sediments but may also have thin beds or lenses of sand (Burt and Dodge 2011).

The Burt and Dodge model actually has three conceptual models: a bedrock model, a 'normal' Quaternary succession, and a tunnel channel model. The bedrock model is quite simple, consisting of an unsubdivided Paleozoic layer and a Precambrian rock surface. The upland or `normal` Quaternary model has 14 layers which can be grouped into three packages based on assumed age. This model includes the late glacial to postglacial deposits of the Algonquin aquifer (GLAF) and Algonquin aquitard (GLAT). The tunnel valley model has seven layers: five

layers representing channel fill sediments and two layers of postglacial lake sediments. The tunnel valley model truncates most of the upland model layers. The postglacial lake sediment layers are common to both overburden models.

Table 2.1 is slightly modified from Table 4 of Burt and Dodge (2011) and provides a summary of the conceptual framework and the layers of the OGS numerical model. Note that Burt and Dodge (2011) use the terms 'glacial deposit' and 'glacial unit' for any sediments deposited in association with glacial activity, not just glacial till. Figure 2.8 gives a graphical representation of the conceptual model, showing stratigraphic and spatial relationships.

The Basal aquifer is a compound unit that combines the zone of weathered carbonate bedrock with younger lag gravel deposits. The five units of the 'lower drift' package are next in the ascending sequence. The three aquitards all contain fine-grained lacustrine deposits along with silty to sandy diamictons. The aquifers are sand to silty sand and are probably mainly lacustrine or glaciolacustrine in origin. With possible ages ranging from the Ontario Subepisode to Illinois Episode, these sediments may be time equivalent to Toronto area units such as the Sunnybrook Drift, the Scarborough Formation, the interglacial Don Formation and the Illinoian York Till (see Barnett 1992).

The 'middle drift' can be divided into the regional aquifer (AF4) plus regional aquitard (AT3) and what Burt and Dodge (2011) call the 'upper aquifer complex' which contains the local aquifer (AF2), local aquitard (AT1) and the regionally significant upper aquifer (AF1). Detrital plant material recovered from the local aquifer unit in OGS borehole BH-35-AKB-2006 gave a carbon-14 (^{14}C) age of 38,860±480 years BP (i.e., the Port Talbot Phase – a relatively warm interstadial period). Burt and Dodge suggest that this material was picked up glacially during a later stage of glacial activity and redeposited during ice recession, possibly during the Brimley Phase, which was prior to the glacial maximum during the Nissouri Phase.

The Newmarket aquitard is mainly composed of the regional Newmarket Till (Port Bruce Phase), 'northern till' – a stony sand till – and minor Kettleby Till (Port Huron Phase), along with some fine-textured glaciolacustrine materials and lenses of sandy sediments (Burt and Dodge, 2011).

The drumlinized, regional coarse-grained till can be called `Newmarket Till` with a high degree of confidence because it is mapped at surface and caps the till uplands. This is not the case for subsurface units, however. Regionally, Quaternary stratigraphic studies of the subsurface are still at an early stage, making correlation of units in the model area with more distant stratigraphic units problematic. According to Burt and Dodge (2011), there has been little success in tracing older glacial units beyond the boundary of their local study area and no suitable material for 14C dating has been recovered below the upper aquifer complex. The chronology in Table 2.1 should be considered at best provisional for older deposits.

The Oro Moraine aquifer (also referred to as the ICSD (for ice-contact stratified drift)) takes in the granular deposits of the Oro Moraine along with a few other bodies of glaciofluvial material of similar age. Fine-grained postglacial lake deposits make up the Algonquin aquitard (GLAT), which is younger than the valley fill sequences (see below) and the Oro Moraine sediments. This unit is capped by the Algonquin aquifer (GLAF), the stratigraphic top of the model, which is made up predominantly of sandy postglacial lake deposits, along with gravelly beach and bar sediments and recent alluvial deposits. Although both of the 'Algonquin' units are found as scattered patches on the till uplands, both are mainly in the tunnel valley systems.

The tunnel valleys cross cut through most of the upland sediment sequence from the Newmarket aquitard (NT) down to the Lower Drift lower aquitard (LD2). The tunnel valley fill sequence consists of three aquifers – lower (CAF3), middle (CAF2), and upper (CAF1) - with two intervening aquitards – lower (CAT2) and upper (CAT1). The uppermost aquifer (CAF1) is capped by the Algonquin aquitard (GLAT). As discussed previously, these sediments represent three fining-upward sedimentary cycles.

The extents and thickness of these units is best appreciated by viewing their isopach maps (see Figure 2.9 to Figure 2.25) and cross sections (See Figure 2.26 through Figure 2.35).

2.3 Climate

Long-term climate data are used to characterize the spatial and temporal distribution of precipitation and to derive the spatial and temporal distribution of evapotranspiration. There are three climate stations established by Environment Canada that are active in the Oro Moraine model area. The Barrie WPCC station (6110557) is located just south of the model area. There are also nine inactive stations with varied periods of record that have historic information. Locations are shown on Figure 2.36.

Climate normal (i.e., averages over 30 years) for 1971 to 2000 have been published by Environment Canada (http://climate.weatheroffice.gc.ca/climate_normals/index_e.html). Monthly average temperature, rainfall, snowfall, and total precipitation values are shown for stations in the model area in Figure 2.37 through Figure 2.40 and are tabulated in Table 2.2. The rainfall and precipitation data are in millimetres (mm). Conversion of snowfall data to equivalent rainfall assumes that 1 centimetre (cm) of snow is equivalent to 1 mm of rainfall.

Monthly average temperature ranges from about -8.3 °C in January to 20.2 °C in July. Temperature data are consistent between the five stations. Monthly rainfall rates for the stations are similar although Orillia TS has generally higher values. Rainfall averages 711 mm/yr. Snowfall rates are more variable with Orillia TS and Coldwater-Warminster being generally high and Barrie WPCC and Midhurst generally low. Snowfall averaged 269 cm/yr. Total precipitation based on these data averaged 980 mm/yr. Precipitation is higher from August to January, averaging 93 mm/month, and lowest from February to April, averaging 63 mm/month. The meteorological data utilized in the numerical model is discussed in more detail in a subsequent chapter.

2.4 Surface Water Characterization

As noted, the model area extends well beyond the boundaries of the Oro North, Oro South, and Hawkestone Creek subwatersheds to include areas that may provide lateral groundwater inflow or that may receive lateral groundwater outflow from these subwatersheds. Figure 2.41 shows the locations of the major streams in the model area and their watersheds as defined by land surface topography. The stream reaches were classified using a Strahler stream order system, which assigns reaches a number depending on their location in the network's branching pattern. The term "headwaters" generally refer to zero-order (unmapped swales), first-order and second-order streams. Typically, at least half the total length of the channels in a stream can be classified as first and second-order. Groundwater discharge to the headwater reaches represents a significant portion of the total baseflow.

As shown on Figure 2.41, a number of wetland features are present within the model area. Land use inventory mapping was reviewed to capture these hydrologic features. Figure 2.42 summaries the Southern Ontario Land Resource Information System (SOLRIS, version 1.2) (MNR, 2008) mapping for the model area. Marshes, bogs, swamps, and ferns represent 15.5% of the model area (125 km^2). Additionally, open water represents 1.1% of the model area (9.0 km^2), mostly reflecting the contribution from Bass Lake and Little Lake. A detailed breakdown of land class is provided on Table 2.4. The land use data employed in the numerical model is discussed in more detail in a subsequent chapter.

Figure 2.41 shows the location of the Water Survey of Canada (HYDAT) stream gauges monitored by Environment Canada. Gauge locations, the period of record, and streamflow statistics for the period of record are presented in Table 2.3. Four active gauges provide a continuous record of streamflow for major streams in the model area. Two gauges on Willow Creek provide historical information and there is another inactive gauge on Sturgeon River at Sturgeon Bay (02ED018) northwest of the model area. There are no gauges on the Oro North or Oro South but information determined by model calibration to flows at the Hawkestone Creek and other gauges was assumed to provide relevant information as the hydrologic and geologic conditions are similar. Additional LSRCA gauges are available but there are only spot flow measurements from these stations.

A Flow Duration Curve (FDC) is an analysis plot that characterizes the probabilistic relationship between magnitude and frequency at a gauge station (Searcy, 1959). Streamflow data (typically daily) is plotted against the fraction of time that the flow rate is equalled or exceeded (the exceedance percentile or probability). The flow duration curve represents an empirical cumulative distribution function of streamflow record at a gauging station (Maidment *et al.*, 1992). FDC's for the four active WSC gauges within the model area are provided as Figure 2.43 through Figure 2.46.

To further characterise the surface water behaviour in the model area, a simple flood frequency analysis was undertaken. Of the WSC gauges in the model area, only Coldwater River at Coldwater (02ED007) had a sufficiently long period of record for this analysis. The peak annual flood series at this gauge was fitted to a Log Pearson III distribution as per Bulletin #17B (Water Resources Council (US), Hydrology Committee, 1981) to derive return intervals. Outlier removal via the Grubbs' Test and the estimation of regional skewness were also implemented as per Bulletin #17B. Qualitatively, most flood events seem to correspond to the spring freshet in the catchment. This agrees with Dickinson's observation that the bulk of the annual flood peaks in rural Ontario watersheds are a result of mixed snowmelt/rain events (Dickinson *et al.*, 1991). Characterizing snowmelt and combined runoff events is necessary for achieving a good model calibration. Return intervals are presented on Figure 2.47 and will be discussed further in relation to model calibration.

When addressing streamflow gauge data, resolution is of extreme importance (Thompson, 2013). Daily data can often obfuscate the natural hydrologic regime as the values represent estimates of the total daily volume flow volume but obscure processes and mechanisms that occur at a higher frequency. This can be of critical importance in flashy urban systems or areas of low permeability soils. To check the adequacy of the temporal resolution of the stream data within the model area, instantaneous streamflow data on a 15-minute time step were obtained from the WSC for the Coldwater River at Coldwater gauge (02ED007). A comparison of the mean daily and instantaneous flow durations curves is provided on Figure 2.48. Mean daily streamflow data appear to adequately represent the hydrologic response in this catchment 99.995% of the time.

The uncertainly within published streamflow data is difficult to precisely quantify. Several authors report a discharge measurement uncertainty of 5% at the 95% confidence interval (Terzi, 1981 and Herschy, 2002). Open water discharge measurements obtained by the WSC are typically fitted to within a 5% window; under ice measurements are fitted to within a 10% window (Hamilton, 2012). Hamilton (2008) observed that this uncertainty cannot be assumed to be uniform across the entire range of possible discharge values. He further goes on to reason that the uncertainly in small discharge and velocity measurements may be high due to unavoidable limits on measurement equipment scale and dimension.

Further uncertainty is associated with estimated mean daily discharge values which are approximated without stage data. The occurrence of estimated values in low flow statistics is about 50% more frequent than the national mean daily dataset (Hamilton, 2008). Awareness of the inherent uncertainty within the stream gauge data is critical when producing model calibration targets.

2.5 Aquifer Heads and Groundwater Flow

Groundwater levels and groundwater flow directions in the model area reflect the complex aquifer layer geometry, recharge patterns, influence of streams, and, to a lesser extent, the effect of groundwater use. Observed groundwater levels (also referred to as aquifer heads or potentials) served as the primary calibration targets for the integrated groundwater/surface water flow model. Groundwater data are discussed below; groundwater use is discussed in a separate section.

2.5.1 Water Level Data Sources

Water-level data are available from three primary sources: the “static water level” data in the Ministry of Environment (MOE) Water Well Information System (WWIS), continuous records from wells in the Provincial Groundwater Monitoring Network (PGMN), and observation wells monitored by other large water users as conditions of their permit to take water (PTTW) issued by the MOE. Compiling the water-level data was necessary for the calibration of the steady-state and transient groundwater flow models and for estimating response to pumping-rate variations and drought conditions.

Static water level data from the MOE WWIS database provide a general insight into the water level patterns in the model area. Well locations are shown in Figure 2.49. Locations are sorted by aquifer based on the midpoint of the screened interval and the interpolated hydrostratigraphic surfaces. It can be seen that some of the aquifer and aquitard units in the tunnel channels have been paired with corresponding units in the till highlands. This was done to simplify the groundwater model and is discussed further on in Section 5. Overall data coverage is good. There are noticeable spatial preferences in the aquifers screened, however, which provides some qualitative information on aquifer presence and yield. For example, many of the bedrock wells are located near the Lake Simcoe shoreline where overburden is absent or thin.

Biases and quality issues are known to exist in the water well record data. Some of these are discussed in the next section. Assessment of the intrinsic error and variation in this data set is discussed at length in Kassenaar and Wexler (2006). Wells with poor location quality codes (QA_CODE > 6) were excluded from the data set. Despite these limitations the vetted WWIS data set provides important insight into regional trends and patterns in the aquifer levels and

was used in the calibration of the steady-state groundwater model. Further discussion of the WWIS data is provided in Section 5.9

PGMN water level data were obtained from the LSRCA. Well construction and location data are provided in Table 2.5. One pair of PGMN wells is located in the Hawkestone Creek subwatershed; the others are located within the Willow Creek or Coldwater Creek subwatersheds (Figure 2.50). The PGMN data provide useful information on natural seasonal and climactic variation in water levels. Quality issues with the PGMN data, such as the location of wells near active pumping sources or quarries, reduces the usefulness of these data.

Private well monitoring data were requested. Data were provided for Edgar Pit located in the Hawkestone Creek subwatershed. Monthly down-to-water measurements for 2012 at Coldwater Fisheries were also provided but the wells are located just north of the model area.

2.5.2 Regional Water Level Patterns

Regional groundwater flow patterns were evaluated using static water level data obtained from the WWIS database and average water levels from long-term monitoring sites.

There are problems that have long been recognized with the static water levels recorded in drillers' logs submitted to the MOE. The data could not be used without some filtering. Sources of error include positional and depth measurement errors and uncertainty as to whether static conditions were achieved prior to measurement. Seasonal and year-to-year water-level variations also introduce noise in the data. The values represent a single "snapshot' in time and place in a data set that spans taken over an extremely long period (about 70 years). The variability is most noticeable when analyzing clusters of water-level data from the same aquifer with pairs of nearby wells showing differences of over 75 m. Although obvious outliers can be eliminated in areas of clustered data, it is often uncertain whether a particular measurement in the data set is accurate and, even if accurate, whether it represents a reasonable measurement of an average water level at that point when data are sparse. The accuracy of maps produced from these data is similarly affected. However, the MOE WWIS data are the only data set with sufficient spatial coverage to allow mapping of potentiometric surfaces over the entire model area and, in general, the water levels and the spatial trends observed in the mapped water level surfaces appear consistent and reasonable.

Observation data for the wells screened in the various aquifers are posted in Figure 2.51 through Figure 2.56. For aquifers where sufficient data exist, the water levels were interpolated using a geostatistical technique known as "kriging" to determine general patterns of groundwater flow. Kriging is a weighted-average interpolation method that attempts to minimize variance and bias in the results while honouring the local values at the data points. Prior to the interpolation, all possible data pairs were examined to determine the relationship between sample variance and lag distance. A theoretical variogram was fitted to the sample data and then used to construct the variance matrix needed to assign weights. Along with interpolated water levels, the kriging analysis produces estimates of the variance and standard error of estimate at each interpolation point. The standard error was used as a measure of confidence in the interpolation and results were "blanked out" in areas of limited data where the standard error exceeded a maximum threshold. Additional elevation data points were added to the kriging process to force the contours to match water surface elevations where the contours intersect the larger streams and lakes.

The interpolated groundwater levels for the AF1-GLAF are shown in Figure 2.57. White areas on the map show where the standard error exceeded 5 m. The highest water level elevations, exceeding 330 masl, are observed in the centre of the model area at Horseshoe Valley. A second high point (329 masl) occurs near Edgar. Another groundwater high occurs on the till upland near Moonstone. Low water levels occur near the Lake Simcoe shoreline and where Willow Creek exits the model area.

Groundwater flow is perpendicular to the contour lines and is radially outward from the groundwater highs towards the streams and lake shore. The contours are generally perpendicular to the topographic watershed divides indicating that cross-watershed flow is not occurring in these areas. Local areas where the lines are not perpendicular, such as near the top of the Oro North watershed or near Shanty Bay in Oro South, may have significant cross-watershed flows. There are pronounced bending of the contours in the vicinity of streams indicating that groundwater is discharging to these features.

Interpolated groundwater levels for the AF4-CAF1 are shown in Figure 2.58. Highest groundwater heads (about 310 masl) are shifted to west and are within the Hawkestone Creek watershed. Some cross-watershed flow is likely occurring here but this is based on a limited number of data points. There is a pronounced low in the centre of the Coldwater Creek watershed with heads less than 210 masl and others at the outlets for Willow and Silver Creeks.

Groundwater is exchanged between aquifers as leakage across the confining units. The direction of vertical flow depends on the difference in head between the overlying and underlying aquifers. Leakage rates vary locally depending on the magnitude of the vertical gradients (i.e., the difference in head divided by the thickness of the confining unit) and the vertical hydraulic conductivity of the confining unit. Leakage is generally downward from the AF1-GLAF to the AF4-CAF1 across the local and regional aquitards (AT1 and AT3) as shown in Figure 2.59. Differences in the interpolated heads greater than 60 m occur in the Moonstone area and values greater than 40 m occur beneath the Oro Moraine although the data to support these observations are sparse. Head differences within the Oro North, Oro South, and Hawkestone Creeks subwatersheds are much less pronounced. Local reversals in the gradient are noted in the vicinity of some streams and along the Lake Simcoe shoreline

Interpolated groundwater levels for the STAF-CAF2, LAF-CAF3, and shallow bedrock are shown in Figure 2.60 through Figure 2.62, respectively. The data are generally too sparse to see any distinctive patterns, although the patterns are likely consistent with those discussed previously (i.e., downward gradients and decreasing heads with depth in the centre of the model area, a reversal of gradients along the shore and in the stream valleys, and radial flow outward from the centre of the model area).

Nugget values determined from the variance analysis suggested that the data have an average systematic error ranging from about ±3 m for all layers after filtering for obvious outliers. This indicates that the model calibration to these data cannot be expected to have a greater accuracy than this intrinsic error.

2.5.2.1 Water Level Fluctuations

Groundwater levels in shallow wells respond to precipitation events and seasonal variations. Typically, seasonal response can be described as:

- Water levels increase in late September through November due to high monthly rainfall rates and decreased evapotranspiration (ET);
- Water levels plateau from mid-December to mid-February as monthly rainfall rates decrease, snow accumulates, and frozen ground conditions restrict infiltration;
- Sporadic water levels increases are observed from mid-February to the end of mid-March due to snowmelt and/or precipitation events.
- Water levels rise dramatically in the mid-March to mid-April spring due to snowmelt and thawing of the ground
- A steep recession in water levels occurs from mid-April to September despite increasing monthly rainfall rates. Few recharge events reach the water table because of high ET rates.

The hydrograph for PGMN well W0000442-1 (Figure 2.63), screened in CAF1 at the edge of the tunnel channel, was (of the PGMN wells in the model area) the most reflective of ambient conditions and least influenced by nearby pumping or quarry activities. Water levels show the rise in the spring, summer recession and limited recovery in the fall. Peak to trough values are about 0.4 m. Year to year variations are noted with a longer-term rising trend in water levels over the interval shown. The effect of an unusually dry 2007 is not seen but the wet years following raised peak water levels 0.4 m (from 248.1 to 248.5 masl). Figure 2.64 shows a relative hydrograph for PGMN wells W0000244 and W0000293-2 which behave somewhat similarly to W0000442-1. Peak to trough values for W0000244 average about 0.5 m while those for W0000293-2 are closer to 0.8 m.

Figure 2.65 shows a comparison of water level response at PGMN well W0000293-2 and precipitation at Barrie-Oro (6117700) for water years 2005 and 2006. There appears to be a reasonable correlation between precipitation events in the fall and spring with more muted responses in the summer and winter months. Some unusual responses are noted as well. For example, there is a decrease in water levels following the large precipitation event in April 2005. This may be due to pumping in the adjacent quarry. Other PGMN wells are not useful for analyzing natural response because they are affected by nearby activities. For example, the hydrograph for PGMN well W0000245 (Figure 2.66), screened in the LAF, is strongly influenced by nearby wells. As can be seen, water levels decline as pumping rates increases. Data from other PGMN wells was deemed to be less reliable.

In summary, the combination of the MOE WWIS and PGMN data provide insight into the regional flow patterns, natural fluctuations in response to seasonal, year-to-year, and daily variation in precipitation, and transient response to other water use. The MOE WWIS data are of considerably lower quality. The PGMN data are generally of better quality but are also subject to data quality problems and some are influenced by nearby activities.

2.6 Tables

Table 2.1: OGS conceptual hydrostratigraphic model (from Burt and Dodge, 2011).

General Chronology	Hydrostratigraphic Unit (Code)	Lithostratigraphic Unit	Summary Lithology	Class
Late glacial to postglacial deposits: late Michigan Subepisode to Hudson Episode	Algonquin aquifer (GLAF)	Lake Algonquin to recent shoreline and nearshore deposits, postglacial to modern river deposits and modern wetlands	Sand and silty sand. Occasional gravel-rich beds. Peat and other organic-rich deposits in wetlands.	Aquifer
	Algonquin aquitard (GLAT)	Lake Algonquin and postglacial Lake Nipissing and Lake Edenvale deep-water deposits	Silt, silty clay and clay	Aquitard
Late glacial deposits: Michigan Subepisode (formerly known as the Late Wisconsinan)	Valley fill: upper aquifer (CAF1)	Tunnel-valley fill: coarse-textured stratified deposits	Sand and silty sand. Rare gravelly beds.	Aquifer
	Valley fill: upper aquitard (CAT1)	Tunnel-valley fill: fine-textured stratified deposits	Silt, silty clay and clay. Rare diamicton beds.	Aquitard
	Valley fill: middle aquifer (CAF2)	Tunnel-valley fill: coarse-textured stratified deposits	Sand and silty sand	Aquifer
	Valley fill: lower aquitard (CAT2)	Tunnel-valley fill: fine-textured stratified deposits	Silt, silty clay and clay. Rare diamicton beds	Aquitard
	Valley fill: lower aquifer (CAF3)	Tunnel-valley fill: coarse-textured stratified deposits	Sand and silty sand. Occasional gravelly beds.	Aquifer
Glacial deposits: Port Bruce Phase of Michigan Subepisode	Oro Moraine aquifer (ICSD)	Oro Moraine and equivalent ice-contact stratified deposits and glacial outwash deposits	Sand and gravel. Rare diamicton beds.	Aquifer
	Newmarket aquitard (NT)	Newmarket Till, northern till and isolated pockets of Kettleby Till, some fine-textured stratified deposits	Sandy and silty sand tills. Silt. Occasional thin sandy beds	Aquitard
Older glacial Deposits (Middle Drift): Elgin Subepisode? (Middle Wisconsinan)	Upper aquifer (AF1)	Regional coarse-textured stratified deposits	Gravel, sand and silty sand	Aquifer
	Local aquitard (AT1)	Local fine-textured stratified deposits	Silt, silty clay, clay	Aquitard
	Local aquifer (AF2)	Local coarse-textured stratified Deposits	Gravel, sand and silty sand	Aquifer
	Regional aquitard (AT3)	Regional fine-textured (deep-water) stratified deposits and till	Silt, silty clay and clay. Silt to clay diamicton beds.	Aquitard
	Regional aquifer (AF4)	Regional coarse-textured stratified deposits	Gravel, sand and silty sand	Aquifer
Old glacial Deposits (Lower Drift): Ontario Subepisode (Early Wisconsinan) to Illinois Episode	Lower drift: upper aquitard (OST)	Lower drift: till and fine-textured (deep-water) stratified deposits	Silty to sandy diamicton, silt, silty clay and rarely clay	Aquitard
	Lower drift: local aquifers (STAF)	Lower drift: local coarse-textured stratified deposits	Sand and silty sand	Aquifer
	Lower drift: middle aquitard (LD)	Lower drift: till and fine-textured (deep-water) stratified deposits	Silty to silty clay diamicton, silt, silty clay and clay	Aquitard
	Lower drift: lower aquifer (LAF)	Lower drift: regional coarse-textured stratified deposits	Sand and silty sand	Aquifer
	Lower drift: lower aquitard (LD2)	Lower drift: till and fine-textured (deep-water) stratified deposits	Silty to sandy diamicton. Silt, silty clay and rarely clay.	Aquitard
Quaternary and Paleozoic contributions	Basal aquifer (BGravel)	Basal gravel lag and weathered bedrock	Sand and gravel, weathered / karst bedrock	Aquifer
Paleozoic and Precambrian	Paleozoic (Ordovician) bedrock (Paleozoic)	Paleozoic bedrock	Shadow Lake, Gull River, Bobcaygeon, and Verulam formations: limestone, shale, siltstone and sandstone	Bedrock
	Precambrian (Mesoproterozoic) bedrock (Precambrian)	Precambrian bedrock	Grenville Province, Central Gneiss Belt : felsic intrusive rocks and derived gneisses and migmatites, metasedimentary gneisses	Bedrock

Table 2.2: Climate normals (1971-2000) for stations in the model area.

Station ID	Station Name	Jan	Feb	Mar	Apr	May	Jun	Jul	Aug	Sep	Oct	Nov	Dec	Annual
		Temperature (°C)												Average
6110557	Barrie WPCC	-8.1	-7.1	-2.2	5.3	12.3	17.7	20.5	19.5	14.9	8.5	2.4	-4.0	6.7
6111769	Coldwater-Warminster	-8.8	-7.8	-2.1	5.5	12.6	17.3	20.1	19.1	14.7	8.4	1.6	-4.5	6.3
6115099	Midhurst	-8.1	-7.6	-2.1	5.2	12.1	17.0	20.0	19.0	14.4	8.2	2.0	-4.5	6.3
6115820	Orillia TS	-8.4	-7.7	-2.1	5.7	12.9	17.1	20.6	19.4	14.8	8.2	2.2	-4.8	6.5
6117684	Shanty Bay	-8.2	-7.2	-1.9	5.5	12.2	17.1	19.9	19.1	14.6	8.5	2.3	-4.3	6.5
		Rainfall (mm/month)												mm/yr
6110557	Barrie WPCC	15.3	13.3	28.9	57.8	77.2	86.6	73.4	92.6	97.6	74.3	62.1	21.3	700.2
6111769	Coldwater-Warminster	21.8	14.8	32.2	55.5	75.7	85.2	84.2	93.2	96.1	81.3	62.1	25.2	727.2
6115099	Midhurst	9.5	14.7	31.2	55.0	66.8	73.9	78.6	88.9	97.8	78.1	61.2	24.3	679.9
6115820	Orillia TS	13.9	15.4	38.4	60.9	77.3	76.4	77.4	102.4	95.3	86.5	77.1	29.6	750.6
6117684	Shanty Bay	18.0	16.5	32.1	53.5	72.4	87.4	73.8	92.4	95.8	72.0	60.9	22.1	696.8
		Snowfall (cm/month)												cm/yr
6110557	Barrie WPCC	80.2	39.5	28.1	5.0	0.1	0	0	0	0	2.5	20.6	62.4	238.4
6111769	Coldwater-Warminster	93.4	54.7	34.7	13.5	1.2	0	0	0	0	6.0	40.2	75.1	318.8
6115099	Midhurst	66.6	37.4	25.3	7.2	0.7	0	0	0	0	4.0	26.3	60.6	228.0
6115820	Orillia TS	89.2	52.6	32.9	11.3	0.4	0	0	0	0	3.2	25.4	77.7	292.6
6117684	Shanty Bay	75.5	41.7	33	11.8	1.2	0	0	0	0	4.4	36.1	63.6	267.3
		Total precipitation (mm/month)												mm/yr
6110557	Barrie WPCC	95.4	52.8	57	62.9	77.3	86.6	73.4	92.6	97.6	76.8	82.6	83.7	938.5
6111769	Coldwater-Warminster	115.1	69.5	66.8	69.0	76.9	85.2	84.2	93.2	96.1	87.3	102.3	100.3	1046.0
6115099	Midhurst	76.1	52.1	56.5	62.2	67.5	73.9	78.6	88.9	97.8	82.1	87.4	84.9	907.9
6115820	Orillia TS	103.1	68.1	71.3	72.2	77.6	76.4	77.4	102.4	95.3	89.7	102.5	107.3	1043.0
6117684	Shanty Bay	93.5	58.3	65.1	65.2	73.6	87.4	73.8	92.4	95.8	76.4	97.0	85.7	964.1

Table 2.3: Summary of WSC gauged catchments in the model area.

Gauge ID	Gauge Name	Start Year	End Year	Status	Catchment Area (km^2)	Average Total Flow (m^3/s)	Median Flow (QP50) (m^3/s)
02EC020	Hawkestone Creek at Hawkestone	2005	2010	Active	35.1	0.54	0.32
02ED007	Coldwater River at Coldwater	1965	2010	Active	168.4	2.31	1.67
02ED030	Silver Creek at Orillia	2005	2010	Active	10.5	0.20	0.15
02ED032	Willow Creek near Minesing	2005	2010	Active	231.1	2.57	1.78
02ED009	Willow Creek above Little Lake	1973	1995	Disco	94.8	0.89	0.34
02ED010	Willow Creek at Midhurst	1973	1998	Disco	127	1.21	0.69
02ED028	Silver Creek near Orillia	1999	2005	Disco	24	0.34	0.23

Table 2.4: Tier 2 study area and model area land use (from SOLRIS v1.2 data (MNR, 2008)).

Generalized Land Class	Coverage (km^2)		Percent Cover	
	Study	Model	Study	Model
Forest Cover	53.7	260.6	29.7%	32.2%
Transportation	7.9	29.6	4.4%	3.7%
Extraction	2.2	5.1	1.2%	0.6%
Built-up Pervious	1.2	7.5	0.7%	0.9%
Built-up Impervious	12.0	41.4	6.7%	5.1%
Swamp/Bog/Marsh	23.2	125.3	12.9%	15.5%
Open Water	0.2	9.0	0.1%	1.1%
Undifferentiated	80.1	331.2	44.4%	40.9%

Table 2.5: PGMN well data.

Well Name	Alternate Well Name	Easting (m)	Northing (m)	Ground Elv. (masl)	Borehole Bottom Elv. (masl)	Screen Top Elv. (masl)	Screen Bottom Elv. (masl)	Strati-graphy
W0000293-2	Oro Pit	613444	4931227	308.3	305.2	308.3	305.2	AF1-GLAF
W0000293-3	Oro Pit BH2	613445	4931228	299.1	296.1	299.1	296.1	AF1-GLAF
W0000244	Midhurst BH2	600110	4920982	221.7	220.2	221.7	220.2	AF1-GLAF
W0000245	Midhurst MW1	600110	4920975	178.4	172.6	178.4	172.6	CAF3-LAF
W0000439-1	BH-19-AKB-2004	612250	4934587	269.0	263.6	269.0	263.6	AF2
W0000440-1		607991	4940031	179	170.6	179	170.6	Bedrock
W0000442-1		603625	4937437	235.7	234.2	235.7	234.2	CAF1-AF4
W0000443-1		603662	4941611	271.5	268.4	271.5	268.4	AF1-GLAF

2.7 Figures

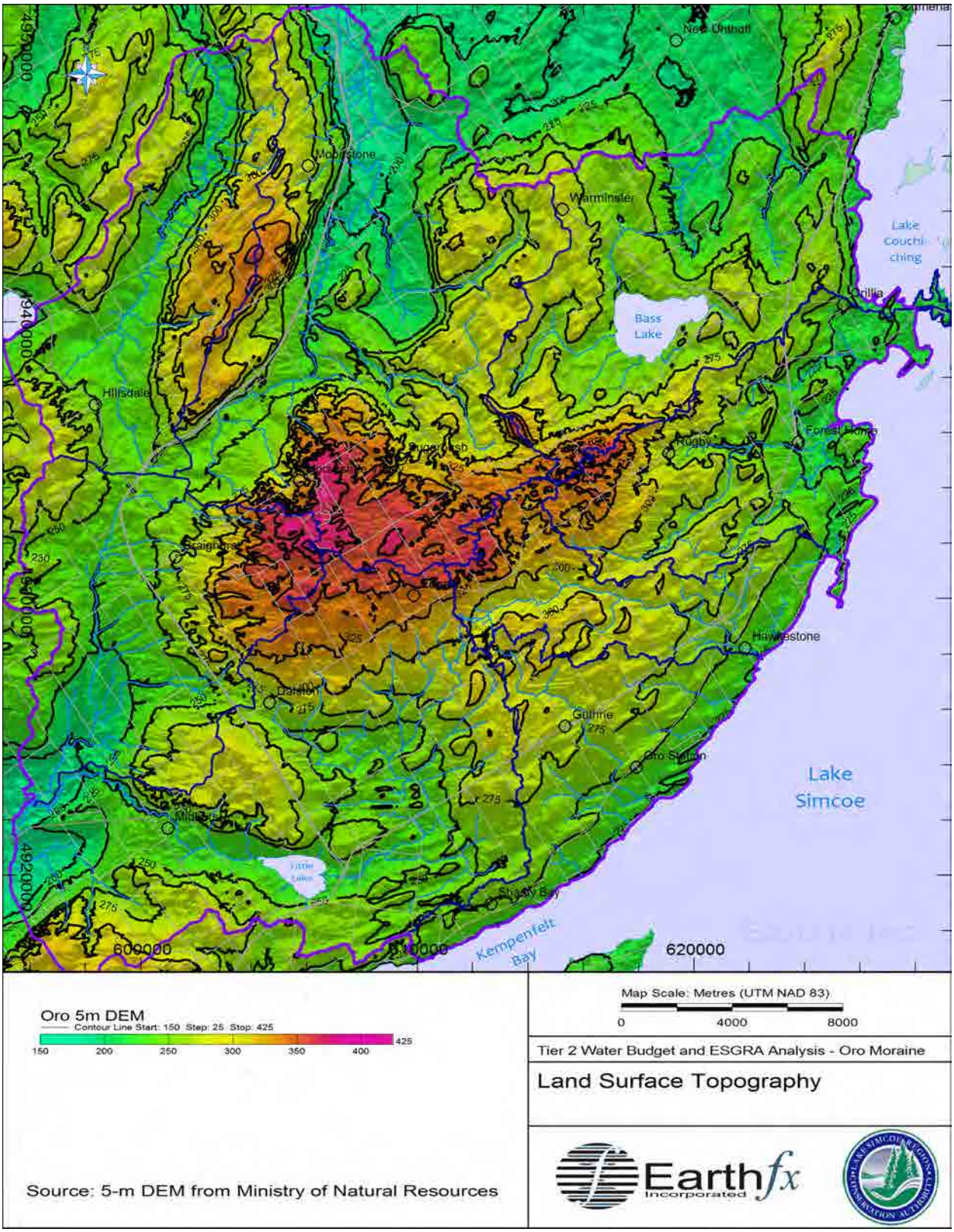

Figure 2.1: Land surface topography from 5-m digital elevation model.

Figure 2.2: Physiographic regions (from Chapman and Putnam (1984) and OGS (2007)).

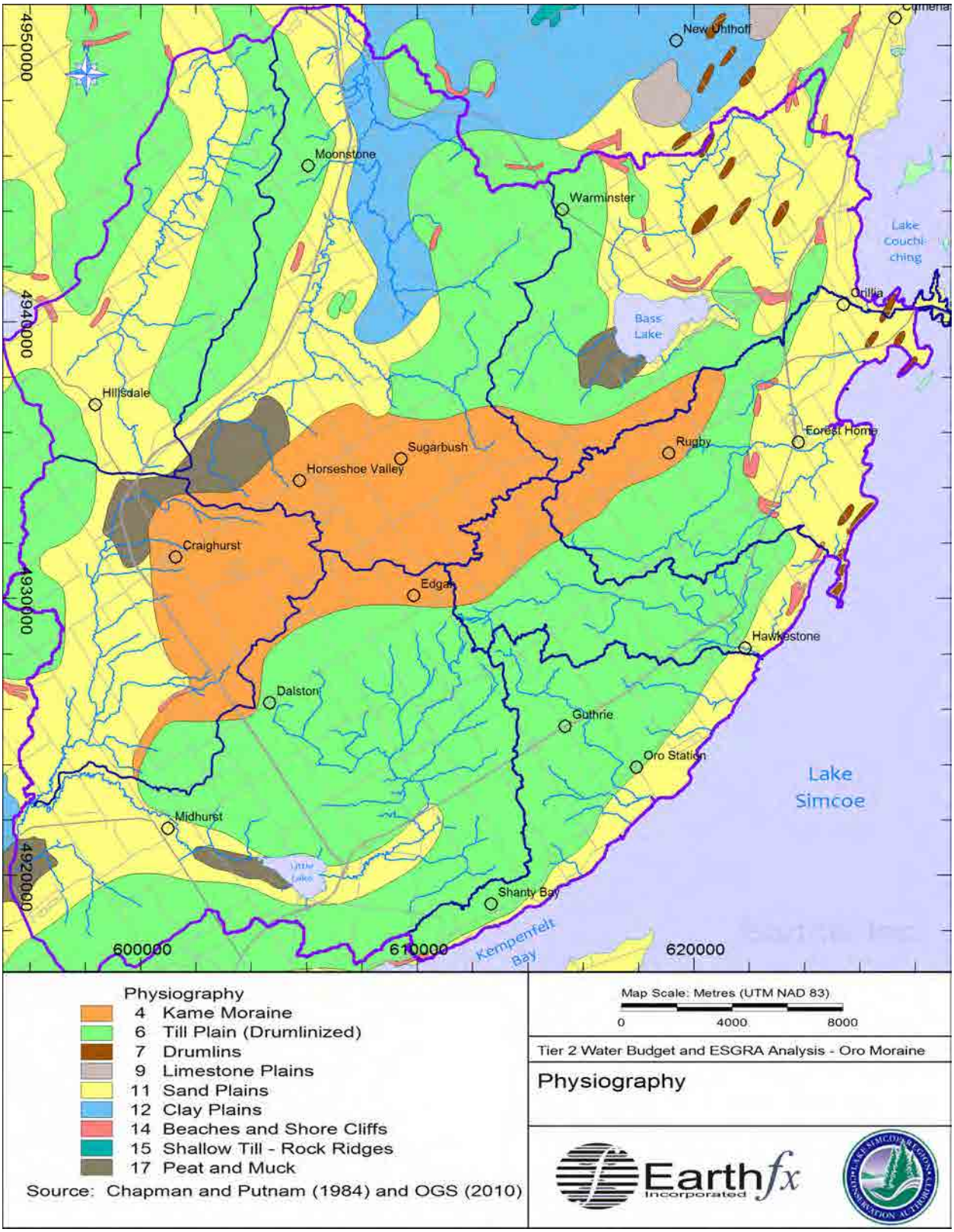

Figure 2.3: Physiography (from Chapman and Putnam (1984) and OGS (2007)).

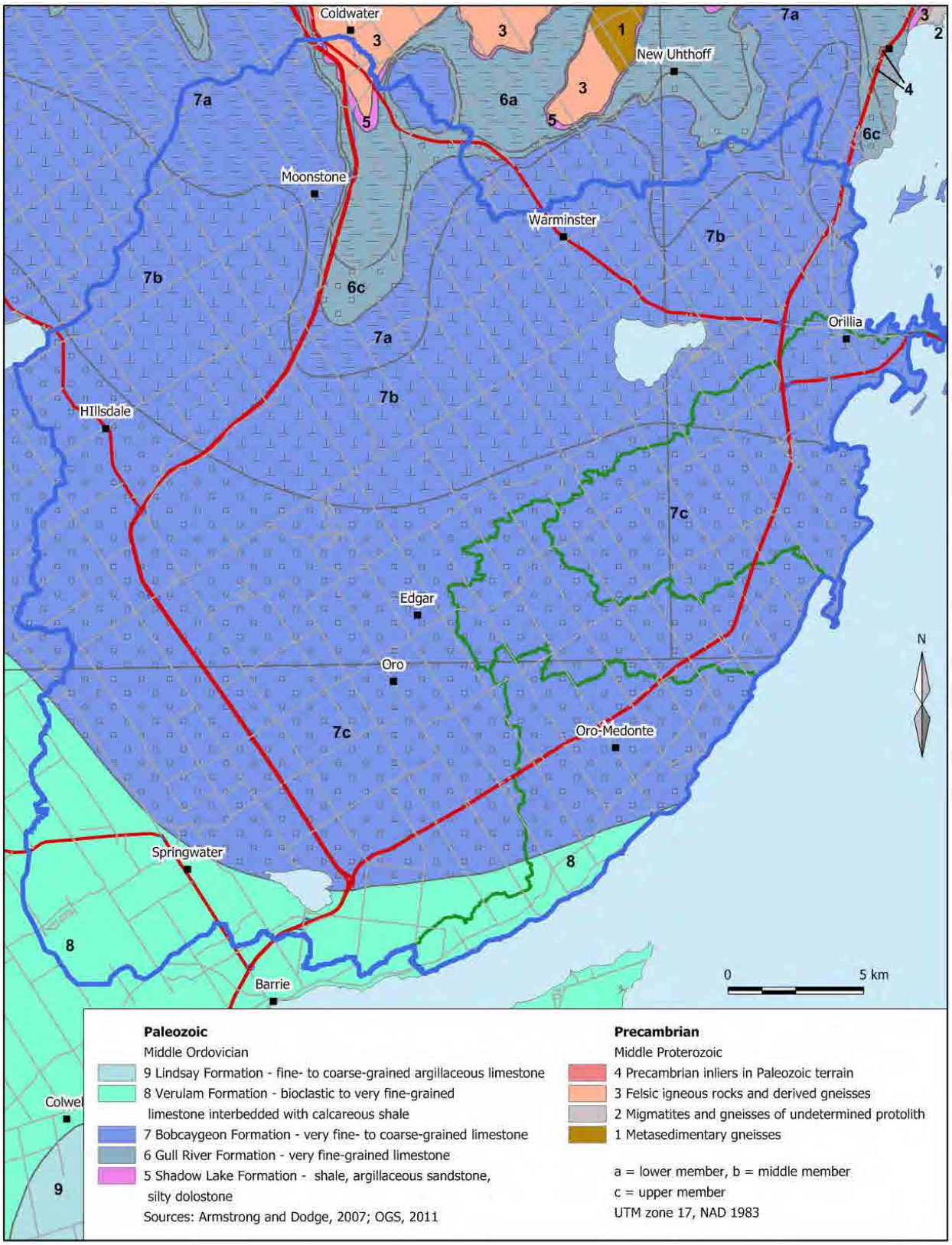

Figure 2.4: Bedrock geology (from Armstrong and Dodge (2007) and OGS (2011)).

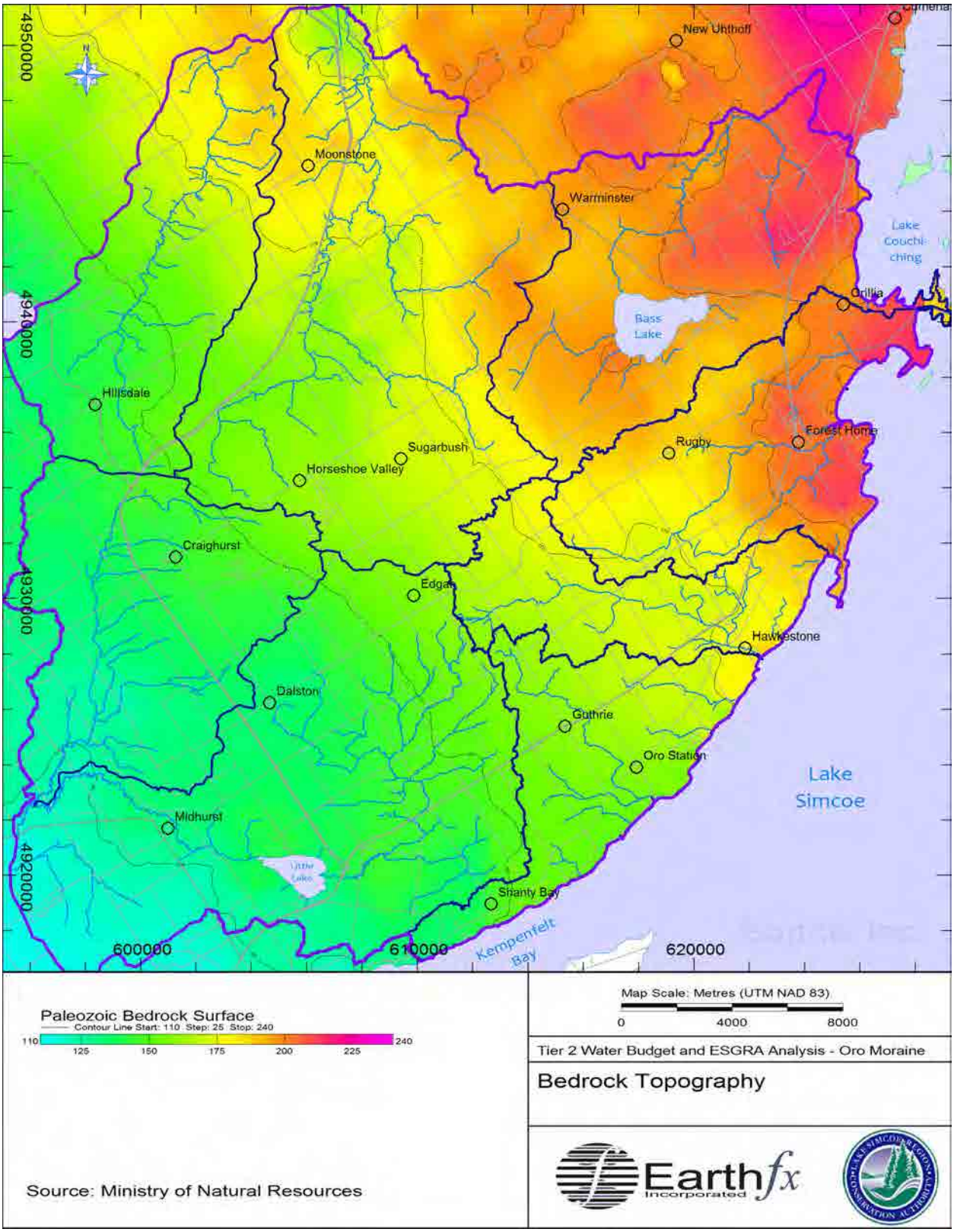

Figure 2.5: Bedrock surface topography (masl).

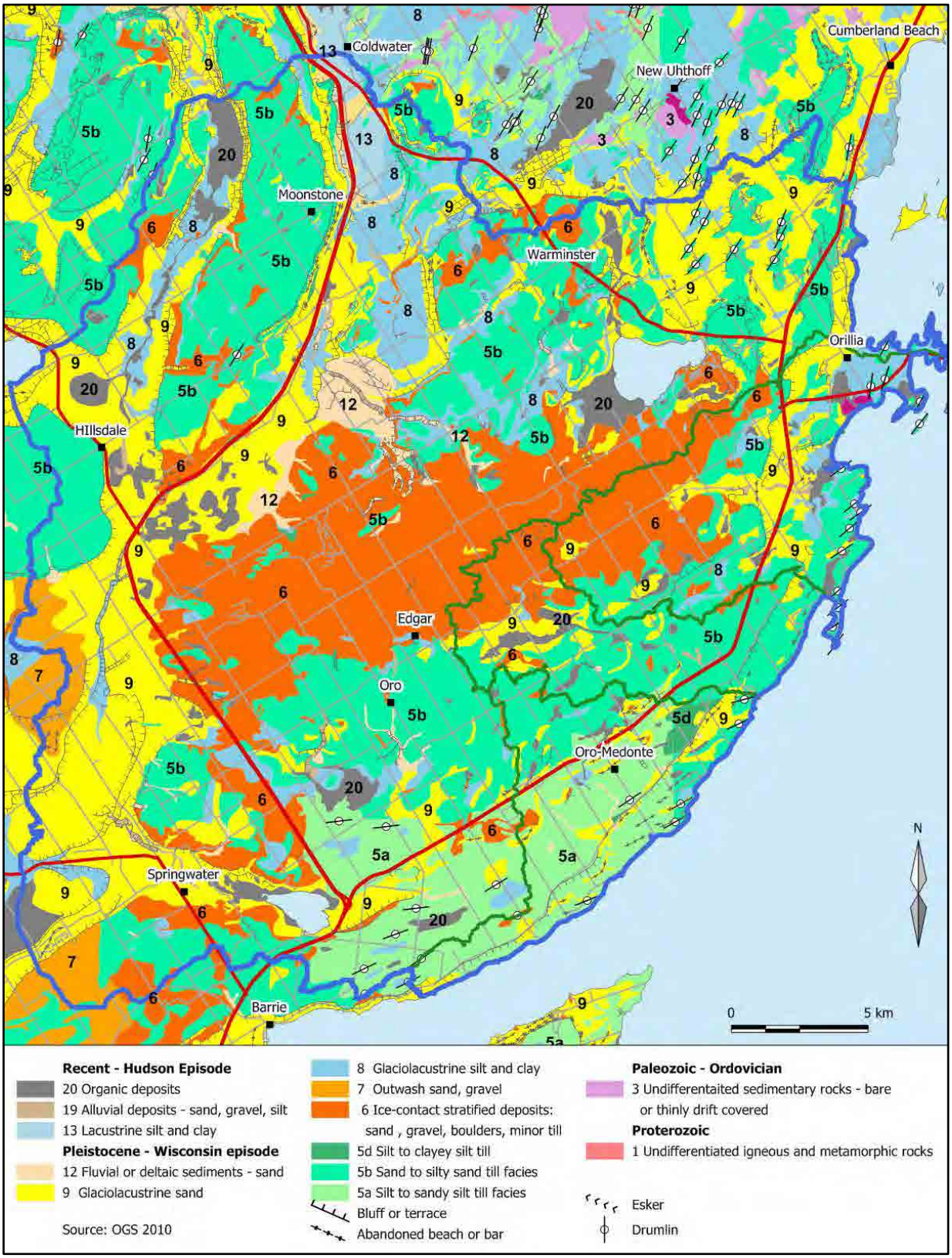

Figure 2.6: Quaternary geology (from OGS (2010)).

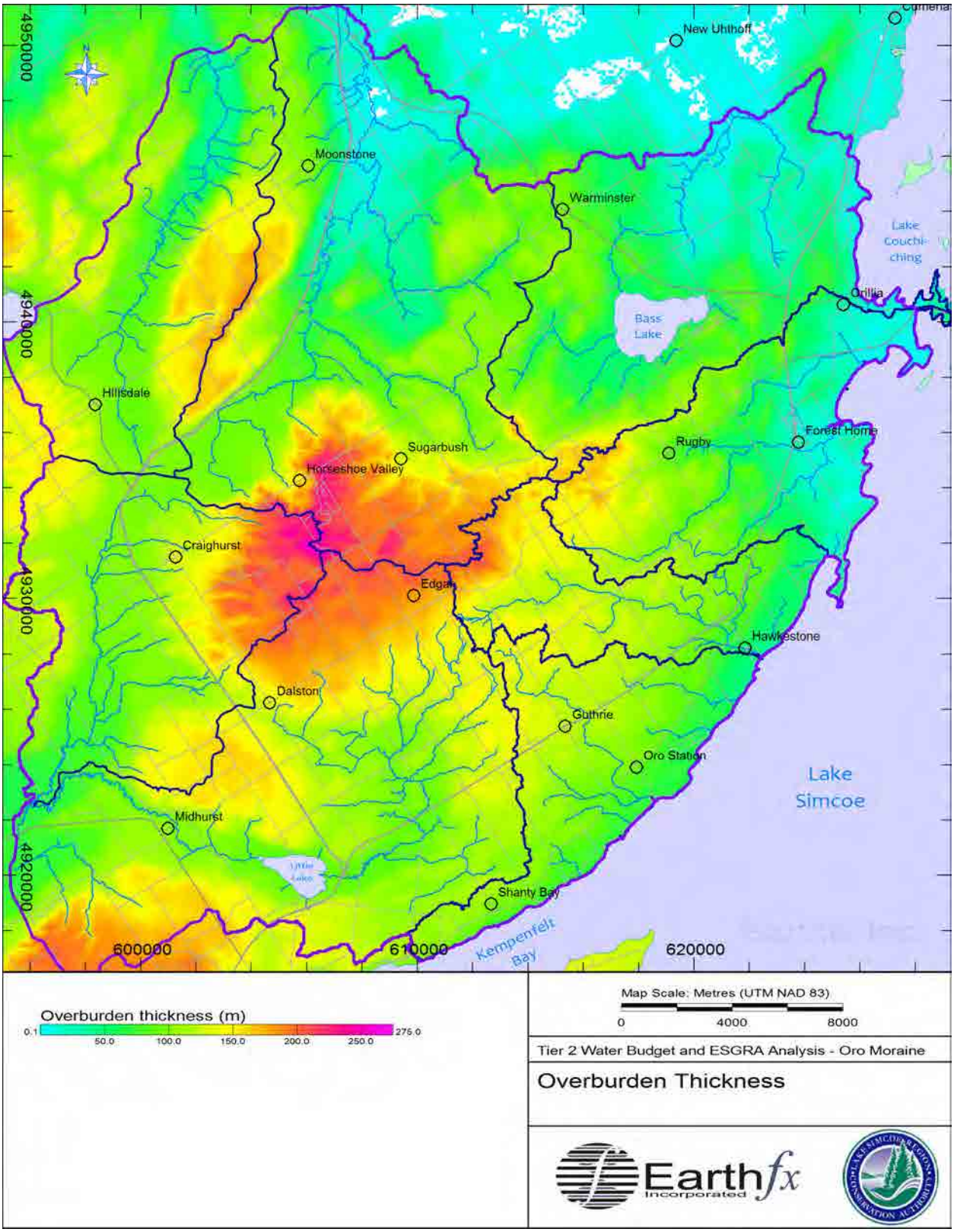

Figure 2.7: Overburden thickness (in metres).

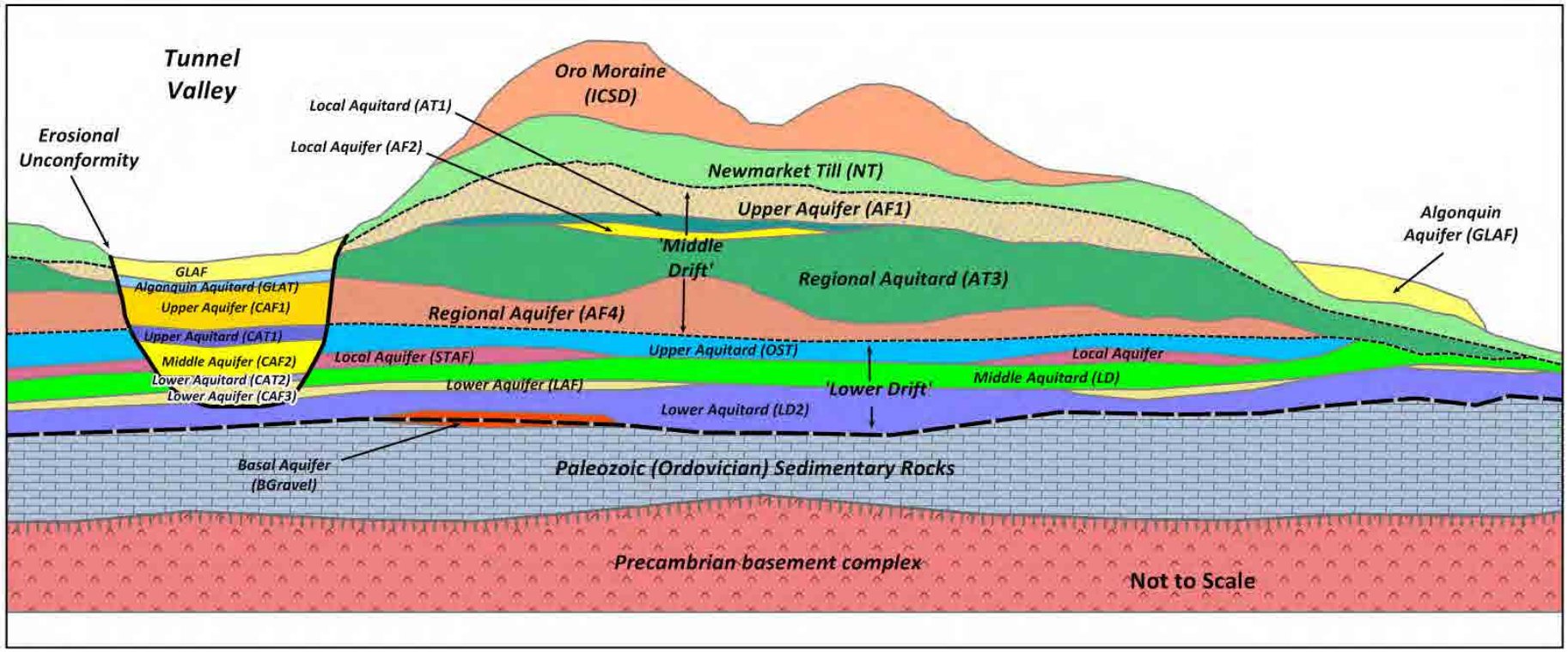

Figure 2.8: OGS conceptual hydrostratigraphic model.

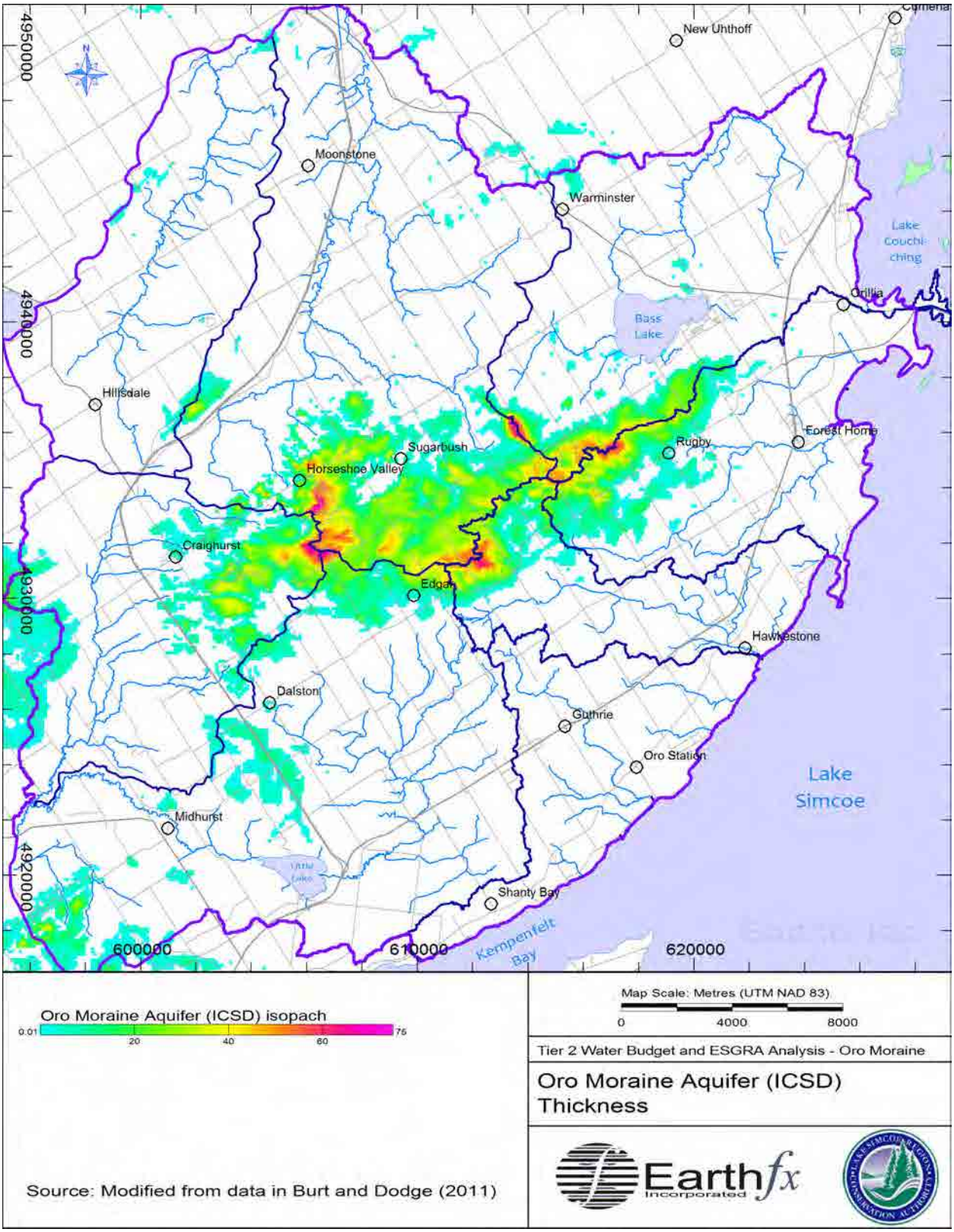

Figure 2.9: Thickness of the Oro Moraine aquifer deposits (ICSD).

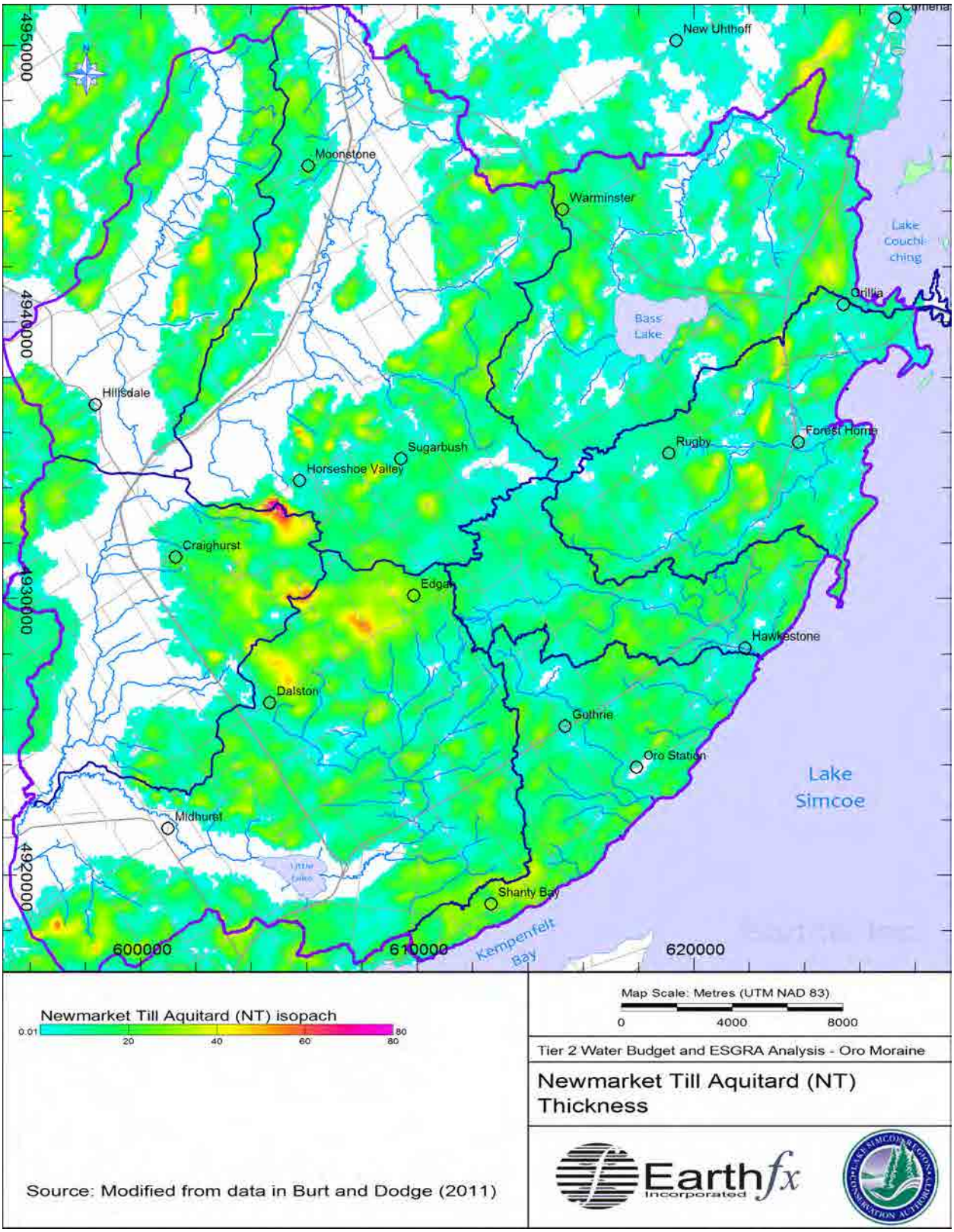

Figure 2.10: Thickness of the Newmarket Till (NT).

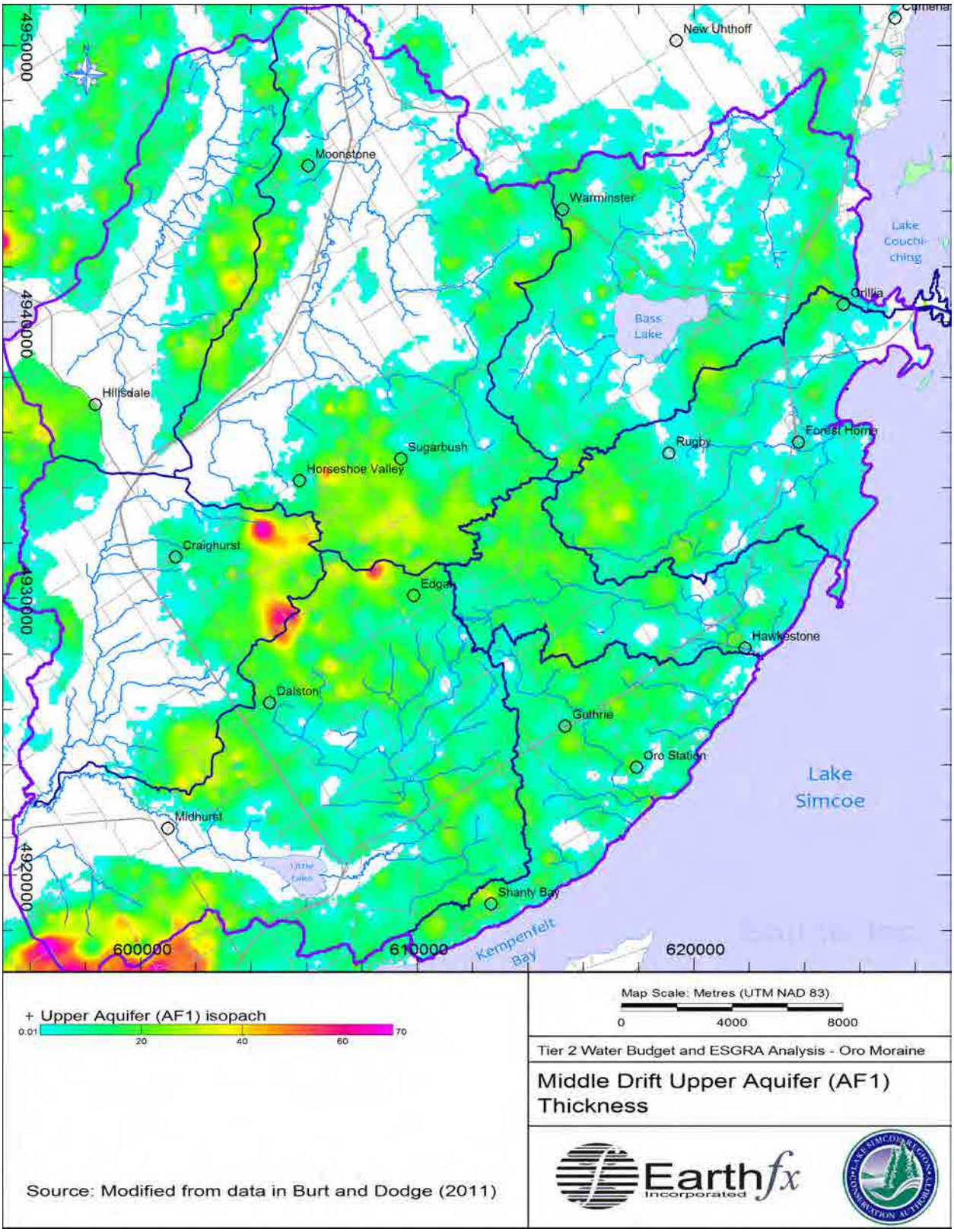

Figure 2.11: Thickness of the Middle Drift Upper Aquifer (AF1).

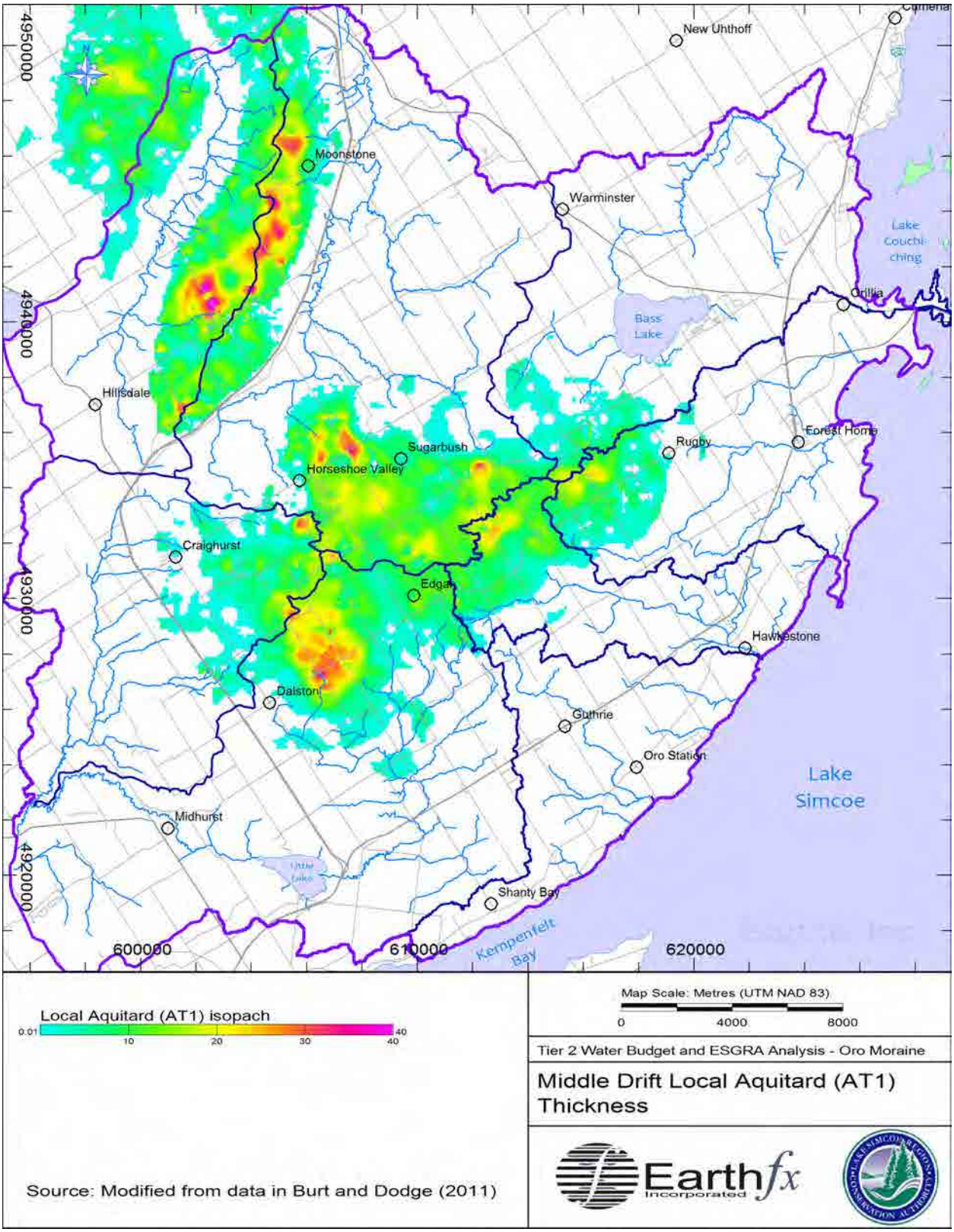

Figure 2.12: Thickness of the Middle Drift Local Aquitard (AT1).

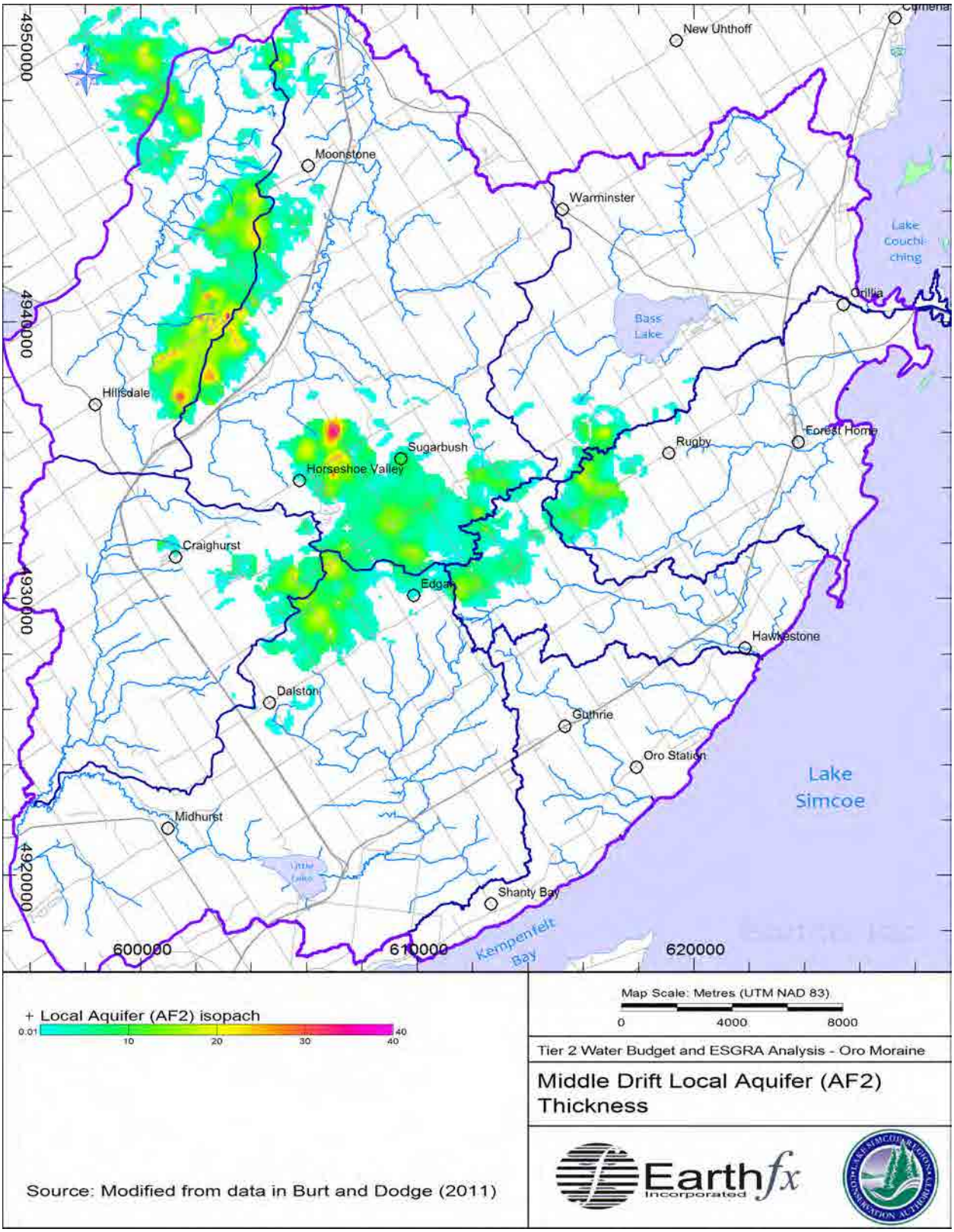

Figure 2.13: Thickness of the Middle Drift Local Aquifer (AF2).

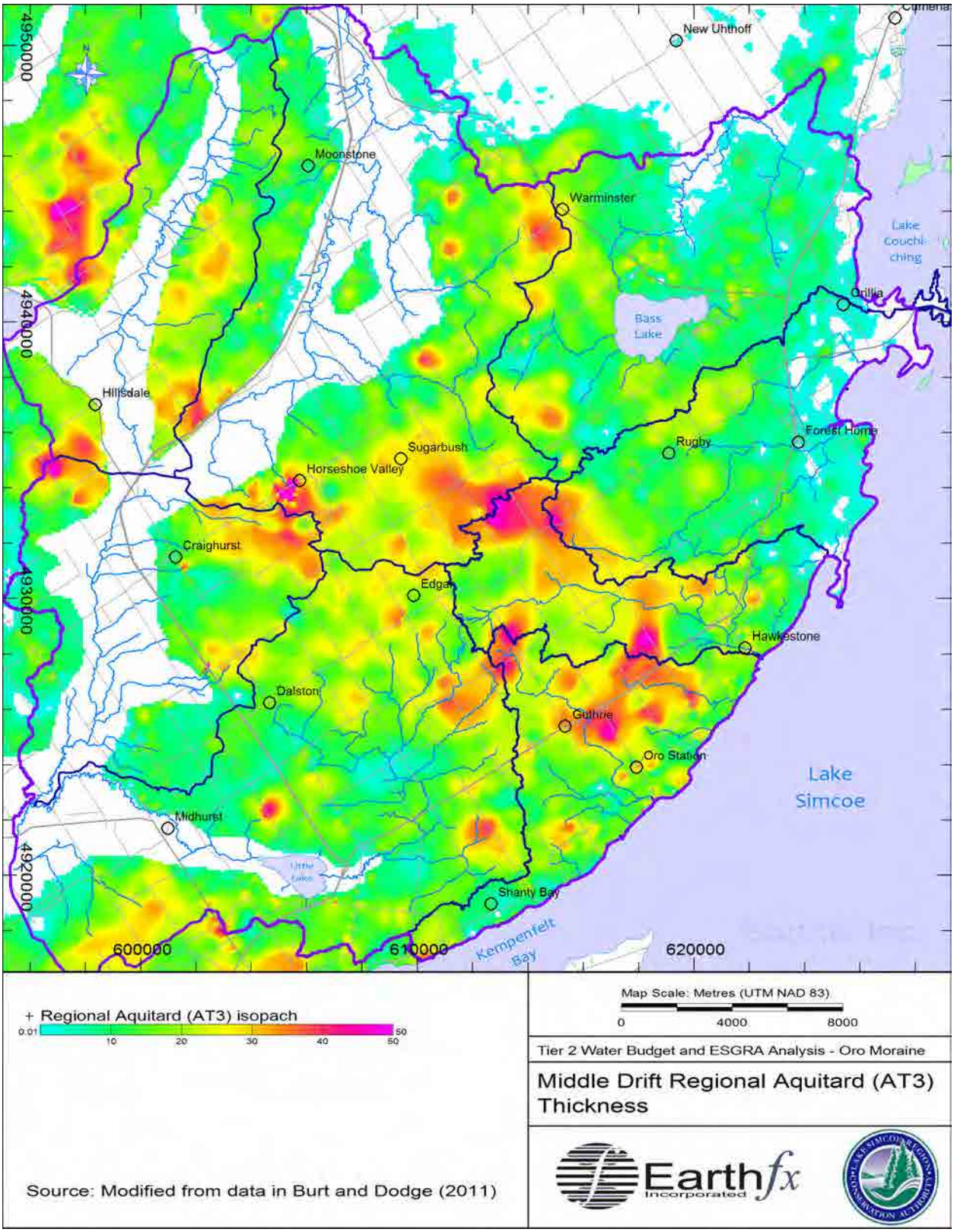

Figure 2.14: Thickness of the Middle Drift Regional Aquitard (AT3).

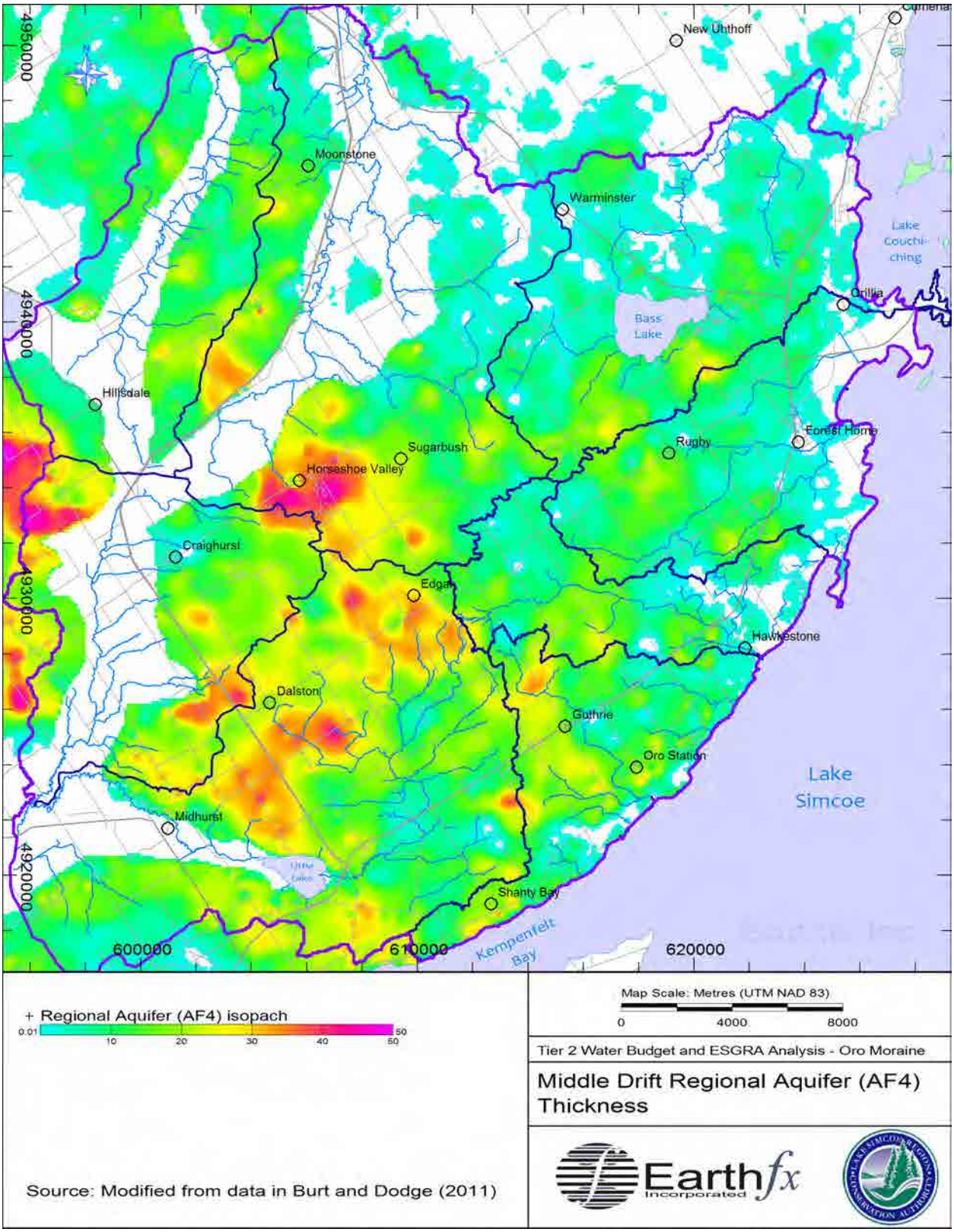

Figure 2.15: Thickness of the Middle Drift Regional Aquifer (AF4).

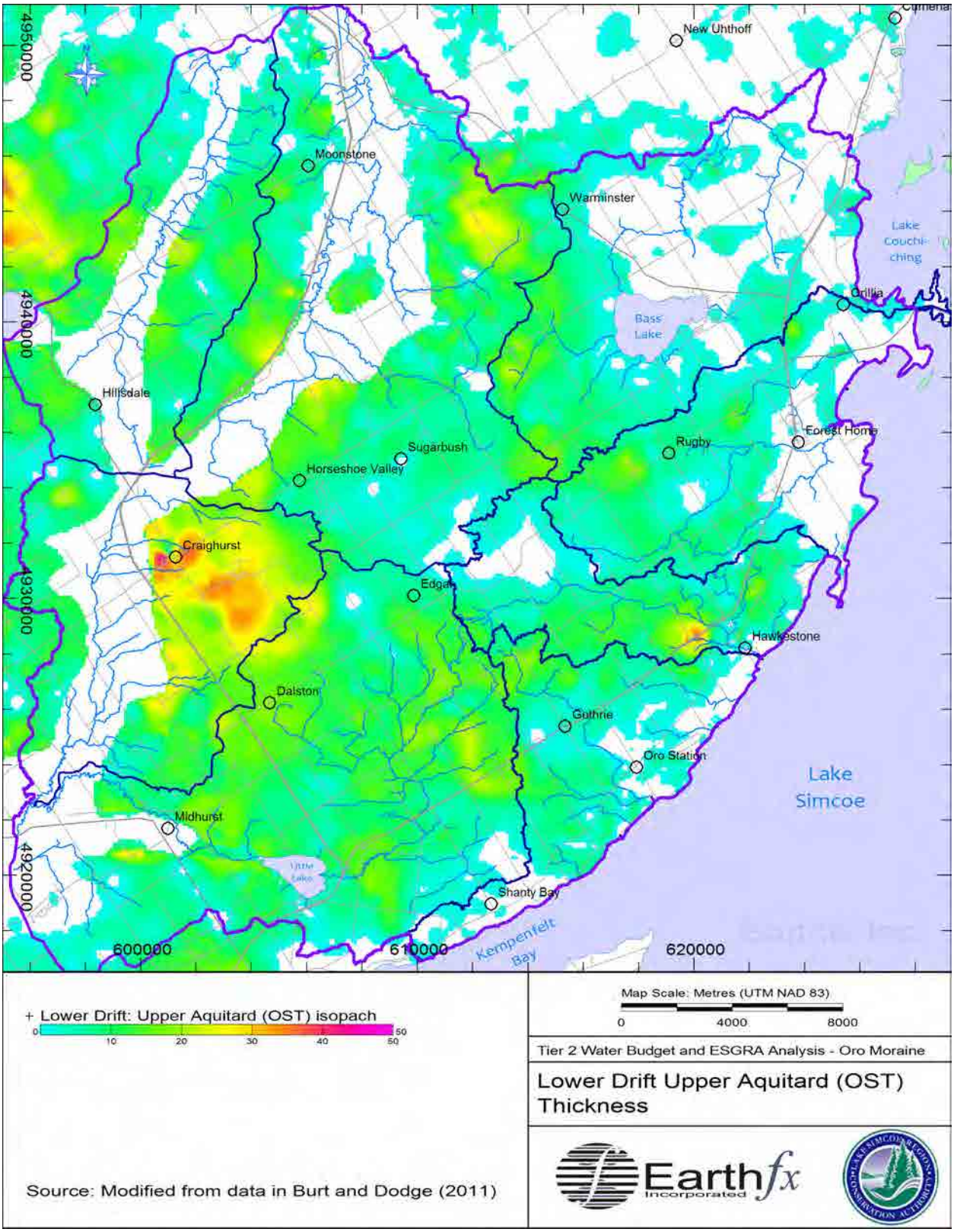

Figure 2.16: Thickness of the Lower Drift Upper Aquitard (OST).

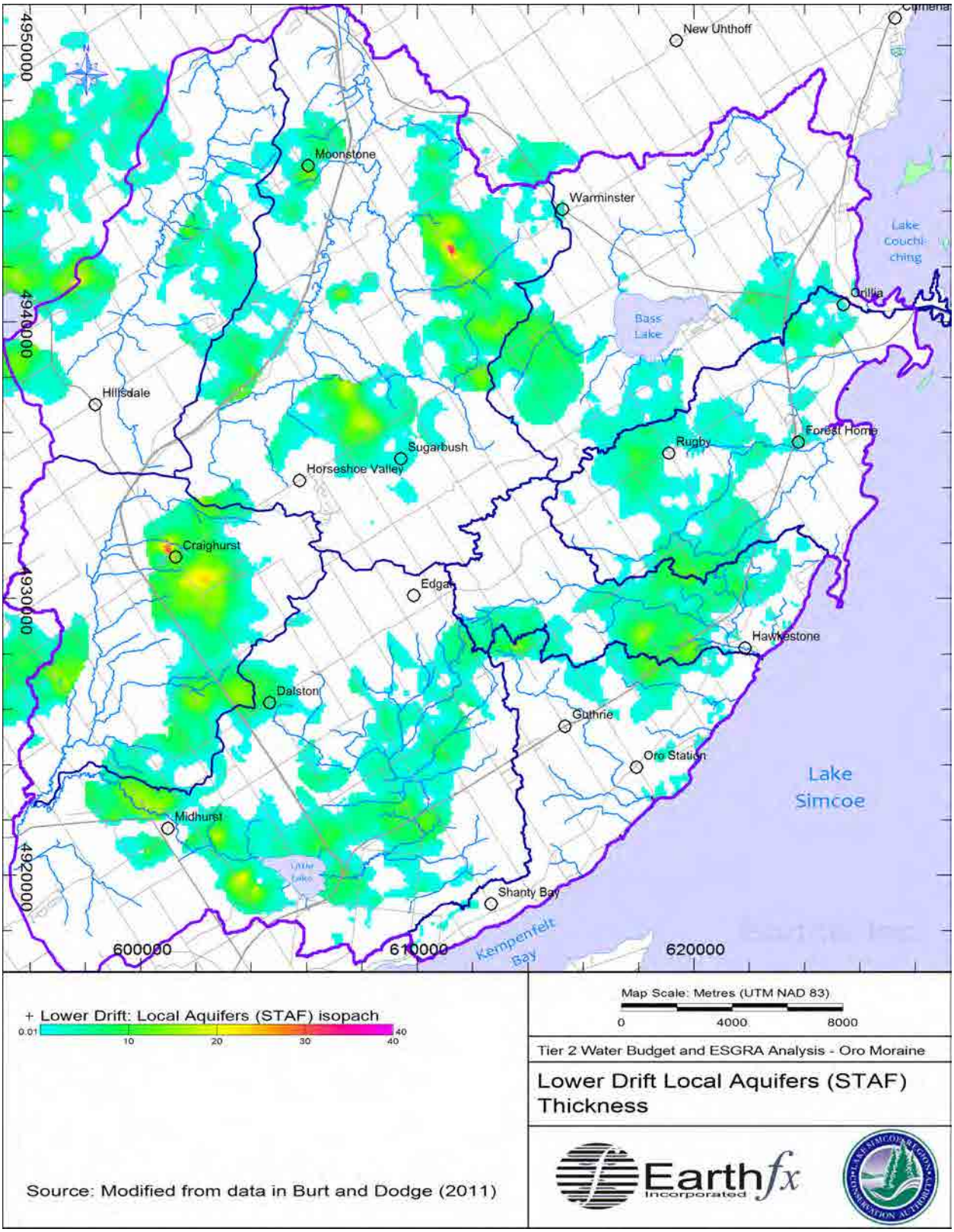

Figure 2.17: Thickness of the Lower Drift Local Aquifers (STAF).

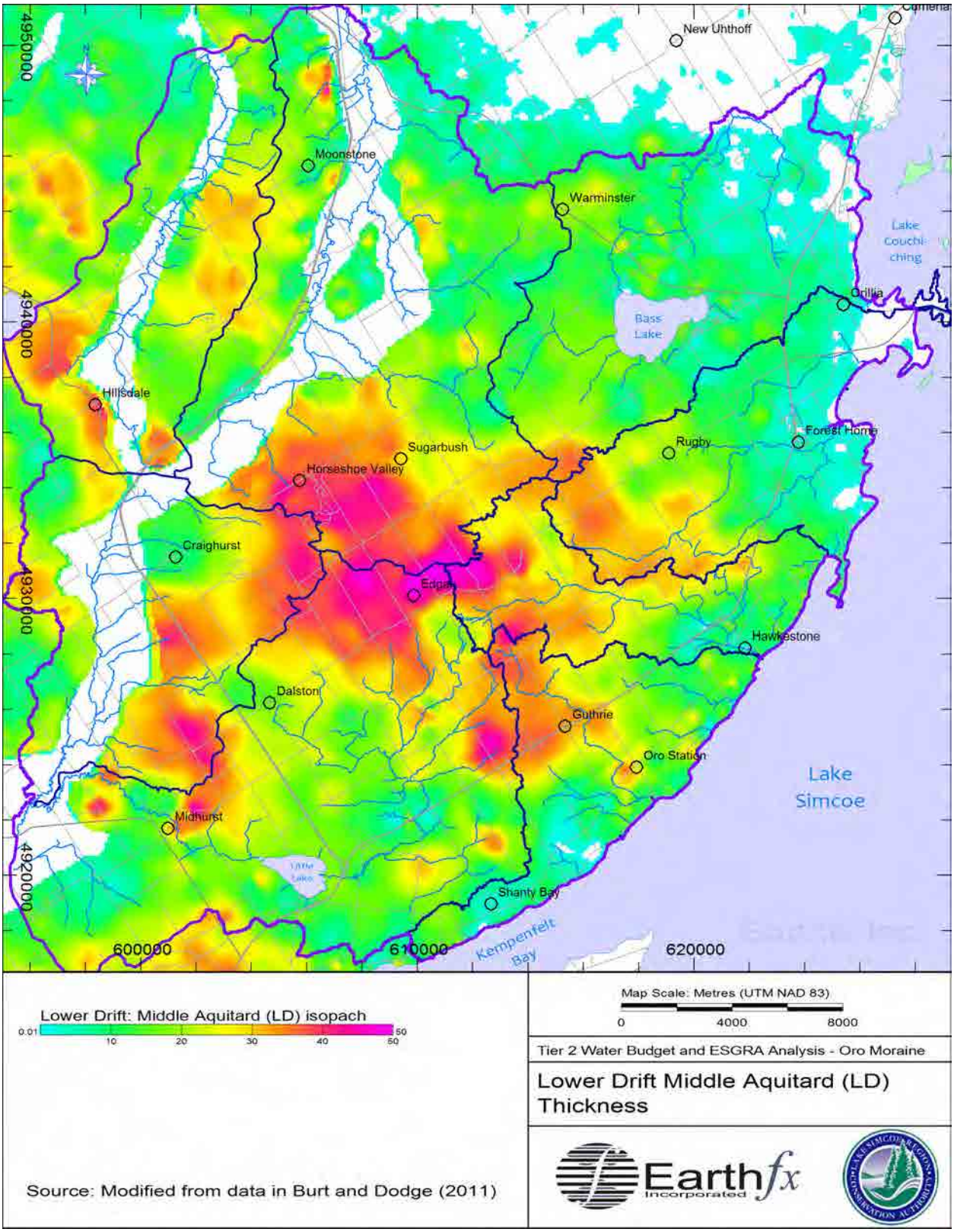

Figure 2.18: Thickness of the Lower Drift Middle Aquitard (LD).

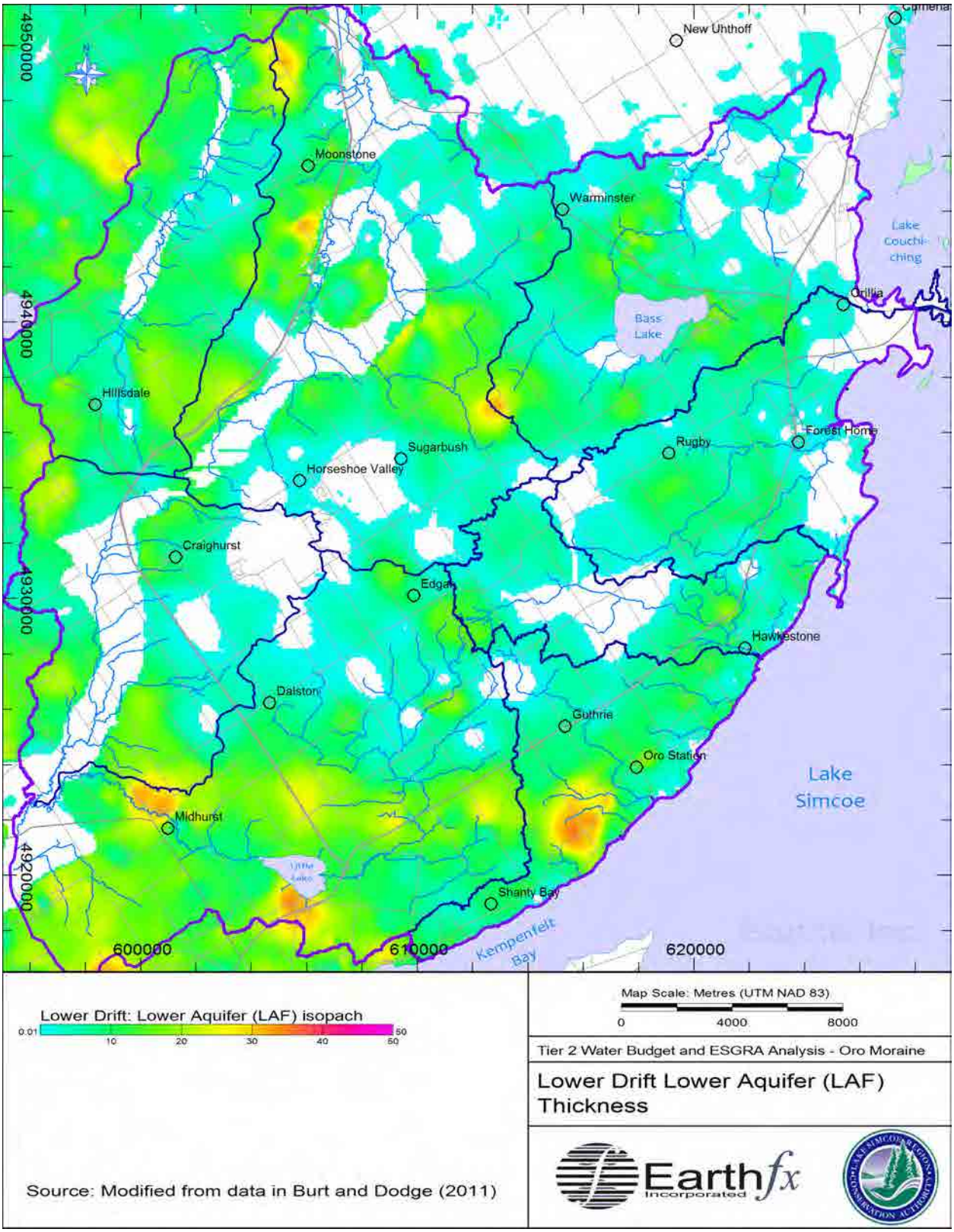

Figure 2.19: Thickness of the Lower Drift Lower Aquifer (LAF).

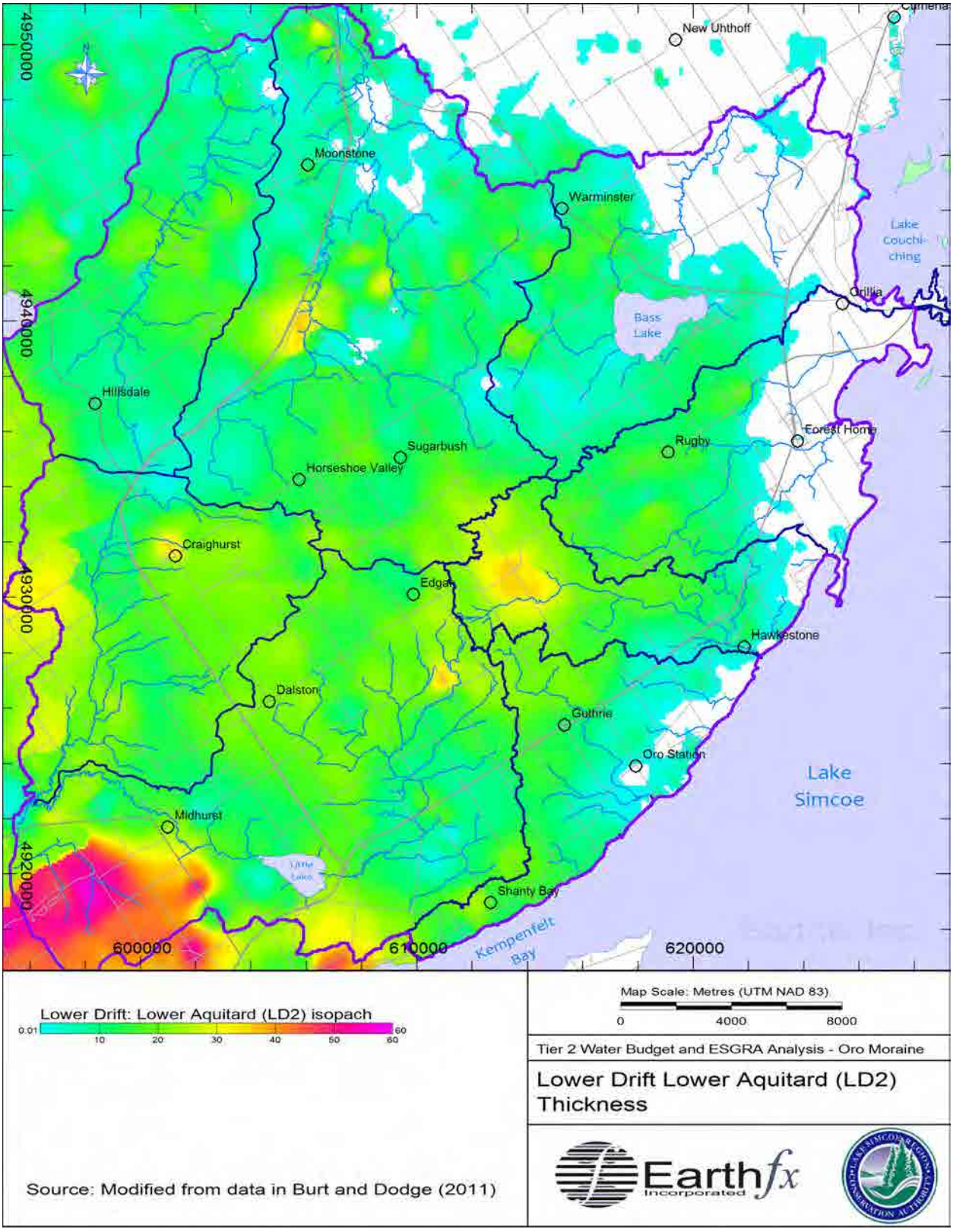

Figure 2.20: Thickness of the Lower Drift Lower Aquitard (LD2).

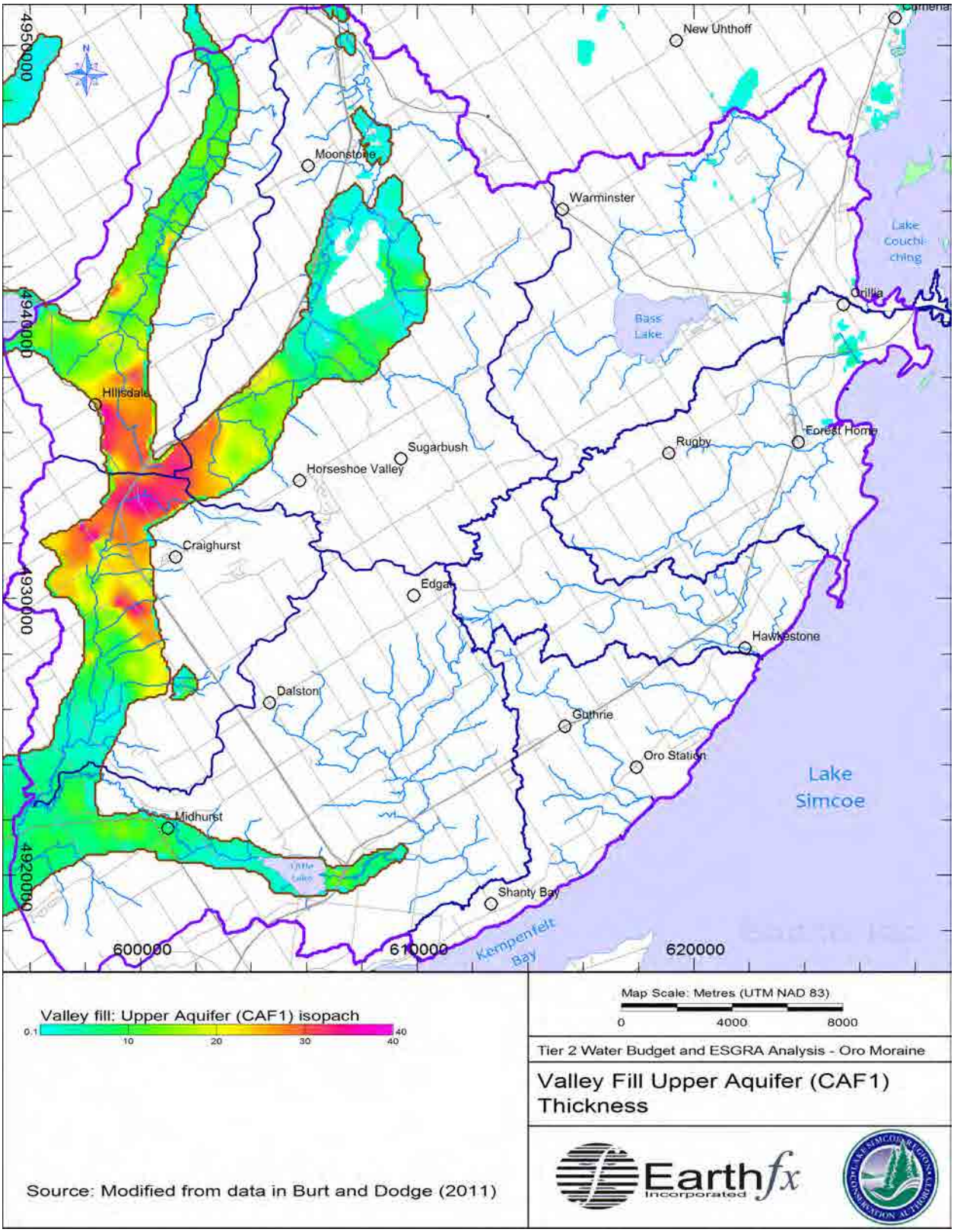

Figure 2.21: Thickness of the Valley Fill Upper Aquifer (CAF1).

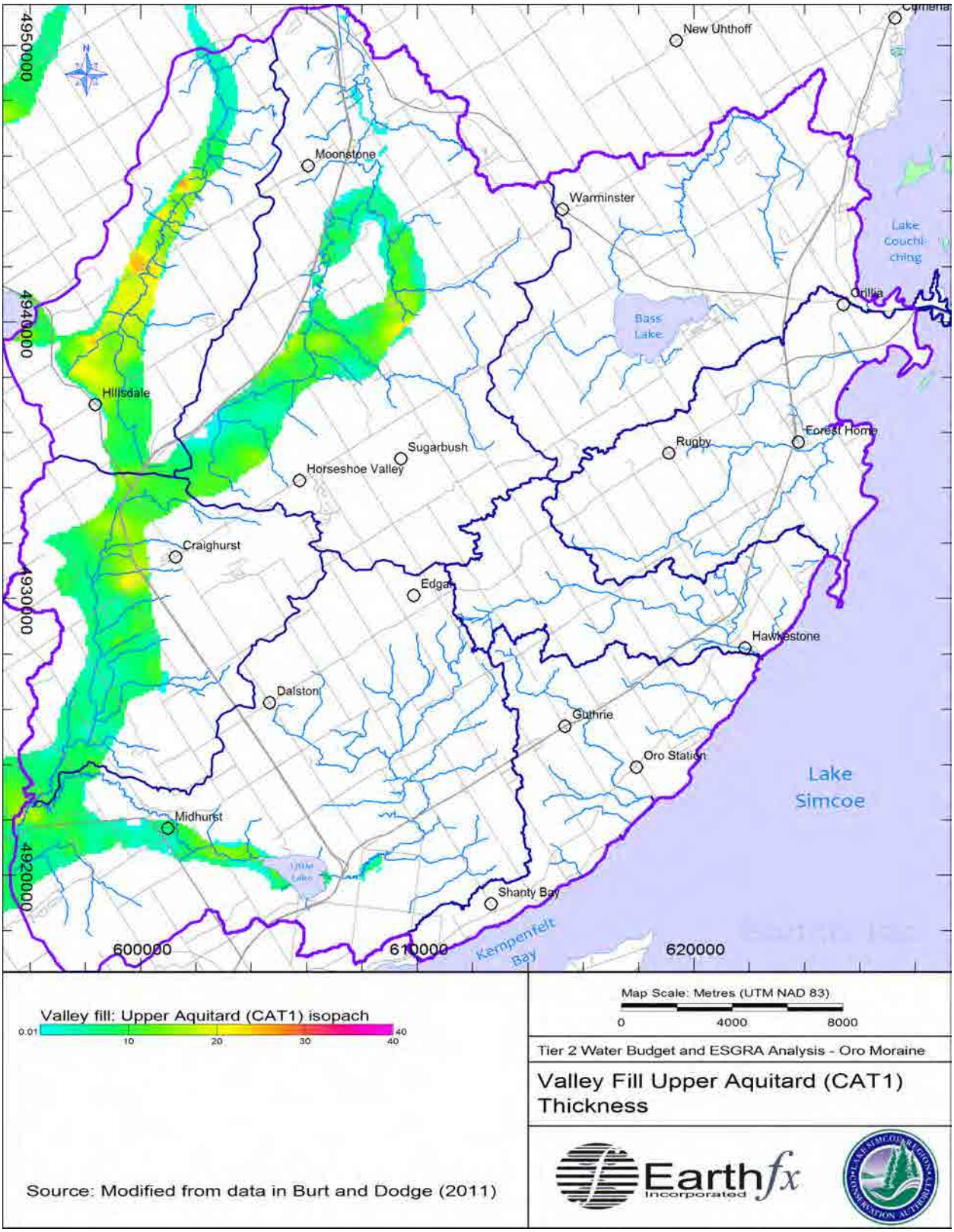

Figure 2.22: Thickness of the Valley Fill Upper Aquitard (CAT1).

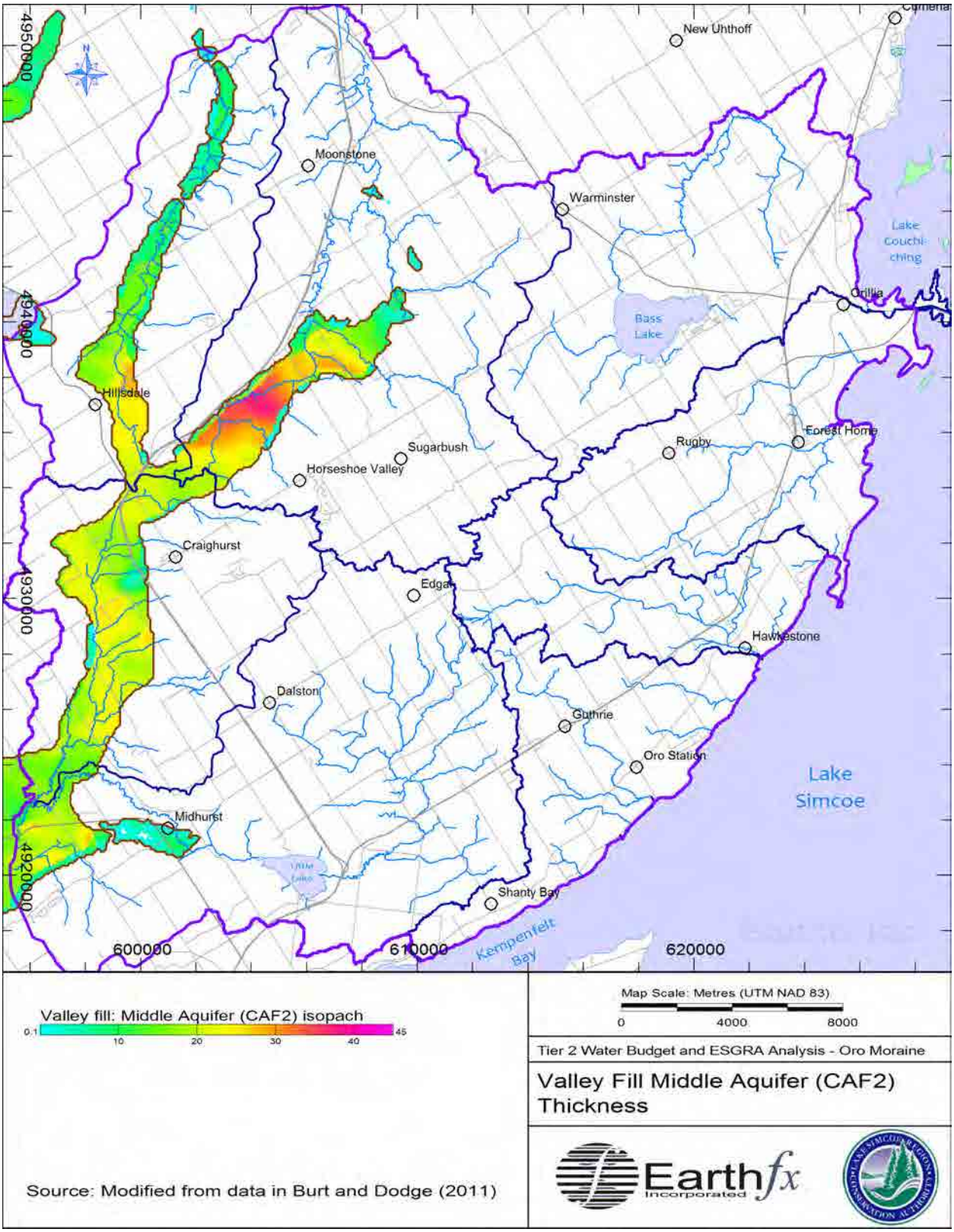

Figure 2.23: Thickness of the Valley Fill Middle Aquifer (CAF2).

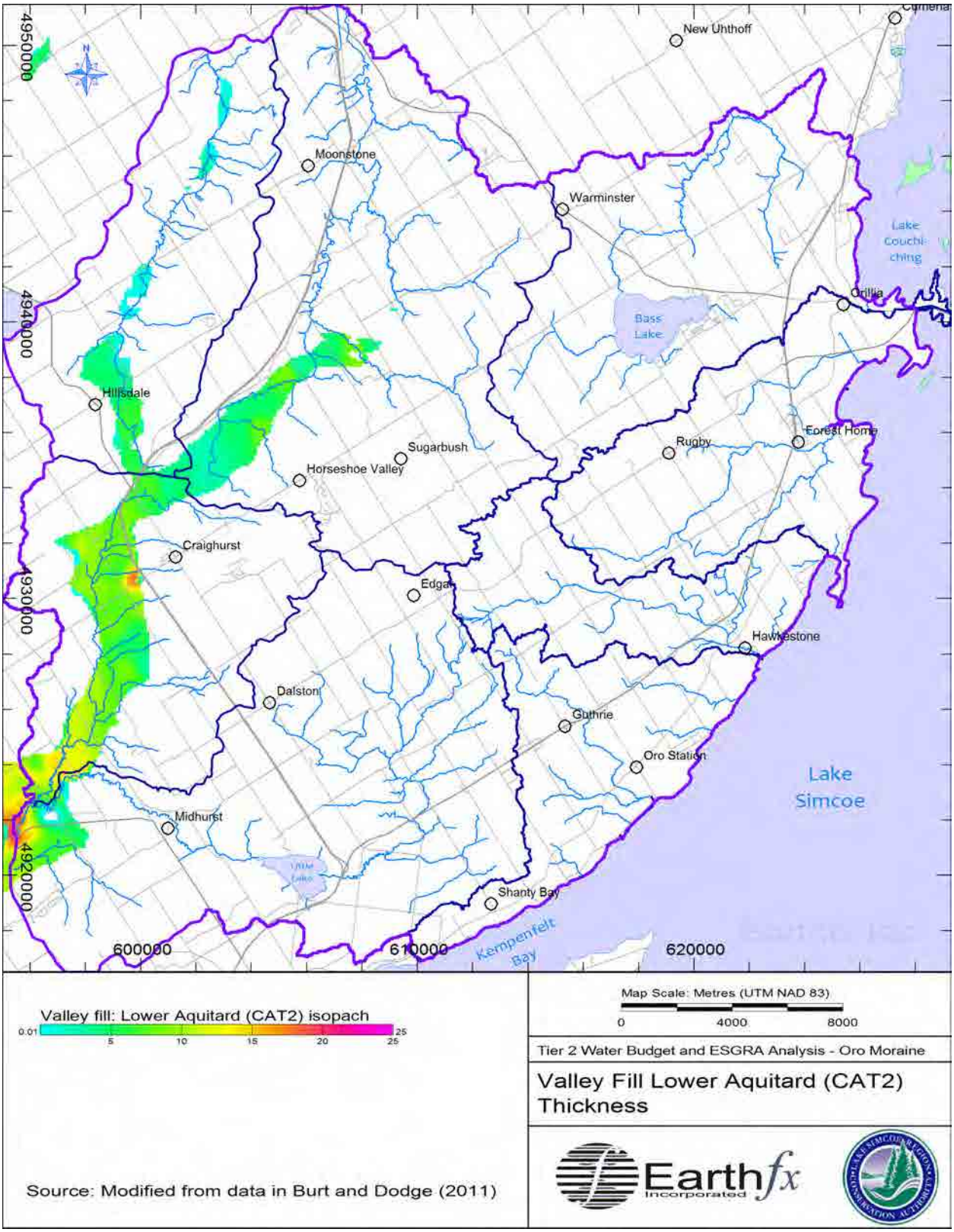

Figure 2.24: Thickness of the Valley Fill Lower Aquitard (CAT2).

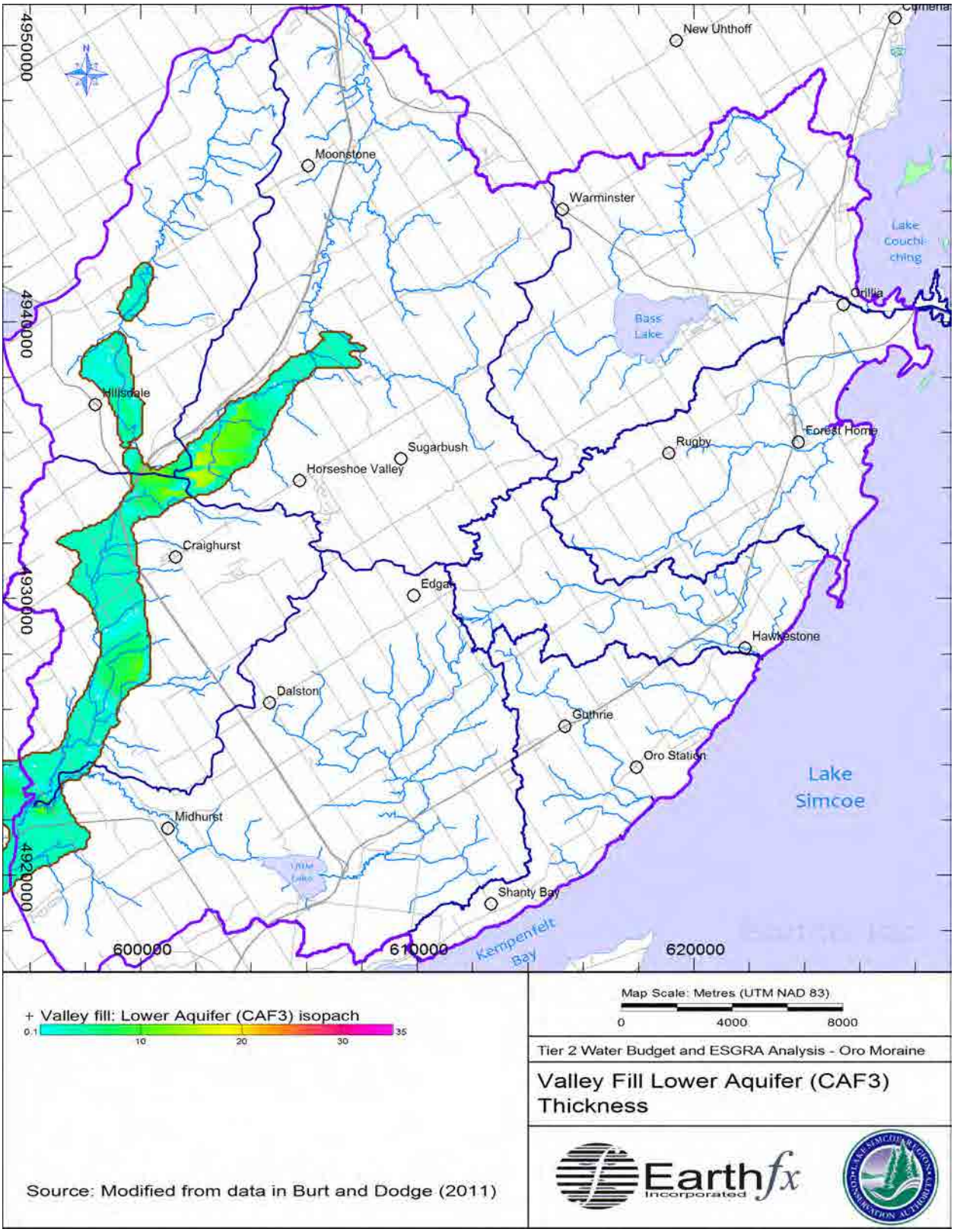

Figure 2.25: Thickness of the Valley Fill Lower Aquifer (CAF3).

Figure 2.26: Cross section locations.

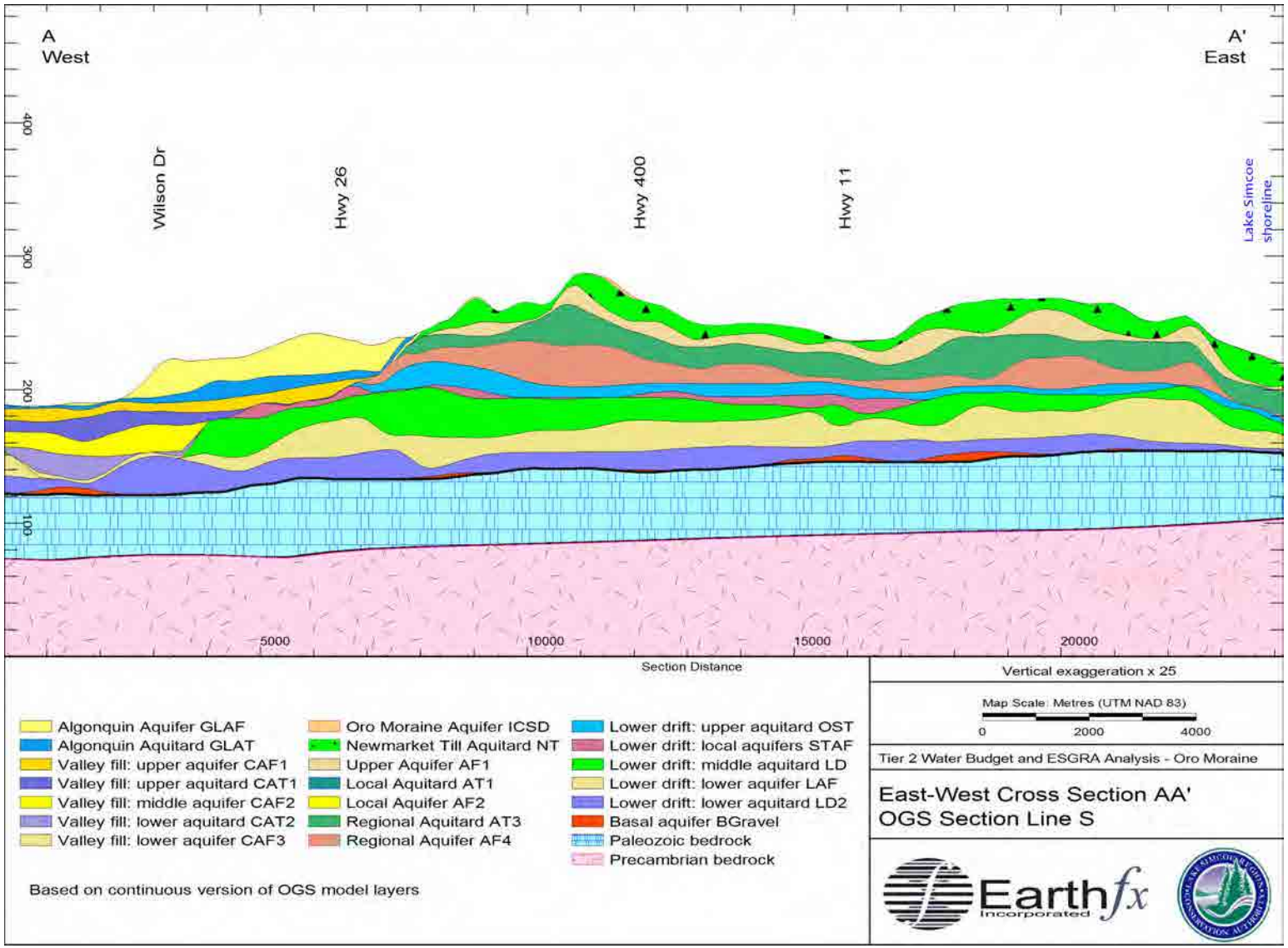

Figure 2.27: Cross section A-A'.

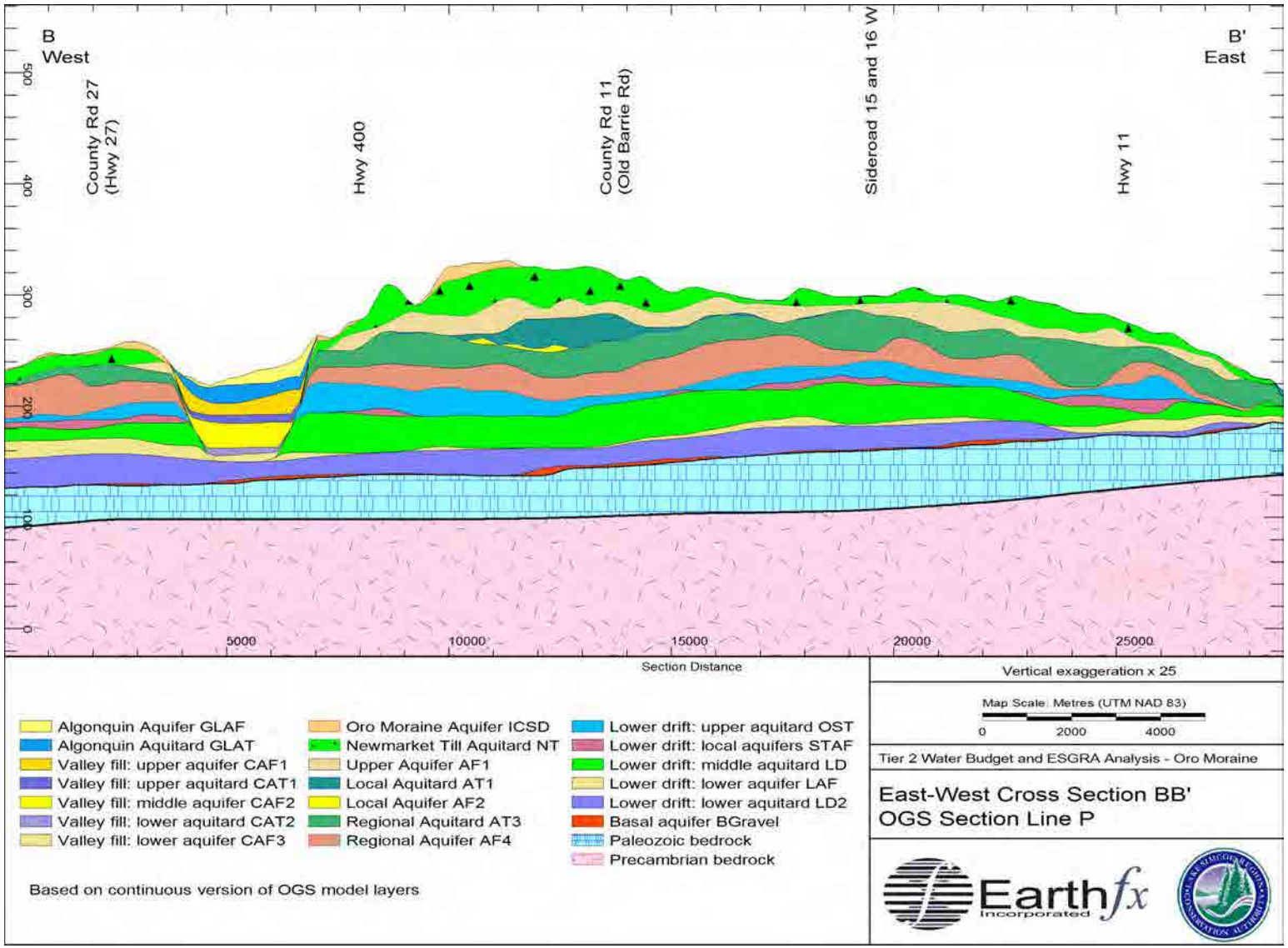

Figure 2.28: Cross section B-B'.

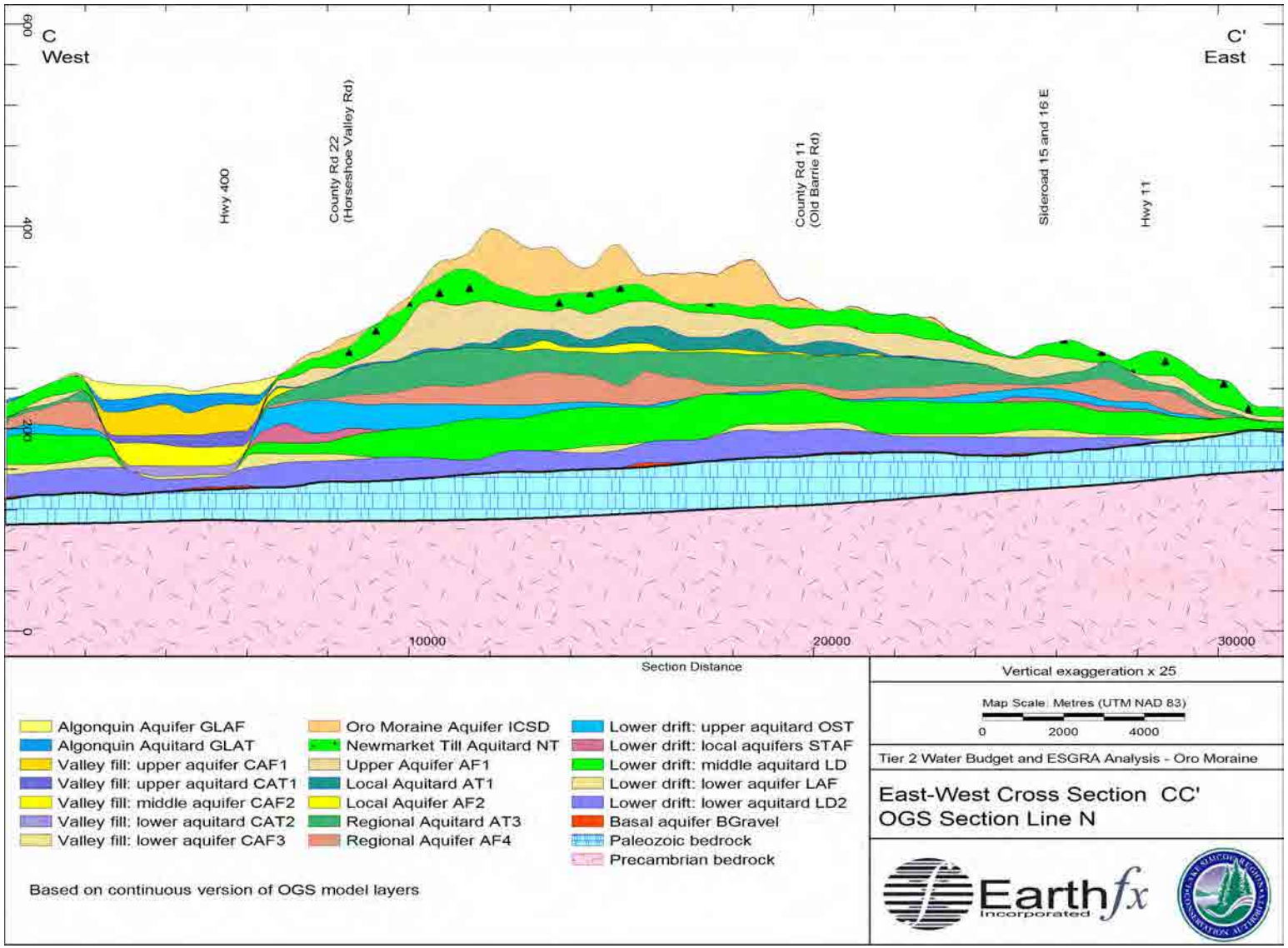

Figure 2.29: Cross section C-C'.

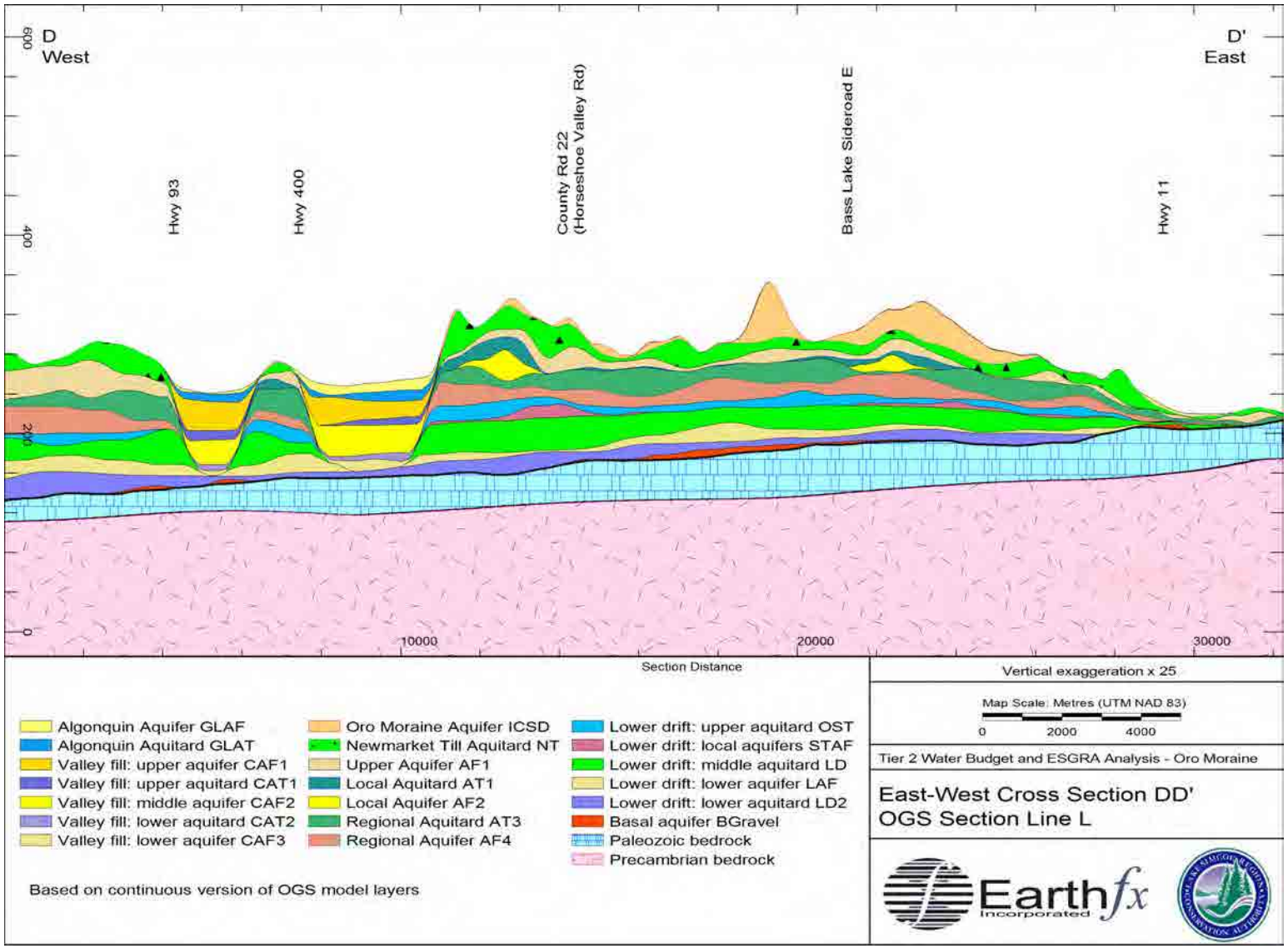

Figure 2.30: Cross section D-D'.

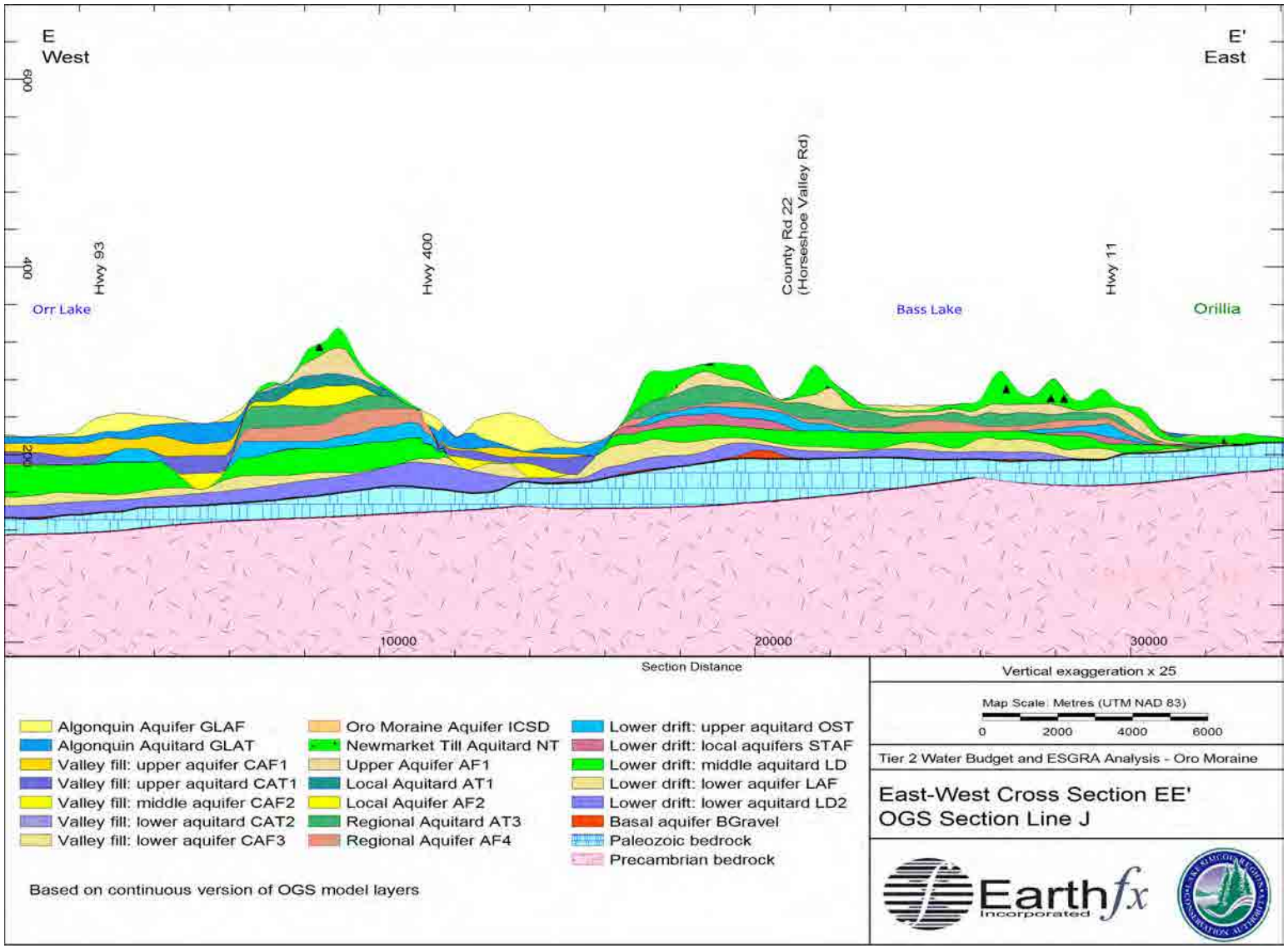

Figure 2.31: Cross section E-E'.

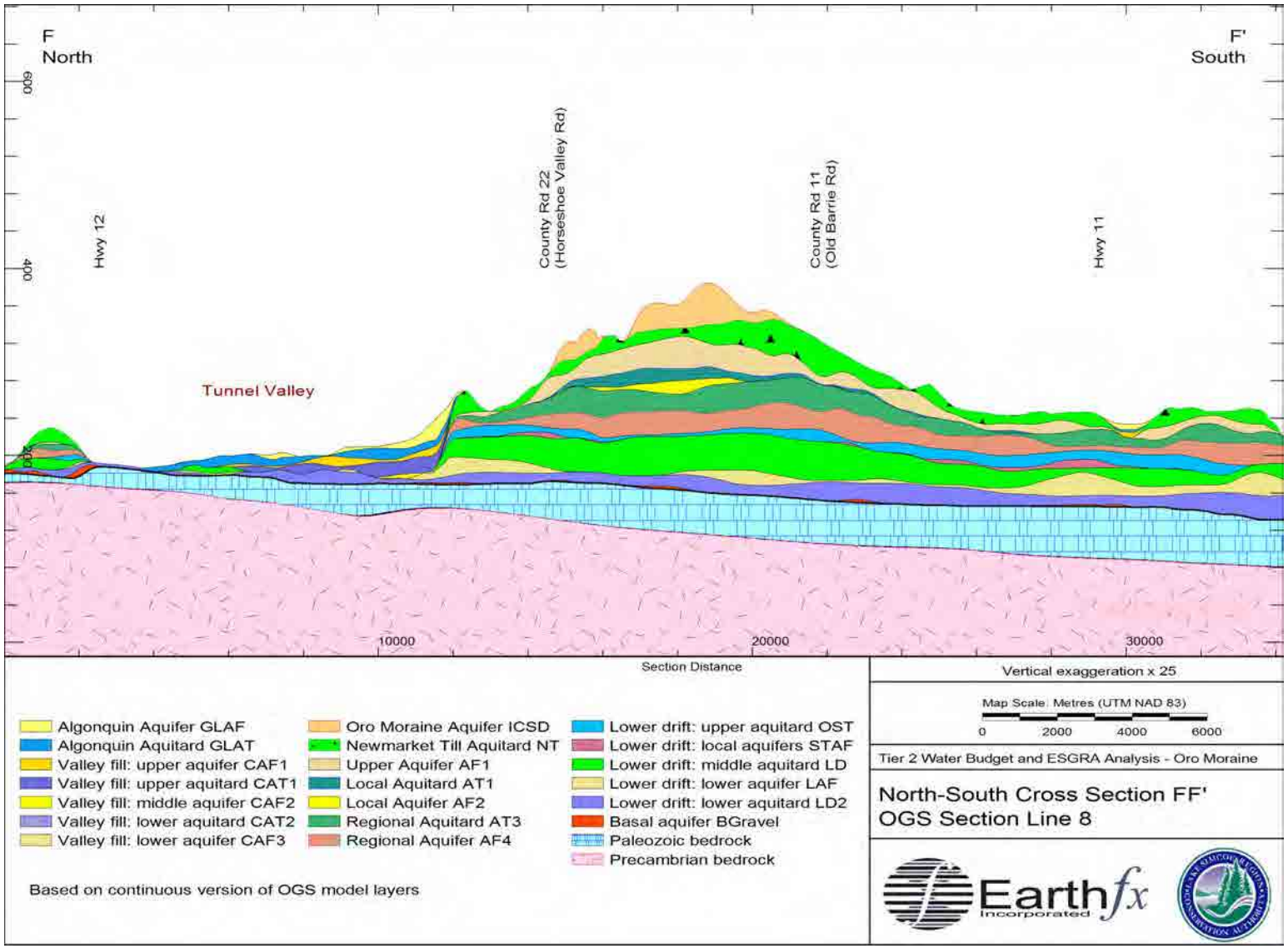

Figure 2.32: Cross section F-F'.

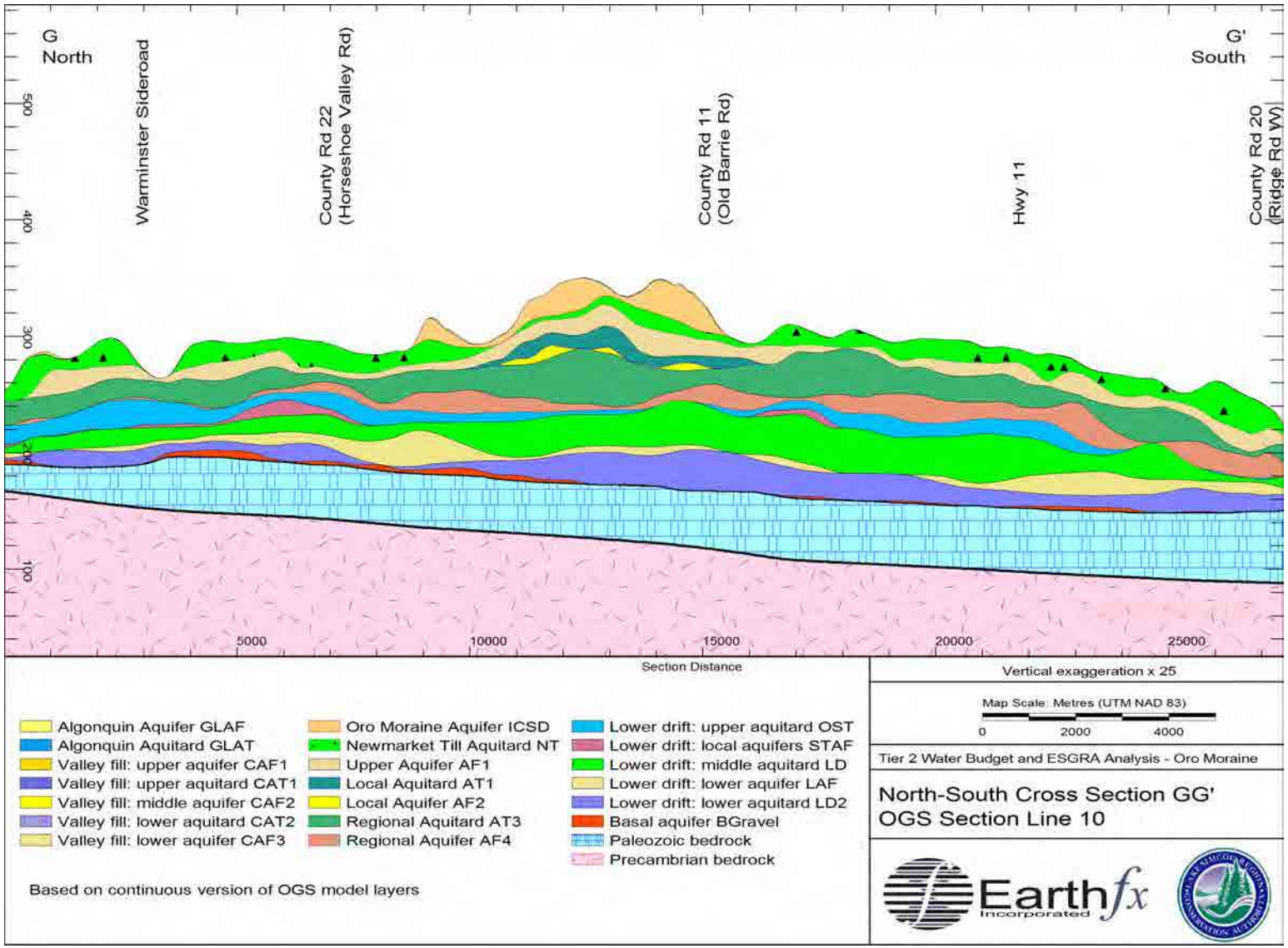

Figure 2.33: Cross section G-G'.

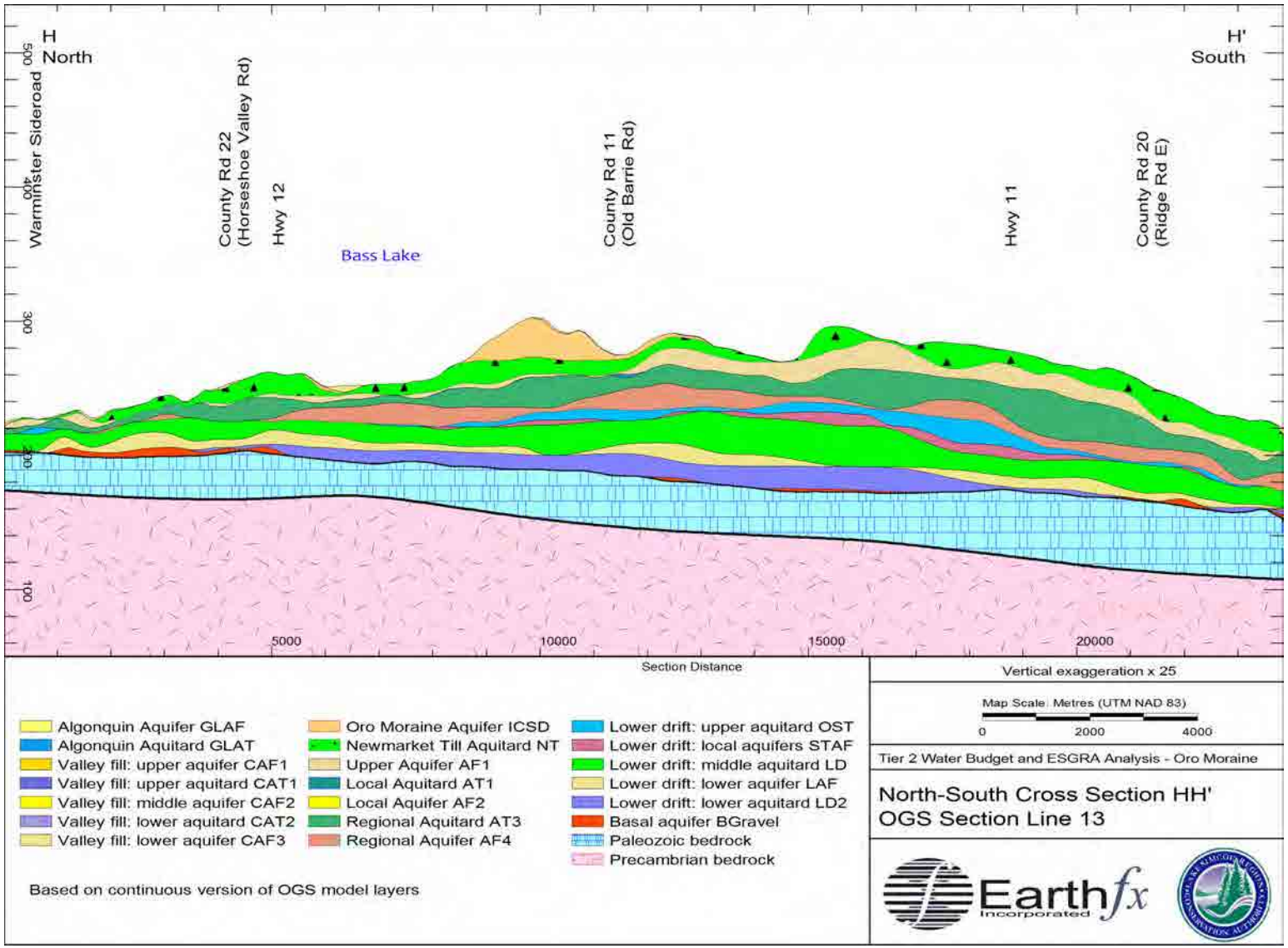

Figure 2.34: Cross section H-H'.

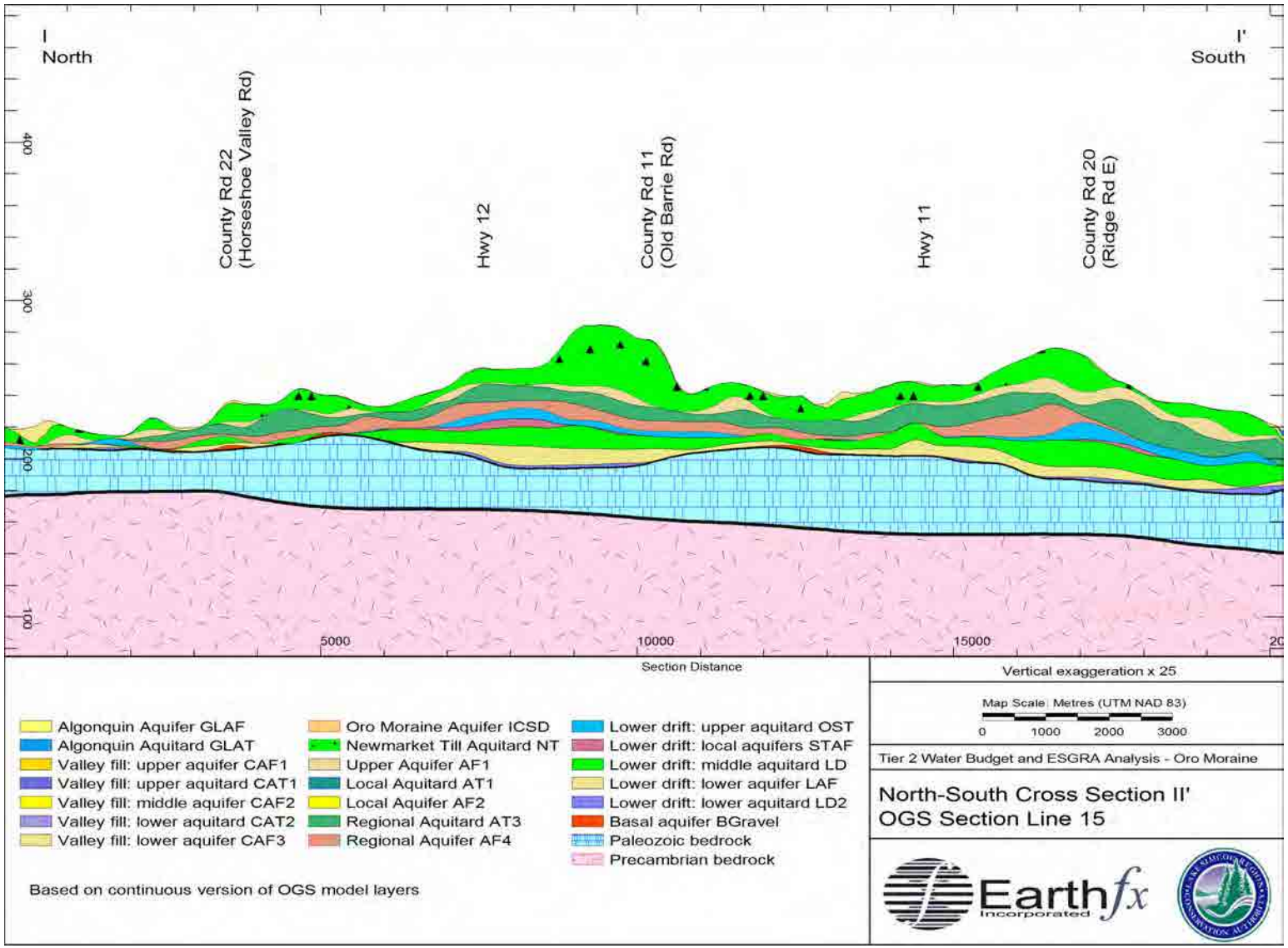

Figure 2.35: Cross section I-I'.

Figure 2.36: Location of active and inactive Environment Canada climate stations.

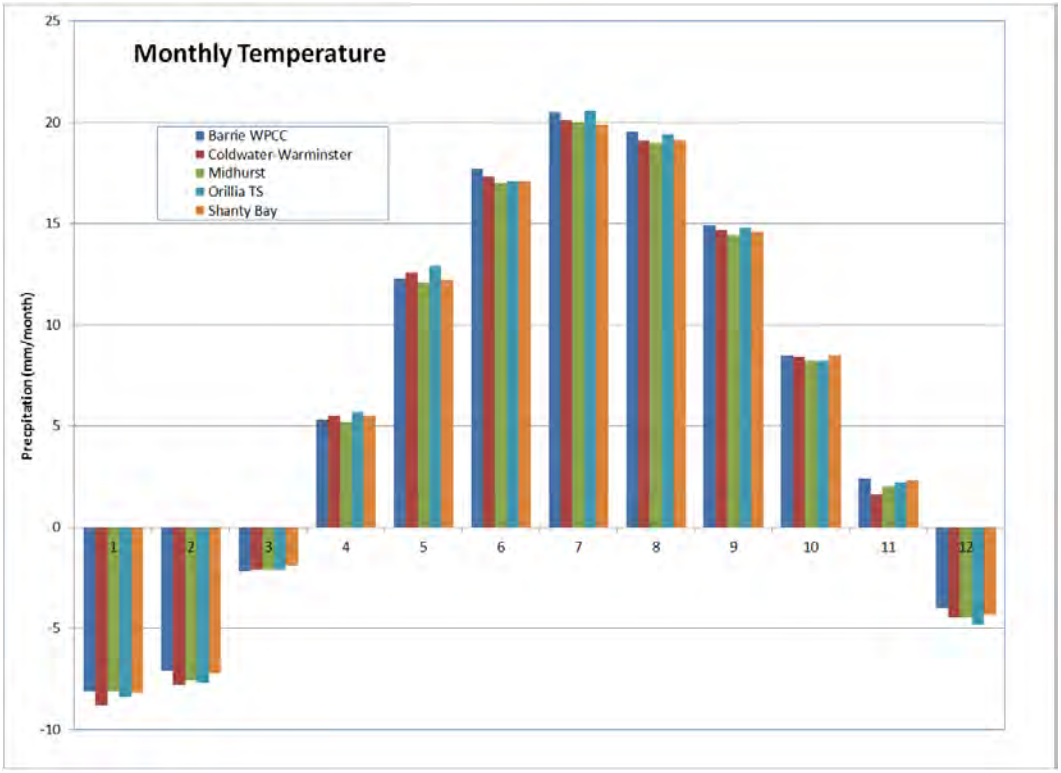

Figure 2.37: Monthly average temperature for stations in the model area (climate normals from Environment Canada (1971-2000)).

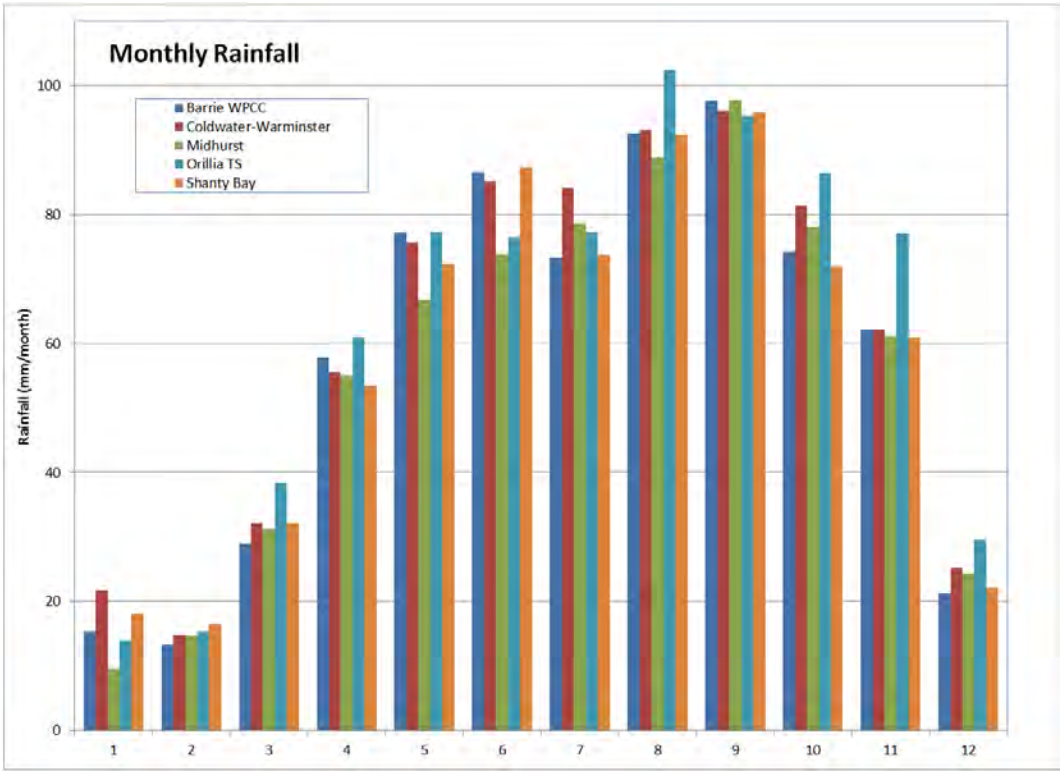

Figure 2.38: Monthly rainfall for stations in the model area (climate normals from Environment Canada (1971-2000)).

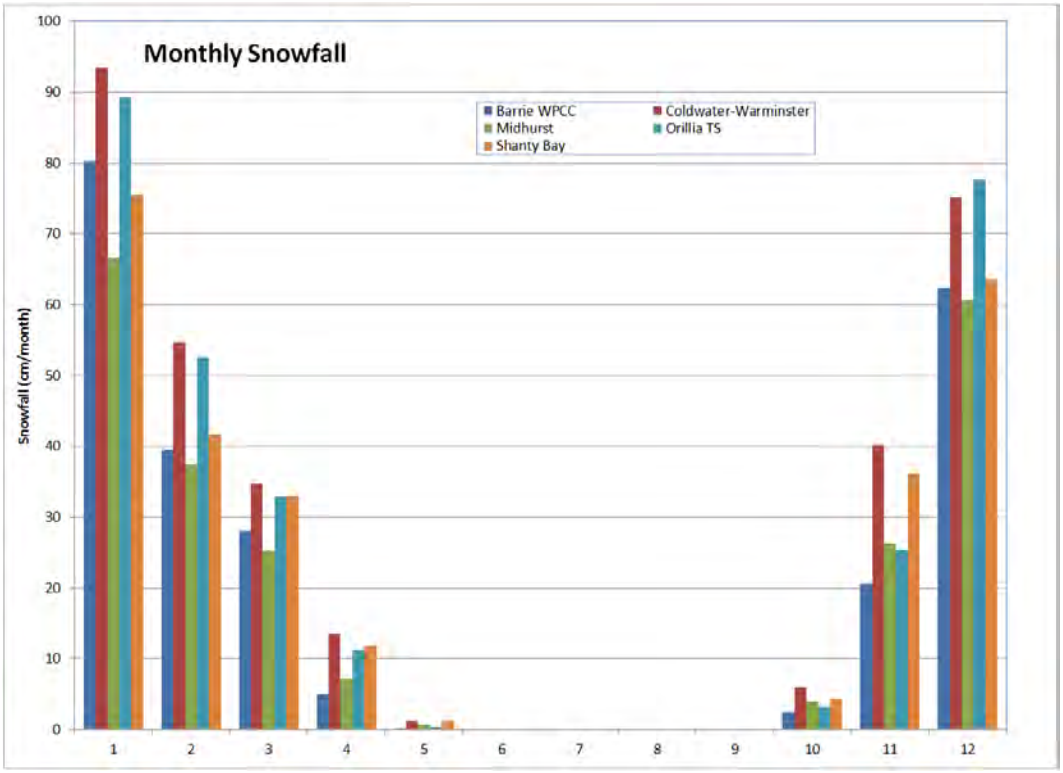

Figure 2.39: Monthly snowfall for stations in the model area (climate normals from Environment Canada (1971-2000)).

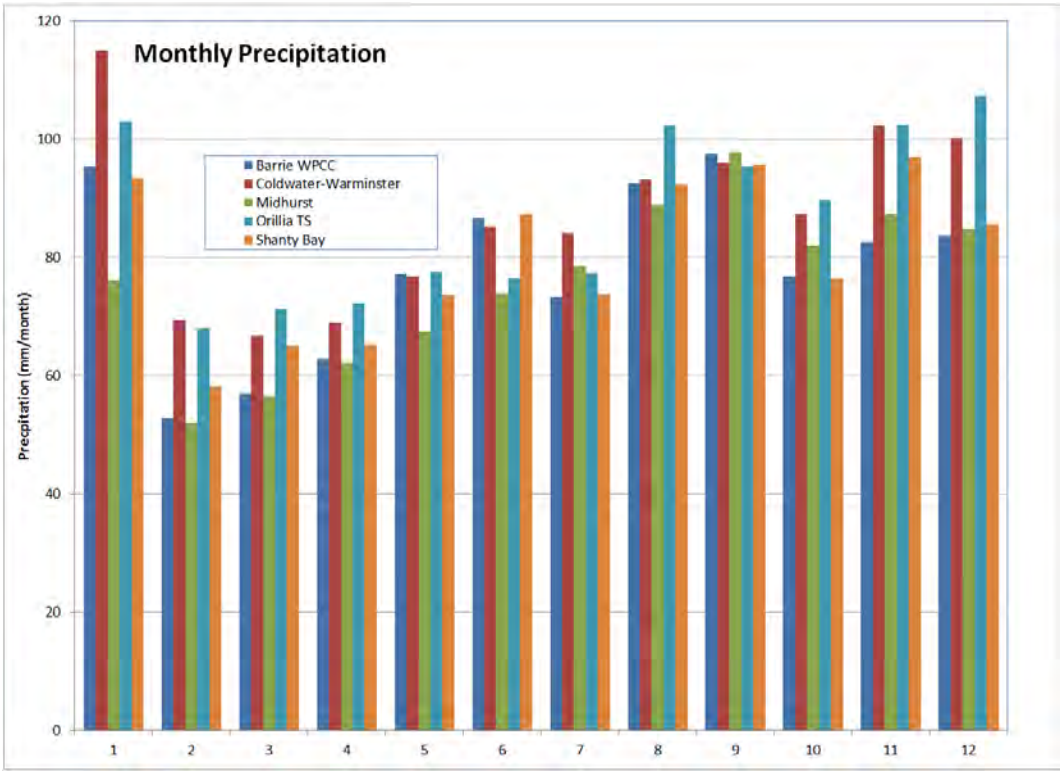

Figure 2.40: Monthly precipitation for stations in the study area (climate normals from Environment Canada (1971-2000)).

Figure 2.41: Surface water features and WSC streamflow gauging stations.

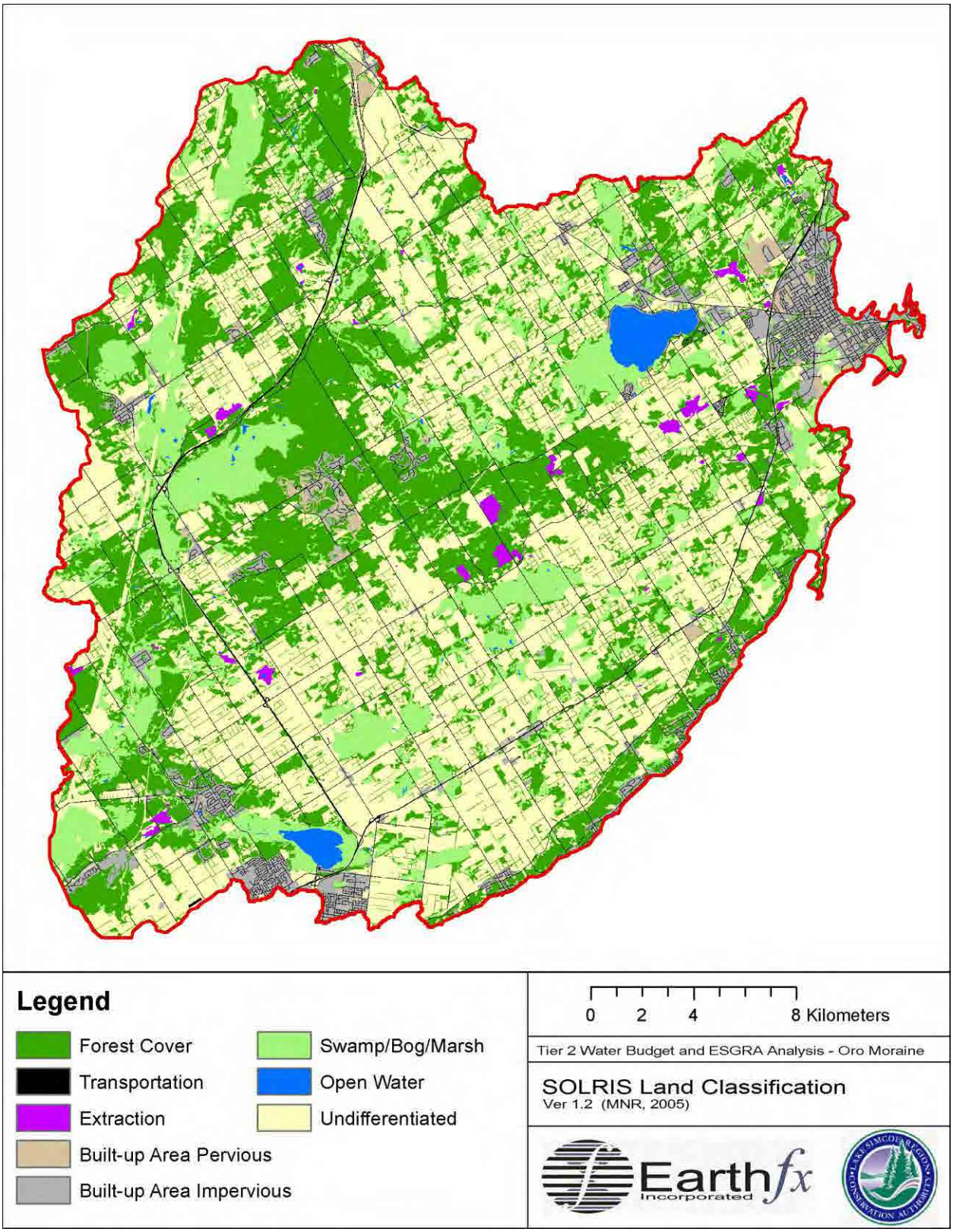

Figure 2.42: Model area land classification after SOLRIS (MNR, 2008).

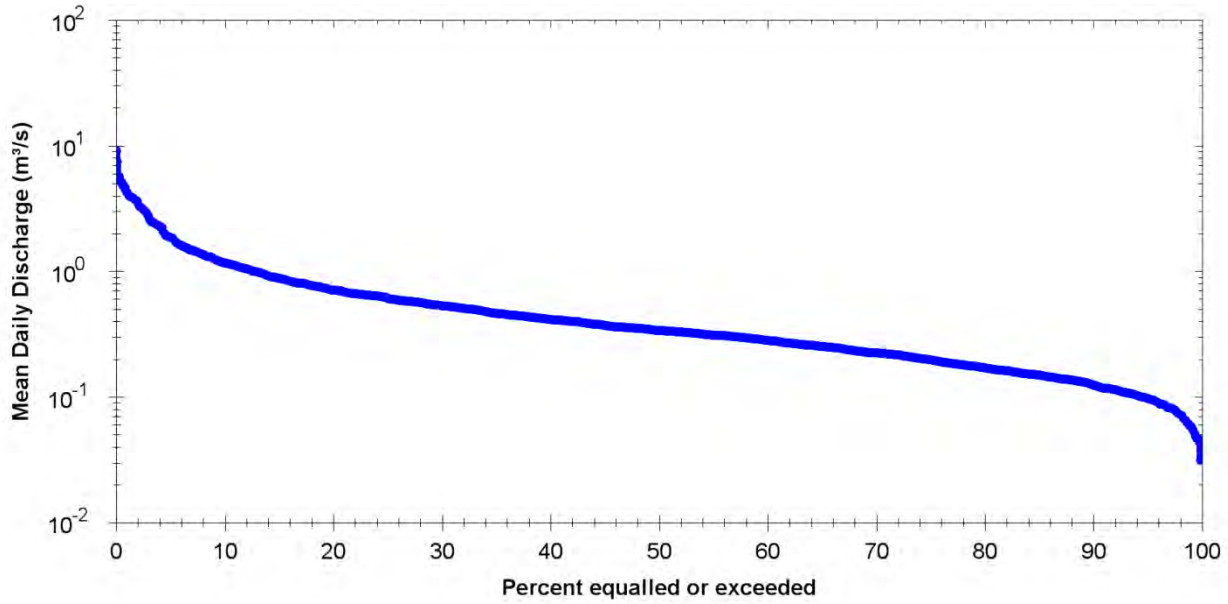

Figure 2.43: Mean daily flow duration curve - Hawkestone Creek at Hawkestone (02EC020).

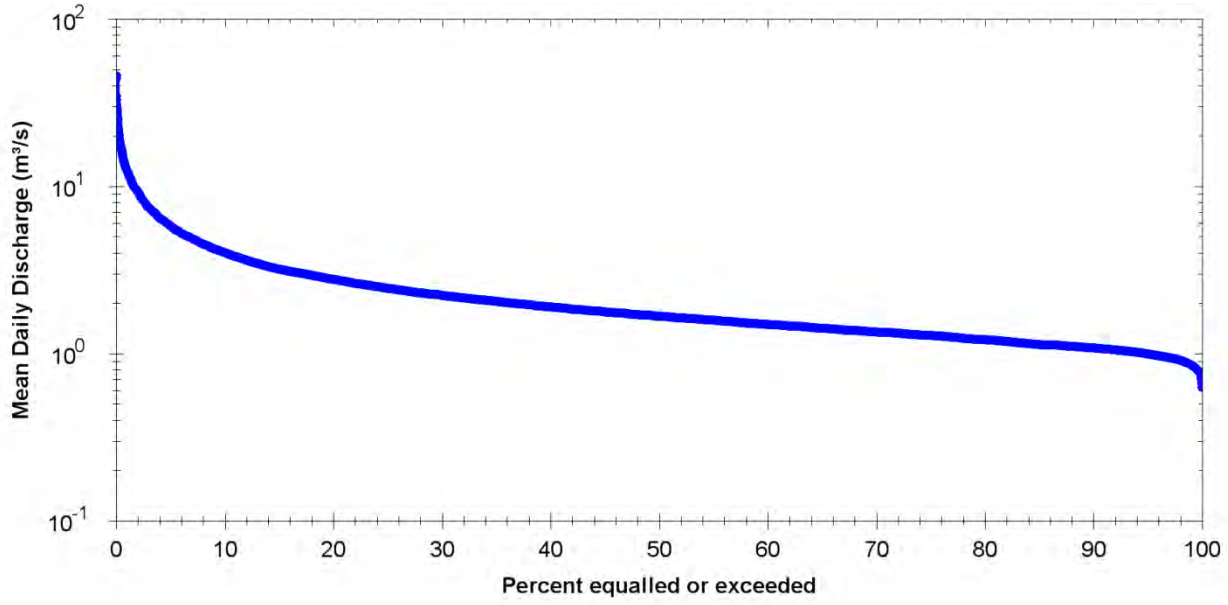

Figure 2.44: Mean daily flow duration curve - Coldwater River at Coldwater (02ED007).

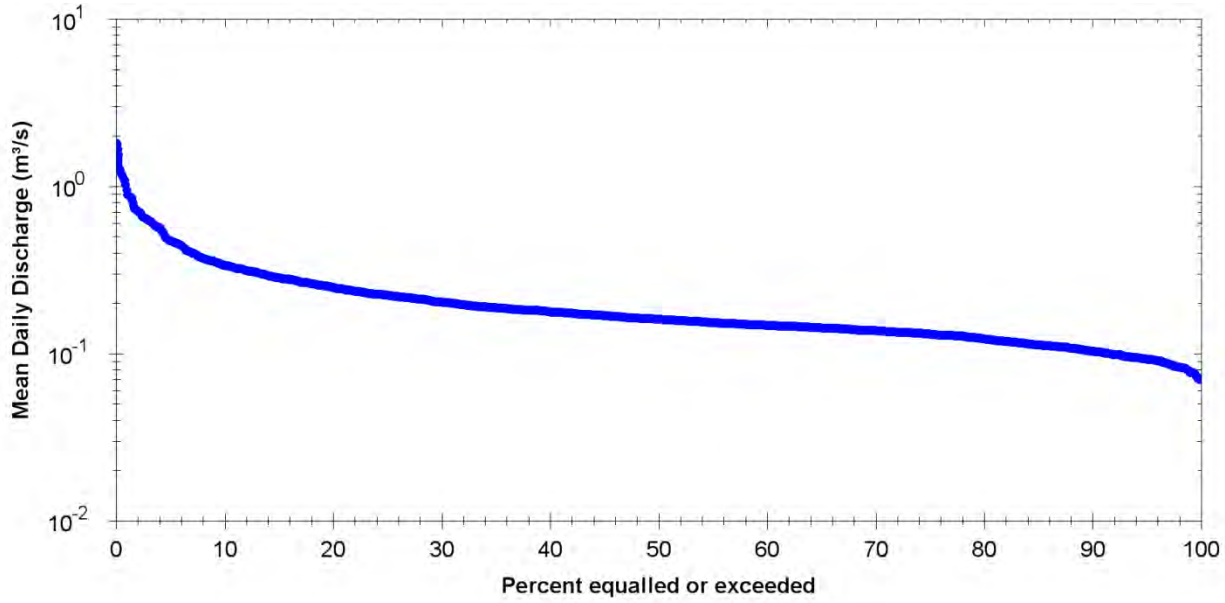

Figure 2.45: Mean daily flow duration curve - Silver Creek at Orillia (02ED030).

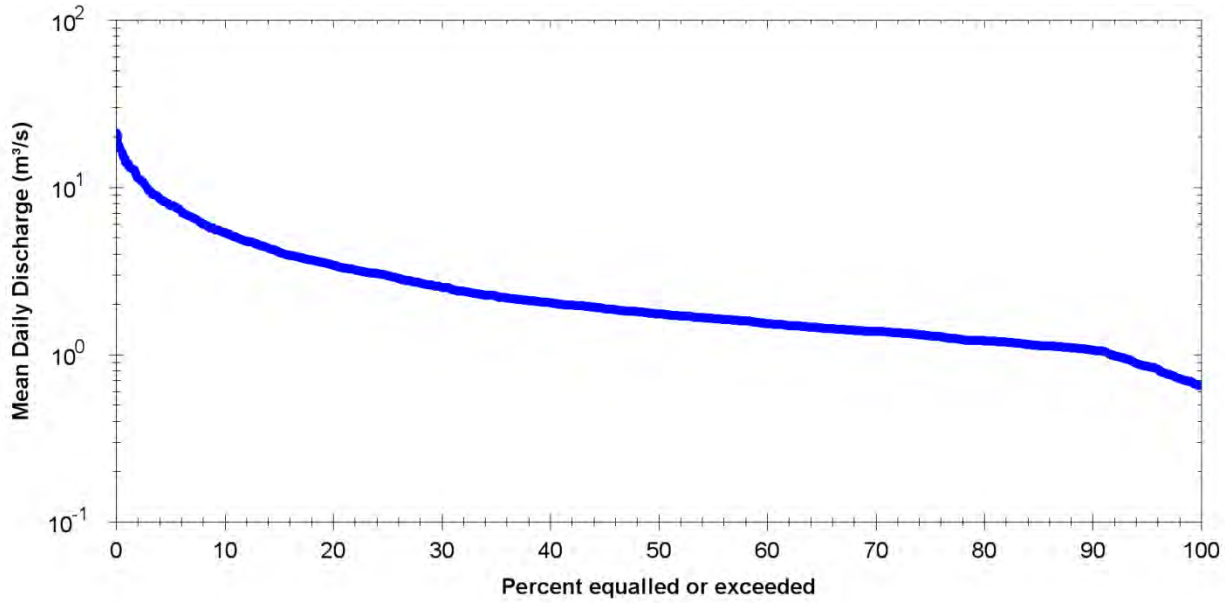

Figure 2.46: Mean daily flow duration curve - Willow Creek near Minesing (02EC032).

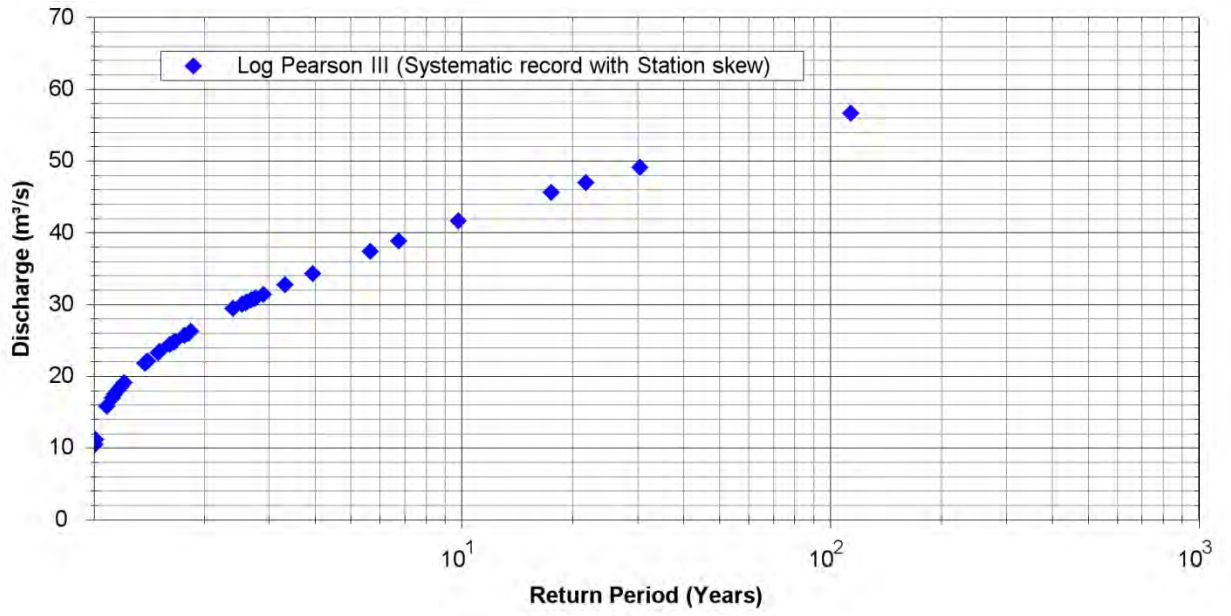

Figure 2.47: Estimated flood return intervals at Coldwater River at Coldwater (02ED007).

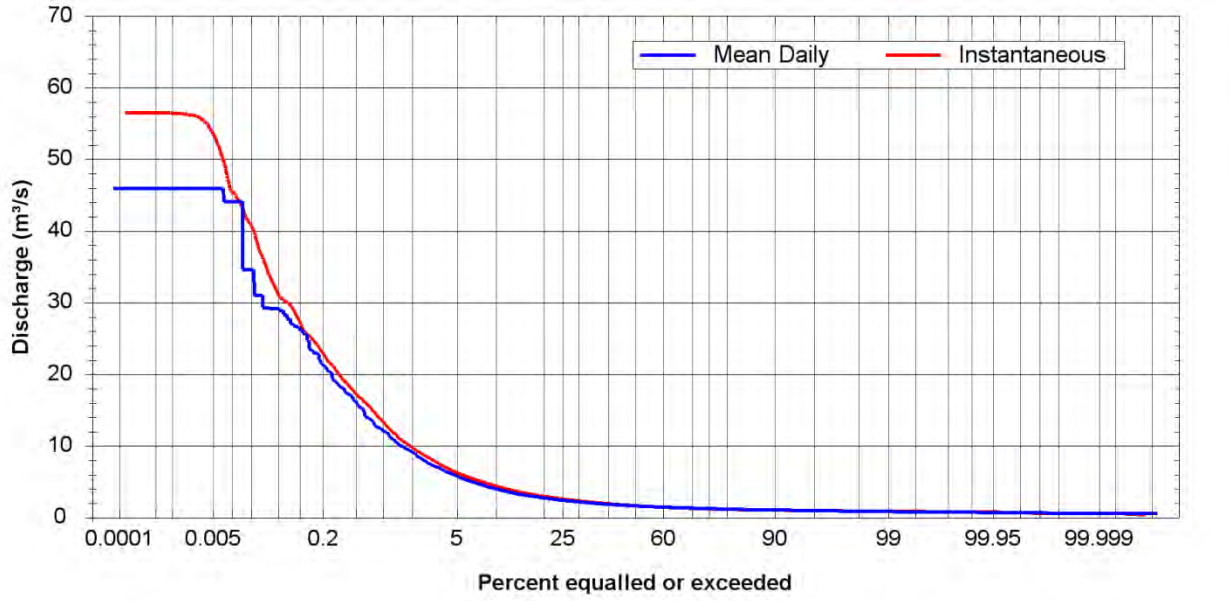

Figure 2.48: Mean daily versus instantaneous (15-minute) discharge at Coldwater River at Coldwater (02ED007).

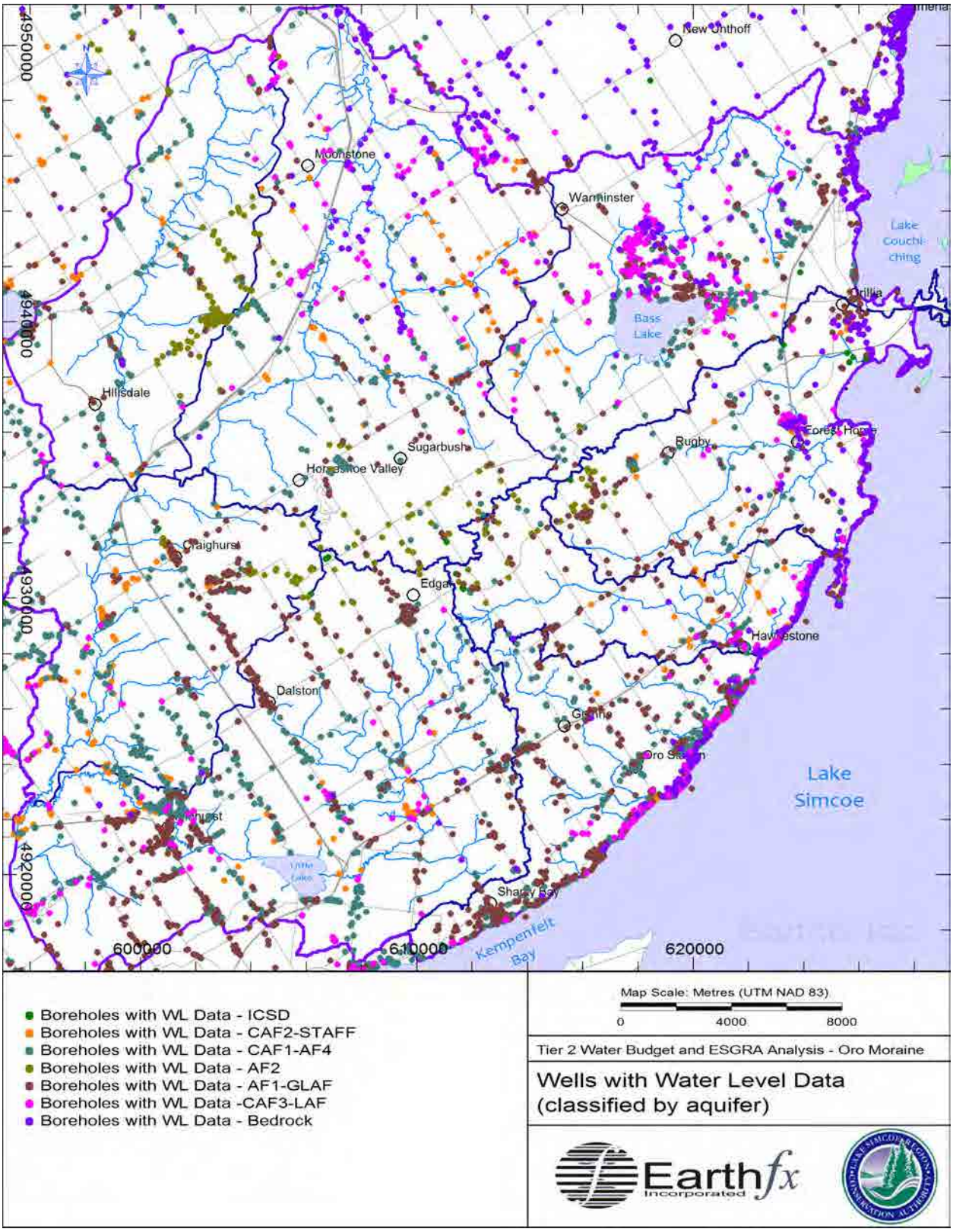

Figure 2.49: Wells with water level data (locations sorted by screened interval classification).

Figure 2.50: Location of PGMN and other monitoring wells.

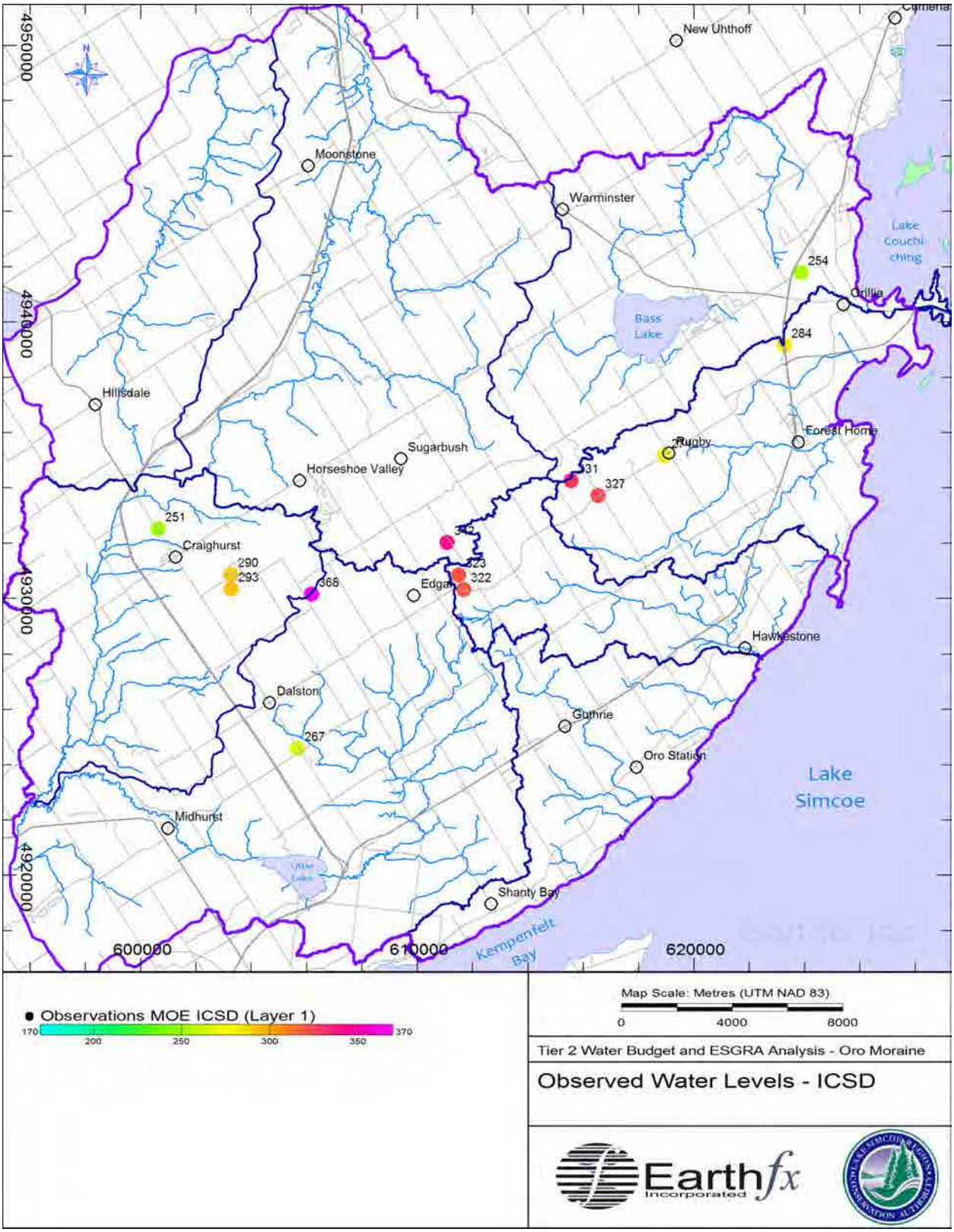

Figure 2.51: Observed static water level data for wells screened in the ICSD.

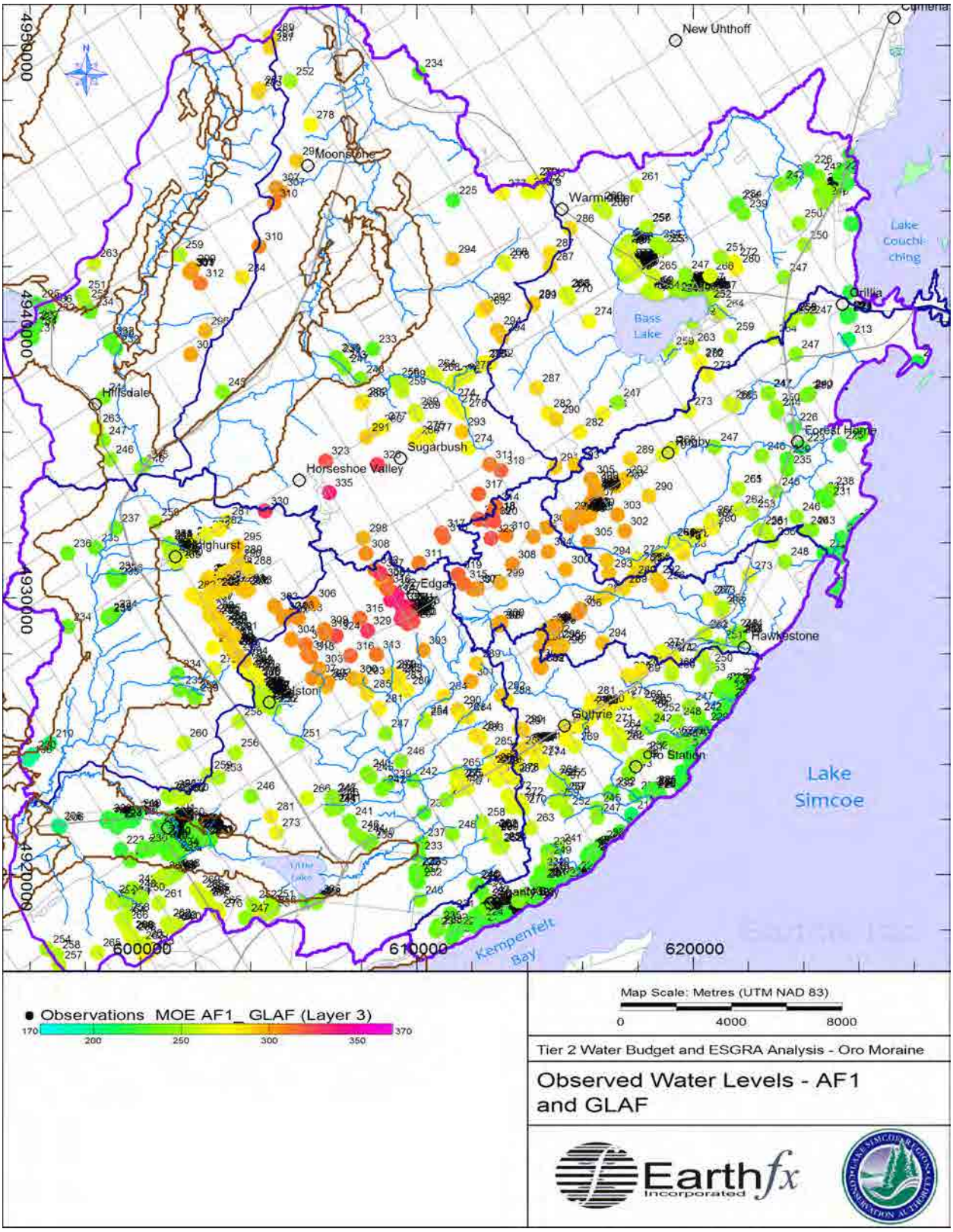

Figure 2.52: Observed static water level data for wells screened in the AF1 and GLAF.

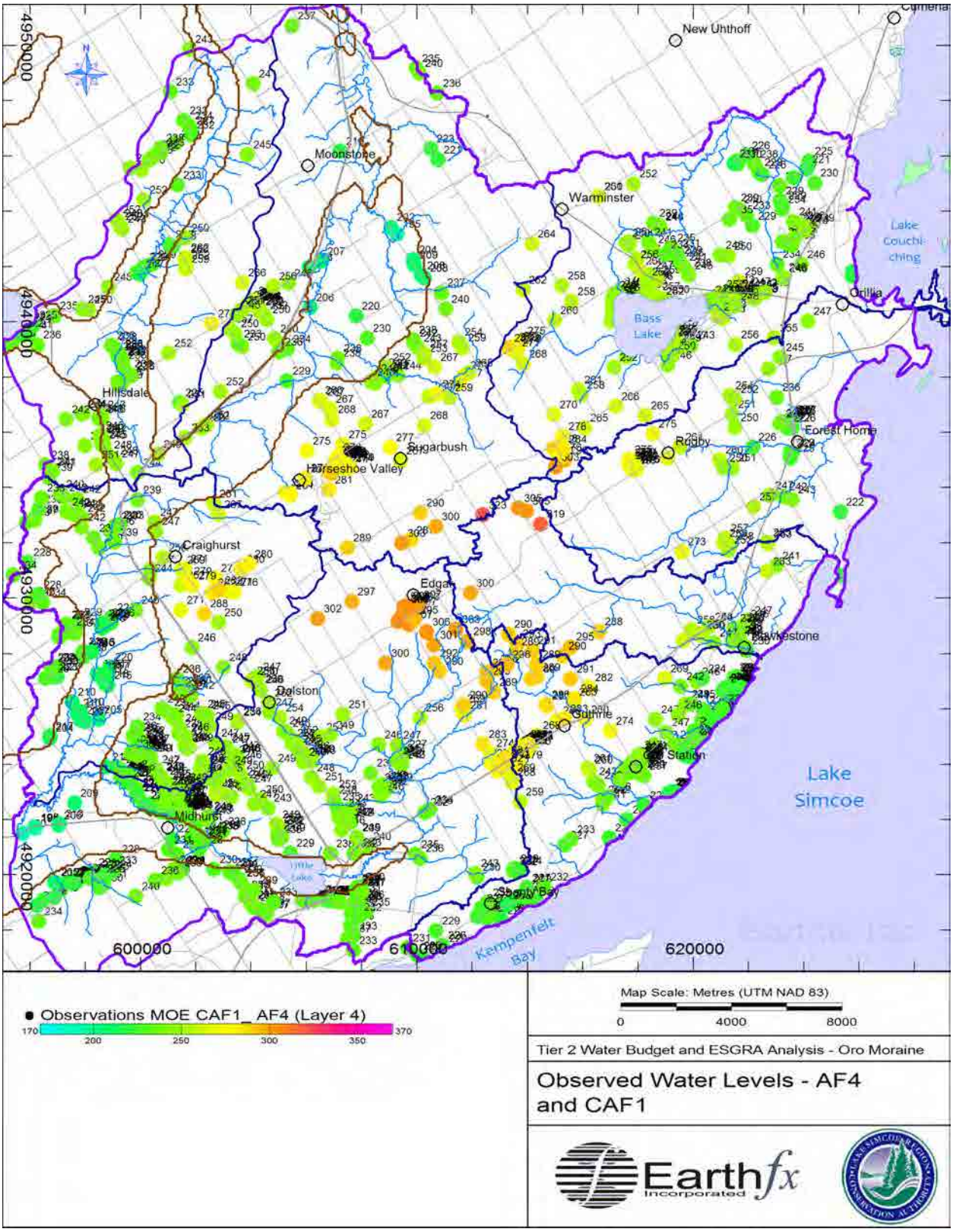

Figure 2.53: Observed static water level data for wells screened in the AF4 and CAF1.

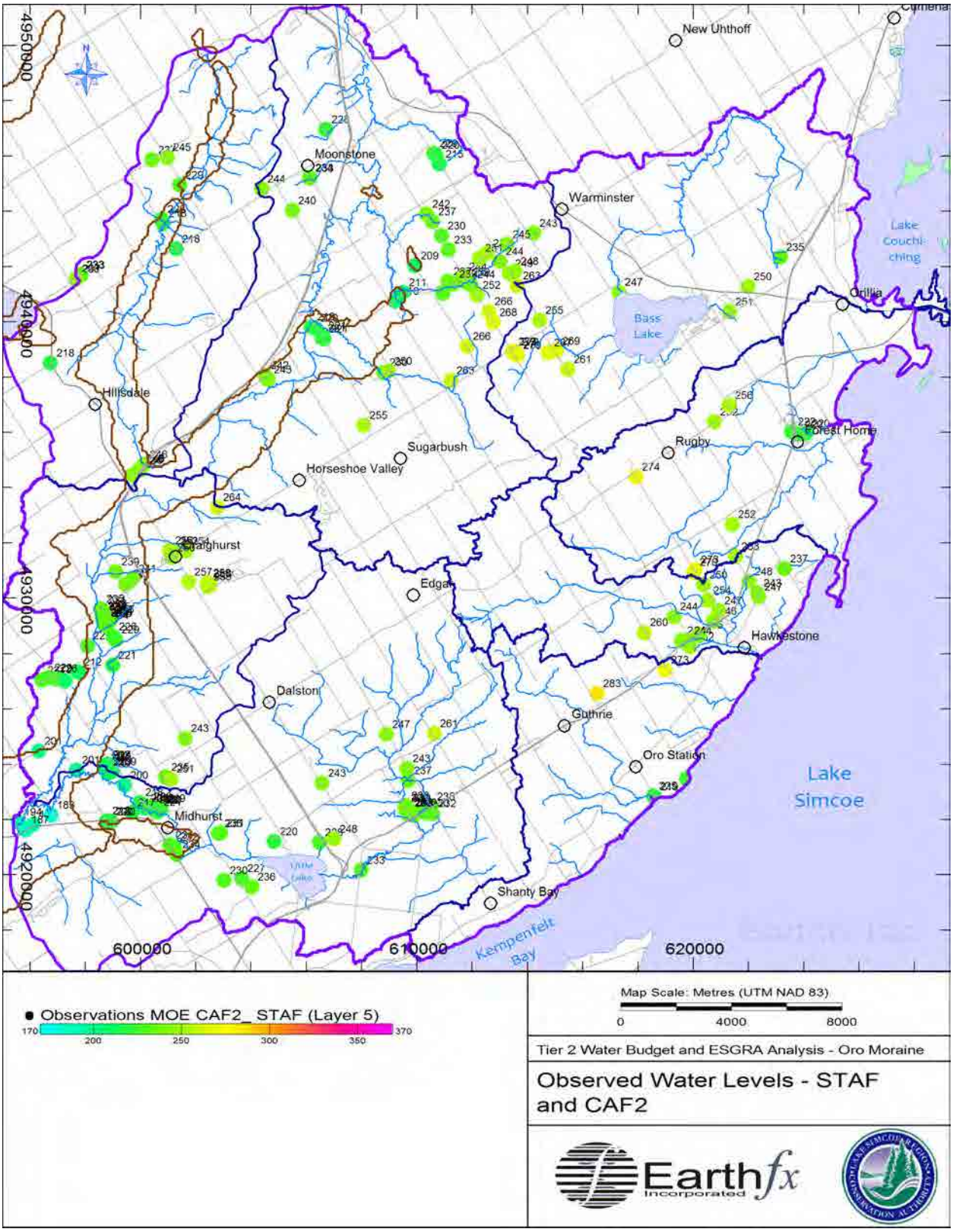

Figure 2.54: Observed static water level data for wells screened in the STAF and CAF2.

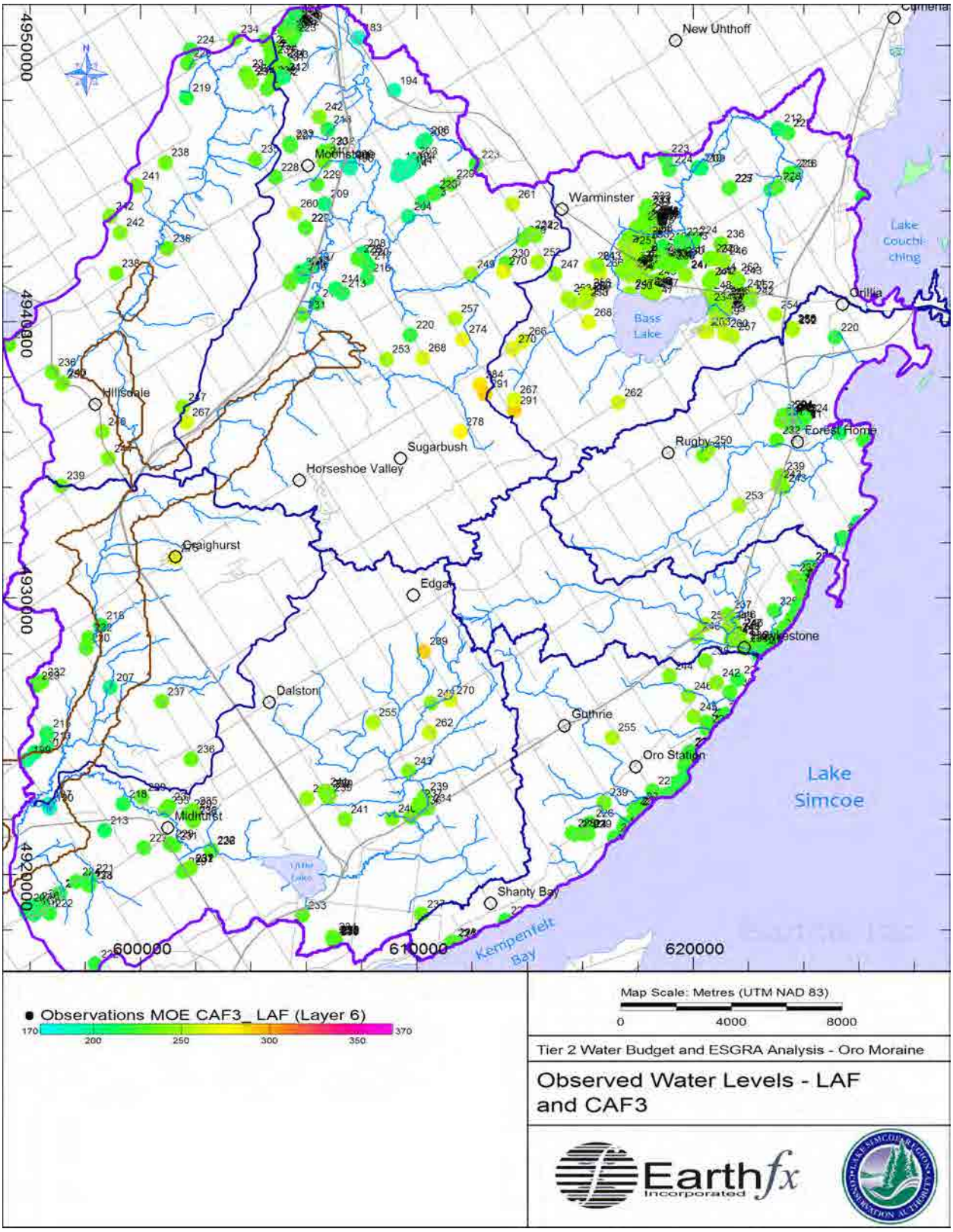

Figure 2.55: Observed static water level data for wells screened in the LAF and CAF3.

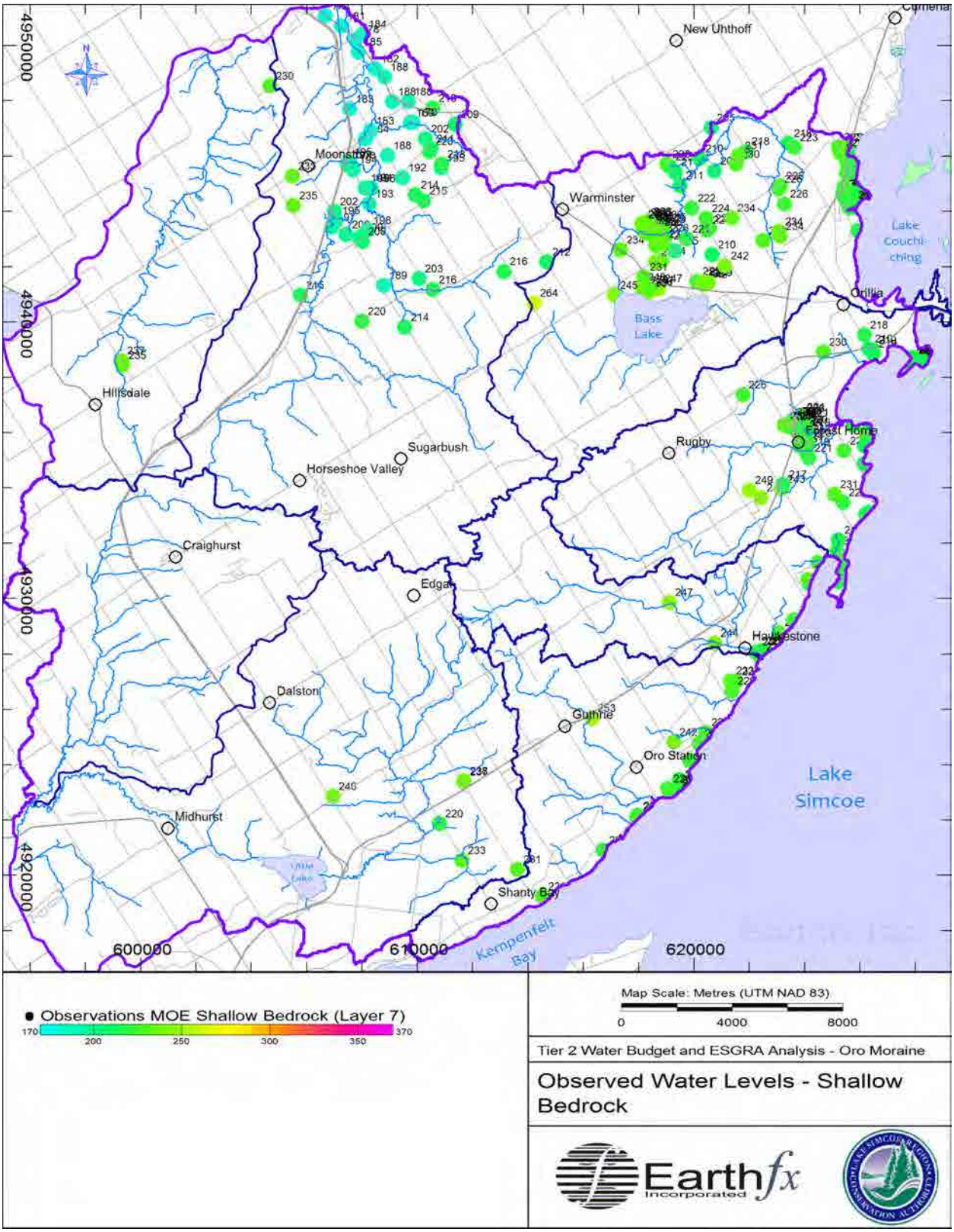

Figure 2.56: Observed static water level data for wells screened in the shallow bedrock.

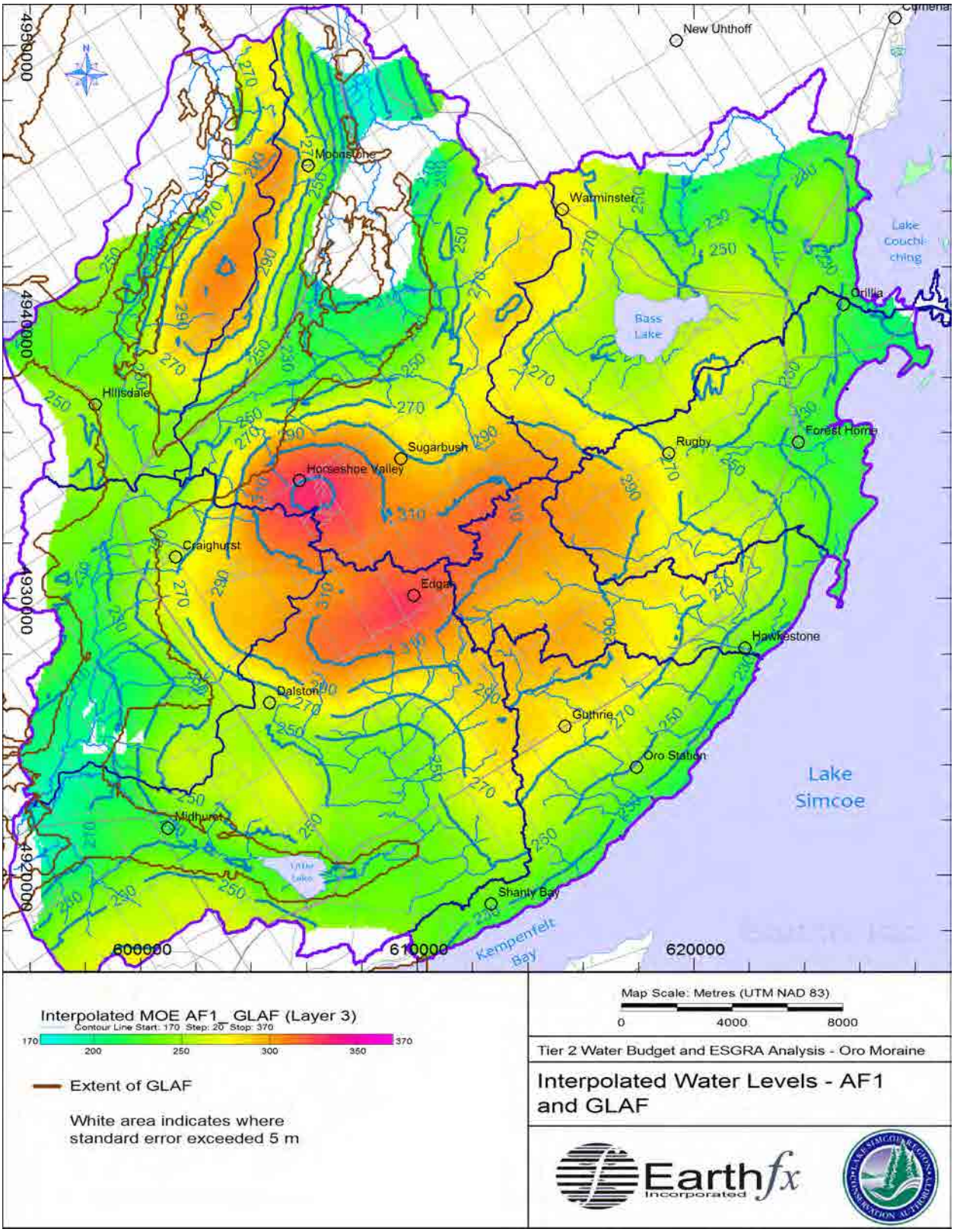

Figure 2.57: Interpolated water levels in the AF1 and GLAF.

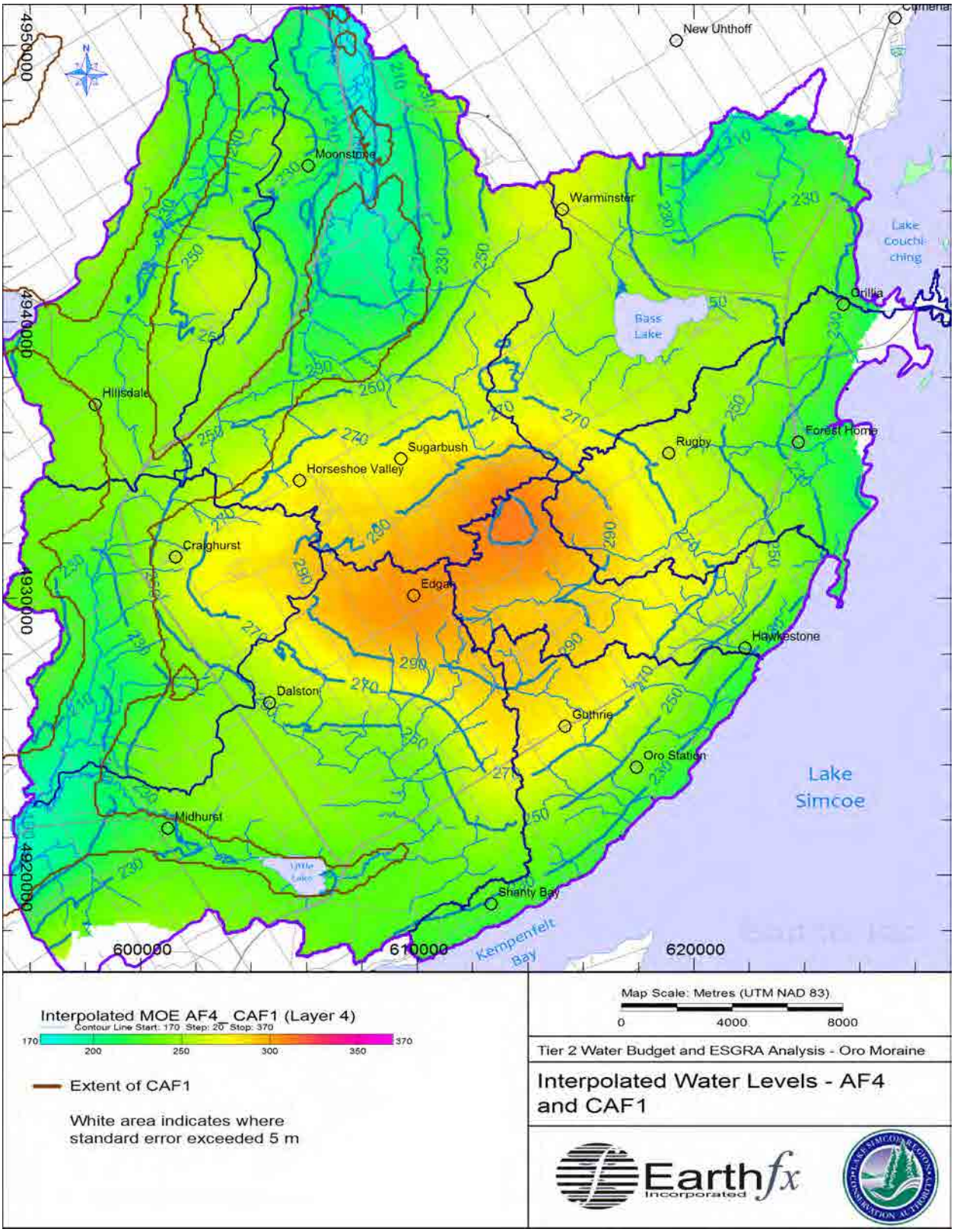

Figure 2.58: Interpolated water levels in the AF4 and CAF1.

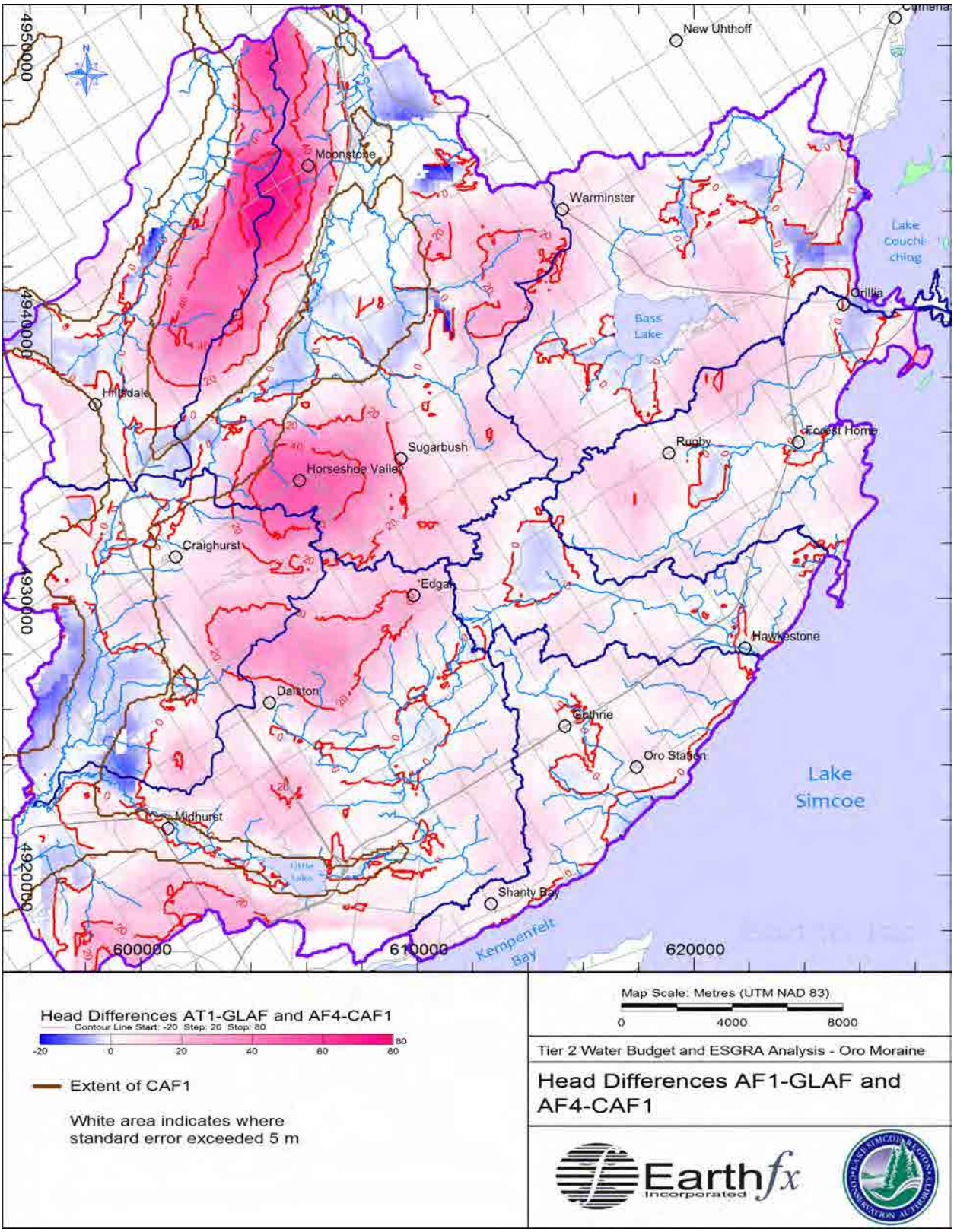

Figure 2.59: Head differences between the AF1-GLAF and AF4-CAF1.

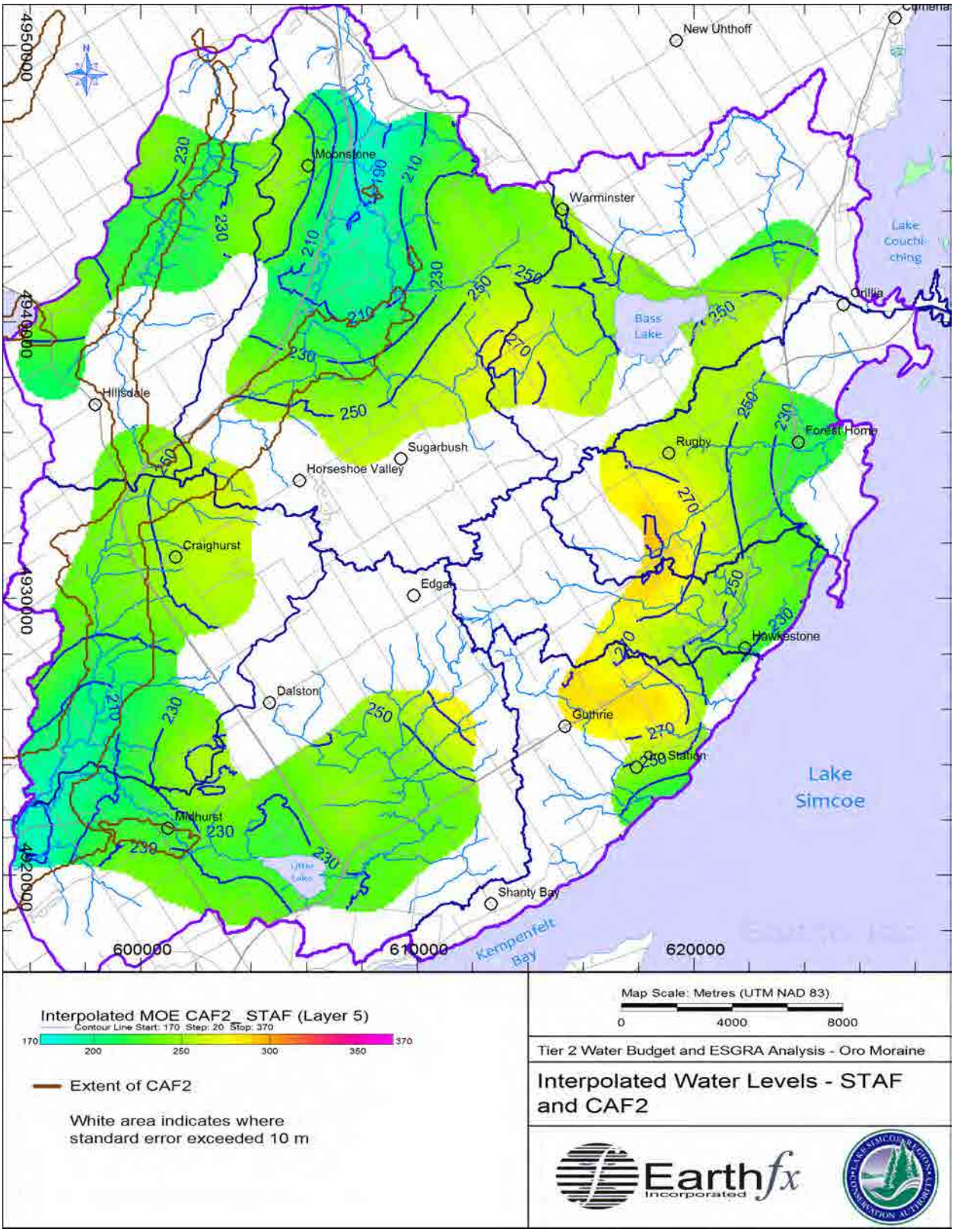

Figure 2.60: Interpolated water levels in the STAF and CAF2.

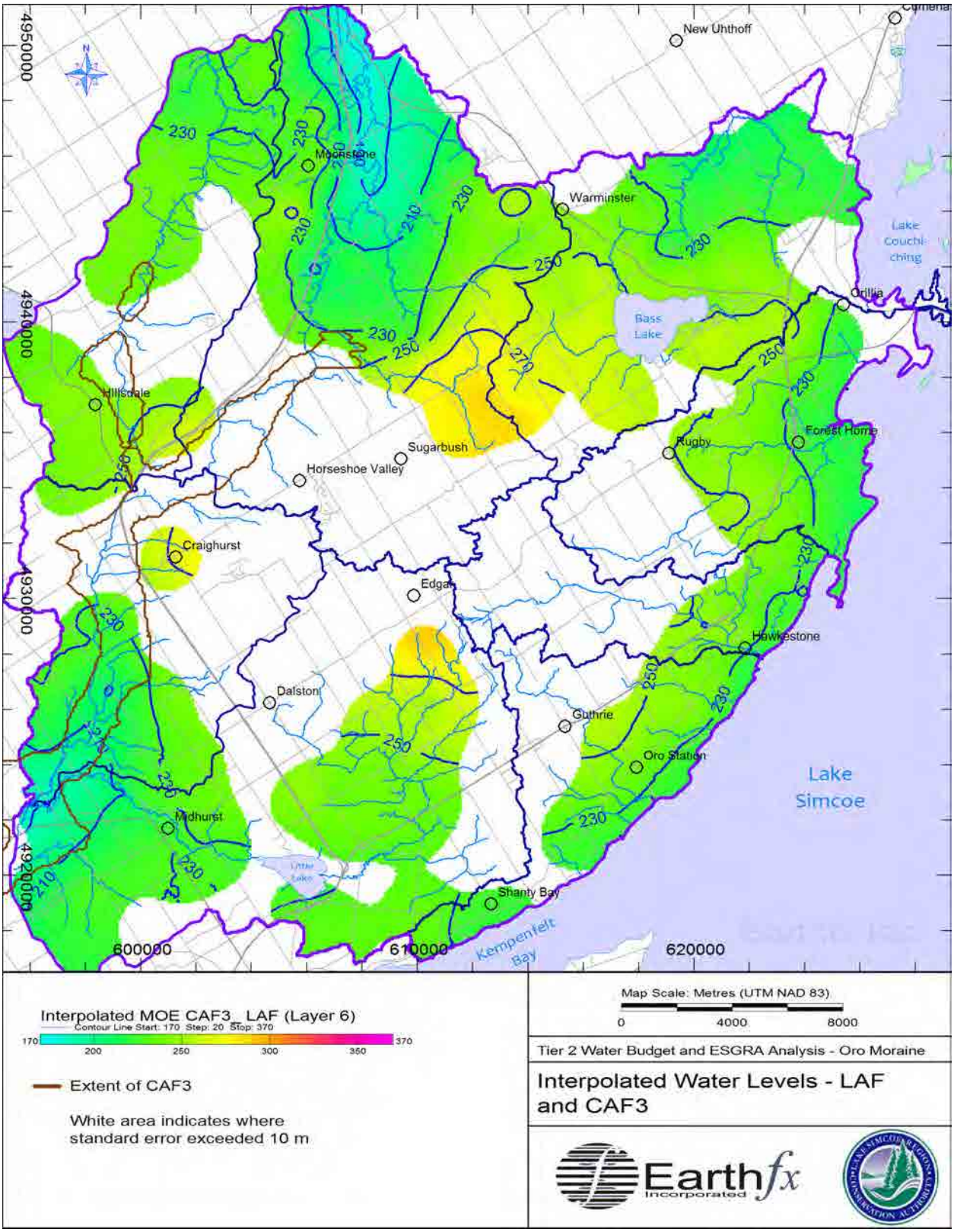

Figure 2.61: Interpolated water levels in the LAF and CAF3.

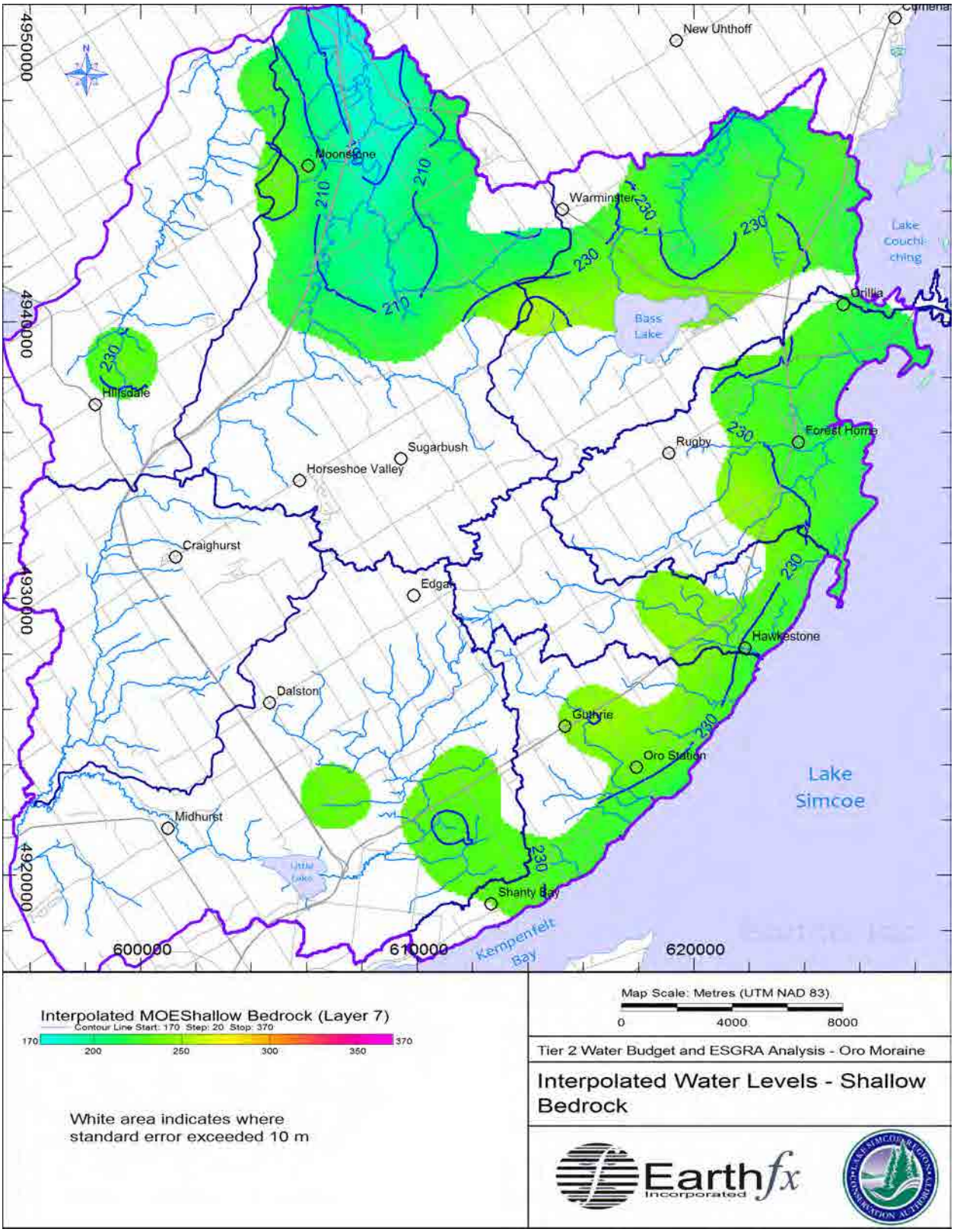

Figure 2.62: Interpolated water levels in the shallow bedrock.

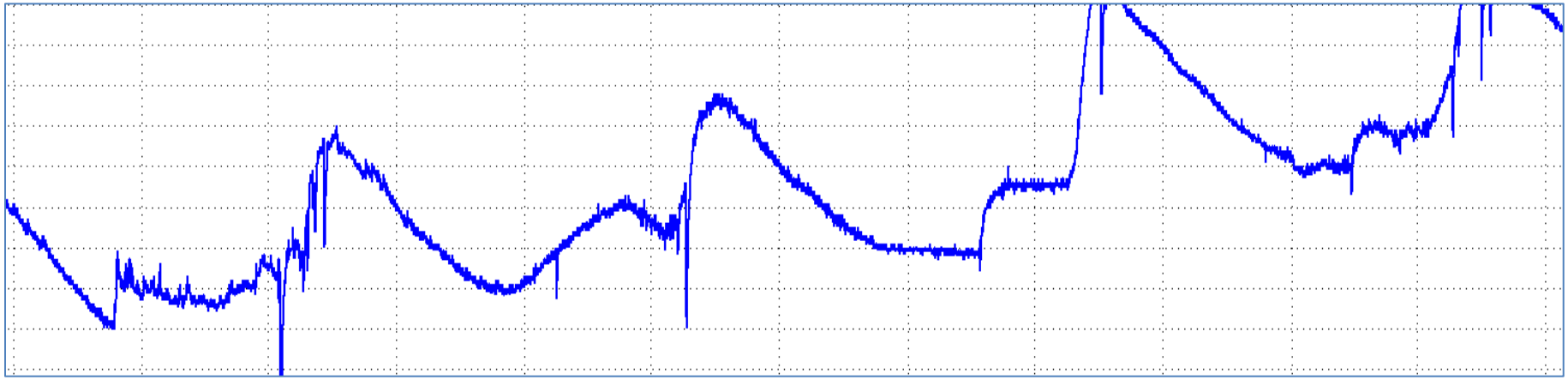

Figure 2.63: Hydrograph for PGMN Well W0000442-1.

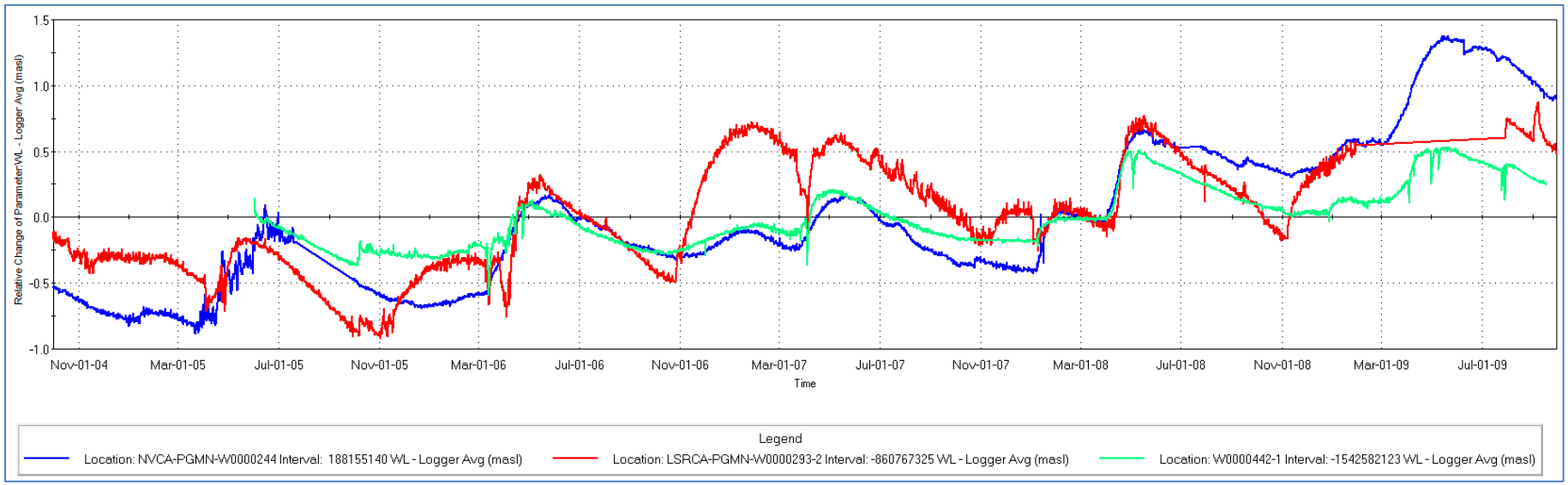

Figure 2.64: Hydrographs of relative water level for PGMN Wells W0000244, W0000293-2, and W0000442-1.

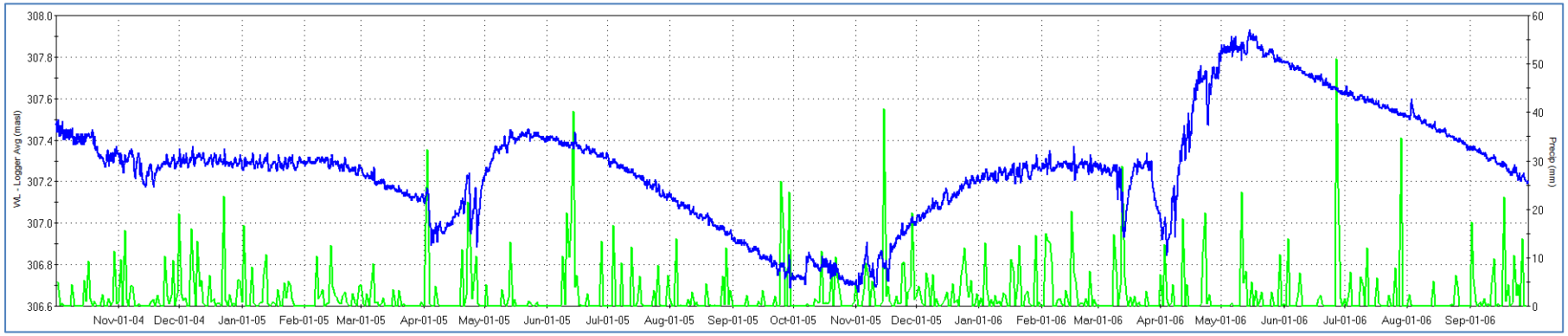

Figure 2.65: Hydrograph for PGMN well W0000293-2 and Precipitation at Barrie-Oro (6117700).

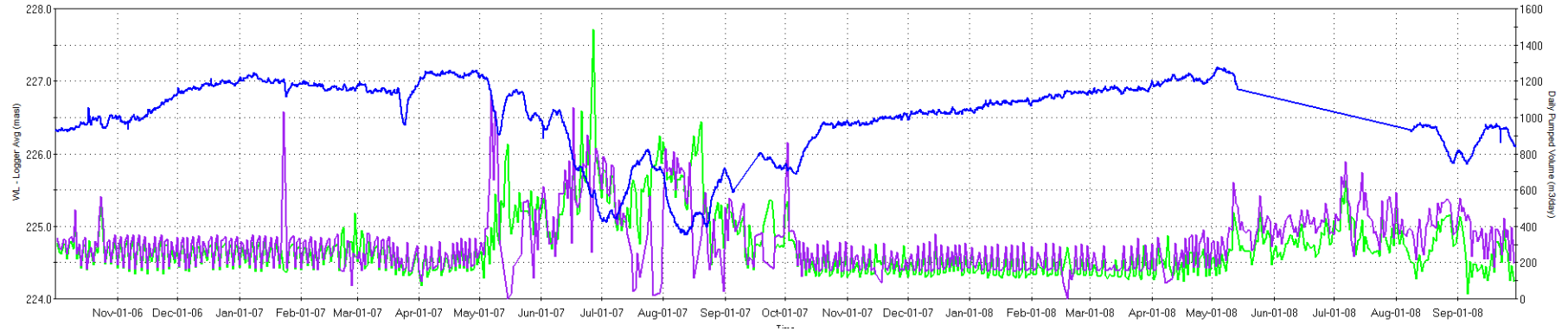

Figure 2.66: Hydrograph for PGMN Well W0000245 and pumping at nearby municipal wells.

3 Water Demand Estimation

3.1 Sources of Demand Estimation Data

The water demand component of the water budget refers to water taken as a result of an anthropogenic activity (e.g., municipal drinking water takings and private water well takings). The water demand can be estimated from a number of information sources, including the Permit to Take Water (PTTW) database, Water Taking Reporting System database, population estimates, census data, and water well records (WWIS database). Water demand was assessed for all Lake Simcoe watersheds in Golder (2006) and LSRCA (2009). Demand estimates were tabulated for each watershed and then adjusted for 'consumptive' demand and seasonal (monthly) extraction rates. The data for the Oro North, Oro South, and Hawkestone subwatersheds were reviewed as part of this study, and refined as necessary. In addition, municipal and other permitted takings were estimated for each user within the entire Oro Moraine model area.

As noted, an important source of consumptive demand data was the MOE Permit to Take Water database which provides information on the permit location, purpose, and maximum taking (in terms of maximum daily rate and number of days per year). The PTTW database does not have a field for the MOE WWIS well ID number which would allow a groundwater permit to be linked to a specific well. The Well ID may be referenced in comment fields or added to the source name for some wells. Withdrawals were assigned to the appropriate model layer based on the placement of the well screen (where the Well ID was known or could be reasonably guessed based on proximity of the permit location to a WWIS well). Where no specific well could be cross-referenced, the model layer was set based on the screen setting of the majority of nearby wells.

Some permits in the PTTW database may have been issued on a temporary basis. Sources classified as a pumping test or temporary construction dewatering were removed from the analysis Further screening eliminated sources that had no location coordinates, were located outside the study area, or had obvious locations errors. For example, one of the sumps for the Uhthoff Quarry was located in Bass Lake. The two other sumps were located in Oro North. The Uhthoff Quarry is actually outside the model area.

Water takings are also classified based on general (e.g., water supply or agriculture) and specific purposes (e.g. campgrounds or municipal water supply). Classifications may have changed since the permitted was issued and data entered into the PTTW database. For example, several communal or municipal wells are still classified as campground water supplies. These were updated for this study and the consumptive use and monthly taking assignments were adjusted accordingly.

Water takings are classified in the PTTW database as either groundwater, surface water or "both". The category of "both" can include ponds that are filled by a well and shallow dug ponds. The classifications are not always consistent, when compared with the original permit. For this study, takings classified as "both" have been included with the groundwater takings.

Actual water use rates are often less than the permitted rates. Verifying and estimating actual consumption is difficult, but Provincial legislation (387/04) requires that actual extraction rates by permit holders be self-reported to the MOE. The Water Taking Reporting System is

maintained as a separate database but takings can be cross-referenced based on the PTTW number. Data for the municipal wells is generally complete for period of 2007-2011. Actual water use was received for most of the non-municipal permitted water users in the model watersheds. Locations of permits with reported data and permits without reported data are shown in Figure 3.1 for the model area and in Figure 3.2 for the Tier 2 study area.

Some known problems exist with the database for non-municipal pumping due to changing permit numbers, incomplete records, transcription errors associated with paper records and electronic submissions, and non-compliance with reporting requirements. Where actual takings were not reported, the demand estimate used the maximum allowable takings from the PTTW database.

Consumptive use can be less than the reported or estimated takings if a portion of the water is returned to its original source. A consumptive use factor can be defined as:

$$Consumptive\,Use\,Factor \equiv \frac{Q_{Pumped} - Q_{\mathrm{Returned}}}{Q_{Pumped}}$$

The consumptive use factor for individual takings can be difficult to determine. Consumptive use factors were assigned to each permitted taking based on the purpose assigned to taking in the database and on recommended values in the Water Budget and Water Quantity Risk Assessment Guide (MOE, 2011). Consumptive use was determined by multiplying the estimated takings by the factors. Water was assumed to return to the aquifer from which it was extracted. There was one exception to this rule. While the Water Budget and Water Quantity Risk Assessment Guide assigns a consumptive use factor of 20% to municipal wells, the LSRCA treated all municipal supply takings as 100% consumptive in their Tier 1 analysis. This practice was followed for this study.

Demand from other non-permitted water use sectors was also estimated. The two types of non-permitted use included unserviced domestic consumption and agricultural operations (irrigation and livestock consumption). Estimates of increased unserviced domestic demand were compiled by LSRCA taking into account population growth estimates for the study area. As noted in the Water Budget and Water Quantity Risk Assessment Guide, Tier 2 analyses should assume that the other permitted demands remain constant in time except where significant land-use changes are anticipated.

3.2 Demand Estimates

3.2.1 Municipal Pumping

Groundwater is the primary source of municipal supply for the various communities in the study area subwatersheds. Additionally, some of the municipal wells for the City of Barrie and the City of Orillia are located within the Oro Moraine area. A total of 45 municipal wells are located within the model area; 12 within the study area. All municipal wells within the model area have reported takings and average pumping was calculated from data in the WTRS database. Table 3.1 summarizes the average pumping values determined for the municipal wells.

Based on conversations with LSRCA staff, future pumping rates were assumed to not change significantly from current rates as no major population growth is expected in the future within the study watersheds. To be conservative, an increase of 10% was applied to the municipal takings in the Tier 2 study area to represent any possible future increases in demand. Future rates for municipal wells outside the Tier 2 study area were not adjusted. It should be noted that the Sandra Drive Well, a part of the Orillia Water Supply System, was discontinued in 2010 and was not considered in the future scenario (LSRCA, 2011). Estimated future pumping rates are summarized on Table 3.2 for the municipal wells in the study area.

3.2.2 Non-municipal Pumping

The PTTW database lists 10 groundwater permits in the study area governing the use of 17 wells. A further 19 groundwater permits (governing 27 wells) were found for subwatersheds outside the study area. Reported actual water use was available for 31 wells; the maximum permitted rate was used for the 13 remaining wells. Table 3.3 summarizes the permitted groundwater takings within the model area.

The PTTW database lists two surface water permits in the study area. Reported takings were available for one of the permits, the maximum permitted rate was used in the analysis of the other. A further 10 permits were found within the model area and were incorporated in the model. Takings were allocated to the model stream reach indicated within the permit. Permitted takings from lakes and ponds were removed from the simulated lakes. Some ponds were too small to represent in the model and the takings were treated as shallow groundwater withdrawals. Table 3.4 summarizes the permitted surface water takings within the model area.

3.2.3 Unserviced Domestic Consumption Estimates

The number of persons in each watershed living outside of the areas with municipal supply is referred to as the “unserviced” population. This population is assumed to be consuming groundwater water from individual wells or small communal supplies.

Estimates of non-serviced domestic water use based on 2006 population census data were taken from the Tier 1 Water Budget and Water Quantity Stress Assessment (LSRCA, 2009). This was corrected for actual consumption (20%) because a significant portion of this water is assumed to be returned to the groundwater system through septic systems and drain fields. The Tier 1 report also included estimates of the future unserviced demand which were incorporated into the assessment of future conditions. No other demand estimates were adjusted for population growth.

Table 3.7 and Table 3.8 present the current and future unserviced demand. These values were incorporated within the steady-state model by decreasing the applied recharge over the each subwatershed by the estimated unserviced demand. Rural areas were defined with SOLRIS land use mapping, version 1.2 (April, 2008) (see Section 2).

3.2.4 Non-Permitted Agricultural Demand

Under the Ontario Water Resources Act (Revised Statutes of Ontario 1990, Chapter O.40), farmers using less than 50 m^3/d and farmers who are taking water for livestock watering but not

storing the water do not require a PTTW and are therefore "non-permitted" agricultural consumers. To estimate agricultural consumption, the Water Budget Assessment Guide suggests using water use coefficients developed by de Loe (2001 and 2005). The 2001 data compiled by de Loe have been allocated to subwatersheds using area weighting to estimate subwatershed water use as per the following process.

Agricultural demand was estimated for each study subwatershed in the Tier 1 Water Budget and Water Quantity Stress Assessment (LSRCA, 2009) using de Loe's methodology. Although this method provides an estimate of total water consumption, there is no method to differentiate what is taken from groundwater versus surface water. Table 3.7 presents the current agricultural demand. These values were incorporated within the steady-state model by decreasing the applied recharge over the each subwatershed by the estimated agricultural demand. The consumption factor for the non-permitted agricultural use (primarily livestock, including dairy operations) was estimated as 80%, close to the recommended factor of 78% suggested by de Loe (2001).

3.2.5 Seasonal Water Use Correction

Many water permit holders do not require the use of water at a constant rate throughout the year. For example, there are several golf course irrigation, snowmaking, campground, and aggregate washing permits in the model area. Additionally, many of the permits in the model area are limited by time, only allowing pumping for a maximum number of days per year. Where WTRS data were available, the actual daily water use was used in estimating demand. Where these data were not available, monthly on/off factors were applied based on Table 3.2 in the Water Budget and Water Quantity Risk Assessment Guide (MNR, 2011) for the different water use purpose categories. Overall, permitted water demand in the model area is higher in the summer due to these activities.

Agricultural demand estimates given by de Loe (2001) were reported on an annual basis. Although it is quite likely that agricultural demand for the summer season exceeds winter demands, there was no information available to allocate seasonal water taking using the data provided by de Loe (2001). Therefore, the annual agricultural water demand estimates were assumed to be constant year-round.

3.2.6 Water Demand Findings

The results of the water demand are presented as a series of summary tables. The overall total water demand includes the permitted usage, unserviced domestic, municipal and agricultural demand, as shown in Table 3.7 and Table 3.8 for current and future scenarios. All values were corrected with consumptive use factors. The total groundwater demand from all sources is 2370 m^3/d in the three study subwatersheds.

In the Oro North and Hawkestone subwatersheds, permitted groundwater takings represent the largest consumers (81% and 74%, respectively). A number of private communities, campgrounds, and golf courses account for these takings. In the Oro South subwatershed, where the population density is higher, municipal and unserviced takings represent nearly 90% of the estimated takings.

As noted, the water demand estimates for the study subwatersheds have been developed from a number of information sources as the PTTW database, WTRS database, WWIS, and Water Budget and Water Quantity Risk Assessment Guide (MNR, 2011). Some simplifying assumptions were made and there is some uncertainty regarding the completeness and accuracy of the data sources. A further discussion of the water demand is included in the later sections of this report, where the demand is compared to the simulated available water supply in the study area subwatersheds.

3.3 Tables

Table 3.1: Pumping rates for municipal supply wells within the model area.

User	Well Name	Sub-watershed	Permit Number	Model Layer	Easting (m)	Northing (m)	Estimated Consumption[1] (m^3/d)	Maximum Permitted Consumption[2] (m^3/d)
Barrie Well Supply	Well #13 at 168 Johnson Street	Willow Creek	8433-6QSRX5	6	607013	4917660	865	6552
Barrie Well Supply	Well #16 at 101 Brown Wood Lane	Willow Creek	8433-6QSRX5	7	604031	4919592	1309	7862
Barrie Well Supply	Well #9 at 168 Johnson Street	Willow Creek	8433-6QSRX5	6	607044	4917651	1128	6552
Bass Lake Woodlands Well Supply	Well #3	North River	87-P-3051	6	619710	4941724	48	494
Bass Lake Woodlands Well Supply	Well No. 1	North River	87-P-3051	6	619709	4941714	29	436
Bass Lake Woodlands Well Supply	Well No. 2	North River	87-P-3051	6	619720	4941704	34	281
Canterbury Subdivision Well Supply	Well 1	**Oro South**	92-P-3028	4	617805	4924105	5	105
Canterbury Subdivision Well Supply	Well 2	**Oro South**	92-P-3028	4	617799	4924108	6	105
Cedar Brook Subdivision Well Supply	Well No.1	**Hawkestone**	4817-6HJPXP	4	621408	4928432	7	104
Cedar Brook Subdivision Well Supply	Well No.2	**Hawkestone**	4817-6HJPXP	4	621415	4928437	8	104
Coldwater Well Supply	Swaile Well (Standby) (WWR 5725508	Coldwater	93-P-3071	7	607215	4951223	2	982
Coldwater Well Supply	Well PW 93-2 (WWR 5729906)	Coldwater	93-P-3071	7	607154	4951202	178	982
Coldwater Well Supply	Well PW93-4 (WWR5729997)	Coldwater	93-P-3071	7	607157	4951179	300	2141
Craighurst Well Supply	Well No.1	Willow Creek	4624-6HKPJW	4	600813	4931474	0	64
Craighurst Well Supply	Well No.2	Willow Creek	4624-6HKPJW	4	600813	4931476	8	140
Craighurst Well Supply	Well No.3	Willow Creek	4624-6HKPJW	4	600816	4931483	13	229
Del Trend Subdivision Well Supply	Del Trend Well #1 (WWR 5728243)	Willow Creek	2372-75VHJ5	6	601776	4920232	19	467
Del Trend Subdivision Well Supply	Del Trend Well #2 (WWR 5728671)	Willow Creek	2372-75VHJ5	6	601788	4920236	24	467
Del Trend Subdivision Well Supply	Del Trend Well #3 (WWR 5733452)	Willow Creek	2372-75VHJ5	6	601768	4920256	86	786

User	Well Name	Sub-watershed	Permit Number	Model Layer	Easting (m)	Northing (m)	Estimated Consumption[1] (m^3/d)	Maximum Permitted Consumption[2] (m^3/d)
Harbourwood Well Supply	Well No.2	**Oro South**	8643-6HKK9K	6	617919	4922286	47	921
Harbourwood Well Supply	Well No.3	**Oro South**	8643-6HKK9K	6	617853	4922342	47	921
Horseshoe Highlands Subdivision Well Supply	Well #1 (5723788)	Coldwater	0404-5UHQDN	4	605950	4934348	290	3371
Horseshoe Highlands Subdivision Well Supply	Well #2 Standby Well (5721850)	Coldwater	0404-5UHQDN	4	605958	4934353	0	527
LSR Airport	Well #2	**Oro South**	5348-6HKP2G	4	615711	4926394	3	36
LSR Airport	Well #3	**Oro South**	5348-6HKP2G	4	615660	4926265	1	36
Maplewood Estates Well Supply	Well (PW #1)	**Oro North**	02-P-1314	6	625395	4932101	24	164
Maplewood Estates Well Supply	Well 2	**Oro North**	0825-89BLY7	6	625444	4932170	0	164
Medonte Hills Well Supply	Well 1	Coldwater	92-P-3029	6	605961	4943415	29	327
Medonte Hills Well Supply	Well 2	Coldwater	92-P-3029	6	605966	4943401	38	393
Midhurst Well Supply	Carson Road Well 5 (formerly Well 4) (WWR 5725264)	Willow Creek	0507-6B9S5G	6	601516	4920130	242	1068
Midhurst Well Supply	Greenpine Well 4	Willow Creek	0507-6B9S5G	6	601425	4921887	206	2000
Midhurst Well Supply	Idlewood Well 2 (WWR 5711983)	Willow Creek	0507-6B9S5G	6	601912	4921975	109	622
Midhurst Well Supply	Idlewood Well 3 (WWR 5718775)	Willow Creek	0507-6B9S5G	6	601898	4921952	346	2900
Orillia Water Supply System	Well 1 & 2	Lake Couchiching	91-P-3036	4	625757	4941830	98	5683
Orillia Water Supply System	Sandra Drive Well	Lake Couchiching	99-P-1256	6	623594	4939744	0	4390
Orillia Water Supply System	Well #3	Lake Couchiching	99-P-1256	6	622904	4940267	712	7920
Orillia Water Supply System	ORILLIA WELL 2	Lake Couchiching	91-P-3036	4	625747	4941678	33	5683
Shanty Bay Well Supply	Well No. 1	**Oro South**	7520-6LJTGX	4	613042	4918915	39	305
Shanty Bay Well Supply	Well No. 2	**Oro South**	7520-6LJTGX	3	613048	4918904	39	305
Shanty Bay Well Supply	Well No. 3	**Oro South**	7520-6LJTGX	4	613028	4918911	78	610
Snow Valley Highlands Well Supply	Well 1 (WWR 5723284)	Willow Creek	7650-6CFRPK	6	597079	4919327	42	700
Snow Valley Highlands Well Supply	Well 2 (WWR 5724900)	Willow Creek	7650-6CFRPK	6	597078	4919342	42	700
Sugar Bush Well Supply	Well #1	Coldwater	1483-5MYQ36	4	609032	4935460	49	851
Sugar Bush Well Supply	Well #2	Coldwater	1483-5MYQ36	4	609404	4934974	188	1636

User	Well Name	Sub-watershed	Permit Number	Model Layer	Easting (m)	Northing (m)	Estimated Consumption[1] (m^3/d)	Maximum Permitted Consumption[2] (m^3/d)
Sugar Bush Well Supply	Well #3	Coldwater	1483-5MYQ36	6	609787	4934894	0	1636
Warminster Well Supply	Well #1	North River	4686-7BQS3T	4	616590	4944537	147	890
Warminster Well Supply	Well #3	North River	4686-7BQS3T	6	616571	4944540	0	890

*__Bold text__ indicates a permit within the Tier 2 study area. 1: Rate estimated from reported taking. 2: Rate estimated from maximum permitted taking. Consumptive use factor assumed equal 1.0.

Table 3.2: Future pumping rates for municipal supply wells within the study area.

User	Well Name	Sub-watershed	Permit Number	Model Layer	Easting (m)	Northing (m)	Future Consumption (m^3/d)
Orillia Water Supply System	Sandra Drive Well	Oro North	99-P-1256	***Discontinued in 2008***			
Maplewood Estates	Well #1	Oro North	02-P-1314	6	625395	4932101	26.0
Cedar Brook Subdivision Well Supply	Well No.1	Hawkestone	4817-6HJPXP	4	621408	4928432	7.8
Cedar Brook Subdivision Well Supply	Well No.2	Hawkestone	4817-6HJPXP	4	621415	4928437	8.8
Lake Simcoe Regional Airport	Well #2	Oro South	5348-6HKP2G	4	615711	4926394	3.6
Lake Simcoe Regional Airport	Well #3	Oro South	5348-6HKP2G	4	615660	4926265	1.2
Canterbury Subdivision Well Supply	Well 1	Oro South	92-P-3028	4	617805	4924105	5.4
Canterbury Subdivision Well Supply	Well 2	Oro South	92-P-3028	4	617799	4924108	6.7
Shanty Bay Well Supply	Well No. 1	Oro South	7520-6LJTGX	4	613048	4918904	42.4
Shanty Bay Well Supply	Well No. 2	Oro South	7520-6LJTGX	3	613048	4918904	43.3
Shanty Bay Well Supply	Well No. 3	Oro South	7520-6LJTGX	4	613028	4918911	86.0
Harbourwood Well Supply	Well No.2	Oro South	8643-6HKK9K	6	617919	4922286	51.9
Harbourwood Well Supply	Well No.3	Oro South	8643-6HKK9K	6	617853	4922342	51.5

Bold text indicates a permit within the Tier 2 study area. 1: Rate estimated from reported taking. 2: Rate estimated from maximum permitted taking. Consumptive use factor assumed equal 1.0

Table 3.3: Permitted groundwater takings (PTTW) within the model area.

Permit Number*	Model Layer	Easting (m)	Northing (m)	Sub-watershed	Category	Specific Purpose	Consumption Factor	Estimated Consumption[1] (m^3/d)[1]	Maximum Permitted Consumption[2] (m^3/d)
1664-6W3MCU	4	596800	4934500	Sturgeon River	Agricultural	Field and Pasture Crops	0.8	0.0	2071.2
0628-78CJEN	6	613527	4937148	North River	Commercial	Bottled Water	1	75.0	873.0
0628-78CJEN	6	613503	4937188	North River	Commercial	Bottled Water	1	83.7	873.0
3524-73QQUA	7	607930	4949745	Coldwater	Commercial	Golf Course Irrigation	0.7	1.9	4.2
5307-7GVLJL	4	604861	4933832	Coldwater	Commercial	Golf Course Irrigation	0.7	44.6	1427.1
1510-7DCLKQ	4	620123	4928370	**Hawkestone**	Commercial	Golf Course Irrigation	0.7	0.3	6.3
1510-7DCLKQ	4	620460	4928540	**Hawkestone**	Commercial	Golf Course Irrigation	0.7	0.0	6.3
1510-7DCLKQ	4	620200	4928057	**Hawkestone**	Commercial	Golf Course Irrigation	0.7	0.1	0.0
1510-7DCLKQ	7	620742	4928397	**Hawkestone**	Commercial	Golf Course Irrigation	0.7	0.0	179.2
0040-733RE2	3	603079	4932549	Willow Creek	Commercial	Golf Course Irrigation	0.7	1.2	45.8
0040-733RE2	3	603729	4933020	Willow Creek	Commercial	Golf Course Irrigation	0.7	105.7	687.4
0386-7AMLUY	4	598296	4919981	Willow Creek	Commercial	Golf Course Irrigation	0.7	21.1	687.4
0386-7AMLUY	6	598296	4919981	Willow Creek	Commercial	Golf Course Irrigation	0.7	37.2	1145.6
3474-759GY9	7	610681	4920539	Willow Creek	Commercial	Golf Course Irrigation	0.7	11.1	140.0
5066-7Y3MJ9	4	606404	4924599	Willow Creek	Commercial	Golf Course Irrigation	0.7	0.7	30.2
1635-8PSQJU	6	605687	4941970	Coldwater	Commercial	Snowmaking	0.2	--	14.8
2742-7E5LEK	4	612130	4930583	**Hawkestone**	Commercial	Snowmaking	0.5	6.2	327.5
4043-8JHKVC	4	612384	4933016	Coldwater	Dewatering	Pits and Quarries	0.25	--	95.9
01-P-1049	3	612906	4932955	**Hawkestone**	Dewatering	Pits and Quarries	0.25	--	57.0
1156-7WTJXC	4	613162	4931320	**Hawkestone**	Industrial	Aggregate Washing	0.25	91.6	95.6
01-P-1157	1	619553	4935633	**Oro North**	Industrial	Aggregate	0.25	158.1	925.0

Permit Number*	Model Layer	Easting (m)	Northing (m)	Sub-watershed	Category	Specific Purpose	Consumption Factor	Estimated Consumption[1] (m^3/d)[1]	Maximum Permitted Consumption[2] (m^3/d)
						Washing			
1635-8PSQJU	6	605713	4941832	Coldwater	Water Supply	Campgrounds	0.2	--	21.7
77-P-3033	5	606119	4945205	Coldwater	Water Supply	Campgrounds	0.2	19.3	115.2
5431-6LRLAA	6	620822	4940037	North River	Water Supply	Campgrounds	0.2	3.5	16.4
5701-6NLJ99	4	621400	4937100	**Oro North**	Water Supply	Campgrounds	0.2	0.1	7.2
5701-6NLJ99	4	621328	4937321	**Oro North**	Water Supply	Campgrounds	0.2	0.2	17.0
5701-6NLJ99	3	621250	4937050	**Oro North**	Water Supply	Campgrounds	0.2	0.4	14.4
5701-6NLJ99	3	621328	4937321	**Oro North**	Water Supply	Campgrounds	0.2	--	7.1
5701-6NLJ99	3	621250	4937050	**Oro North**	Water Supply	Campgrounds	0.2	--	6.9
5701-6NLJ99	5	621250	4937050	**Oro North**	Water Supply	Campgrounds	0.2	--	5.4
99-P-1053	3	626042	4935947	**Oro North**	Water Supply	Campgrounds	0.2	--	4.4
7528-8M5QPX	7	621947	4927551	**Oro South**	Water Supply	Campgrounds	0.2	--	16.5
3772-6EQGSY	5	597740	4923757	Willow Creek	Water Supply	Campgrounds	0.2	--	3.9
3772-6EQGSY	7	597843	4923884	Willow Creek	Water Supply	Campgrounds	0.2	--	6.8
3772-6EQGSY	5	597684	4923768	Willow Creek	Water Supply	Campgrounds	0.2	--	4.6
5353-5W4LB8	3	598021	4922077	Willow Creek	Water Supply	Campgrounds	0.2	7.7	71.4
0077-79UPRS	5	605590	4944977	Coldwater	Water Supply	Communal	0.2	26.1	168.4
8786-7GVNFK	3	605451	4933595	Coldwater	Water Supply	Communal	0.2	0.3	178.8
8786-7GVNFK	4	605467	4933708	Coldwater	Water Supply	Communal	0.2	0.0	59.0
8786-7GVNFK	4	605423	4933719	Coldwater	Water Supply	Communal	0.2	0.8	1112.8
4076-7HFJB6	6	612542	4937184	North River	Water Supply	Communal	0.2	0.0	202.2
4076-7HFJB6	6	612542	4937184	North River	Water Supply	Communal	0.2	0.0	202.2
91-P-3105	6	617632	4937655	North River	Water Supply	Communal	0.2	--	157.2
1586-62FLP2	4	611554	4918074	**Oro South**	Water Supply	Communal	0.2	0.6	16.2

*__Bold text__ indicates a permit within the Tier 2 study area. 1: Rate estimated from reported taking. 2: Rate estimated from maximum permitted taking.

Table 3.4: Permitted surface water takings (PTTW) within the model area.

Permit Number*	UTM Easting (m)	UTM Northing (m)	Subwatershed	Category	Specific Purpose	Consumption Factor	Days per year	Reported Consumption[2] (m^3/day)	Maximum Consumption[2] (m^3/d)
1510-7DCLKQ	620200	4928057	**Hawkestone**	Commercial	Golf Course Irrigation	0.7	100	19.7	194
3041-77VHXW	603690	4920430	Willow Creek	Commercial	Golf Course Irrigation	0.7	35	*No Data*	103
3041-77VHXW	604034	4920278	Willow Creek	Commercial	Golf Course Irrigation	0.7	120	114.4	403
3474-759GY9	610681	4920539	Willow Creek	Commercial	Golf Course Irrigation	0.7	42	69.4	230
3524-73QQUA	607930	4949745	Coldwater	Commercial	Golf Course Irrigation	0.7	160	110.4	637
5205-6CJH4Y	623231	4941925	North River	Commercial	Golf Course Irrigation	0.7	60	127.7	298
6556-83SQ94	609691	4923429	Willow Creek	Commercial	Golf Course Irrigation	0.7	180	28.8	202
84-P-3007	614658	4939586	North River	Commercial	Golf Course Irrigation	0.7	150	69.9	224
8680-6A9M3V	606404	4924599	Willow Creek	Commercial	Golf Course Irrigation	0.7	127	1	63
1635-8PSQJU	606475	4942498	Coldwater	Commercial	Snowmaking	0.5	90	*No Data*	2014
7166-7F3L2Q	614125	4929975	**Hawkestone**	Miscellaneous	Other - Miscellaneous	1	365.25	*No Data*	114
5353-5W4LB8	597977	4922110	Willow Creek	Recreational	Other - Recreational	0.1	365.25	169	1890

* **Bold text** indicates a permit within the Tier 2 study area

Table 3.5: Monthly pumping rates for municipal supply wells within the model area (m^3/day).

User	Well Name	Jan	Feb	Mar	Apr	May	Jun	Jul	Aug	Sep	Oct	Nov	Dec
Barrie Well Supply	Well #13 at 168 Johnson Street	160	81	463	456	964	1389	1727	1559	1183	745	679	606
Barrie Well Supply	Well #16 at 101 Brown Wood Lane	910	829	911	947	1286	2233	2740	2298	1447	1343	494	34
Barrie Well Supply	Well #9 at 168 Johnson Street	236	117	693	616	1274	1756	2436	2002	1391	1184	757	598
Bass Lake Woodlands Well Supply	Well #3	10	13	12	20	80	124	107	102	54	26	13	14
Bass Lake Woodlands Well Supply	Well No. 1	15	23	15	17	24	18	56	50	57	35	27	15
Bass Lake Woodlands Well Supply	Well No. 2	67	53	50	54	41	16	1	1	8	26	42	55
Canterbury Subdivision Well Supply	**Well 1**	4	3	3	3	5	8	8	7	5	4	4	4
Canterbury Subdivision Well Supply	**Well 2**	4	3	3	4	5	8	8	19	5	4	4	4
Cedar Brook Subdivision Well Supply	**Well No.1**	7	6	7	7	7	8	9	8	7	7	6	7
Cedar Brook Subdivision Well Supply	**Well No.2**	8	7	7	7	8	10	10	9	8	7	7	7
Coldwater Well Supply	Swaile Well (Standby) (WWR 5725508	1	2	2	1	2	2	1	2	2	5	4	4
Coldwater Well Supply	Well PW 93-2 (WWR 5729906)	179	135	141	156	223	244	179	113	154	181	222	204
Coldwater Well Supply	Well PW93-4 (WWR5729997)	272	323	319	293	273	274	342	417	325	279	240	248
Craighurst Well Supply	Well No.1	0	0	0	0	0	0	0	0	0	0	0	0
Craighurst Well Supply	Well No.2	6	5	5	6	9	12	12	10	8	7	7	8
Craighurst Well Supply	Well No.3	10	8	8	11	16	20	19	17	13	13	13	13
Del Trend Subdivision Well Supply	Del Trend Well #1 (WWR 5728243)	10	9	10	12	57	48	15	10	13	18	17	18
Del Trend Subdivision Well Supply	Del Trend Well #2 (WWR 5728671)	12	10	10	12	41	68	31	8	14	19	31	32
Del Trend Subdivision Well Supply	Del Trend Well #3 (WWR 5733452)	55	53	55	71	66	68	210	195	136	61	28	32
Harbourwood Well Supply	**Well No.2**	16	20	23	31	49	74	76	74	64	63	37	25
Harbourwood Well Supply	**Well No.3**	65	62	55	56	52	48	46	38	29	20	42	58
Horseshoe Highlands Subdivision Well Supply	Well #1 (5723788)	205	202	211	191	351	443	448	447	355	237	177	205

User	Well Name	Jan	Feb	Mar	Apr	May	Jun	Jul	Aug	Sep	Oct	Nov	Dec
Horseshoe Highlands Subdivision Well Supply	Well #2 Standby Well (5721850)	0	0	0	0	0	0	0	0	0	0	0	0
LSR Airport	**Well #2**	2	2	1	2	3	3	5	5	5	4	4	4
LSR Airport	**Well #3**	1	1	0	0	1	1	2	2	2	2	1	1
Maplewood Estates Well Supply	**Well (PW #1)**	19	20	19	21	24	28	28	30	24	24	24	19
Maplewood Estates Well Supply	**Well 2**	0	0	0	0	0	0	0	0	0	0	0	0
Medonte Hills Well Supply	Well 1	21	22	23	23	29	34	36	34	31	31	31	29
Medonte Hills Well Supply	Well 2	33	31	32	33	34	42	51	46	42	36	34	41
Midhurst Well Supply	Carson Road Well 5 (formerly Well 4)	163	148	147	179	286	404	369	356	281	203	182	183
Midhurst Well Supply	Greenpine Well 4	124	126	118	132	262	335	345	349	227	163	138	142
Midhurst Well Supply	Idlewood Well 2 (WWR 5711983)	66	67	64	80	137	169	176	169	129	91	74	77
Midhurst Well Supply	Idlewood Well 3 (WWR 5718775)	209	216	198	234	417	543	565	541	421	295	240	257
Orillia Water Supply System	Well 1 & 2 (rates combined with Well 2-Obs Well)	35	28	61	65	96	79	125	160	167	113	158	85
Orillia Water Supply System	Sandra Drive Well	0	0	0	0	0	0	0	0	0	0	0	0
Orillia Water Supply System	Well #3	341	260	122	428	965	1013	1012	864	795	825	1016	879
Orillia Water Supply System	ORILLIA WELL 2	2	1	4	2	19	43	69	111	76	36	15	13
Shanty Bay Well Supply	**Well No. 1**	64	69	56	62	57	13	3	2	20	19	45	61
Shanty Bay Well Supply	**Well No. 2**	48	42	48	51	43	17	33	36	37	31	40	49
Shanty Bay Well Supply	**Well No. 3**	2	2	1	6	84	214	211	201	110	64	24	3
Snow Valley Highlands Well Supply	Well 1 (WWR 5723284)	33	34	35	38	48	54	54	50	46	39	34	37
Snow Valley Highlands Well Supply	Well 2 (WWR 5724900)	33	34	33	39	48	51	53	49	46	43	34	38
Sugar Bush Well Supply	Well #1	46	48	37	36	55	55	54	52	48	49	49	50
Sugar Bush Well Supply	Well #2	158	166	166	172	182	196	251	221	196	171	178	180
Sugar Bush Well Supply	Well #3	0	0	0	0	0	0	0	0	0	0	0	0
Warminster Well Supply	Well #1 WWR 5708757	190	184	184	179	138	144	149	134	129	127	127	107
Warminster Well Supply	Well #3 WWR 5708758	0	0	0	0	0	0	0	0	0	0	0	0

Table 3.6: Monthly permitted groundwater takings (PTTW) within the model area (m^3/day).

Permit Number	Consumption Factor	Jan	Feb	Mar	Apr	May	Jun	Jul	Aug	Sep	Oct	Nov	Dec
0040-733RE2	0.7	0.3	0.3	0.4	1.1	1.9	2.2	2.3	2.3	1.9	1.2	0.6	0.2
0040-733RE2	0.7	0.0	0.0	0.0	69.4	139.6	258.0	324.1	268.4	138.8	61.6	0.0	0.0
0077-79UPRS	0.2	23.1	22.7	23.2	24.6	30.4	28.9	34.5	29.6	24.3	23.7	23.1	24.2
01-P-1049	0.25	0.00	0.00	0.00	0.00	97.25	97.25	97.25	97.25	97.25	97.25	97.25	0.00
01-P-1157	0.25	0.0	0.0	0.0	101.7	367.2	371.4	305.5	342.3	218.9	130.2	49.7	0.0
0386-7AMLUY	0.7	0.0	0.0	0.0	24.9	37.9	52.9	87.7	30.1	17.8	0.7	0.0	0.0
0386-7AMLUY	0.7	0.0	0.0	0.0	41.7	59.0	81.5	152.1	75.2	27.7	1.1	4.9	0.0
0628-78CJEN	1	58.5	62.3	63.3	65.7	65.1	81.2	85.8	82.0	88.3	81.0	93.7	73.1
0628-78CJEN	1	65.5	64.8	73.4	62.7	84.9	91.7	93.1	96.2	99.2	93.7	89.7	88.4
1156-7WTJXC	0.25	0.0	0.0	100.1	124.2	139.9	139.9	139.9	139.9	139.9	113.1	56.2	0.1
1510-7DCLKQ	0.7	0.0	0.0	0.0	0.3	0.6	0.7	0.8	0.7	0.6	0.3	0.0	0.0
1510-7DCLKQ	0.7	0.0	0.0	0.0	0.0	0.1	0.1	0.0	0.1	0.0	0.0	0.0	0.0
1510-7DCLKQ	0.7	0.0	0.0	0.0	0.1	0.2	0.2	0.2	0.2	0.2	0.1	0.0	0.0
1510-7DCLKQ	0.7	0.0	0.0	0.0	0.0	0.0	0.0	0.0	0.0	0.0	0.0	0.0	0.0
1586-62FLP2	0.2	0.8	0.6	0.5	0.6	0.5	0.6	0.6	0.7	0.6	0.6	0.6	0.6
1635-8PSQJU	0.2	60.00	60.00	0.00	0.00	0.00	0.00	0.00	0.00	0.00	0.00	0.00	60.00
1635-8PSQJU	0.2	0.00	0.00	0.00	0.00	51.80	51.80	51.80	51.80	51.80	0.00	0.00	0.00
1664-6W3MCU	0.8	0.0	0.0	0.0	0.0	0.0	0.0	0.0	0.0	0.0	0.0	0.0	0.0
2742-7E5LEK	0.5	0.0	0.0	0.0	0.0	22.0	0.0	0.0	22.0	0.0	0.0	0.0	29.3
3474-759GY9	0.7	0.0	0.0	0.0	0.0	0.0	7.6	63.6	39.6	17.8	0.0	0.0	0.0
3524-73QQUA	0.7	0.0	0.0	0.0	2.0	3.4	4.1	4.2	4.2	3.4	1.1	0.0	0.0
3772-6EQGSY	0.2	0.00	0.00	0.00	7.80	7.80	7.80	7.80	7.80	7.80	0.00	0.00	0.00
3772-6EQGSY	0.2	0.00	0.00	0.00	13.60	13.60	13.60	13.60	13.60	13.60	0.00	0.00	0.00
3772-6EQGSY	0.2	0.00	0.00	0.00	9.20	9.20	9.20	9.20	9.20	9.20	0.00	0.00	0.00
4043-8JHKVC	0.25	0.00	0.00	0.00	0.00	163.66	163.66	163.66	163.66	163.66	163.66	163.66	0.00
4076-7HFJB6	0.2	0.0	0.0	0.0	0.0	0.0	0.0	0.0	0.0	0.0	0.0	0.0	0.0

Permit Number	Consumption Factor	Jan	Feb	Mar	Apr	May	Jun	Jul	Aug	Sep	Oct	Nov	Dec
4076-7HFJB6	0.2	0.0	0.0	0.0	0.0	0.0	0.0	0.0	0.0	0.0	0.0	0.0	0.0
5066-7Y3MJ9	0.7	0.0	0.0	0.0	0.6	1.2	1.6	1.3	1.5	1.3	0.9	0.2	0.0
5307-7GVLJL	0.7	99.8	0.1	0.0	16.8	48.6	46.3	85.8	56.0	33.1	13.3	20.1	108.6
5353-5W4LB8	0.2	10.4	0.0	0.0	0.0	0.0	0.0	14.0	17.0	13.6	13.4	13.7	0.0
5431-6LRLAA	0.2	0.0	0.0	0.0	0.6	4.0	6.0	11.4	11.3	7.0	0.5	0.0	1.0
5701-6NLJ99	0.2	1.0	0.0	0.0	0.0	0.0	0.0	0.0	0.0	0.0	0.0	0.0	0.0
5701-6NLJ99	0.2	2.3	0.0	0.0	0.0	0.0	0.0	0.0	0.0	0.0	0.0	0.0	0.0
5701-6NLJ99	0.2	4.5	0.0	0.0	0.0	0.0	0.0	0.0	0.0	0.0	0.0	0.0	0.0
5701-6NLJ99	0.2	0.00	0.00	0.00	0.00	17.00	17.00	17.00	17.00	17.00	0.00	0.00	0.00
5701-6NLJ99	0.2	0.00	0.00	0.00	0.00	16.40	16.40	16.40	16.40	16.40	0.00	0.00	0.00
5701-6NLJ99	0.2	0.00	0.00	0.00	0.00	13.00	13.00	13.00	13.00	13.00	0.00	0.00	0.00
7528-8M5QPX	0.2	0.00	0.00	0.00	0.00	39.28	39.28	39.28	39.28	39.28	0.00	0.00	0.00
77-P-3033	0.2	18.4	16.8	17.3	17.8	22.7	23.8	21.3	22.4	18.5	16.8	16.0	19.5
8786-7GVNFK	0.2	0.6	0.3	0.2	0.1	0.3	0.3	0.5	0.4	0.2	0.2	0.1	0.6
8786-7GVNFK	0.2	0.0	0.0	0.0	0.0	0.0	0.0	0.0	0.0	0.0	0.0	0.0	0.0
8786-7GVNFK	0.2	5.9	0.1	0.1	0.1	0.2	0.3	0.7	0.3	0.2	0.1	0.1	1.0
91-P-3105	0.2	157.20	157.20	157.20	157.20	157.20	157.20	157.20	157.20	157.20	157.20	157.20	157.20
99-P-1053	0.2	0.00	0.00	0.00	0.00	10.60	10.60	10.60	10.60	10.60	0.00	0.00	0.00

Table 3.7: Current groundwater consumption summary.

Current Groundwater Consumption (m^3/yr)					
Watershed Name	**Municipal**	**Unserviced**	**PTTW**	**Agricultural**	**Total Consumption**
Oro North	8,644	64,390	66,723	15,000	154,757
Hawkestone	5,504	33,185	56,702	10,000	105,391
Oro South	96,987	117,482	6,240	13,000	233,709

Table 3.8: Future groundwater consumption summary.

Future Groundwater Consumption (m^3/yr)					
Watershed Name	**Municipal**	**Unserviced**	**PTTW**	**Agricultural**	**Total Consumption**
Oro North	9,508	90,146	66,723	15,000	181,377
Hawkestone	6,054	46,460	56,702	10,000	119,216
Oro South	106,686	164,475	6,240	13,000	290,401

3.4 Figures

Figure 3.1: Permitted water users within the model area.

Figure 3.2: Permitted water users within the study area subwatersheds.

4 PRMS Model Development and Calibration

4.1 Introduction

Surface water and hydrological processes were simulated using the U.S. Geological Survey (USGS) Precipitation-Runoff Modeling System (PRMS) code. The original version of the code is documented in Leavesley *et al.* (1983); a modified version of the code was implemented as a sub-model in GSFLOW (Markstrom *et al.*, 2008). The PRMS submodel in GSFLOW can run separately or in a fully-integrated manner, which combines the PRMS model with the MODFLOW-NWT groundwater model. The following section describes the construction and initial calibration of the PRMS portion of the GSFLOW model. GSFLOW provides the ability to run the groundwater/surface water models separately which simplifies model construction; however, during this model development stage, feedback from the groundwater flow system must be assumed negligible.

4.2 Model Description

The PRMS is an open-source code for calculating all components of the hydrologic cycle at a watershed, subwatershed, or cell-based scale. PRMS is a modular, deterministic, physically-based distributed-parameter model developed to evaluate the impacts of various combinations of precipitation, climate, topography, soil type, and land use on streamflow and groundwater recharge. The modular design provides a flexible framework for model enhancement. The PRMS code is extremely well documented in Leavesley *et al.* (1983) and has been used recently in many applications across the US, in Europe (Barth, 2005; Ely, 2006; Yeung, 2005), and in nearby watersheds (e.g., TRCA, 2008, Earthfx, 2008, CLOCA 2008, Earthfx, 2010a, and Earthfx 2010b). When run independently (i.e., in PRMS-only mode), a simple cell-based linear groundwater reservoir is used in place of the links to the MODFLOW-NWT code.

To use PRMS, the study area is first discretized into a planimetric grid, herein referred to as cell-based hydrologic response units (HRUs). Each cell HRU is then characterized based on slope, slope aspect, elevation, vegetation type, soil type, land use, and surficial geology; such that every cell HRU within the model domain has a unique set of properties. Daily climate data (i.e., rainfall, snowfall, and minimum and maximum temperature) are assigned to each cell based on an inverse-squared-distance weighting scheme, and daily solar radiation is adjusted for cell slope and aspect by the model. As previously discussed, distributed hourly rainfall rates were derived from NEXRAD radar data to better capture the spatial and temporal distribution of small-scale storm events. Water and energy balances were computed at every time step for every cell HRU. The routing of water between cells is defined by a cascade flow network based on basin topography. The cascade directs outflows (i.e., runoff and interflow) of one (or many) upslope cell(s) into inflow (i.e., run-on) to one (or many) downslope cells.

For this study, square cells, 50 m on a side, were found to adequately represent the distribution of land use, topography, and soil properties within the model boundary. The PRMS grid contained 740 rows and 740 columns (547,600 cells). The grid covered the entire study area and extended beyond the boundaries of the groundwater model, covering an area of 1370 square kilometres (km²).

A flow chart describing the operation of the PRMS code is shown in Figure 4.1. The reader is referred to Leavesley *et al.* (1983) and Markstrom *et al.* (2008) for a more complete description of the program code and underlying theory. The model tracks volumes of water for each cell in a number of storage reservoirs. These include interception storage, depression storage, snowpack storage, capillary soil moisture zone storage, gravity soil moisture zone storage (i.e., water in excess of field capacity), preferential flow storage, and groundwater storage (if GSFLOW is run in PRMS-only mode). A two-layer, energy-balance model for the snowpack, shown schematically in Figure 4.2, computes snowpack depth, density, albedo, temperature, sublimation, and snowmelt on a daily basis using maximum and minimum air temperature, solar radiation, and precipitation data. The energy-balance snowpack model is combined with an aerial snow-depletion curve to simulate the sub-cell spatial coverage of the snowpack during the snowmelt phase at shallow snowpack depths (DeWalle and Rango, 2008).

Each cell can contain both pervious and impervious surfaces and the water balance for every cell is computed independently at every time step. For both types of areas, the model first computes interception by vegetation. The amount intercepted depends on vegetation type, precipitation type (rain, snow, or mixed) and winter/summer vegetation cover density. When interception storage capacity is exceeded, the surplus is allowed to fall though onto the snowpack, if present, or directly onto the ground surface (a process commonly termed throughfall or net rainfall). In impervious areas, the model computes the capture of precipitation by depression storage. When depression storage capacity is exceeded, the surplus is allowed to runoff. Water is removed from the depression storage reservoir in each cell by evaporation.

The snowpack energy balance model is used to determine the amount of snowmelt on pervious and impervious areas on a sub-daily basis to account for differences in the night and day energy flux. For a detailed description of the model, see Anderson (1968), Obled and Rosse (1977), or Leavesley *et al*. (1983). The snowpack is treated as a porous media, where liquid water can be stored and potentially re-freeze.

During precipitation events, the model first determines whether a snowpack exists. If the temperature is below a user-defined base (or critical) temperature (T_b), all throughfall (i.e., precipitation in excess of interception storage) is added to the snowpack as new snow. If the temperature is higher, the throughfall is added as rain to the snowpack and is used to raise the temperature of the snowpack through sensible and latent heat exchange. If the energy input is high enough and the snowpack has become isothermal, all or part of the snowpack can melt and runoff. The snowpack can also melt or refreeze based on air temperature change and is subject to sublimation.

Snowmelt is assumed to infiltrate the soil up to a maximum daily amount and any excess is allowed to runoff. For this study, a maximum rate of frozen soil infiltration was assigned based on a proportion of the saturated hydraulic conductivity of the soil type (assumed to be 5% of the non-frozen hydraulic conductivity).

Throughfall in the absence of a snowpack is partitioned between infiltration and runoff. The stand-alone PRMS code included a “contributing area” method to partition flows (Dickinson and Whiteley, 1970) when using daily precipitation data and a modified Green and Ampt (1911) method when precipitation data are available at shorter time intervals. Earthfx has adopted the PRMS Green and Ampt module (Dawdy *et al.*, 1972) in GSFLOW to allow hourly precipitation data to be used. In this module, infiltration is computed with the Green and Ampt equation using information on the saturated hydraulic conductivity of the soil, the volume of water in the

soil (i.e., antecedent conditions), and the capillary drive. Runoff is calculated as the excess over the infiltration capacity.

Percolation to groundwater is assumed to have a maximum daily limit and excess infiltration is diverted to runoff when the soil zone storage reservoirs reach capacity. This form of runoff is termed "Dunnian" runoff (Markstrom *et al.*, 2008) and is the predominant form of runoff in humid climates such as the Oro study area. The maximum daily infiltration limit was assigned based on the saturated vertical hydraulic conductivity of the surficial soils (assuming a unit gradient). Water held in the soil zone is updated every time step. The soil storage reservoir is depleted by ET, discharge to downslope HRUs as interflow, or percolation to the groundwater reservoir as gravity drainage over time.

During PRMS-only simulations, percolation is fed to a linear groundwater reservoir associated with every HRU cell. Lateral groundwater movement can be handled either using a separate groundwater reservoir cascade algorithm or by assigning a single groundwater reservoir for an entire sub-catchment. The latter option was used in this calibration step. Discharge to streams from the groundwater reservoirs occurs at a rate dependent on the volume of water stored in the groundwater reservoir and a linear decay coefficient that can be pre-determined using gauge discharge records (Linsley *et al*., 1975). In the integrated model (i.e., in GSFLOW mode), the cascading linear groundwater reservoirs are not used, as MODFLOW takes care of the groundwater processes and groundwater discharge to surface water bodies..

As previously noted, unique values for all parameters were assigned for each 50 m cell in the model. To simplify parameter assignment and to enforce consistency across the study area, cells were first assigned classes based on land-use and soil type mapping (discussed further on). Parameter values were then assigned to model cells using tables of lookup values assigned to each land use and surficial geology class. For example, soil properties such as porosity and hydraulic conductivity were assigned to soil classes while properties such as percent imperviousness were assigned to land-use class. VIEWLOG-GIS was used as a data pre-processor to assign classes and perform the lookups needed to assign parameters.

4.3 Input Data for the PRMS Model

A variety of input data and model parameters were defined prior to PRMS analysis. Consistent assumptions and parameter values were applied across all subwatersheds within the study area (i.e. consistent values for forested Newmarket Till were used in each subwatershed). The discussion of model parameters is grouped into five sub-sections, including:

1. topography-related properties (e.g., slope and slope aspect);
2. soil properties that can be correlated to surficial geology;
3. vegetative cover and imperviousness that can be related to land-use;
4. climate-based properties such as daily climate inputs (precipitation, minimum and maximum air temperature, and solar radiation); and
5. other parameters related to hydrological processes such as stream discharge (total flow and baseflow), evapotranspiration and other losses, groundwater recharge, and surface water takings.

4.3.1 Topography

Topography for the model area is based on a 5 m lidar digital elevation model (DEM) provided by MNR which was re-sampled to the 50 m cells. Re-sampling was done by averaging the 100 elevation values located within every 50 m cell HRU.

Slope and slope aspect are utilized to correct the amount of shortwave solar radiation arriving at land surface used in snowmelt and evapotranspiration (ET) calculations. Recorded solar irradiation data are corrected in the PRMS model for land-surface slope and slope aspect as well as for time of year. For example, a north-facing valley slope will get less solar radiation than the south-facing slope and will therefore have lower potential ET rates and a longer persisting snowpack. Slope and slope aspect values were calculated from the DEM using a nine-point planar regression technique that fits a plane to every cell and its eight surrounding cells, in a similar fashion to Moore *et.al.* (1991). Slope data are also used to generate the cascade flow network.

As noted earlier, the PRMS code incorporates a cascading flow algorithm that routes overland flow and interflow from one cell to adjacent cells (Markstrom *et al.*, 2008). In other (simpler) catchment models, runoff generated at any point within the model is routed directly to stream channels, without having the possibility of infiltrating somewhere along the pathway to its ultimate destination, the stream network. The cascading algorithm transfers runoff from one cell and adds it (as run-on) to the total volume of water available for infiltration and/or runoff in the downslope cell. Accumulation of runoff from upstream cells and the convergence of the generally dendritic flow network results in more physically realistic patterns of ET distribution, runoff contributing to streams, and enhanced recharge in the downslope areas.

Terrain analysis was required to define the cascade overland flow routing network. An 8-direction steepest decent method was used because it generates an efficient many-to-one cascade network (i.e., only one outflow path per cell is defined) and it avoids undesirable upslope numerical dispersion (see Seibert and McGlynn, 2007).

A sample cascade flow network is shown in Figure 4.3. Cascades are directed to adjacent cells until a stream reach or a swale (i.e., a closed depression) is encountered. The amount of runoff allowed to cascade is dependent on the cell slope. Two model parameters are used to define this amount.

4.3.2 Surficial Geology and the Soil Zone

Soil properties have a significant influence on hydrological processes because they control the amount of water that can infiltrate and be transmitted to the water table as well as the amount of water lost to evaporation and transpiration by plants (i.e., actual ET). In PRMS, the soil zone is divided into two main reservoirs: the capillary reservoir represents the tension storage above field capacity and is susceptible to ET losses; the gravity reservoir represents the remaining available storage within the soils column where water can drain freely to recharge the groundwater system. Soil water movement is controlled by two main factors: (i) the ability of the soil to transmit water (hydraulic conductivity); and (ii) the gravity and suction forces acting on the soil water. The PRMS model simplifies the simulation of unsaturated flow in the soil zone by assuming that storage within this zone can be filled within a day at a rate limited by the Green and Ampt model. For PRMS-only simulations, all water above field capacity (remaining after ET) is available to percolate to the water table. If the soil permeability is low, water will be

retained in the gravity reservoir and will gradually percolate over a period of days. Soil water-holding capacity in the capillary and gravity reservoirs (see Markstrom et al., 2008) are given as model parameters that are a function of soil zone thickness, porosity, field capacity, and wilting point. These values were assigned to each surficial geology type and then assigned to each HRU cell based on surficial geology mapping, with some exceptions as described below.

OGS (2003) surficial geology maps were used to assign soil types found in the study area. The surficial geology classes and associated parameters used by the PRMS model are listed in Table 4.1. Consistent parameter values were assigned to each geologic material type across the basin. Hydraulic conductivities and other soil properties were estimated initially from the available literature (e.g., Chow, 1964; Linsley et al., 1975; Fetter, 1980; Todd, 1980; DeWalle and Rango, 2008) and refined (where necessary) during model calibration to improve the match between observed and simulated flows. The PRMS code expects inputs in a mix of imperial and metric units. Conversions were applied to the tabulated values in the data pre-processors.

Some soil properties were estimated based on land-use types specific to agriculture, natural areas (i.e., forests and wetlands), and urban areas. It was assumed that soil characteristics that relate to wilting point, field capacity, and porosity should be relatively consistent for the soils in these three land use types for the region. For example, all agricultural soils were assumed to be a sandy loam with a large Plant Available Water (PAW) store (Ward and Trimble, 2003) having a wilting point, field capacity, and porosity of 0.1, 0.2, and 0.4, respectively. Natural areas, which exist mainly in riparian areas, were assumed to be rather peaty having a wilting point, field capacity, and porosity of 0.05, 0.1, and 0.9, respectively (Fetter, 1980; Todd, 1980). Urban areas were assumed to be mostly grass lawns and parks 6 inches deep and were given a wilting point, field capacity, and porosity of 0.1, 0.2, and 0.4, respectively. Making this assumption reduced the amount of parameterization and allowed the calibration effort to focus on adjusting effective soil depth values through model calibration. The proportion of the model area consisting of natural, agricultural and urban areas is 48%, 40%, and 9%, respectively; the remaining 3% consists of other land use type such as pits and quarries.

4.3.3 Land Use

Land use patterns were defined using the LSRCA ELC land use coverage which covered all of the immediate study area (Oro North, Hawkestone, and Oro South watersheds). SOLRIS data (MNR, 2008) was used to infill the remaining areas outside of the Lake Simcoe Watershed. Land use types applied are listed in Table 4.2: Land use lookup table.

The type of land cover has a strong effect on the water balance. Interception and ET are directly influenced by vegetation type and cover density, which in turn, affect runoff and infiltration rates. Conversion of natural to non-natural land use generally increases the amount of impervious cover leading to increased evaporation from depression storage and increased runoff. At the same time however, ET from interception and soil zone storage are decreased, making the net impact to groundwater recharge more difficult to predict intuitively, and thus it is best done using a distributed water-balance model such as PRMS and GSFLOW.

Consistent parameter values were assigned to each land-use type across the study area. Vegetation type was determined from land-use classifications. Cover density and transmission factors were estimated initially from the available literature (e.g., Hardy et al., 2004) and refined (where necessary) during model calibration to improve the match between observed and simulated flows.

4.3.4 Climate Data

Climate data (i.e., precipitation as rain, precipitation as snow, daily maximum temperatures, daily minimum temperatures, and daily solar irradiation) were collected from a variety of sources. Precipitation and temperature data for Water Year (WY) 1980 to WY 2011 were obtained from Environment Canada stations, MNR infilled data, and NEXRAD data. For the model calibration runs, hourly rainfall values from the NEXRAD data were interpolated to each cell HRU using an inverse-distance squared weighting technique. For the long-term hydrologic assessment and drought simulations, hourly climate data were obtained using the MNR infilled climate dataset (Schroeter and Associates Inc. and AquaResources (2008)). Hourly infill data sets were generated for Barrie WPCC (6110557), Coldwater-Warminster (6111769), Midhurst (6115099), and Orillia Brain (6115811). The infilled data cover the period of 1950 to 2005 and were used for drought analysis. The 20-year long term simulation ran from WY1986 to WY2006.

Hourly data were used in the integrated groundwater/surface water model to calculate runoff and infiltration. Data for the study period were estimated from **Nex**t-Generation **Rad**ar (NEXRAD) data, available from the U.S. National Weather Service (USNWS) - an agency of the National Oceanic and Atmospheric Administration (NOAA). The data, which come in the form of a Digital Precipitation Array (DPA), provide a near-continuous hourly dataset covering the past decade. Publically available EC climate data are not officially verified or calibrated after 2006.

The NEXRAD high-resolution Doppler radar station KBUF (Buffalo, NY) is closest (within 200 km) to the study area. The KBUF dataset has 9087 distributed cells which span a radius of 232 km. Figure 4.4 shows the layout of the NEXRAD cells superimposed on the model boundary. The centroids of each cell were designated as a Virtual Climate Station (VCS). Every VCS had a unique temporal precipitation dataset and a simple inverse-distance-squared technique was used to interpolate the data between the virtual stations.

The NEXRAD dataset covers a period from February 23, 1996 to August 30, 2011. Figure 4.5 plots the cumulative missing data-days and shows that only 79 days out of a total of 5668 (or 1.4%) were missing. The longest continuous data gap was 9 days.

A more detailed NEXRAD error analysis and ground-truthing was completed to reduce possible systematic and random errors associated with the radar data when compared to measurements made at ground locations. From this analysis, NEXRAD DPA correction factors were determined for the months of March through November (i.e., the non-winter months). Winter-month precipitation estimates were derived from the other sources mentioned above.

The incoming solar radiation dataset was built based in the average from the measurements from four climate stations maintained by Environment Canada after 1985; these stations include: 611KBE0: Egbert CARE; 6142285: Elora Research Station; 6158350: Toronto; and 6158740: Toronto MET Research Station. Unfortunately, the most recent record among these four gauges occurs on August 31, 2003; therefore the remaining date up to the end of the study period (2011) had to be infilled using data from the University of Waterloo and the University of Toronto Mississauga campus. Averaging of these records was done because the data quality is typically quite poor for all stations and no station has a period of record that extends across the entire modelling period. In all, the solar radiation record extends from 1956 to present.

In GSFLOW, the incident solar radiation is adjusted at every HRU based on slope and slope aspect, vegetation type, winter/summer cover density, and winter transmission factor (i.e., percentage of short-wave radiation passing through the winter vegetation canopy). This data

input is the primary driver of potential evaporation and contributes a large portion to the snowpack energy balance formulation which influences snowmelt.

Two stream discharge targets were used for the preliminary PRMS-only calibration efforts: WSC gauge 02EC020: Hawkestone Creek at Hawkestone, and 02ED007: Coldwater River at Coldwater.

4.3.5 Evapotranspiration

Water entering the soil in pervious areas is subject to evapotranspiration (ET). The PRMS code has three methods for calculating potential evapotranspiration (PET). The Jensen and Haise method, which requires only two climate parameters (temperature and incident radiation), was used in this study to estimate daily PET.

Actual evapotranspiration (AET) depends on several factors including: PET, the amount of water in interception storage, the amount of water in depression storage, the soil type and the amount of water in the soil zone. In PRMS, the soil zone is stratified into two layers, of which the capillary soil zone is susceptible to ET. Water is extracted from the gravity soil zone, if available, to replenish the capillary zone when it is not at capacity. The capillary zone has an evaporation extinction depth, below which only transpiration can occur.

AET processes are assumed to follow a hierarchy whereby if the amount of water in interception storage and depression storage is insufficient to meet PET demand, the deficit is extracted from the capillary zone (i.e. the upper soil zone) at a rate based on soil type and the ratio of the current volume of water stored in the capillary zone to its maximum storage capacity. If PET demand is still not met, moisture is extracted from the gravity soil zone reservoir to replenish the capillary deficit (Markstrom *et al.*, 2008). Once below the evaporation extinction depth, transpiration continues at a rate dependent on canopy coverage, vegetation type, soil type, and the ratio of the current volume of water stored in the capillary soil zone to its maximum storage capacity. Soil zone depth is defined by the average rooting depth of the predominant vegetation and adjusted during model calibration. Initial storage in the upper soil zone was set to 50% of soil zone capacity. The water available for AET is equal to the difference between the water stored and wilting point. Once PET has been satisfied, any excess water, defined as the soil moisture above field capacity (i.e., the amount of free-draining water in the gravity soil zone), is allowed to percolate to the groundwater reservoirs as groundwater recharge.

4.4 Model Construction

A preliminary step to the construction of the GSFLOW model was to test the model's ability to simulate distributed surface water processes, which include:

a) The accounting and distribution of incoming rainfall, snowfall, temperature, and solar radiation;
b) The separation of precipitation between interception and throughfall;
c) The simulation of snowmelt processes;
d) The parsing of throughfall, snowmelt, and upslope contributions between runoff and infiltration by a combination of infiltration capacity (i.e., Hortonian runoff) and saturation

excess (i.e., Dunnian runoff) mechanisms, and impervious areas based on land use mapping;
e) The accounting of soil moisture amongst the capillary and gravity soil zone stores;
f) The routing of runoff and interflow downslope, following the model area's topography relating to slope (i.e., cascading flow);
g) Recharge from the gravity store of the groundwater reservoir; and
h) The rate at which the groundwater reservoir releases its storage in the form of baseflow.

The testing was accomplished by running PRMS independently of MODFLOW. With the exception of the final process (h.) the parameterization used to test the surface water model processes are completely transferable to GSFLOW running as a fully-integrated surface water/groundwater model.

When considering the limitations and uncertainty of the input and calibration target data and accepting the fact that absolute knowledge of distributed hydrological processes is impossible (due primarily to the uncertainty associated with discharge measurements, precipitation and temperature measurements including errors associated with spatial interpolation, and due to the limits of model conceptualization and set boundary conditions) there is a high probability that there will exist no true unique/global solution to the surface water model. With this in mind, the PRMS-only calibration was completed while considering the probable range and sensitivities of parameter values that will likely need adjusting once influences of groundwater become a factor. With this prior knowledge, the GSFLOW calibration efforts were reduced as the hydrological element to this modelling exercise was well investigated during this step.

4.5 PRMS Modelling Results

The following section will present results from the 9-year PRMS-only calibration in which the long-term average groundwater recharge was applied to the steady-state MODFLOW model. Because this does not represent the final calibration, the results presented herein will be brief. Final GSFLOW calibration and results will be presented below.

The PRMS model was calibrated at various times depending on the period of record of the calibration gauge. Much of the calibration effort was focussed on the Hawkestone and Coldwater Creek watersheds as the former makes up most of the immediate study area, while the latter covers much of the Oro Moraine immediately north of the study area. After calibration, the PRMS model was run from WY 2001 and WY 2010 (inclusive) using the NEXRAD dataset in order to produce a long term average hydrological condition. Four distributed outputs are shown:

1. Figure 4.6: average annual precipitation
2. Figure 4.7: average annual evapotranspiration
3. Figure 4.8: average annual cascading flow
4. Figure 4.9: average annual groundwater recharge

According to NEXRAD, annual average precipitation for the past decade varies greatly as one proceeds north from Lake Simcoe. Above the Hawkestone gauge an average of 1150 mm/yr has fallen whereas only 850 mm/yr fell above the Coldwater creek gauge. Evapotranspiration (ET) patterns are highly dependent on surficial geology distribution. First, it is evident that low

ET (<200 mm/yr) occurs in urban areas. For urban areas, there is a reduction on pervious areas, thus a reduction in soil zone water holding capacity and vegetative surfaces. Atop the moraine, ET is reduced as this area experiences greater recharge and thus less water is available to evaporate. In contrast, more water is kept from percolating on the Newmarket Till plain resulting in higher ET rates.

Generated runoff is defined as the runoff generated at specific locations and does not include incoming cascading runoff from up-slope cells; while cascading flow defines the average volume of water that is likely to pass a given location. Visually, the difference between the two maps is that the cascading flow paths are not apparent on the generated runoff map, which is useful when highlighting the impacts of urbanization. The cascading runoff map (Figure 4.8) highlights the role topography has on the distribution of runoff. For example, it is apparent that runoff from the till plains follow a series of dendritic ephemeral channels not covered by the MNR stream mapping; however, by utilizing the high resolution DEM, these pathways become clear. In some cases, one can see how the rill formation extends from the headwater streams, in a dendritic pattern one would expect. Because the water is distributed in this fashion, it potential to recharge and evaporate and transpire also follows these patterns.

Figure 4.10 presents a comparison of the average annual recharge derived for this study (Figure 4.9) with the recharge presented in the Lake Simcoe Basin PRMS model report (Earthfx, 2010a). Groundwater recharge is 145mm higher on average over the study area in the revised PRMS model. Recharge is higher on the Oro Moraine and has been reduced at areas with tills at surface. The reason for this discrepancy is twofold; firstly the WSC stream gauge on Hawkestone Creek at Hawkestone (02EC020) was not employed in the calibration of the LSRCA PRMS model as the period of record did not overlap the study period. With no calibration targets, model parameters were blindly extended into the Oro Creeks and Hawkestone watersheds; the limitations of this approach are discussed in the final report (Earthfx, 2010a). Secondly, the current approach incorporates an updated geological interpretation of the study area which has altered the parameterization of PRMS model variables.

Lastly, groundwater recharge is mostly dominated by surficial geology. Greater recharge tends to occur above on Moraine compared to the quarries and the till regions adjacent to the moraine. Recharge occurring in the wetlands should not be evaluated using these results, as these areas often prove to be areas of groundwater discharge not modelled in these PRMS-only runs.

4.6 Conclusions

This section serves to describe the PRMS model structure, input, and preliminary results. These results are not to be confused with the final GSFLOW results presented below. The main point of this calibration exercise was to get the PRMS model to perform as best as possible prior to integrating it with MODFLOW (i.e., GSFLOW) in order to expedite the calibration process. As it stands, however, the PRMS results are promising and minor improvements were expected upon full integration.

4.7 Tables

Table 4.1: List of Surficial Geology types used in the PRMS model.

Description	Permeability	Proportional coverage of model area
Till: Moderately Stoney To Stoney Sandy Silt To Silt Till	Low-Medium	38%
Pleistocene Ice-Contact Deposits: Pleistocene Ice-Contact Deposits (Sand And Gravel)	High	22%
Glaciofluvial Outwash: Fine To Coarse Sand, Minor Gravel	High	1%
Glaciolacustrine Deposits: Silt Clay Sand (Fine Grained)	Low	8%
Glaciolacustrine Deposits: Sand And Gravel	High	4%
Glaciofluvial/Lacustrine Deposits: Sand	High	19%
Fluvial, Alluvial, Deltaic: Pleistocene	Variable	2%
Lacustrine: Fine-Grained, Clay Silt	Low	1%
Peat And Muck: Wetlands (Organic Deposits)	High	5%

Table 4.2: Land use lookup table

Description	Land use source	Percent Impervious	Depression Storage (mm)	Winter Cover Density	Summer Cover Density	Snow Interception Storage (mm)	Summer Rain Interception Storage (mm)	Winter Rain Interception Storage (mm)
Active Aggregate	OMNR, 2007	100%	100	0%	0%	0.0	0.0	0.0
Inactive Aggregate	OMNR, 2007	5%	10	95%	95%	1.6	1.6	1.6
Commercial	OMNR, 2007	81%	1.6	19%	19%	1.6	1.6	1.6
Estate Residential	OMNR, 2007	17%	1.6	83%	83%	1.7	1.9	1.7
Golf Course	OMNR, 2007	5%	1.6	95%	95%	1.7	1.9	1.7
Intensive Agriculture: Market Garden	OMNR, 2007	0%	0	4%	75%	2.5	2.5	2.5
Intensive Agriculture: Orchard	OMNR, 2007	0%	0	30%	75%	2.5	2.5	2.5
Intensive Agriculture: Row Crop	OMNR, 2007	0%	0	4%	85%	4.0	4.0	4.0
Intensive Agriculture: Sod	OMNR, 2007	0%	0	100%	100%	1.5	1.5	1.5
Intensive Agriculture: Tree Farm	OMNR, 2007	0%	0	34%	85%	2.5	2.5	2.5
Industrial	OMNR, 2007	40%	1.6	60%	60%	1.6	1.6	1.6
Institutional	OMNR, 2007	30%	1.6	70%	70%	1.6	1.8	1.6
Manicured Open Space	OMNR, 2007	5%	1.6	95%	95%	1.5	1.5	1.5
Non-Intensive Agriculture: Hay	OMNR, 2007	0%	0	4%	75%	4.0	4.0	4.0
Non-Intensive Agriculture: Pasture	OMNR, 2007	0%	0	100%	100%	1.6	1.8	1.6
Natural Heritage Feature: Open Alvar	OMNR, 2007	0%	0	100%	100%	1.6	1.8	1.6
Natural Heritage Feature: Shrub Bog	OMNR, 2007	0%	0	6%	10%	2.5	2.5	2.5
Natural Heritage Feature: Treed Bog	OMNR, 2007	0%	0	4%	10%	2.5	2.5	2.5
Natural Heritage Feature: Cultural Meadow	OMNR, 2007	0%	0	100%	100%	1.8	2.1	1.8
Natural Heritage Feature: Cultural Plantation	OMNR, 2007	0%	0	34%	85%	2.5	2.5	2.5
Natural Heritage Feature: Cultural Thicket	OMNR, 2007	0%	0	60%	100%	2.5	2.5	2.5
Natural Heritage Feature: Cultural Woodland	OMNR, 2007	0%	0	54%	90%	2.5	2.5	2.5
Natural Heritage Feature: Open Fen	OMNR, 2007	0%	0	100%	100%	1.5	1.5	1.5

Description	Land use source	Percent Impervious	Depression Storage (mm)	Winter Cover Density	Summer Cover Density	Snow Interception Storage (mm)	Summer Rain Interception Storage (mm)	Winter Rain Interception Storage (mm)
Natural Heritage Feature: Shrub Fen	OMNR, 2007	0%	0	30%	75%	2.5	2.5	2.5
Natural Heritage Feature: Coniferous Forest	OMNR, 2007	0%	0	100%	100%	3.8	3.8	3.8
Natural Heritage Feature: Deciduous Forest	OMNR, 2007	0%	0	40%	100%	2.5	2.5	2.5
Natural Heritage Feature: Mixed Forest	OMNR, 2007	0%	0	60%	100%	3.0	3.0	3.0
Natural Heritage Feature: Meadow Marsh	OMNR, 2007	0%	0	100%	100%	1.8	2.1	1.8
Natural Heritage Feature: Shallow Marsh	OMNR, 2007	0%	0	100%	100%	1.8	2.1	1.8
Natural Heritage Feature: Open Water	OMNR, 2007	0%	0	0%	0%	0.0	0.0	0.0
Natural Heritage Feature: Floating-Leaved Shallow Aquatic	OMNR, 2007	0%	0	100%	100%	1.8	2.1	1.8
Natural Heritage Feature: Mixed Shallow Aquatic	OMNR, 2007	0%	0	100%	100%	1.5	2.3	1.5
Natural Heritage Feature: Submerged Shallow Aquatic	OMNR, 2007	0%	0	0%	0%	0.0	0.0	0.0
Natural Heritage Feature: Coniferous Swamp	OMNR, 2007	0%	0	100%	100%	3.8	3.8	3.8
Natural Heritage Feature: Deciduous Swamp	OMNR, 2007	0%	0	40%	100%	2.5	2.5	2.5
Natural Heritage Feature: Mixed Swamp	OMNR, 2007	0%	0	60%	100%	3.0	3.0	3.0
Natural Heritage Feature: Thicket Swamp	OMNR, 2007	0%	0	60%	100%	2.5	2.5	2.5
Natural Heritage Feature: Open Tallgrass Prairie	OMNR, 2007	0%	0	100%	100%	1.5	1.5	1.5
Rural Development	OMNR, 2007	20%	1.6	80%	80%	1.7	2.0	1.7
Rail	OMNR, 2007	15%	1.6	85%	85%	1.7	1.9	1.7
Road	OMNR, 2007	50%	1.6	50%	50%	1.7	1.9	1.7
Urban	OMNR, 2007	80%	1.6	20%	20%	1.6	1.8	1.6
Open Cliff And Talus	OMNR, 2007	10%	1.6	0%	0%	2.5	2.5	2.5
Alvar	OMNR, 2007	0%	0	100%	100%	1.6	1.8	1.6
Shoreline	OMNR, 2007	0%	0	0%	0%	2.5	2.5	2.5

Description	Land use source	Percent Impervious	Depression Storage (mm)	Winter Cover Density	Summer Cover Density	Snow Interception Storage (mm)	Summer Rain Interception Storage (mm)	Winter Rain Interception Storage (mm)
Open Shoreline	OMNR, 2007	0%	0	0%	0%	2.5	2.5	2.5
Open Bluff	OMNR, 2007	0%	0	0%	0%	2.5	2.5	2.5
Open Sand Barren And Dune	OMNR, 2007	0%	0	0%	0%	2.5	2.5	2.5
Treed Sand Barren And Dune	OMNR, 2007	0%	0	0%	0%	2.5	2.5	2.5
Open Tallgrass Prairie	OMNR, 2007	0%	0	100%	100%	1.5	1.5	1.5
Tallgrass Savannah	OMNR, 2007	0%	0	100%	100%	2.0	2.8	2.0
Tallgrass Woodland	OMNR, 2007	0%	0	34%	85%	2.5	2.5	2.5
Forest	OMNR, 2007	0%	0	60%	100%	3.0	3.0	3.0
Coniferous Forest	OMNR, 2007	0%	0	100%	100%	3.8	3.8	3.8
Mixed Forest	OMNR, 2007	0%	0	60%	100%	3.0	3.0	3.0
Deciduous Forest	OMNR, 2007	0%	0	40%	100%	2.5	2.5	2.5
Plantations - Tree	OMNR, 2007	0%	0	34%	85%	2.5	2.5	2.5
Hedge Rows	OMNR, 2007	0%	0	60%	100%	2.5	2.5	2.5
Transportation	OMNR, 2007	50%	1.6	50%	50%	1.7	1.9	1.7
Extraction	OMNR, 2007	100%	100	0%	0%	0.0	0.0	0.0
Built-Up Area Pervious	OMNR, 2007	5%	1.6	95%	95%	1.7	1.9	1.7
Built-Up Area Impervious	OMNR, 2007	80%	1.6	20%	20%	1.6	1.8	1.6
Swamp	OMNR, 2007	0%	0	60%	100%	3.0	3.0	3.0
Fen	OMNR, 2007	0%	0	100%	100%	1.5	1.5	1.5
Bog	OMNR, 2007	0%	0	6%	10%	2.5	2.5	2.5
Marsh	OMNR, 2007	0%	0	100%	100%	1.8	2.1	1.8
Open Water	OMNR, 2007	0%	0	0%	0%	0.0	0.0	0.0
Undifferentiated	OMNR, 2007	0%	0	4%	85%	4.0	4.0	4.0
Idle Agricultural Land (5-10 Years)	LSRCA ELC	0%	0	4%	85%	4.0	4.0	4.0
Idle Agricultural Land (Over 10 Years)	LSRCA ELC	0%	0	4%	85%	4.0	4.0	4.0
Built Up	LSRCA ELC	80%	1.6	20%	20%	1.6	1.8	1.6
Berries	LSRCA ELC	0%	0	30%	75%	2.5	2.5	2.5
Corn System	LSRCA ELC	0%	0	4%	85%	4.0	4.0	4.0
Cherries	LSRCA ELC	0%	0	30%	75%	2.5	2.5	2.5
Extraction	LSRCA ELC	100%	100	0%	0%	0.0	0.0	0.0

Description	Land use source	Percent Impervious	Depression Storage (mm)	Winter Cover Density	Summer Cover Density	Snow Interception Storage (mm)	Summer Rain Interception Storage (mm)	Winter Rain Interception Storage (mm)
Extraction Pits And Quarries	LSRCA ELC	100%	100	0%	0%	0.0	0.0	0.0
Extraction Topsoil Removal	LSRCA ELC	100%	100	0%	0%	0.0	0.0	0.0
Grazing System	LSRCA ELC	0%	0	100%	100%	1.6	1.8	1.6
Hay System	LSRCA ELC	0%	0	4%	75%	4.0	4.0	4.0
Pasture System	LSRCA ELC	0%	0	100%	100%	1.6	1.8	1.6
Specialty Agriculture	LSRCA ELC	0%	0	30%	75%	2.5	2.5	2.5
Extensive Field Vegetables	LSRCA ELC	0%	0	4%	85%	4.0	4.0	4.0
Market Gardens/Truck Farms	LSRCA ELC	0%	0	4%	75%	2.5	2.5	2.5
Nursery	LSRCA ELC	0%	0	34%	85%	2.5	2.5	2.5
Tobacco System	LSRCA ELC	0%	0	4%	85%	4.0	4.0	4.0
Mixed System	LSRCA ELC	0%	0	4%	85%	4.0	4.0	4.0
Grain System	LSRCA ELC	0%	0	4%	85%	4.0	4.0	4.0
Orchard	LSRCA ELC	0%	0	30%	75%	2.5	2.5	2.5
Orchard-Vineyard	LSRCA ELC	0%	0	30%	75%	2.5	2.5	2.5
Continuous Row Crop	LSRCA ELC	0%	0	4%	85%	4.0	4.0	4.0
Peaches-Cherries	LSRCA ELC	0%	0	30%	75%	2.5	2.5	2.5
Peaches	LSRCA ELC	0%	0	34%	85%	2.5	2.5	2.5
Recreation	LSRCA ELC	5%	1.6	95%	95%	1.7	1.9	1.7
Sod Farm	LSRCA ELC	0%	0	100%	100%	1.5	1.5	1.5
Unknown	LSRCA ELC	0%	0	4%	85%	4.0	4.0	4.0
Vineyard	LSRCA ELC	0%	0	30%	75%	2.5	2.5	2.5
Vineyard-Orchard	LSRCA ELC	0%	0	30%	75%	2.5	2.5	2.5
Water	LSRCA ELC	0%	0	0%	0%	0.0	0.0	0.0
Swamp, Marsh Or Bog	LSRCA ELC	0%	0	60%	100%	3.0	3.0	3.0
Woodland	LSRCA ELC	0%	0	60%	100%	3.0	3.0	3.0
Pastured Woodland	LSRCA ELC	0%	0	34%	85%	2.5	2.5	2.5
Reforestation	LSRCA ELC	0%	0	60%	100%	3.0	3.0	3.0

4.8 Figures

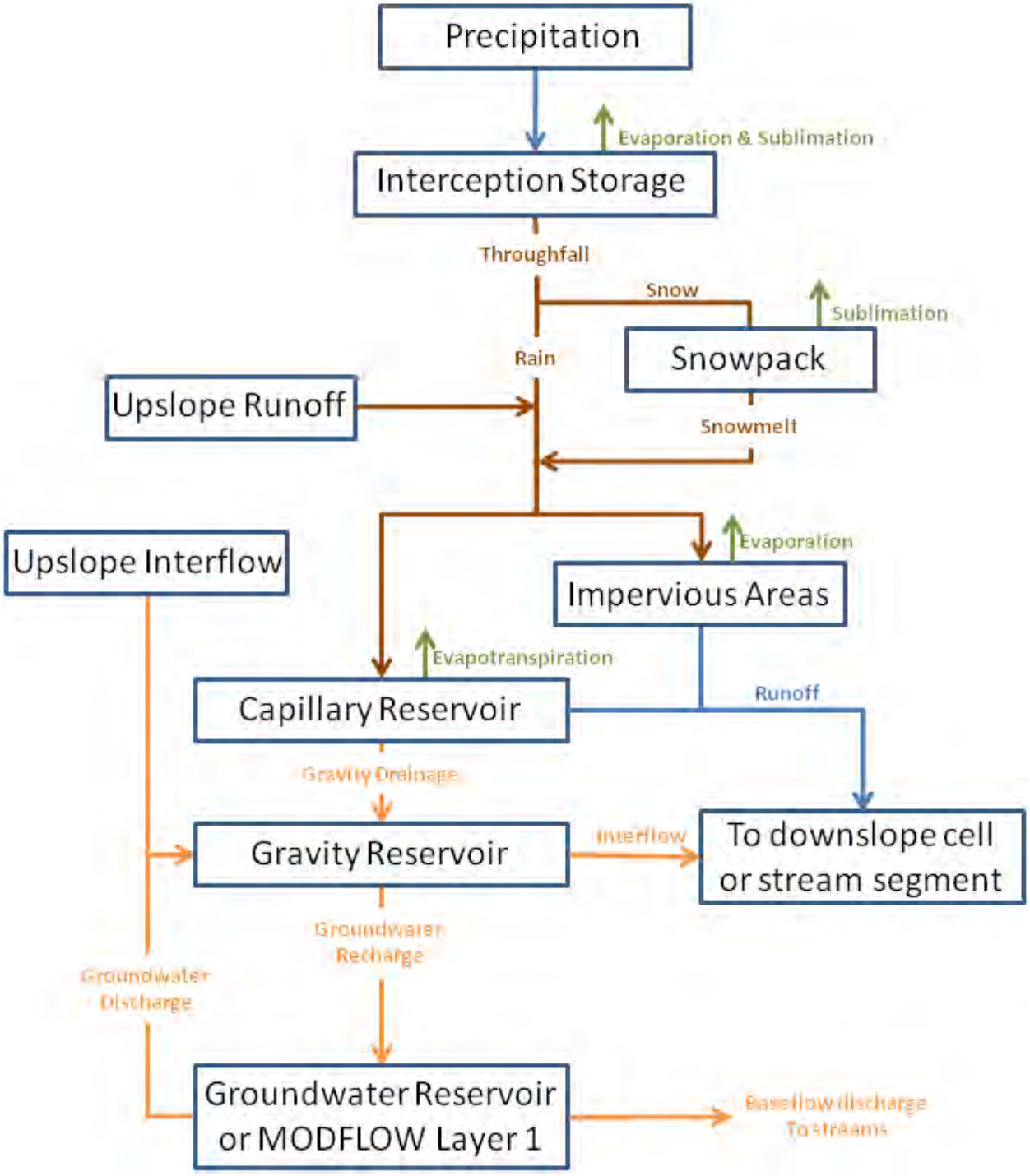

Figure 4.1: Flow chart of PRMS hydrological processes.

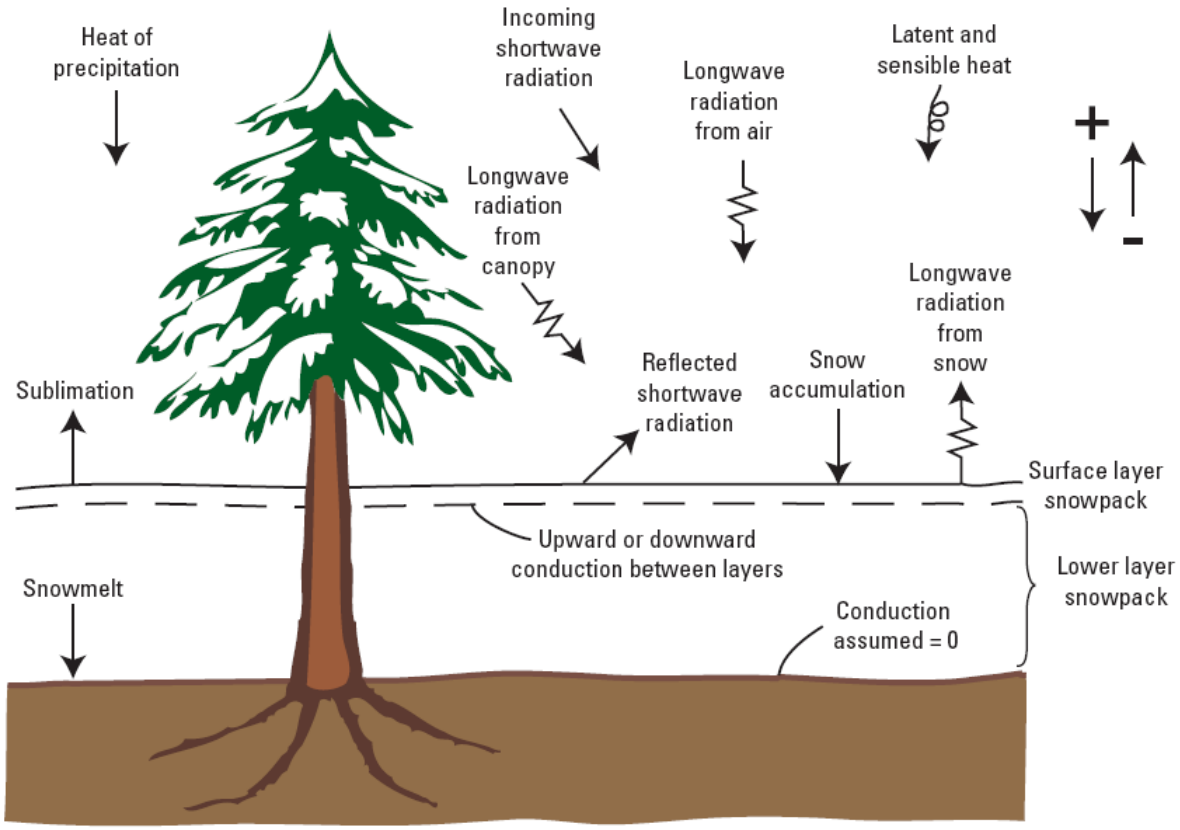

Figure 4.2: PRMS 2-layer snowpack conceptualization and the processes accounted for in the energy balance snowmelt algorithm.

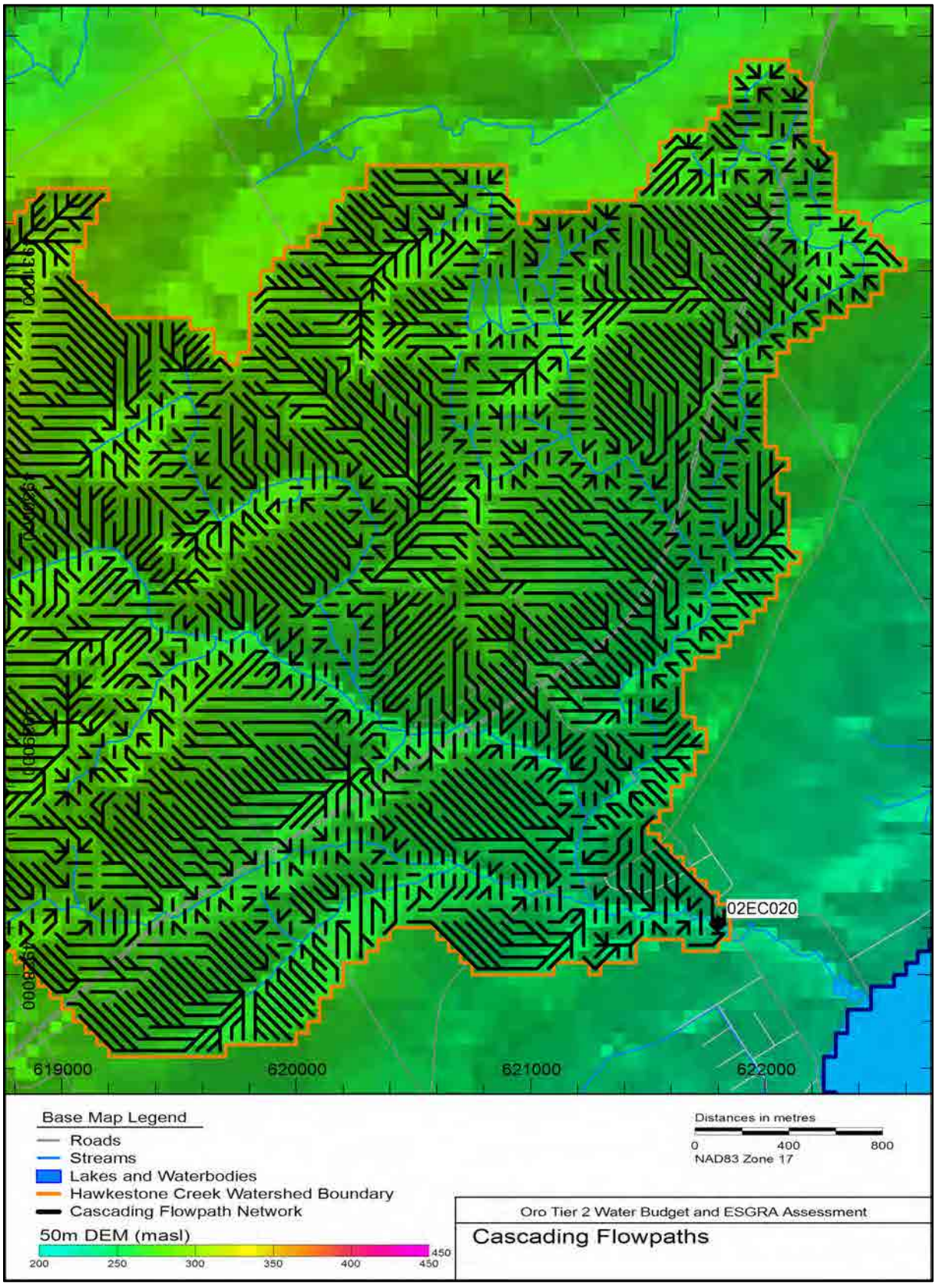

Figure 4.3: The cascade flow network superimposed over the DEM.

Figure 4.4: Location of NEXRAD Virtual Climate Stations relative to climate monitoring stations.

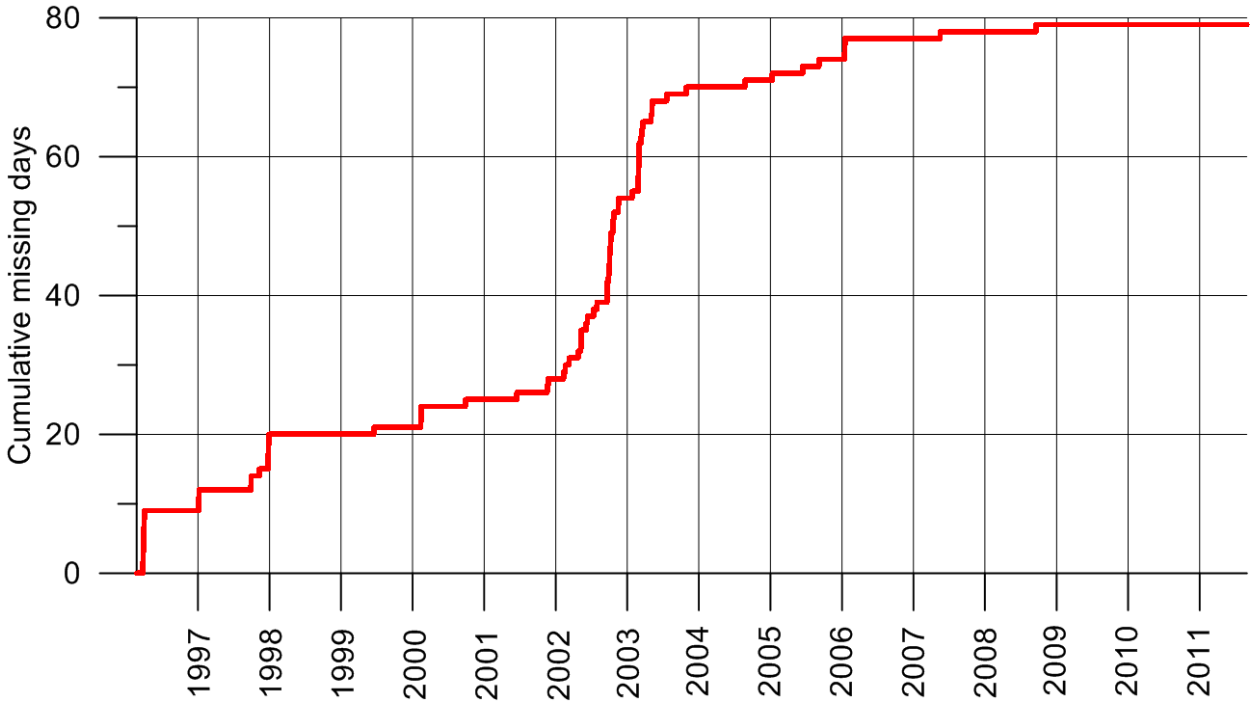

Figure 4.5: Data quality of the NEXRAD dataset.

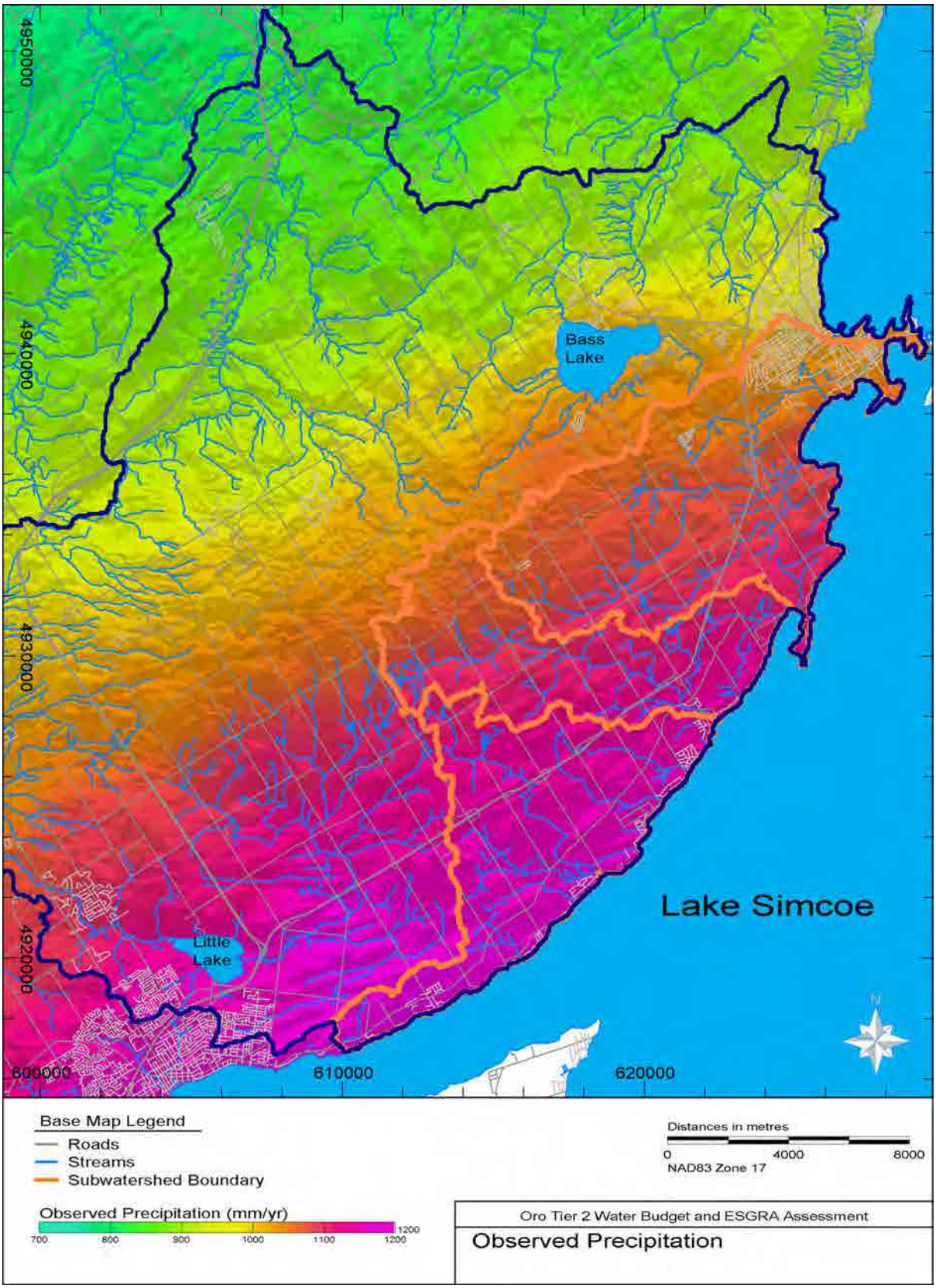

Figure 4.6: Distribution of long-term NEXRAD precipitation (2000-2009)

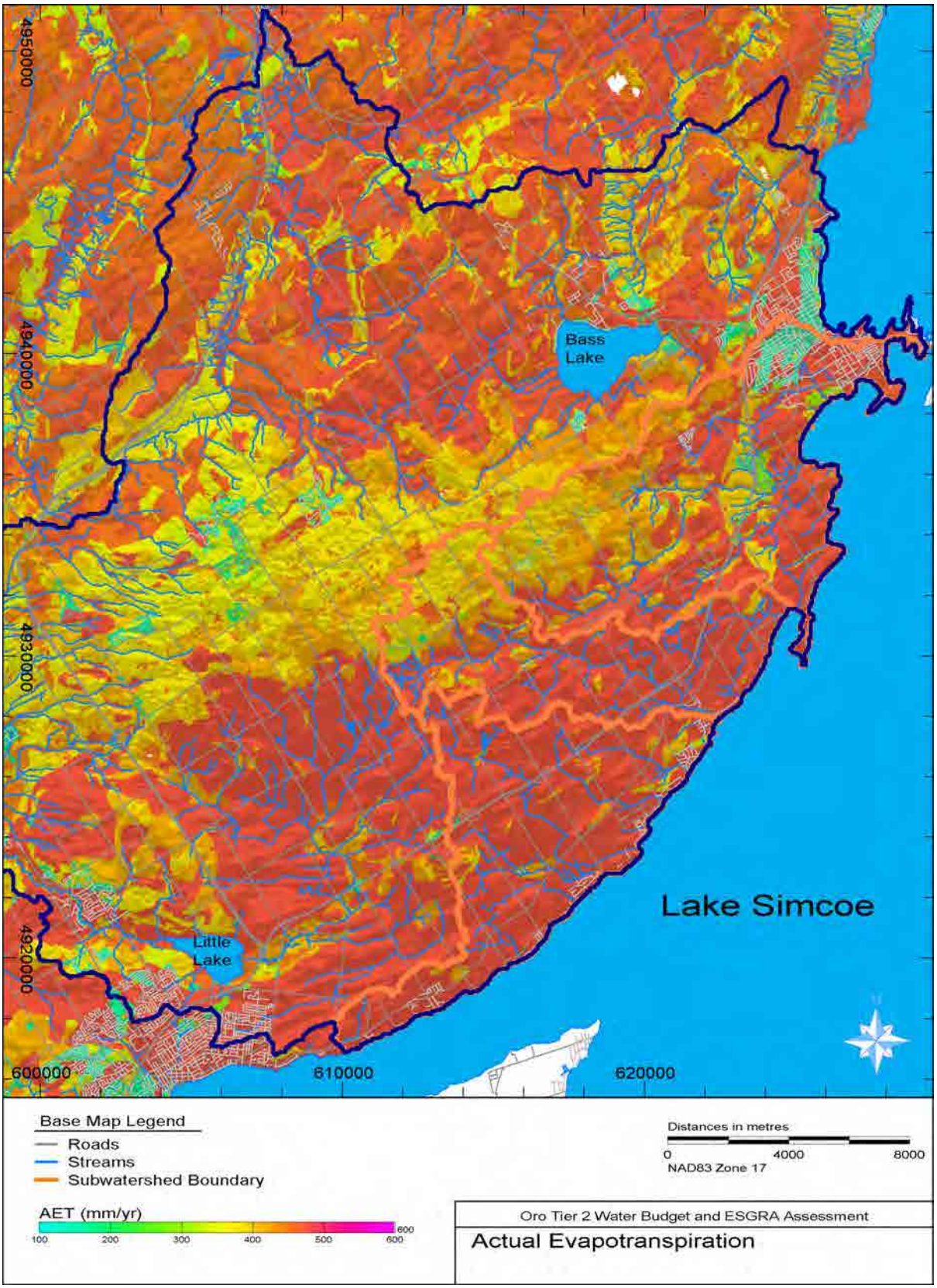

Figure 4.7: PRMS-predicted distribution of evapotranspiration.

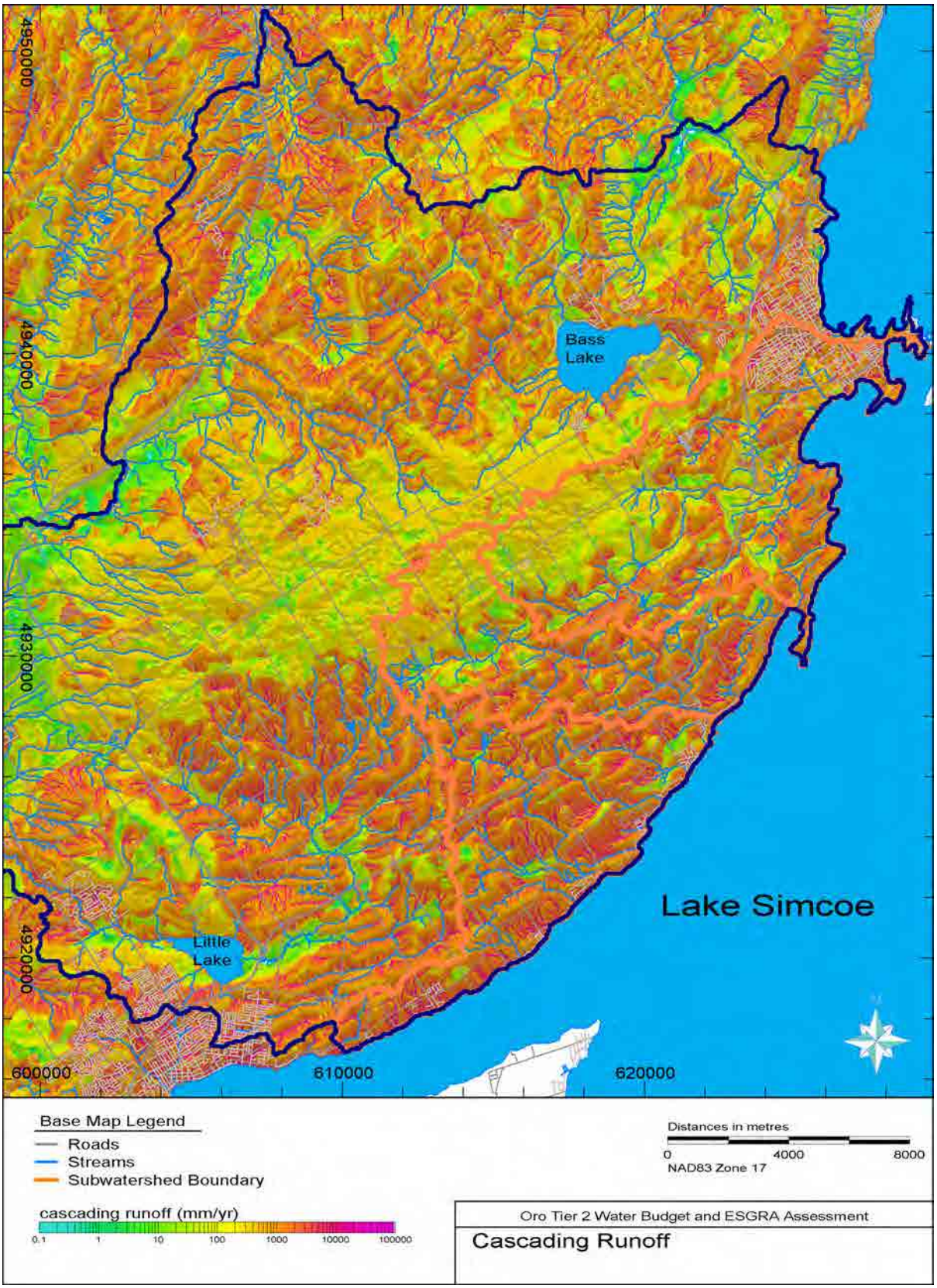

Figure 4.8: PRMS-predicted distribution of accumulated cascading runoff.

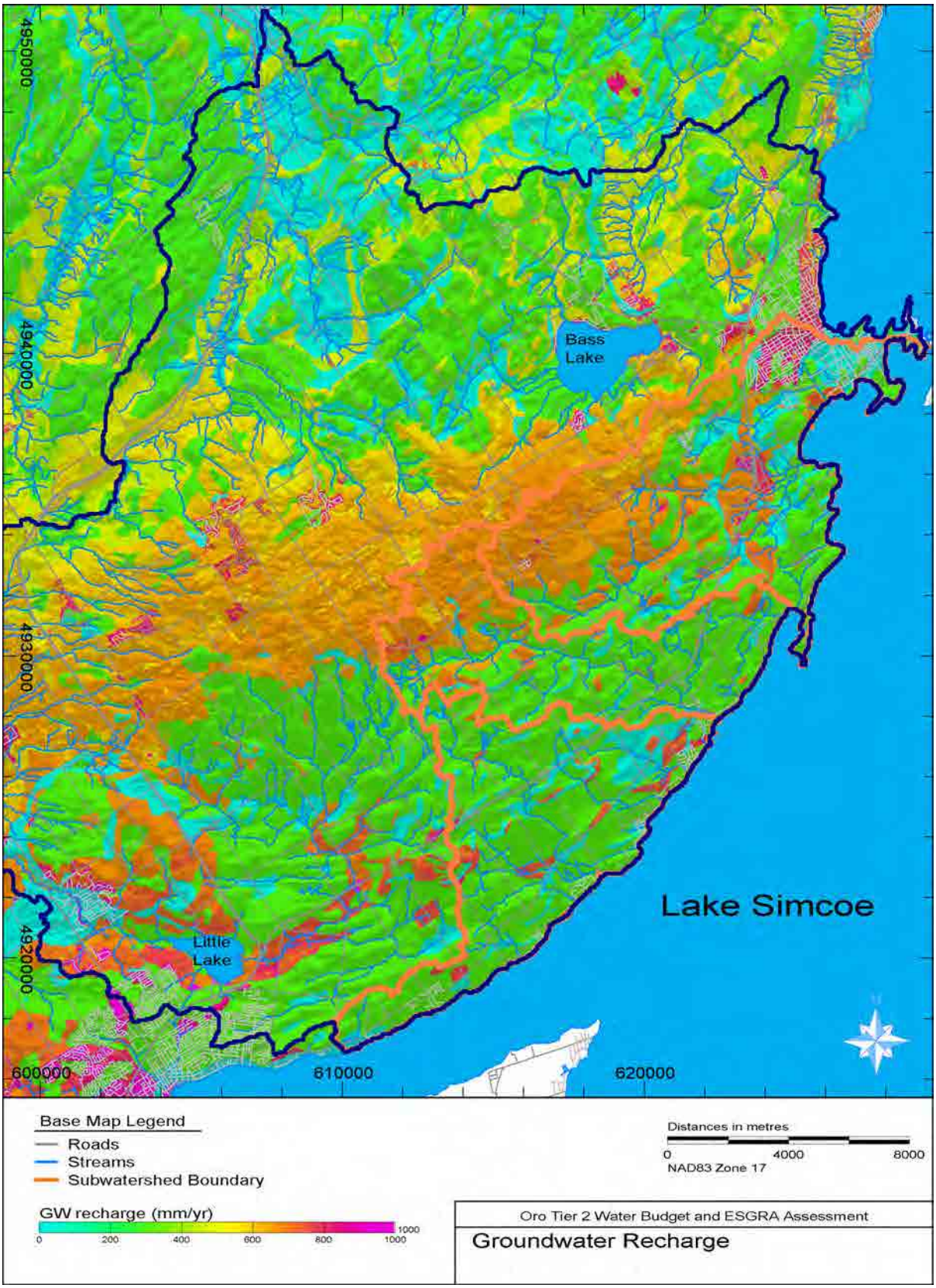

Figure 4.9: PRMS-predicted distribution of groundwater recharge.

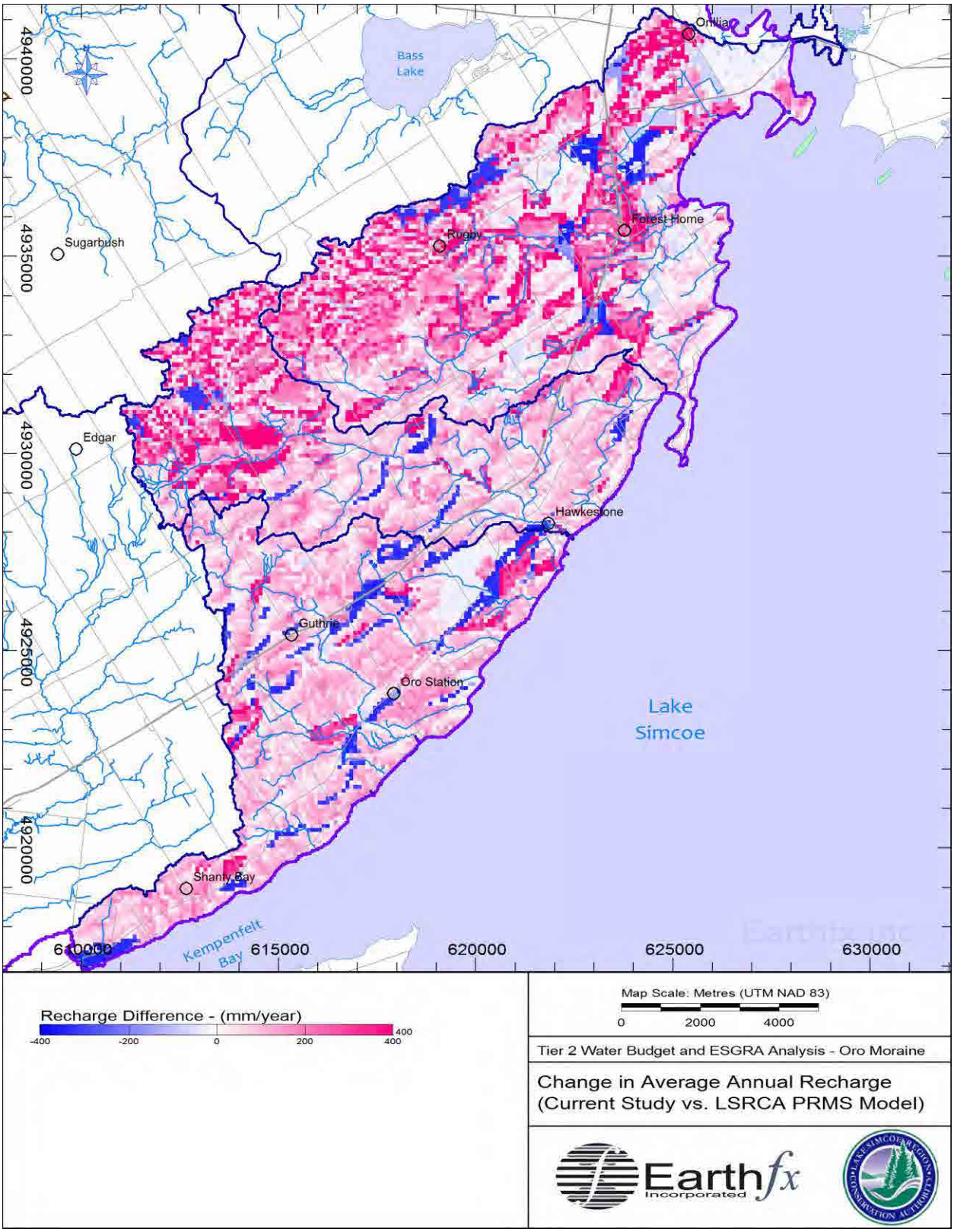

Figure 4.10: Difference in modelled Average Annual Recharge between current study and LSRCA PRMS model (Earthfx, 2010a).

5 Groundwater Model Development

5.1 Overview

A primary objective of this study was to develop an integrated groundwater and surface-water model capable of addressing the specific requirements of the Tier 2 water budget and stress assessment. A Tier 2 water budget analysis must consider the surface water and groundwater flow systems as well as the interaction linkage between them. For this reason, an integrated groundwater/surface water model was developed for the Oro Moraine model area using the USGS GSFLOW code (Markstrom *et al.*, 2008). As noted earlier, GSFLOW represents an integration of the two widely-recognized USGS models: PRMS and the modular groundwater flow model MODFLOW (Harbaugh, 2005). In addition to determining groundwater levels in the model area, the groundwater sub-model provides estimates of the rates of groundwater discharge to streams and wetlands along with other groundwater budget items such as the exchange of water between shallow and deeper aquifers, and lateral groundwater inflow and outflow across catchment boundaries. Lateral groundwater inflow across the subwatershed boundaries and groundwater discharge to streams are two important components of the Tier 2 stress analysis discussed further on.

The MODFLOW code is extremely suitable for modelling transient groundwater flow in multi-layered aquifer systems such as in the Oro Moraine model area and can easily account for irregular boundaries, complex stratigraphy, and variations in hydrogeologic properties. The most recent version of GSFLOW (v1.1.5) incorporates MODFLOW-NWT (Niswonger *et al.*, 2011), a version of MODFLOW especially well-suited for representing thin aquifers and sharp changes in model layer stratigraphy, such as that occurring along the edges of the till uplands, within the Oro Moraine, and in the tunnel channels.

MODFLOW uses the finite-difference method and requires that the model area be subdivided vertically into several layers, where each layer can represent a hydrogeologic unit or subunit (such as the ICSD or the weathered bedrock layer). The model area is also subdivided horizontally into a grid of small rectangular cells. Aquifer properties, such as top and bottom elevations for each layer, hydraulic conductivity, and storage coefficients are assigned to each cell. Boundary conditions are specified for cells that lie along lines corresponding to the physical boundaries of the flow system. The main output from the model is simulated groundwater potentials in each model cell at the end of each time period. Flows between model cells and across model boundaries can be derived from the simulated potentials.

This section briefly discusses the groundwater flow equation, model code, grid design, boundary conditions, model calibration, and numerical model results. As was the case for the PRMS sub-model, it is possible to develop and calibrate the groundwater submodel independently of GSFLOW. Early efforts focussed on developing a steady-state MODFLOW-only model with estimates of groundwater recharge supplied by PRMS-only model runs. Integrated transient model runs were conducted once the calibration of the independent groundwater model had been taken as far as needed to conduct the steady-state analyses required for the Tier 2 study.

5.2 Groundwater Flow Model

A groundwater flow model is a simplified representation of the complex physical, hydrologic and hydrogeological processes and factors that affect the rates and direction of groundwater flow. These processes and factors relate to physical characteristics of the model area and include:

- stratigraphy (i.e., the bedrock and overburden stratigraphic layers, unit top and bottom elevations, lateral extent of the formations, and unit thickness);
- hydrostratigraphy (i.e., descriptions of the aquifers and aquitards in the model area, their top and bottom surface elevations, and their lateral extent, thickness, and degree of continuity;
- aquifer and aquitard properties (i.e., estimated hydraulic conductivity, anisotropy, saturated thickness, transmissivity, and storage properties);
- inputs to the hydrologic system (i.e., rates of groundwater recharge and discharge and the underlying processes that affect these rates (e.g., precipitation, evapotranspiration, overland runoff, infiltration, and baseflow));
- properties of the surface-water system and factors controlling groundwater/surface water interaction;
- anthropogenic inputs and outputs from the groundwater system (pumping rates and return flows); and
- other significant features (e.g., surficial geology and topographic features such as slope that may affect recharge and discharge).

The groundwater flow model was developed based on a synthesis of information presented earlier in this report. The conceptual model was refined over the course of this study as our understanding of the model area and the behaviour of the groundwater system and its response to changes in stress improved. Key features of the conceptual model have been presented in the previous report sections. This section primarily describes features of the conceptual model directly related to the construction of the numerical groundwater flow model.

5.3 Groundwater Flow Equation

Groundwater flow is governed by Darcy's Law, which states that flow is proportional to the hydraulic gradient and to the hydraulic conductivity of the aquifer material. Darcy's Law can be written as:

— (Eq. 1)

where q is the specific discharge or rate of flow per unit area, K is the hydraulic conductivity, and dh/dx is the hydraulic gradient (change in hydraulic head per unit length). Groundwater flow is also governed by the Law of Conservation of Mass which states that all inflows to an area must be balanced by outflows and/or by a change in aquifer storage. When the mass balance equation is combined with Darcy's Law, it yields the governing equation for three-dimensional groundwater flow.

$$\frac{\partial}{\partial x}\left(K_{xx}\frac{\partial h}{\partial x}\right)+\frac{\partial}{\partial y}\left(K_{yy}\frac{\partial h}{\partial y}\right)+\frac{\partial}{\partial z}\left(K_{zz}\frac{\partial h}{\partial y}\right)=S_0\frac{\partial h}{\partial t} \quad \text{(Eq. 2)}$$

where: K_{xx} = Hydraulic conductivity in the x direction;
K_{yy} = Hydraulic conductivity in the y direction;
K_{zz} = Hydraulic conductivity in the z direction;
h = hydraulic head;
S_0 = Specific storage

Hydraulic conductivity is a measure of how easily water can pass through the pores in the geologic unit. Specific storage is a measure of how much water is released from aquifer storage per unit decline in aquifer head per unit volume of aquifer. Water is released from storage when the head decreases due to expansion of the water and due to compression of the pore structure by the increase in intergranular stress. The intergranular stress increases as the water pressure decreases because total stress due to the weight of the overburden remains constant.

In the hydraulic approach to aquifer flow (see Bear, 1979), Equation 2 can be simplified by integrating over the thickness of the aquifer. The resulting equation for two-dimensional flow in a confined aquifer of thickness B with recharge, discharge, and leakage from above and below can be written mathematically (Bear, 1979) as:

$$\frac{\partial}{\partial x}\left(T_{xx}\frac{\partial h}{\partial x}\right)+\frac{\partial}{\partial y}\left(T_{yy}\frac{\partial h}{\partial y}\right)+\left[\frac{K'_U}{B'_U}\left(H_U-h\right)\right]+\left[\frac{K'_O}{B'_O}\left(H_O-h\right)\right]+N-\sum_{k=1}^{Nwell}Q'_k=S\frac{\partial h}{\partial t} \quad \text{(Eq. 3)}$$

where: T_{xx} = Transmissivity in the x direction (where $T_{XX} = K_{XX}B$);
T_{yy} = Transmissivity in the y direction;
h = hydraulic head;
K' = vertical hydraulic conductivity of an overlying (or underlying) confining unit
B' = thickness of the overlying (or underlying) confining unit;
H_O/H_U = head in the aquifer layer overlying/underlying the confining unit;
N = rate of groundwater recharge;
Q'_K = Pumping rate (per unit area) at well k
S = Storativity or storage coefficient (where $S = S_0B$)

A similar equation can be written for each aquifer in a layered sequence of aquifers and confining units. When an aquifer layer is unconfined, the transmissivity terms T_{XX} and T_{YY} are replaced by the effective transmissivity, equal to $K_{XX}(h-b)$ and $K_{YY}(h-b)$, where b is the elevation of the base of the aquifer. The storage coefficient for an unconfined aquifer is usually replaced with the specific yield, S_Y, which is used to represent water "released from storage" due to the draining of the pore space above the water table as the water table drops. S_Y is generally several orders of magnitude larger that compressive storage.

Equation 3 is a differential equation which formed the basis of the mathematical model developed for the Oro Moraine area. The equation is "solved" to determine aquifer heads at all points in the model area. Information in the form of aquifer properties, recharge and discharge rates, and conditions along the model boundaries, are provided as input to the model to make the solution unique to the model area. Numerical methods are needed to solve Equation 3

because model area boundaries are irregular and aquifer/aquitard properties, aquifer geometry (stratigraphy), and rates of recharge and discharge vary spatially within the model area.

If the variation of head over time is considered to be small, for example, when considering equilibrium or long-term average conditions, the term on the right hand side of Equation 5 can be set to zero. This yields the steady-state form of the groundwater flow equation. The steady-state equation is often solved first because it provides information on aquifer hydraulic conductivity properties independent of the aquifer storage properties. Once the hydraulic properties are adjusted sufficiently through calibration to average flows and water levels, then the transient form can be solved to refine estimates of hydraulic properties and determine the storage properties of the aquifer.

The U.S. Geological Survey (USGS) MODFLOW code was developed to solve Equation 3 using the finite-difference method. The basic MODFLOW-2005 code is documented in Harbaugh (2005) and the MODFLOW-NWT version of the code is documented in Niswonger *et al.* (2011). Several enhancements to the basic model code are documented in other USGS reports and were cited above. Best practices for groundwater modelling and professional judgement were followed when applying and calibrating the numerical models as outlined in the ASTM (2000) standards for groundwater flow modelling. The study made extensive use of VIEWLOG (VIEWLOG Systems Inc., Version 3.9) to view, analyze, and manage hydrogeologic data. VIEWLOG allowed a direct link to the extensive relational database that was constructed for this study. Along with the ability to facilitate geologic data analysis and spatial data management, VIEWLOG has add-on modules with pre-and post-processing functions for MODFLOW and GSFLOW. The MODFLOW and GSFLOW modules were used to facilitate model construction and model calibration as well as for the interpretation and presentation of model results.

5.4 Model Extents and Model Grid

As noted earlier, the model boundaries extend well beyond the Oro North, Oro South, and Hawkestone Creeks subwatersheds to encompass all of the Oro Moraine and the other associated subwatersheds. Model extents and the location of the subwatersheds mentioned are shown in Figure 5.1.

MODFLOW uses the finite-difference method and requires that the model area be subdivided vertically into several layers, where each layer can represent a hydrogeologic unit or subunit (such as the Maple Formation or the weathered bedrock layer). The model area is also subdivided horizontally into a grid of small rectangular cells. Aquifer properties, such as top and bottom elevations for each layer, hydraulic conductivity, and storage coefficients are assigned to each cell. Boundary conditions are specified for cells that lie along lines corresponding to the physical boundaries of the flow system.

On particular feature of the GSFLOW formulation is that the PRMS grid used for the soil water balance can be different than the one used for the groundwater flow. As discussed in the previous chapter, a grid composed of uniform square cells, 50 metres on a side, was used for the PRMS submodel. A uniform cell-size grid was designed for the MODFLOW sub-model with square cells 100 m on a side as shown in Figure 5.1. Recharge from the PRMS model was averaged over the MODFLOW cell. Groundwater discharge to surface and groundwater ET rates calculated by MODFLOW were subdivided equally when passing the information back to PRMS.

The cell size selected provided a high degree of resolution around the important features of the model area (i.e., streams, wetlands, and municipal wells). The model grid consists of 350 rows and 343 columns and contains 120,050 grid cells for each of seven model layers. A finer grid could have been used but model run times are strongly dependent on the number of MODFLOW cells.

MODFLOW works in a local, grid coordinate system based on row and column numbers. The VIEWLOG pre-processor was used to help translate geo-referenced map data into MODFLOW coordinates. The local origin for the model grid is at UTM coordinates 595000 E and 49165000 N. The grid was aligned with the 50-m grid used for the PRMS sub-model. All digital maps and well data for the model area were referenced using NAD83 (UTM Zone 17) grid coordinates.

5.5 Model Layers

There are a several possible approaches that can be used to represent hydrostratigraphy with the MODFLOW code. For this study, the Oro Moraine model area was subdivided vertically into layers, where each layer represented a separate hydrostratigraphic unit, either an aquifer or aquitard. Layering follows the OGS hydrostratigraphic model (discussed in 2.2.4) with some simplification as discussed below. Model layers differed between the tunnel channels and the till uplands although common layers are found at depth. Model layers are shown schematically in the table below:

Table 5.1: MODFLOW layer structure (V indicates a virtual layer)

Layer	Oro Moraine/Till Upland	Tunnel Channels
1	Oro Moraine Aquifer (ICSD)	(GLAF)
2	Newmarket Till	(GLAF)
3	Upper Aquifer - AF1	Algonquin Aquifer - GLAF
V3a	Local Aquitard - AT1	
V3a	Local Aquifer - AF2	Algonquin Aquitard - GLAT
V3a	Regional Aquitard - AT3	
4	Regional Aquifer - AF4	Valley Fill: Upper Aquifer - CAF1
V4a	Lower Drift - Upper Aquitard OST	Valley Fill: Upper Aquitard - CAT1
5	Lower Drift - Local Aquifers - STAF	Valley Fill: Middle Aquifer - CAF2
V5a	Lower Drift - Middle Aquitard - LD	Valley Fill: Lower Aquitard - CAT2
6	Lower Drift - Lower Aquifer - LAF	Valley Fill: Lower Aquifer - CAF3
V6a	Lower Drift - Lower Aquitard LD2	Lower Drift - Lower Aquitard LD2
7	Basal Aquifer - Bgravel	Basal Aquifer - Bgravel
7	Weathered Bedrock	Weathered Bedrock

The uppermost model layer outside of the tunnel channels represents the Oro Moraine ICSD deposits, where present, along with patches of glaciofluvial material found on the till highlands. Layer 2 represents the Newmarket Till aquitard, the upper till on the till uplands. Layer 3 represented the upper regional aquifer (AF1). The local aquifer, AF2, is patchy over most of the model area, and for simplicity, was grouped with the Local aquitard (AT1) and Regional Aquitard (AT3) into one aquitard unit. The MODFLOW code has an option to represent aquitards as virtual layers located between the primary aquifer layers. When this option is used, flow in the aquitards is assumed to be in the vertical direction only. This approach was adopted to represent the AT1/AF2/AT3 unit. Virtual layers only need information on the thickness and equivalent vertical hydraulic conductivity. The model does not solve for the heads in the virtual layer, but flow across the unit can be determined based on the simulated heads in the adjoining aquifers and the vertical conductance (i.e., the vertical hydraulic conductivity divided by the aquitard thickness).

Layer 4 represents the regional aquifer, AF4, Layer 5 represents local aquifers within the lower drift (STAF), and Layer 6 represents the lower regional aquifer, LAF. Virtual layers were used to represent the intervening upper aquitard (OST) and the middle aquitard (LD), and the underlying lower aquitard (LD2).

Within the tunnel channels, the uppermost unit is the Algonquin aquifer (GLAF) composed of sandy postglacial lake deposits, gravelly beach and bar sediments, and recent alluvium. To keep the number of model layers the same as for the till uplands, the GLAF was subdivided and represented in Layers 1, 2, and 3. The Algonquin Aquitard was represented as a virtual layer separating the GLAF and upper valley-fill aquifer (CAF1). Layer 4 represents the upper valley-fill aquifer (CAF1), Layer 5 represents the middle valley-fill aquifer (CAF2), and Layer 6 represents the lower valley fill aquifer (CAF3). Virtual layers represent the intervening upper and lower aquitards, CAT1 and CAT2.

The lower aquitard (LD2) is assumed to be present beneath the entire model area (including the tunnel channels) and is the first of the common units. The basal gravel beneath LD2 is patchy and, for simplicity, was combined with the weathered bedrock in Layer 7. The base of the model is represented by the top of the unweathered bedrock.

An important consideration in translating the conceptual model layers to numerical model layers is that the MODFLOW code requires continuity of aquifer layers whereas the hydrostratigraphic model can have zero thickness. Where physical layers pinched out (i.e., had a zero thickness), the layer was assigned a minimum thickness (2.0 m for aquifers and 1.0 m for aquitards) and hydraulic properties were assigned based on those of the underlying layer. Figure 5.2 shows a west to east section through the model area showing the numerical model layers corresponding to the hydrostratigraphic model layers shown in Figure 2.29.

5.6 Model Boundary Conditions

Physical conditions along the model boundaries must be provided as input to the numerical model. MODFLOW can represent three general types of conditions along the physical boundaries of the model. All three boundary condition types, constant head, no-flow, and head-dependent discharge boundaries, were employed in the numerical model to represent natural hydrologic boundaries.

5.6.1 Constant-Head Boundary Conditions

Figure 5.1 shows the location of constant head and no-flow boundaries (in red). Cells along the edge of Lake Simcoe and Lake Couchiching have a fixed elevation set to average lake levels of 219 masl. Constant heads were also set along the edge of Orr Lake at 220 masl.

It was not practical to extend the model boundary to Georgian Bay or the Minesing Swamp. Instead, constant head boundaries were set across the stream valleys where Willow Creek, Coldwater Creek, Sturgeon River, and Silver Creek exit the model area. Constant head values were extrapolated from the DEM.

A no-flow boundary condition was applied along the remaining lateral boundaries of the model area, indicating that flow across the external boundaries was expected to be small to negligible. The boundaries represent the topographic divides delineating the major subwatersheds. A no-flow boundary condition was also applied at the base of the lowest model layer representing the assumption that little flow is exchanged between the model layers and deep bedrock.

5.6.2 Stream Boundaries

A third type of boundary condition (head-dependent discharge boundary) was used extensively to represent groundwater/surface water interaction processes within the active model area. Flow was assumed to be exchanged as "leakage" across a lake bed or streambed assumed to be of lower hydraulic conductivity compared to the underlying aquifer. The rate of flow is determined based on Darcy's Law where:

$$Q_{Leak} = \frac{K'}{B'} A_L (H_L - h) \qquad \text{(Eq. 6)}$$

where:
- Q_{LEAK} = volumetric flow rate between aquifer and stream or lake;
- K' = vertical hydraulic conductivity of the stream or lake bed;
- B' = thickness of the streambed or lake bed;
- A_L = wetted area of the streambed or lake bed and sides;
- H_L = stream or lake stage; and
- h = head in the aquifer

Stream-aquifer interaction is handled by the SFR2 module in MODFLOW. A dendritic stream network was created by defining stream "segments" and junctions at the confluence of two or more tributary segments as in the sketch below. Segments were numbered from upstream to lowest downstream such that all upstream flows are calculated when two sub-networks join at a junction (for example, Segment 1 in the sketch joins Segment 3 at a junction and the confluent flow moves downstream to Segment 4). Stream segments are defined as the portion of a stream reach within a model cell. These are also numbered in downstream order.

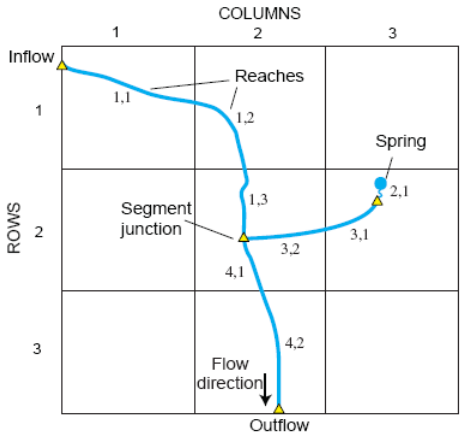

Stream reaches were defined by overlaying the model grid on the stream segment network. All mapped stream segments (all Strahler classes, including the smallest headwater streams) in the model area were simulated. Maps of the existing streams were obtained from MNR stream coverages. Streams were classified based on Strahler code and assigned section properties on that basis. The stream, lake, and wetland network is shown in Figure 2.41. The model area contained 1728 stream segments broken into 14945 stream reaches. Stream properties including stream cross-sections, roughness (Mannings n), streambed thickness, and streambed hydraulic conductivity were defined for each segment. The hydraulic conductivity of the streambed material was set to $5x10^{-7}$ metres per second (m/s) for all streams which is in the range of silt to silty-fine alluvial sand and bed thickness was set to 0.2 m. Stream slope was defined for each reach as estimated from the DEM.

Stream stage in each reach is calculated based on the sum of upstream inflows, precipitation, evaporation, and overland flow to the reach (as calculated by PRMS). Leakage to or from the aquifer is then calculated based on the difference between stream stage and the head in the underlying aquifer. Net outflow from each reach is routed to a downstream segment. Because leakage downstream can affect upstream aquifer levels, streamflow routing and the groundwater flow equations are solved in an iterative manner for each time step until convergence is achieved (i.e., changes in simulated flows and heads between successive iterations fall below threshold levels). Stream segments can terminate in a lake or wetland (as shown in the schematic below) or exit the model area.

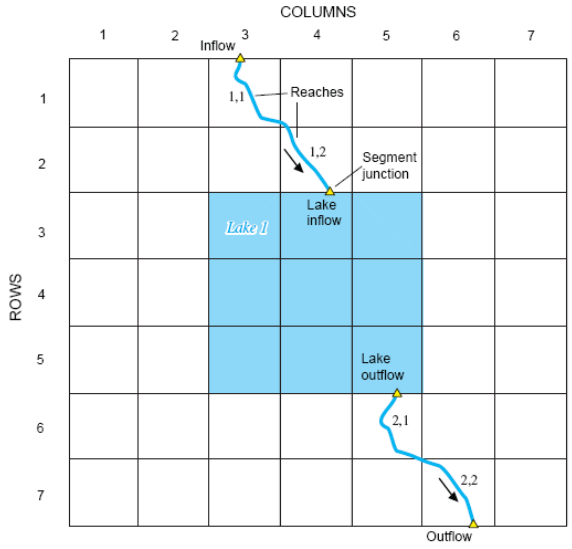

The input data for simulating lakes and streams and lake simulation can be quite large when using mapped streams. VIEWLOG was used to construct the stream network topology (i.e., assigning reach and segment numbers, defining junctions, and assigning segment-based properties) and overlay the stream network on the model grid to determine the reach length and slope.

The lake simulation (LAK3) module (Merritt and Konikow, 2000) was used to represent Bass Lake, Little Lake, and 83 other water bodies within wetlands. The module computes a separate water balance for each lake or wetland based on computed inflows (e.g., precipitation, runoff, and incoming stream discharge) and outflows (e.g., evaporation, groundwater leakage, surface water takings, and outflowing stream discharge). Lakes are represented as occupying part of the volume of the model as shown in the plan view sketch above and in the associated cross-section view below. As shown in the schematic cross section below, lakes can penetrate one or more groundwater model layers, allowing interaction with multiple aquifer layers.

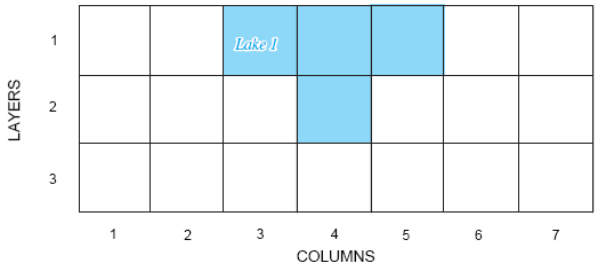

Lake areas were defined in VIEWLOG by overlaying the polylines representing the wetlands and lakes (from the MNR hydrography coverage) over the model grid. Some of the line work was modified to delineate portions of the mapped wetlands that were likely to have standing water during some part of the year based on historic aerial photography. Some wetlands expected to have similar hydrologic response were aggregated by assigning the cells the same lake ID number and a single stage was computed for the wetland chain. All lakes were contained in the uppermost model layer. (Note: the peripheral areas of the wetlands, where standing water is not readily observed, were represented with appropriate wetland soil zone parameters.)

Leakage to or from the aquifer is calculated based on the difference between lake stage and the head in the underlying aquifer. Lake stage was updated daily using a stage-storage relationship established based on the area of cells occupied by the lake and the elevation of the lake bottom. Lake bottoms were defined by adjusting the top of Layer 2 (i.e., the top of Newmarket Till) such that the difference between the initial estimate of lake stage and the top of Layer 2 represented the average lake depth. Average lake depths were obtained from bathymetry data for Bass and Little Lakes. Wetland lakes were assigned a depth of 1.5 metres. Lake bed conductance (i.e. vertical hydraulic conductivity divided lakebed thickness) was assigned to each lake. A value of $5x10^{-7}$ m/s/m was assigned to Bass and Little Lakes. A value of $7x10^{-8}$ m/s/m was assigned to the wetland lakes.

Discharge from the lake is calculated by the SFR2 package with rates determined by a specified lake stage/discharge relationship. For most outlets, flow was controlled based on the properties of the downstream stream segment. Obvert elevations were assigned based on the DEM. It is recognized that simulating the wetlands as MODFLOW lakes is a simplification because neither the slope of the water surface nor the velocity variation within the wetland are calculated. The wetlands simulated tend to be relatively small and using a single stage value was thought to be a reasonable approximation.

5.7 Groundwater Recharge

Groundwater recharge rates for the steady-state simulations were estimated from the average of annual recharge rates from the PRMS-only simulations (Figure 4.9). Rates range from near zero to 600 mm/year and reflect the combined effects of climate, topography, land cover, and soil property variation. For transient GSFLOW simulations, the PRMS submodel is run on an hourly basis and net recharge is applied to the unsaturated portion of the groundwater model on a daily basis. Because the position of the water table can affect the amount of net recharge, in GSFLOW the PRMS submodel is run iteratively with the MODFLOW submodel until convergence is achieved between the two models and a mass balance is obtained for the time step (Markstrom & Niswonger, 2008).

5.8 Model Layer Properties

Initial estimates for the aquifer and aquitard hydraulic conductivities were determined from other studies in similar settings and then adjusted as part of the model calibration procedure. Due to lack of data, constant values were assumed for some of the hydrostratigraphic units. Hydraulic conductivities were adjusted manually to best match the observed water levels. Automated parameter estimation techniques (Watermark Numerical Computing, 2010) were employed to help refine the calibration.

Maps showing the spatial distribution of the final calibrated hydraulic conductivity values for Layers 1 through 6 are presented in Figure 5.3 through Figure 5.9, respectively. Some of the variation in the layers is due to the assignment of hydraulic conductivities from underlying layers in areas where the main unit is not present. Vertical hydraulic conductivity within the virtual layers is presented in Figure 5.10 through Figure 5.13.

Vertical conductance values, a MODFLOW term describing the average vertical hydraulic conductivity divided by the distance between the midpoints of the layers, were calculated in VIEWLOG based on the layer thicknesses and the assigned hydraulic conductivity values and anisotropy factors (i.e. the ratios of vertical to horizontal hydraulic conductivities) as:

$$VC = \frac{1}{\frac{\Delta Z_1}{2\alpha_1 K_1} + \frac{\Delta Z_2}{2\alpha_2 K_2}} \qquad \text{(Eq. 5)}$$

where:

VC	=	Vertical conductance [1/t];
ΔZ	=	Layer thickness [L];
K	=	Horizontal hydraulic conductivity [L/t]; and
α	=	Anisotropy factor.

Anisotropy factors were set uniformly to 0.5 for all the aquifer layers except for Layer 3 which was set to 1 (AF1/GLAF). All the aquitards were set to 0.33. Base values for anisotropy were set to 0.3 for Layer 2 and 0.1 for Layer 4.

Discharge of groundwater to streams, wetlands and lakes and losses of water from surface water to the underlying aquifer are other areas of groundwater/surface water interaction. Representing these processes in a consistent manner is the principal objective of the GSFLOW

code. As shown in the sketch below (modified from Markstrom *et al.*, 2008), the MODFLOW sub-model in GSFLOW accounts for the saturated and unsaturated zone components of flow as well as the surface water flow components (i.e., lakes, wetlands, and streams) while PRMS accounts for the soil water balance and overland flow routing.

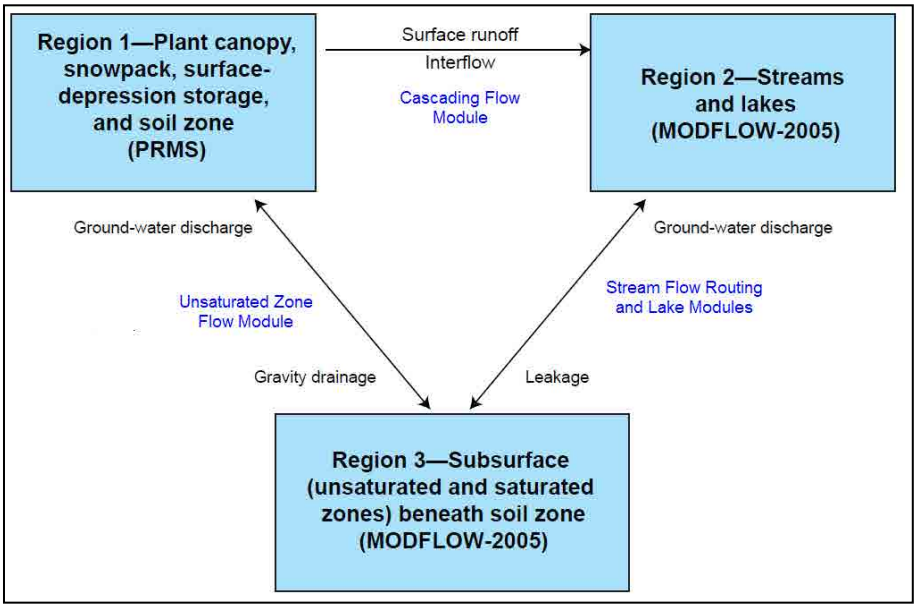

The UZF unsaturated flow package (Niswonger *et al.*, 2005) is incorporated into the MODFLOW sub-model in GSFLOW to simulate the percolation of excess moisture (infiltration minus losses to evapotranspiration) from the soil zone to the water table, groundwater ET processes, and the return of excess infiltration to the surface. The UZF module handles the particularly complex problem of the water table rising into the soil zone which can occur in portions of the model area, for example, perched water table conditions within the Oro Moraine.

A second add-on to the MODFLOW sub-model in GSFLOW is the SFR2 streamflow routing module (Niswonger and Prudic, 2005) which routes flow and calculates leakage between streams and the underlying aquifer. A third add-on is the lake simulation (LAK3) module (Merritt and Konikow, 2000) which is used in this study to represent lakes and shallow wetlands in the model area. The module computes a separate water balance for each lake/wetland based on computed inflows and outflows. Within the model, 85 water features were modelled as lakes, the largest being Bass and Little Lakes. The remaining 83 features represent ponds and other open water portions of wetland complexes identified from aerial photography. Figure 5.14 illustrates the location of lake features within the model area (shown in purple).

As discussed in the previous section, the hydrologic processes simulated in the PRMS sub-model are driven by hourly climate inputs (rainfall, snowfall, air temperature, and solar radiation) supplied to the groundwater sub-model on a daily basis. Changes in the groundwater stress (e.g., pumping or changes in reservoir operations) can be input to the model at the start of a daily time step. The SFR2 module routes streamflow on a daily basis and calculates average daily streamflow, stream stage, leakage, and stream discharge. Similarly, the LAK3 module determines average daily lake stage, change in storage volume, leakage and outflow.

Developing and calibrating an integrated model is therefore more complicated than developing separate surface water and groundwater models. The integrated model, however, can provide a much more realistic representation of the complex interactions between the groundwater and

surface water systems and can be used to evaluate the effects of factors as land-use change, climate variability, and groundwater withdrawals on surface and subsurface flow.

5.9 Model Calibration Approach and Targets

The primary targets for model calibration were the groundwater heads and flow patterns observed from static water levels obtained from the MOE database. Processing and filtering of the data as well as statistical error in the data are discussed in a previous section. MOE water levels were used to calibrate the steady state model.

Calibration of the groundwater flow model was initiated using a systematic trial-and-error process in which results of successive model runs were used to improve the initial estimates of hydraulic conductivity, vertical anisotropy, and recharge rates. Spatial analysis of residuals (i.e., the difference between simulated and observed values) helped to highlight areas where the model was or was not performing well. Statistical tests, in which the observed and simulated groundwater heads were compared, helped determine whether the calibration met the required goodness-of-fit criterion. After the initial manual calibration, calibration refinement was undertaken via automated parameter estimation methods, namely PEST (Watermark Numerical Computing, 2010) applied to the steady state model.

A second important target for the model calibration was discharge at WSC streamflow gauges within the model area. A key advantage of an integrated modelling approach is that total streamflow within a reach or segment can be estimated. This negates the need for baseflow separation techniques and the estimation of a single average value for the observed catchment groundwater discharge Transient modelling efforts were undertaken over a 5 year calibration period (October 2004 to September 2009). Further discussion of transient calibration efforts will be provided in the Phase 2: ESGRA reporting.

5.10 Model Results

5.10.1 Steady State Calibration

Figure 5.15 through Figure 5.19 illustrate the simulated groundwater heads output from the calibrated steady state model. A scatterplot comparing the observed MOE water levels to the simulated heads in each layer is shown in Figure 5.20. Ideally, all data points should fall on the 45° line shown on the graph. The scatterplots show that most data points fall within bands defined by ±10 m.

In addition to visual checks that the simulated water levels matched the MOE observed values reasonably well, three calibration statistics were used to assess and demonstrate model accuracy: the mean error (ME), mean absolute error (MAE), and root mean squared error (RMSE). These are given by Anderson and Woessner (1992) as:

$$\text{Mean Error} = \frac{1}{n}\sum_{1}^{n}(h_O - h_S)_i \qquad \text{(Eq. 6)}$$

$$\text{Mean Absolute Error} = \frac{1}{n}\sum_{1}^{n}\left|(h_O - h_S)_i\right| \qquad \text{(Eq. 7)}$$

$$\text{Root Mean Squared Error} = \sqrt{\frac{1}{n}\sum_{1}^{n}(h_O - h_S)_i^2} \qquad \text{(Eq. 8)}$$

where:

h_o = Observed hydraulic head;
h_s = Simulated hydraulic head; and,
n = Number of wells.

Values for the calibration statistics are provided in Table 5.2. The magnitude of the absolute error for the overall dataset is relatively small and the positive sign on the Mean Error (ME value) indicates that simulated values are generally lower than the observed values by 0.3m. Mean Absolute Error (MAE) and the Root Mean Squared Error (RMSE) are 5.8m and 8.1m respectively for the entire model domain.

The MAE and RMSE provide a good estimate of the average magnitude of the difference between the observed and simulated values. Values for MAE and RMSE are often compared to the overall response of the model (Anderson and Woessner, 1992); in this case, the range in heads over the model area approximately 190 m. The RMSE as a percent of range for the upper layers is less that 10%, and under 5% for the overall model. Spitz and Moreno (1996) state that a RMSE of less than 10% of the observed water level range indicates an acceptable calibration. The MODFLOW mass balance error for the steady state model was less than one tenth of a percent.

5.10.2 Transient Model Results

The transient fully integrated GSFLOW model was calibrated for the period spanning October 1, 2004 and September 30, 2009. This calibration period was selected because it contained the optimum coverage of calibration data, including PGMN water levels, MOE actual water takings, WSC streamflow and NEXRAD hourly climate data. Figure 5.21 through Figure 5.31 compare simulated transient heads to observed water levels at several groundwater monitoring locations in the model area. Specifically, Figure 5.21 through Figure 5.26 represent locations in or near the Oro and Hawkestone watersheds. The transient model reasonably matches the complex longer term rising water level trend observed through this time period. Shorter term seasonal patterns are also matched by the GSFLOW model in these key boreholes. It should be noted that the effects of pumping can be observed in the observation data, and that the model provides a reasonable match, even given the uncertainty in the actual water taking data. In summary, the transient groundwater calibration is excellent.

Figure 5.32 through Figure 5.35 compare simulated streamflow to the four active WSC stream gauges in the model area. The calibration to the key Hawkestone gauge (Figure 5.32) is very good, matching both the peaks and the recession patterns, a particularly complex scenario given the large wetland located in the upper-middle portion of the watershed (see the green wetland area shown in Figure 2.41). Also note how the Hawkestone gauge calibration reasonably matches both the 2007 summer drought flows, as well as the higher flows of the 2008 wet year. The calibration at the Coldwater gauge (Figure 5.34) is also particularly good. Monthly runoff volumes (Figure 5.36, Figure 5.37) compare favourably between the model results and the recorded discharge and the WSC gauge stations.

5.11 Conclusions

Given the low overall ME and RMSE calibrations statistics demonstrated in the steady-state model, and the good match between groundwater and streamflow hydrographs in the transient model, the calibration is of sufficient quality to proceed to the Tier 2 water balance calculations. In summary, the GSFLOW integrated GW/SW calibration in the model area provides considerable confidence in the model development, since the one model can represent such a complex range of long term and seasonal patterns in both surface water and groundwater conditions.

Further discussion and insights from the transient model will be provided in the Phase 2 ESGRA report.

5.12 Tables

Table 5.2: Model calibration statistics

Model Result By Aquifer/Layer	No. of Wells (n)	ME (m)	MAE (m)	RMSE (m)	Range (Obs) (m)	RMSE as % of Range (%)
Simulated heads in Layer 1 versus observed heads in the *ICSD*	14	-1.5	7.5	10.1	166.9	6.1%
Simulated heads in Layer 3 versus observed heads in the *AF1-GLAF* Aquifer	1254	0.1	5.0	7.1	140.5	5.1%
Simulated heads in Layer 4 versus observed heads in the *AF4-CAF1* Aquifer	1223	1.1	5.4	7.1	132.4	5.4%
Simulated heads in Layer 5 versus observed heads in the *STAF-CAF2* Aquifer	203	-0.5	6.2	7.9	100.6	7.8%
Simulated heads in Layer 6 versus observed heads in the *LAF-CAF3* Aquifer	491	1.8	8.7	11.2	107.6	10.4%
Simulated heads in Layer 7 versus observed heads in the *Bedrock* Aquifer	251	-3.8	6.7	9.8	85.8	11.4%
Overall	**3436**	**0.3**	**5.8**	**8.1**	**190.24**	**4.3%**

5.13 Figures

Figure 5.1: Model extent, boundaries, and finite-difference grid.

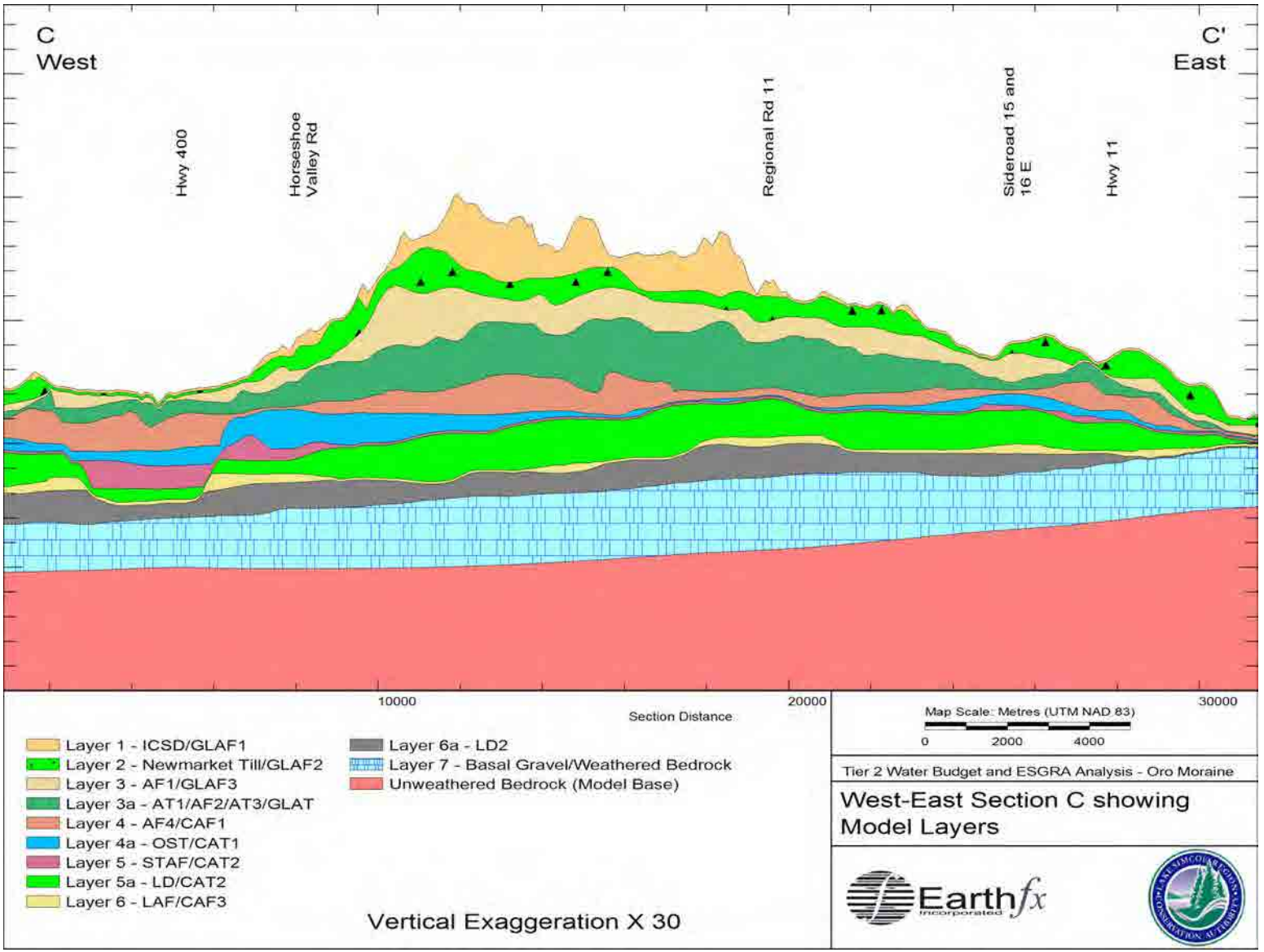

Figure 5.2: West-East cross section showing numerical model layers.

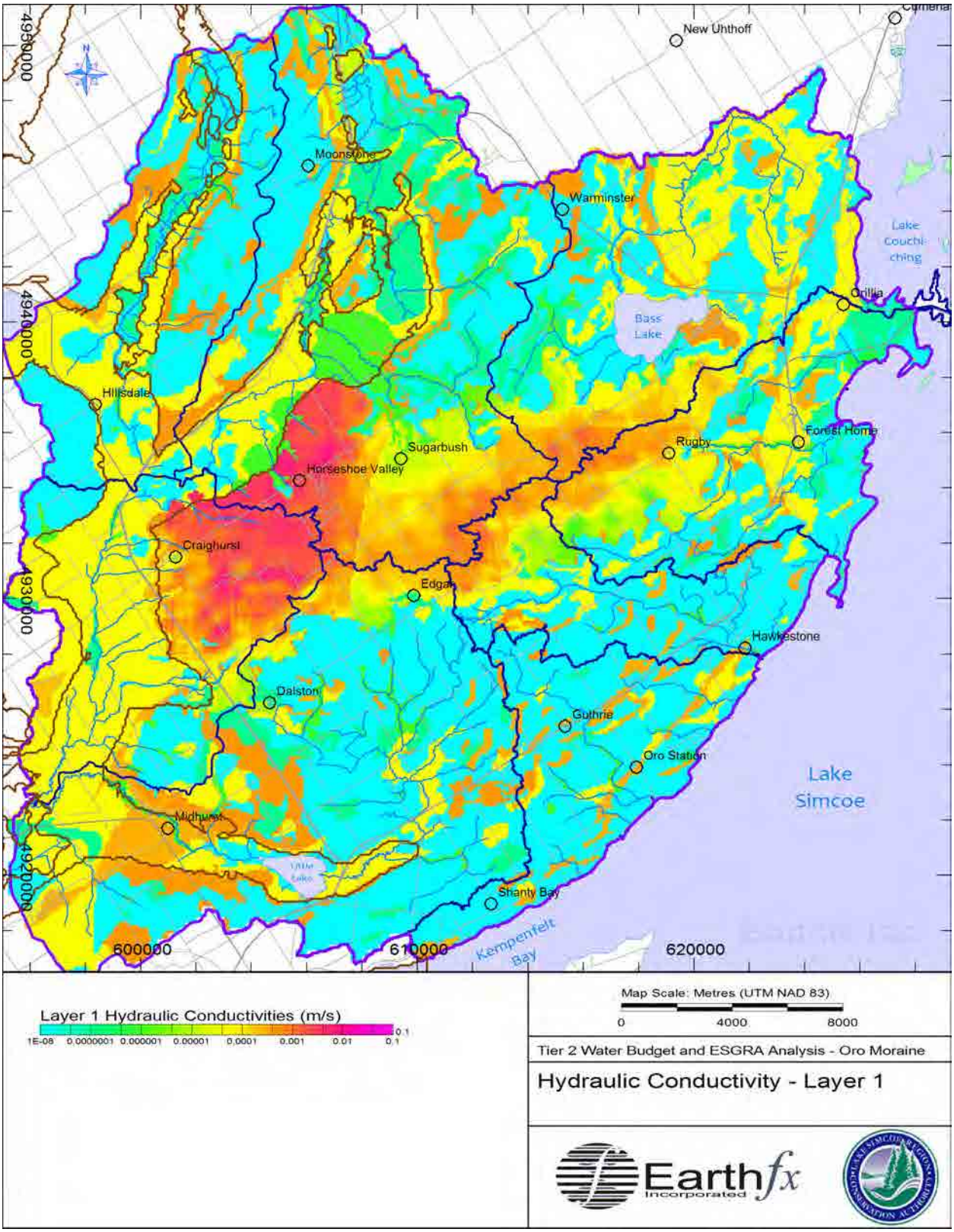

Figure 5.3: Hydraulic conductivity for Layer 1 representing the ICSD and GLAF.

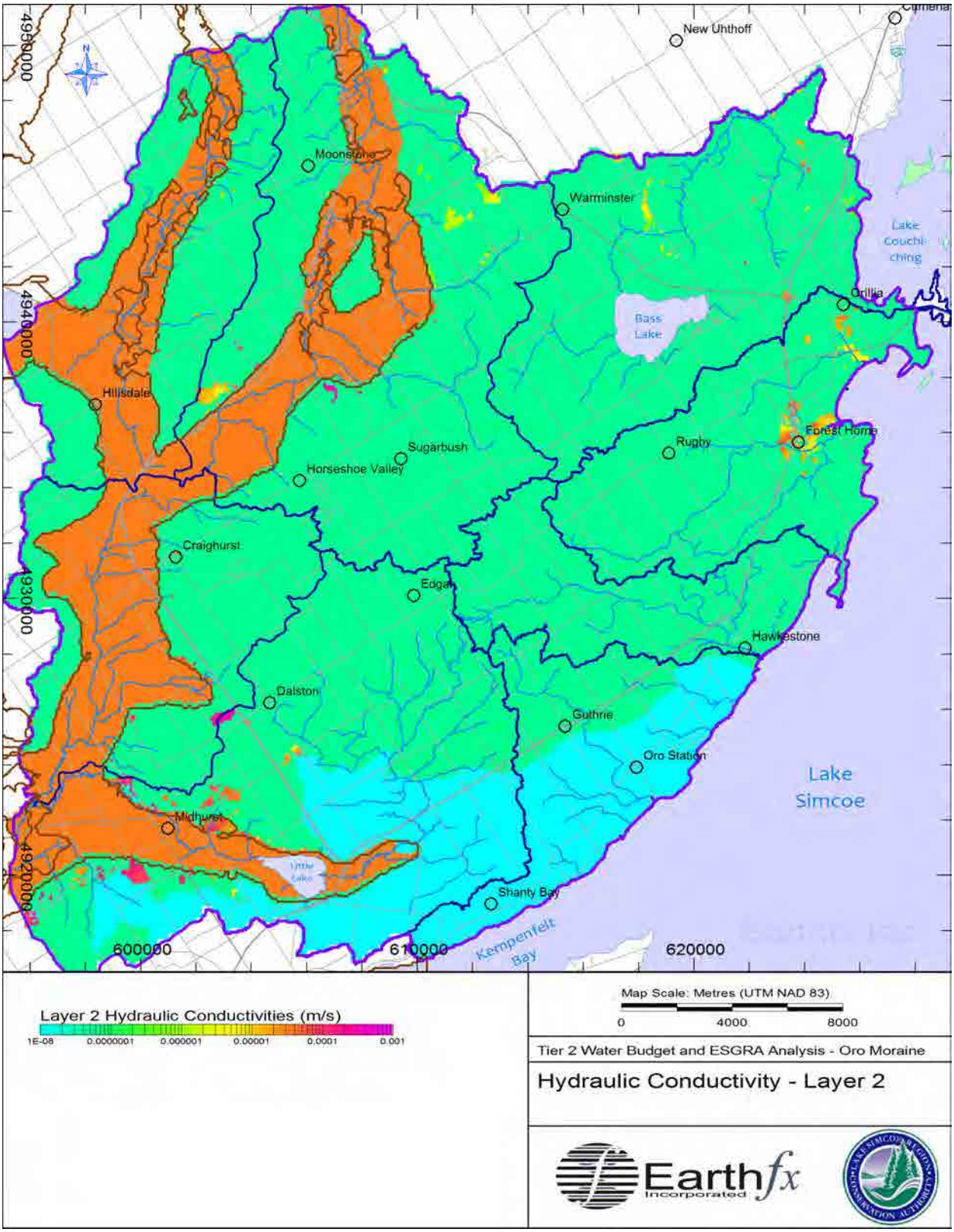

Figure 5.4: Hydraulic conductivity for Layer 2 representing the Newmarket Till/GLAF

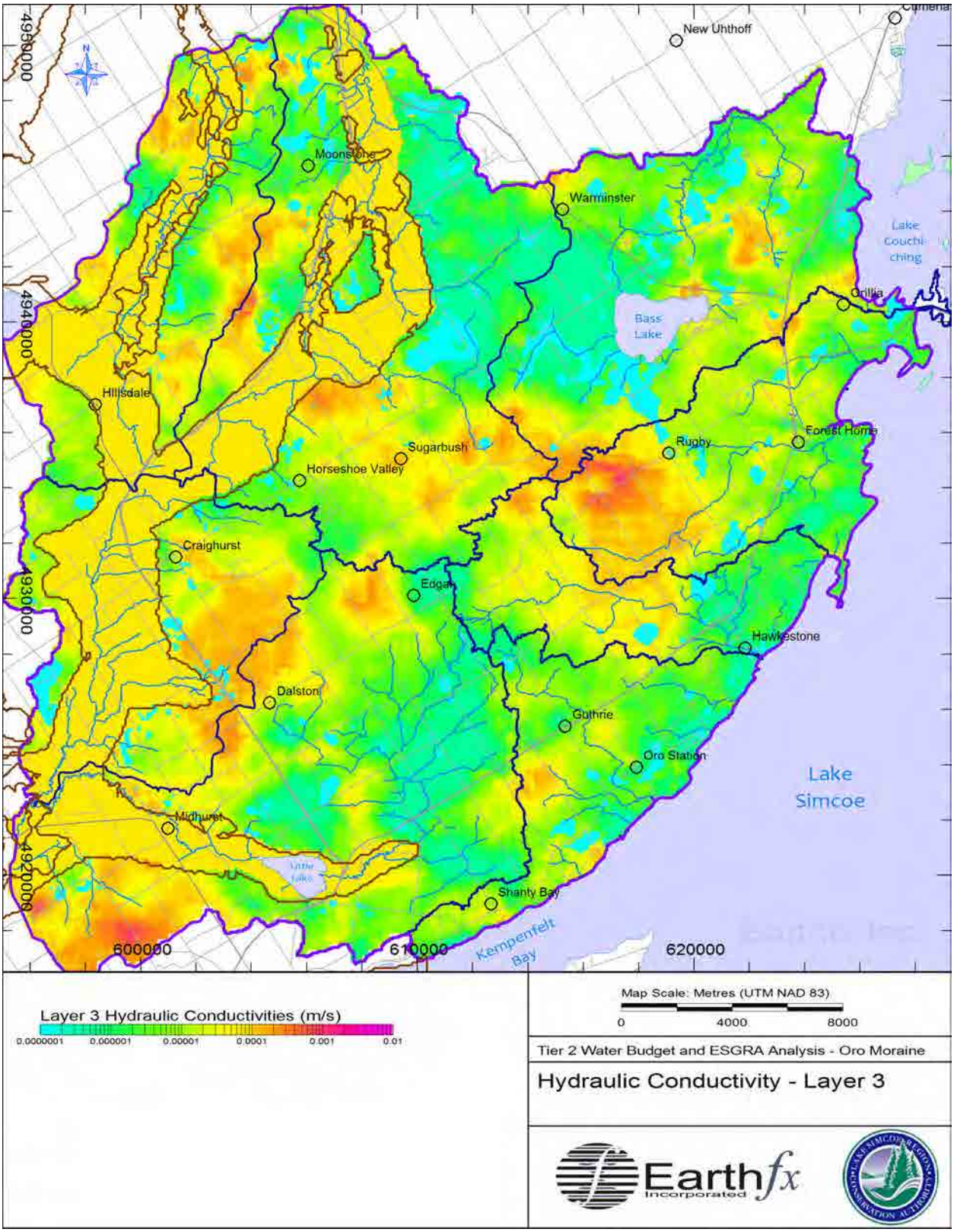

Figure 5.5: Hydraulic conductivity for Layer 3 representing AF1I/GLAF.

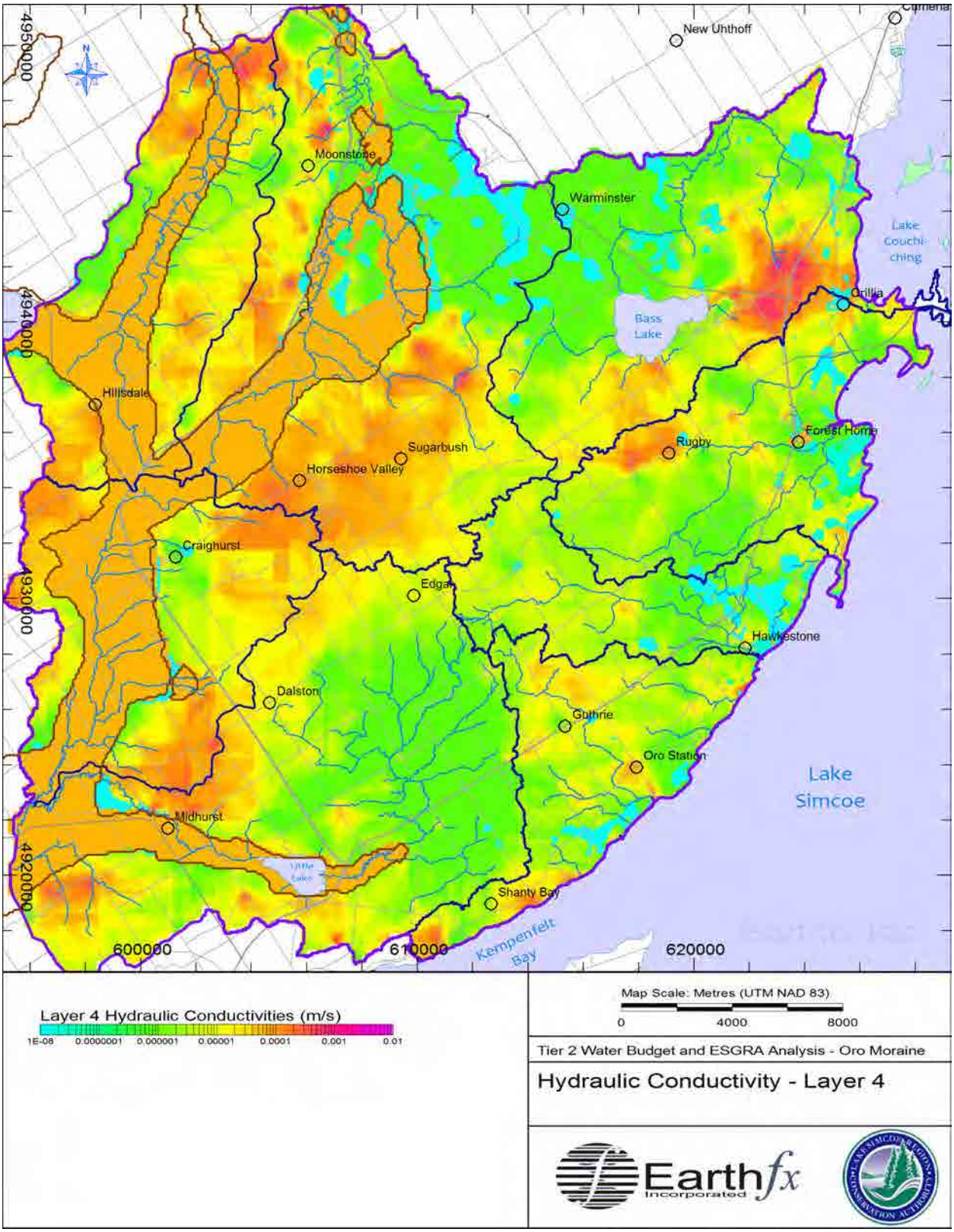

Figure 5.6: Hydraulic conductivity for Layer 4 representing the AF4/CAF1.

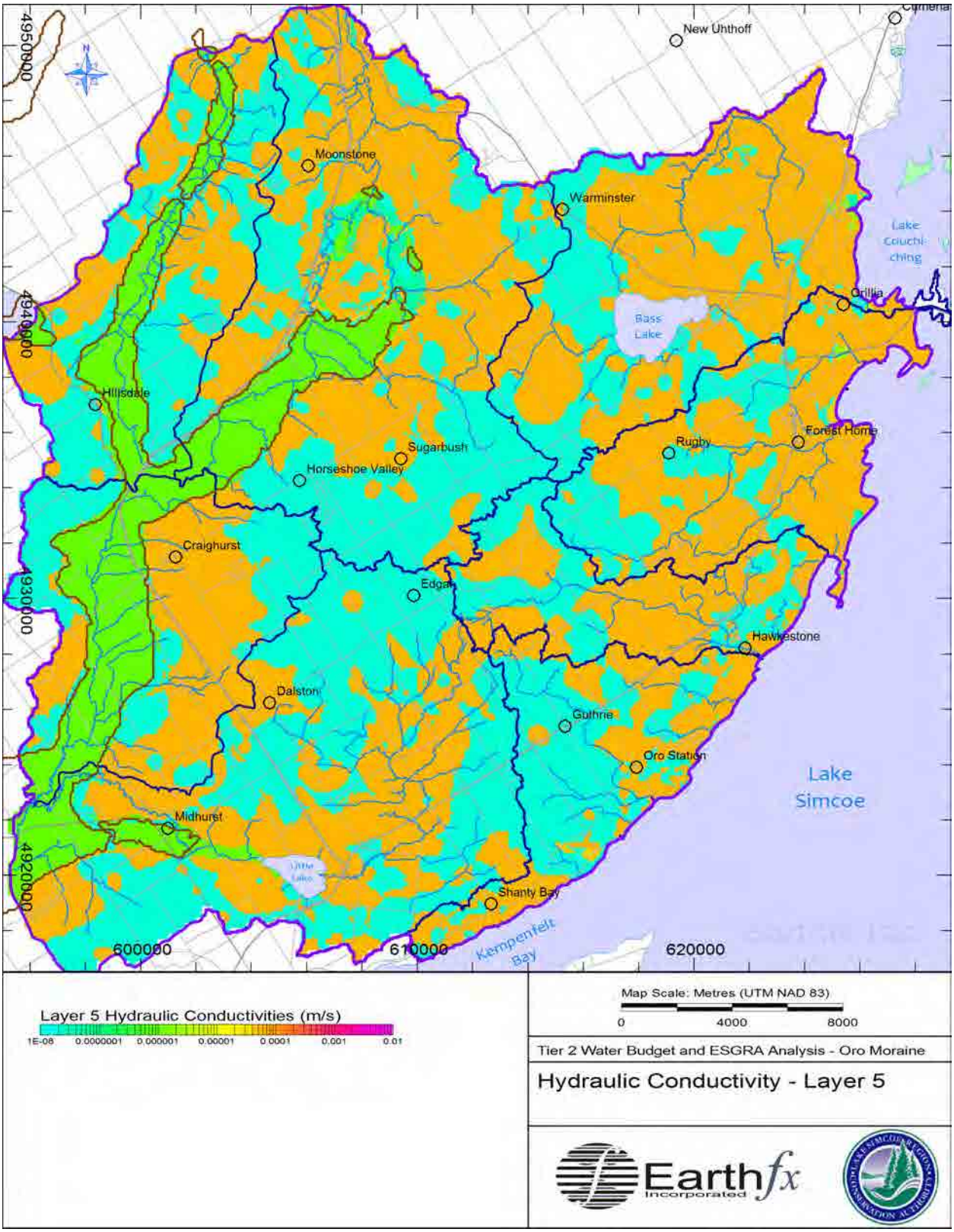

Figure 5.7: Hydraulic conductivity for Layer 5 representing the STAF/CAF2.

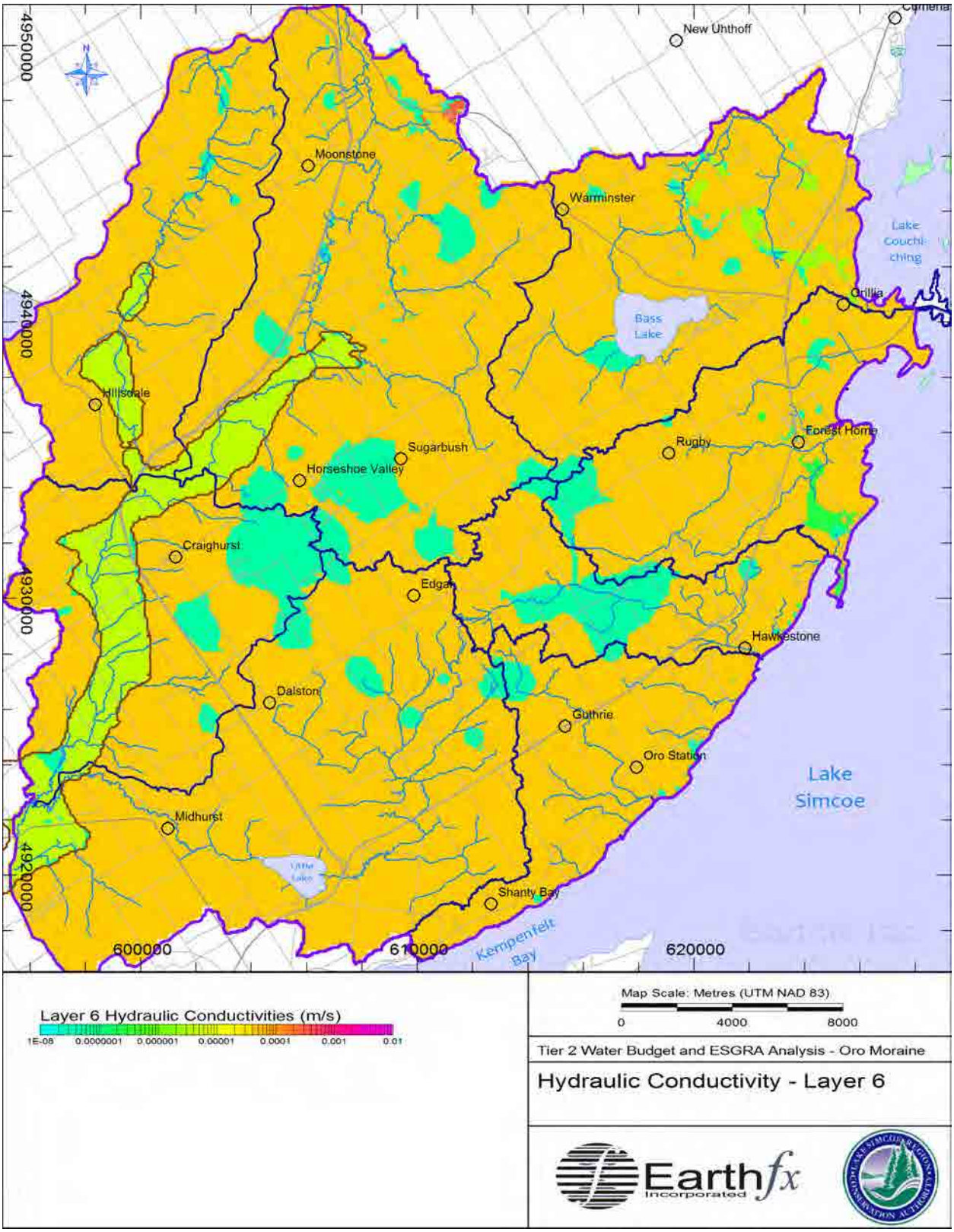

Figure 5.8: Hydraulic conductivity for Layer 6 representing the LAF/CAF3.

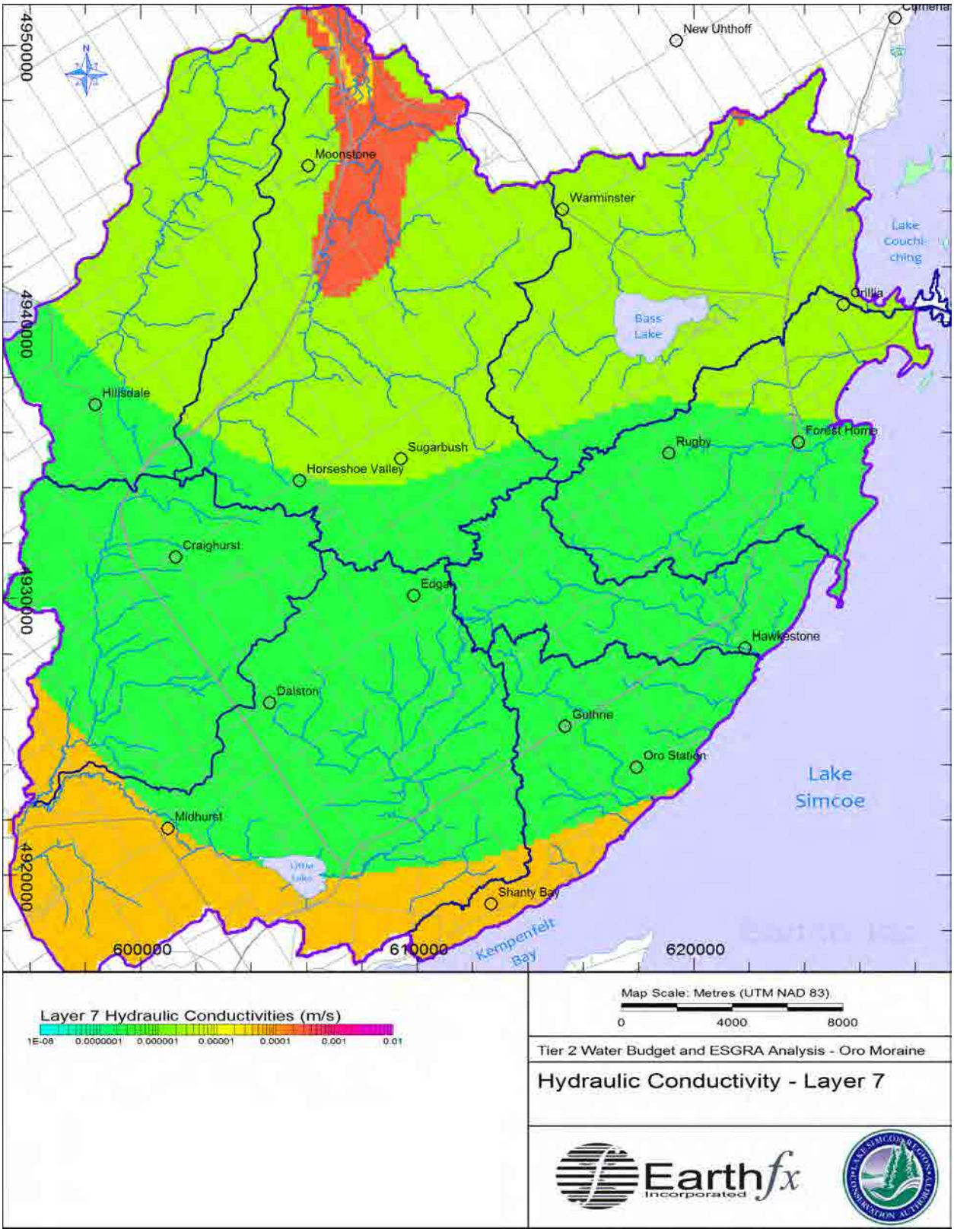

Figure 5.9: Hydraulic conductivity for Layer 7 representing the weathered bedrock.

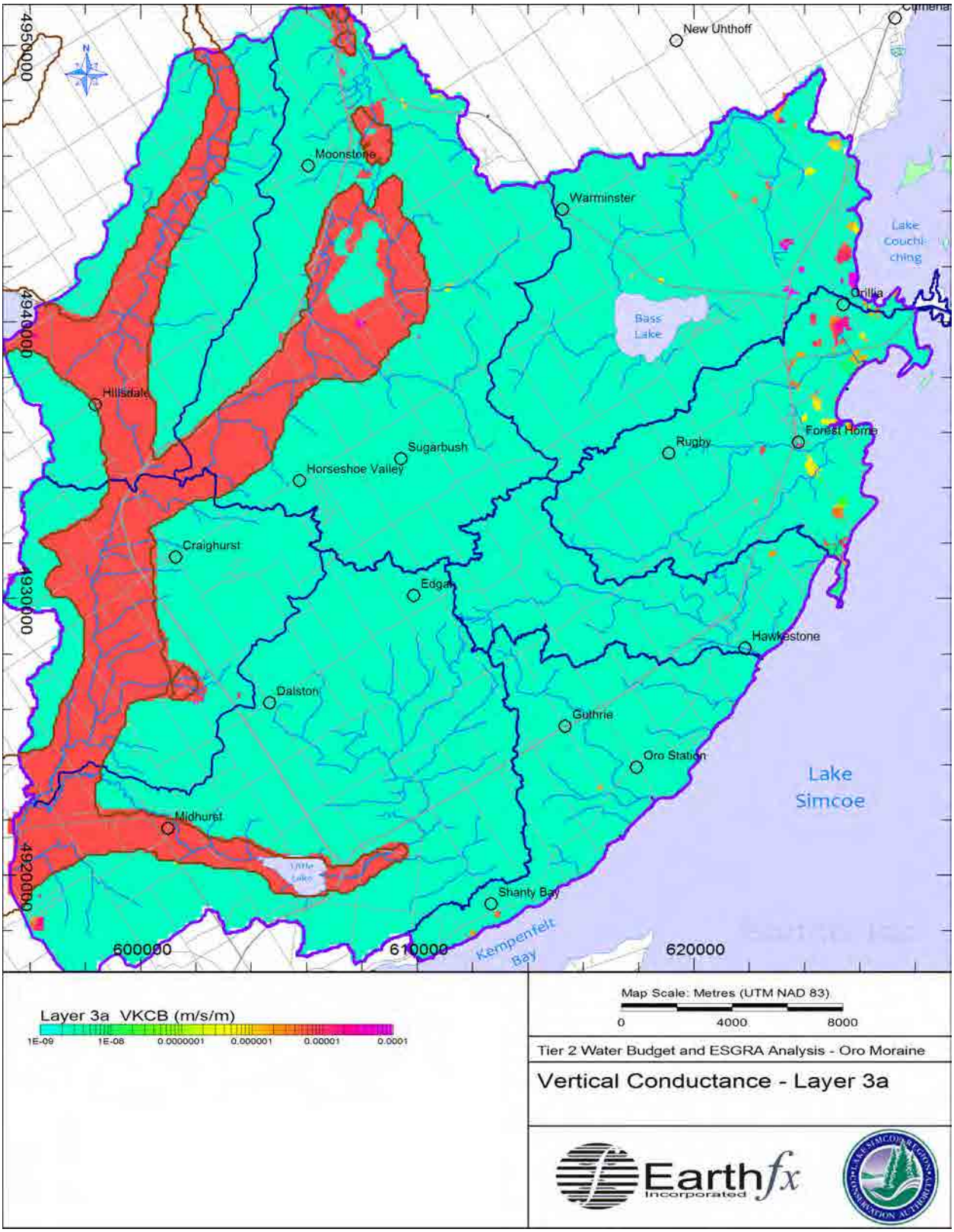

Figure 5.10: Vertical conductance - Virtual Layer 3a representing the AT1/AF2/AT3/GLAT.

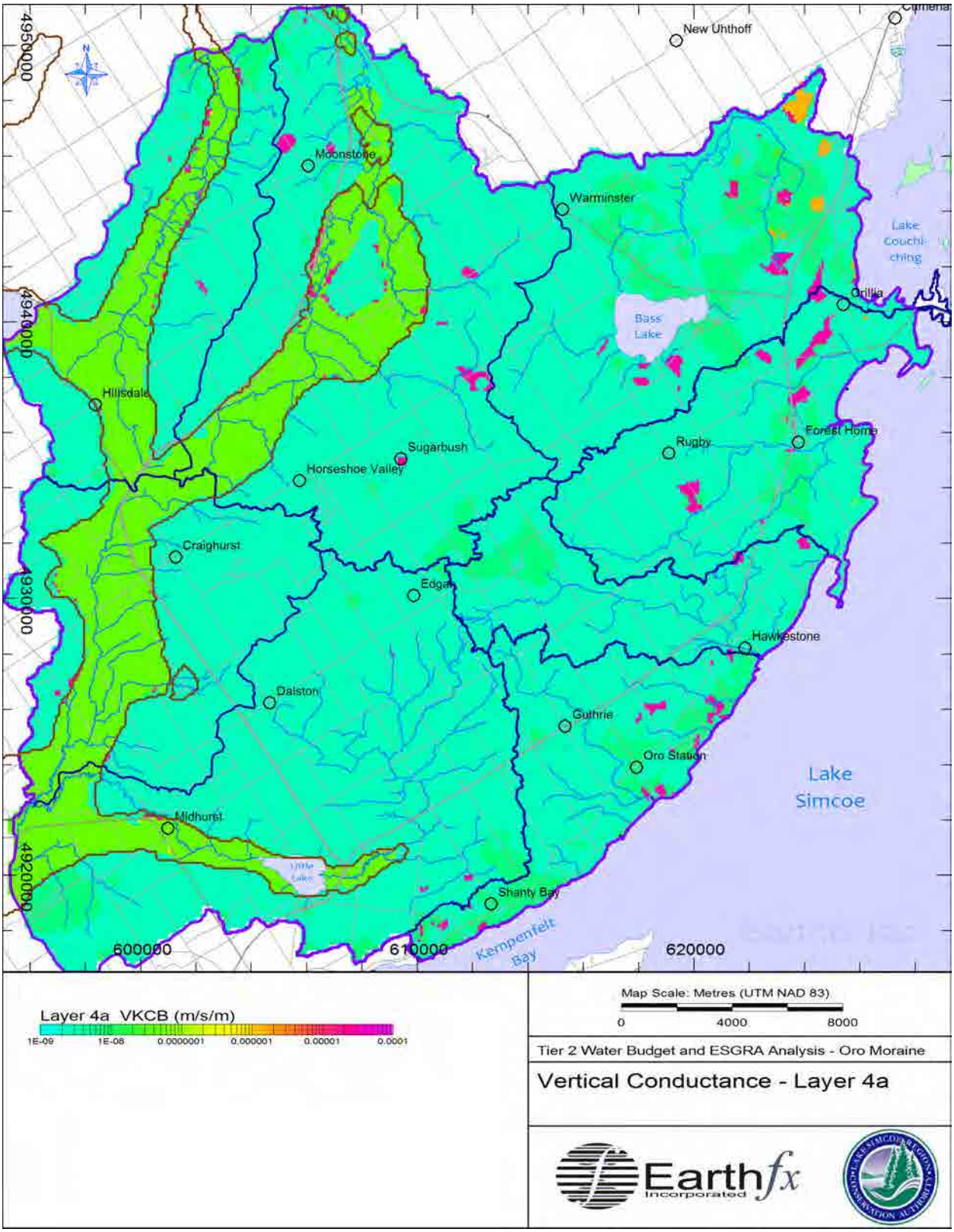

Figure 5.11: Vertical conductance - Virtual Layer 4a representing the OST/CAT1.

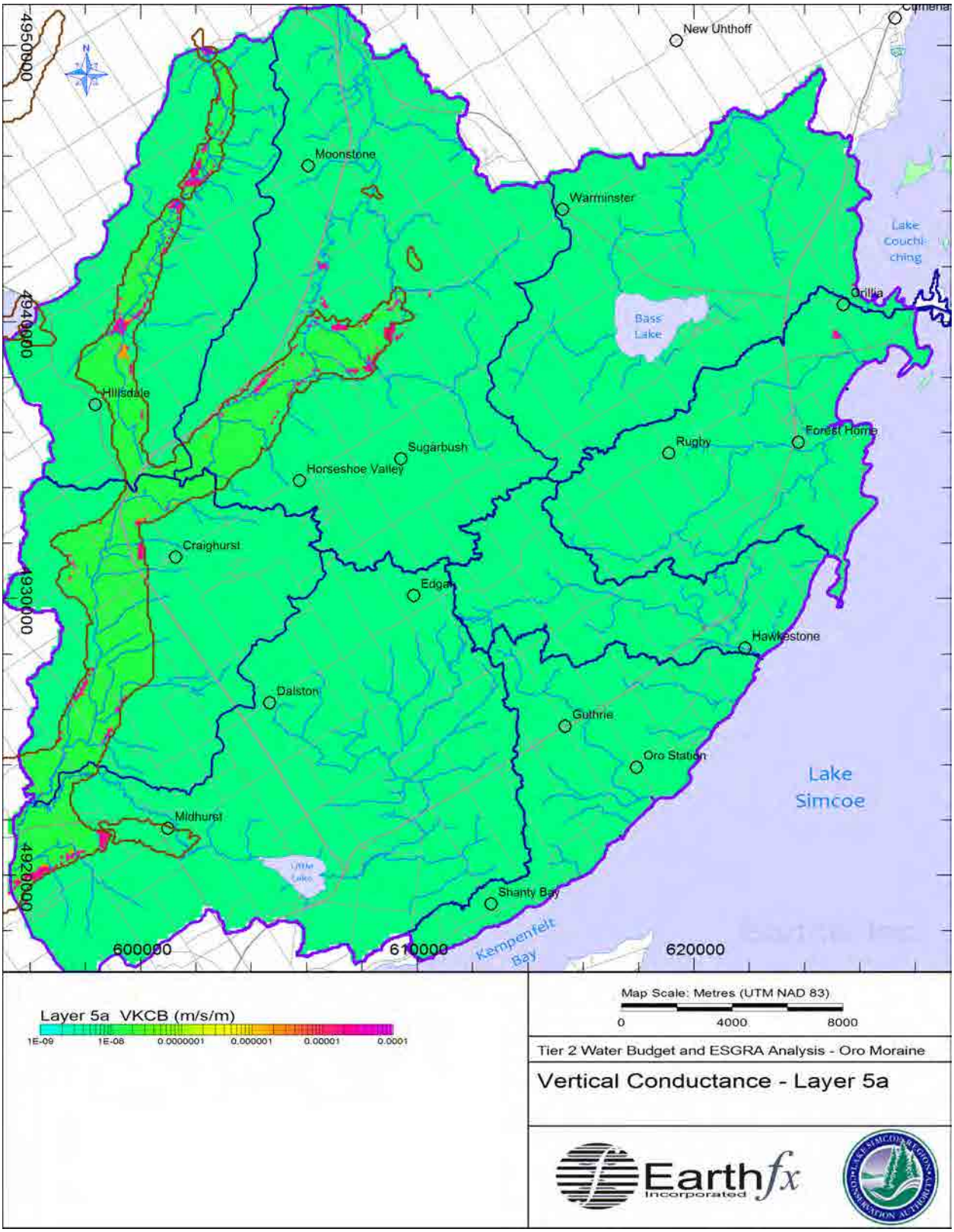

Figure 5.12: Vertical conductance - Virtual Layer 5a representing the LD/CAT2.

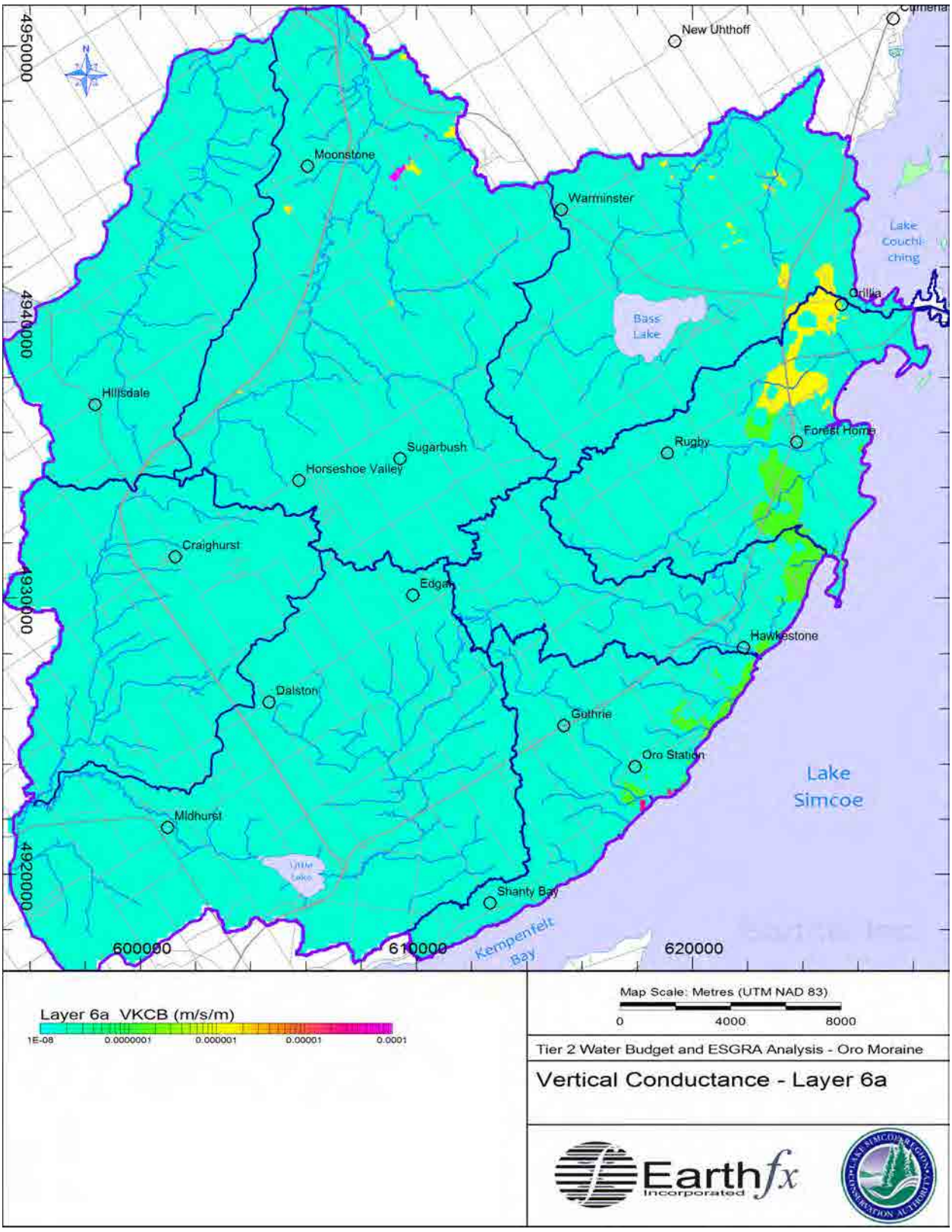

Figure 5.13: Vertical conductance - Virtual Layer 6a representing the LD2.

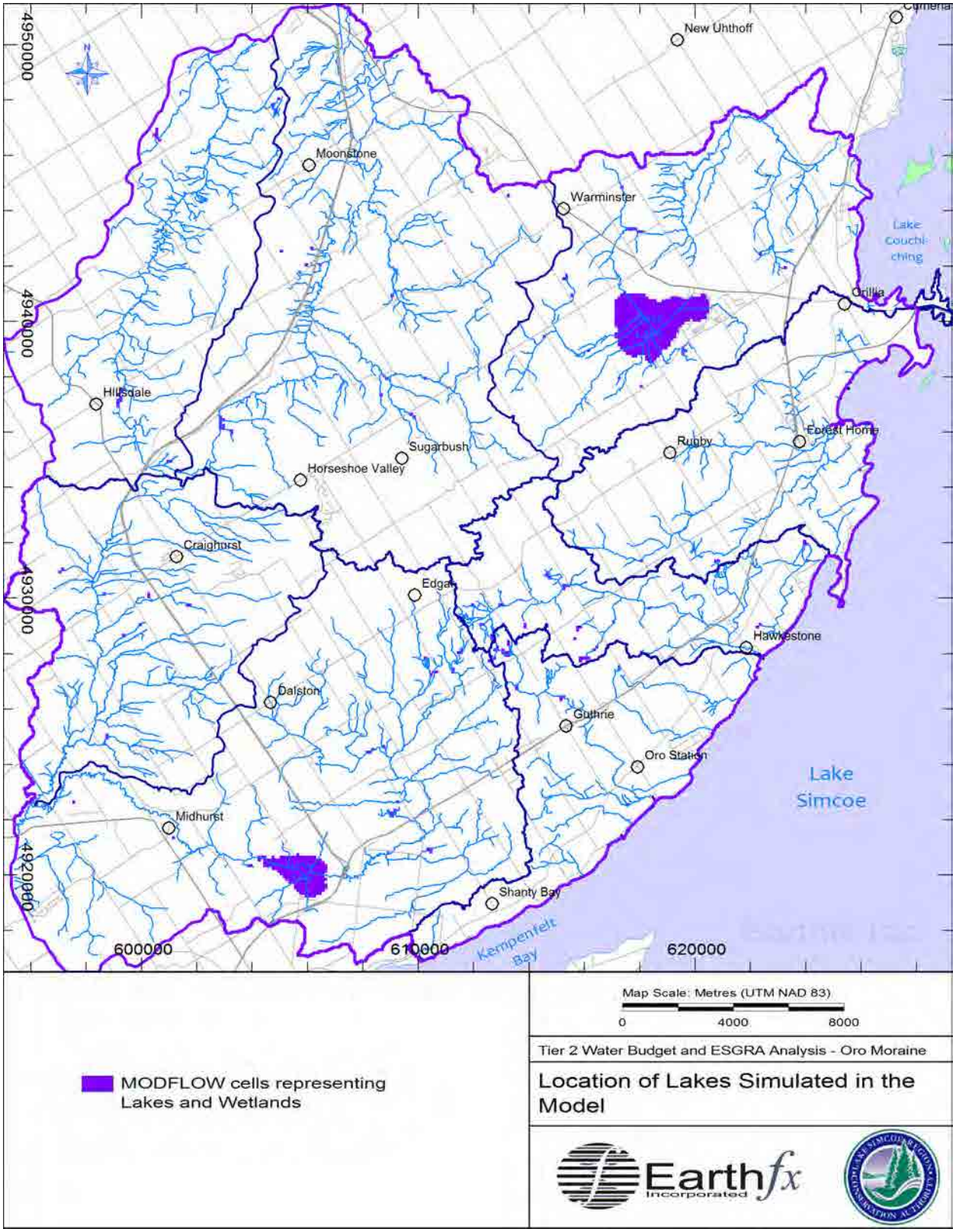

Figure 5.14: Location of simulated lakes and wetland-lake features.

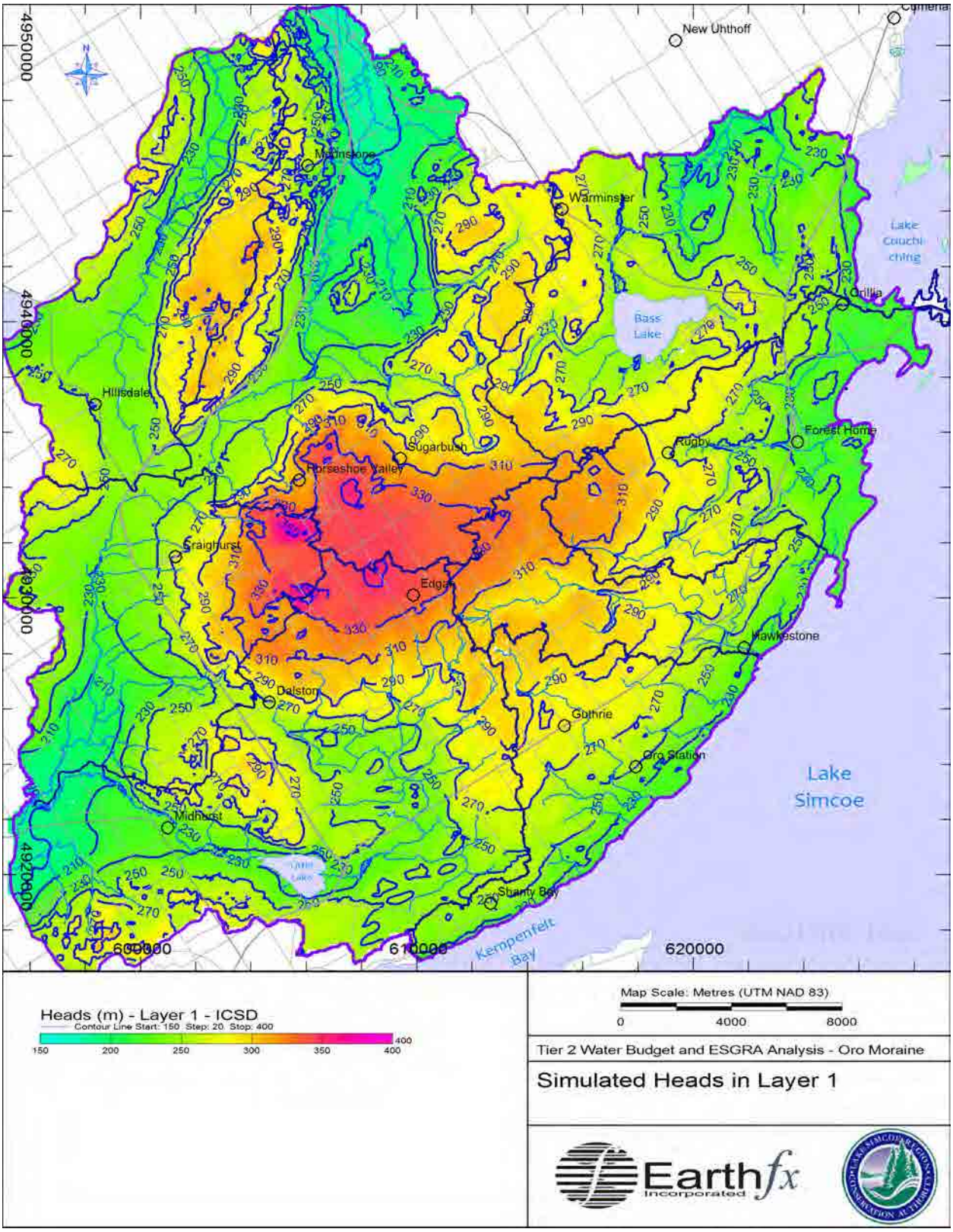

Figure 5.15: Simulated heads in Layer 1.

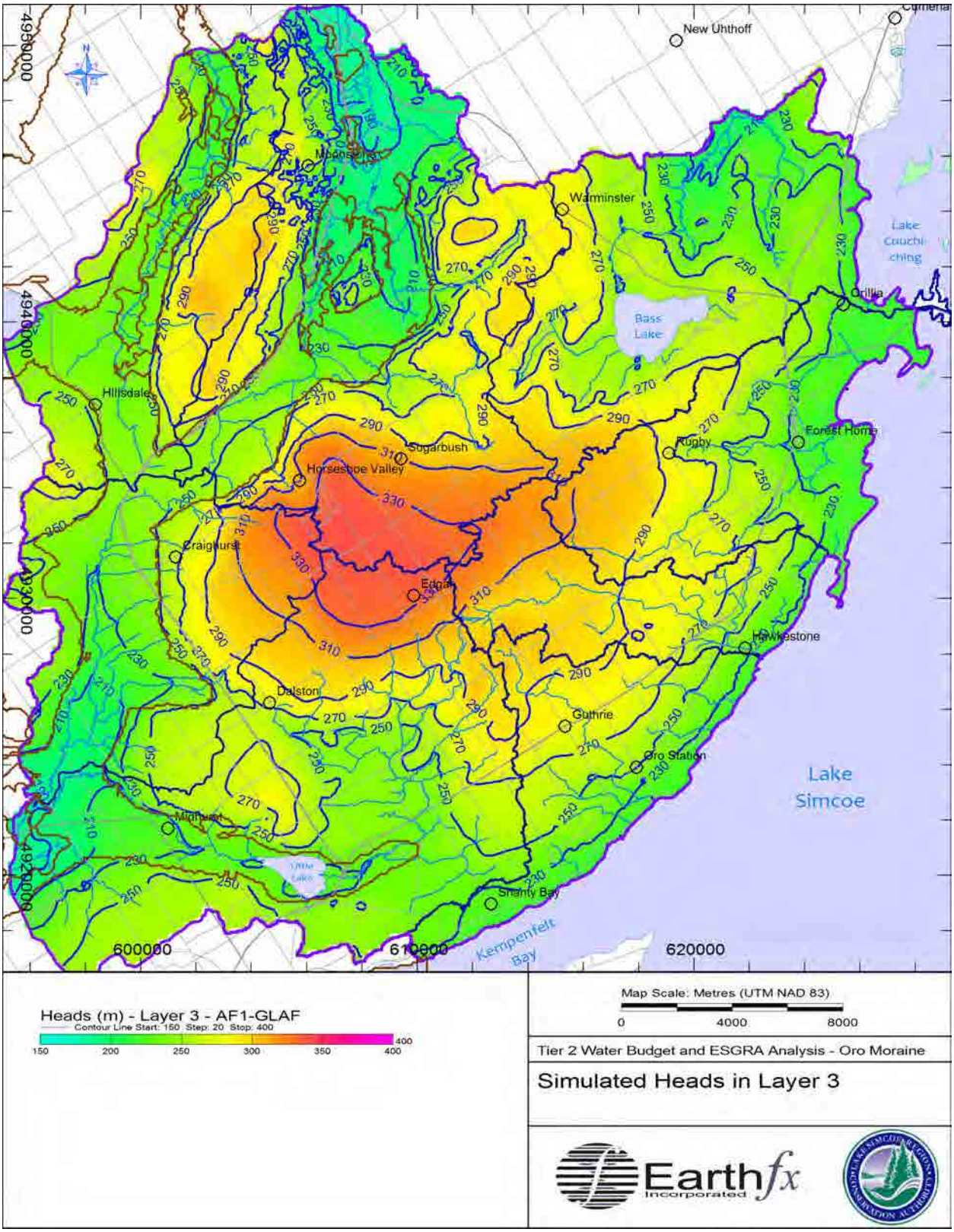

Figure 5.16: Simulated heads in Layer 3.

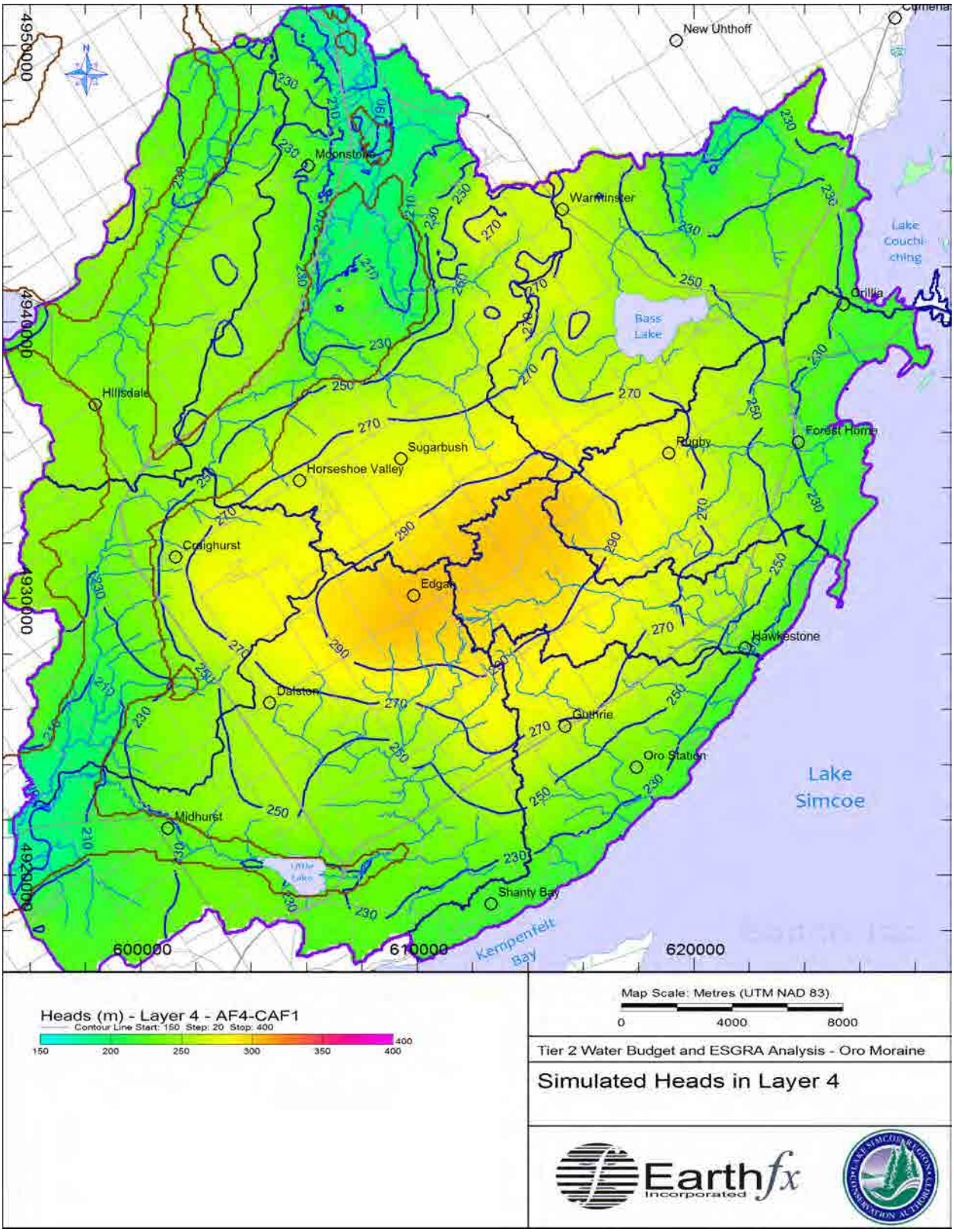

Figure 5.17: Simulated Heads in Layer 4.

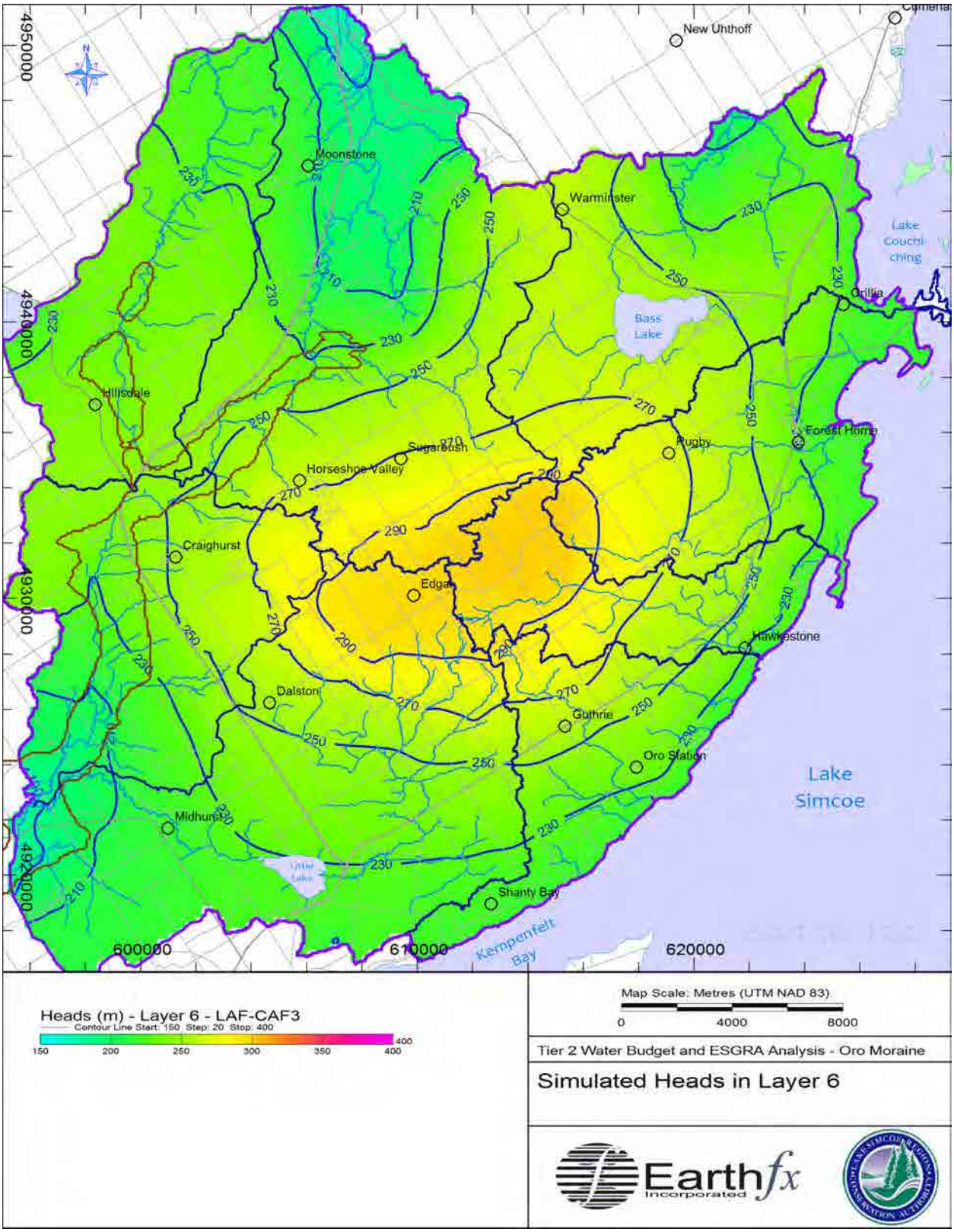

Figure 5.18: Simulated heads in Layer 6.

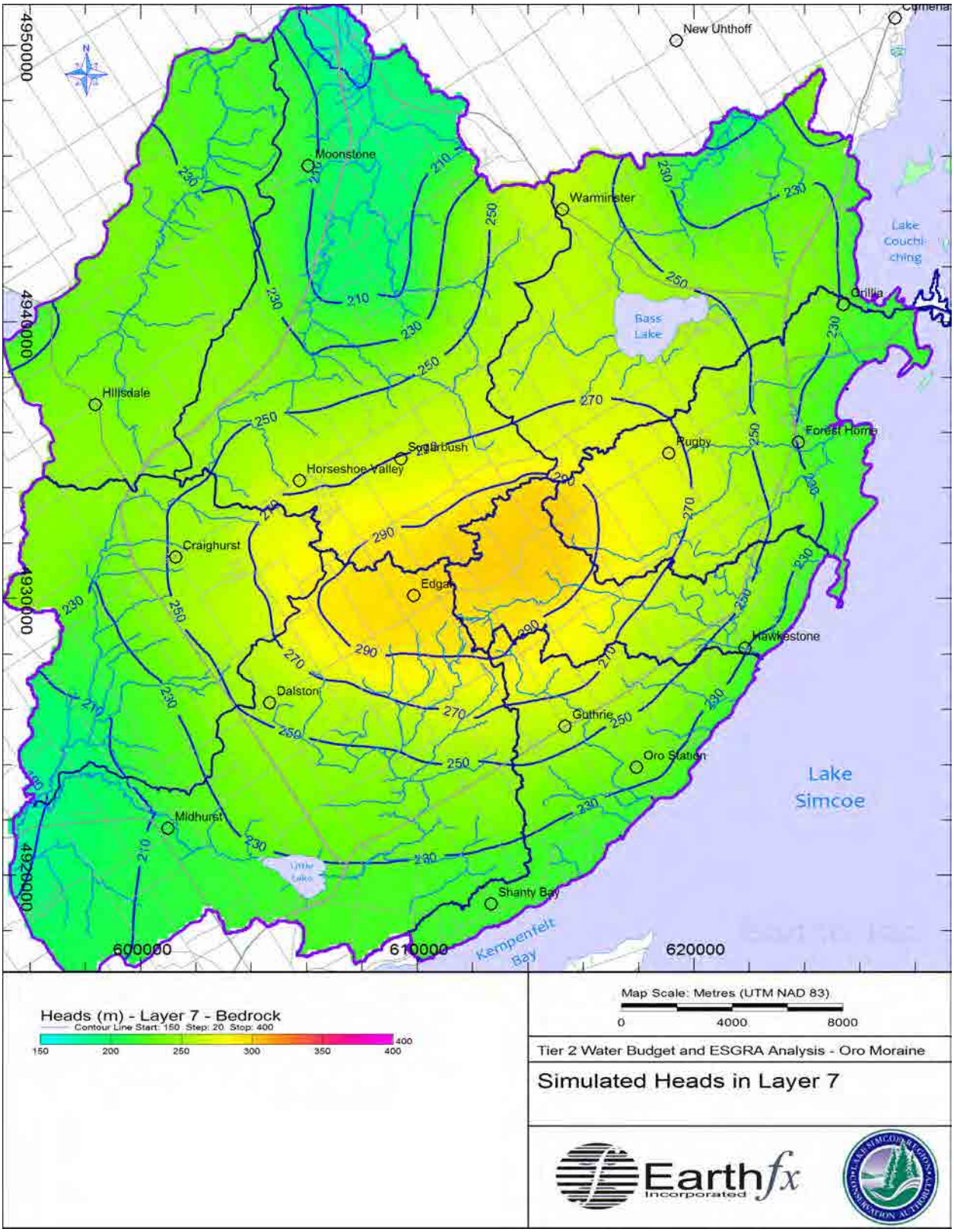

Figure 5.19: Simulated heads in Layer 7.

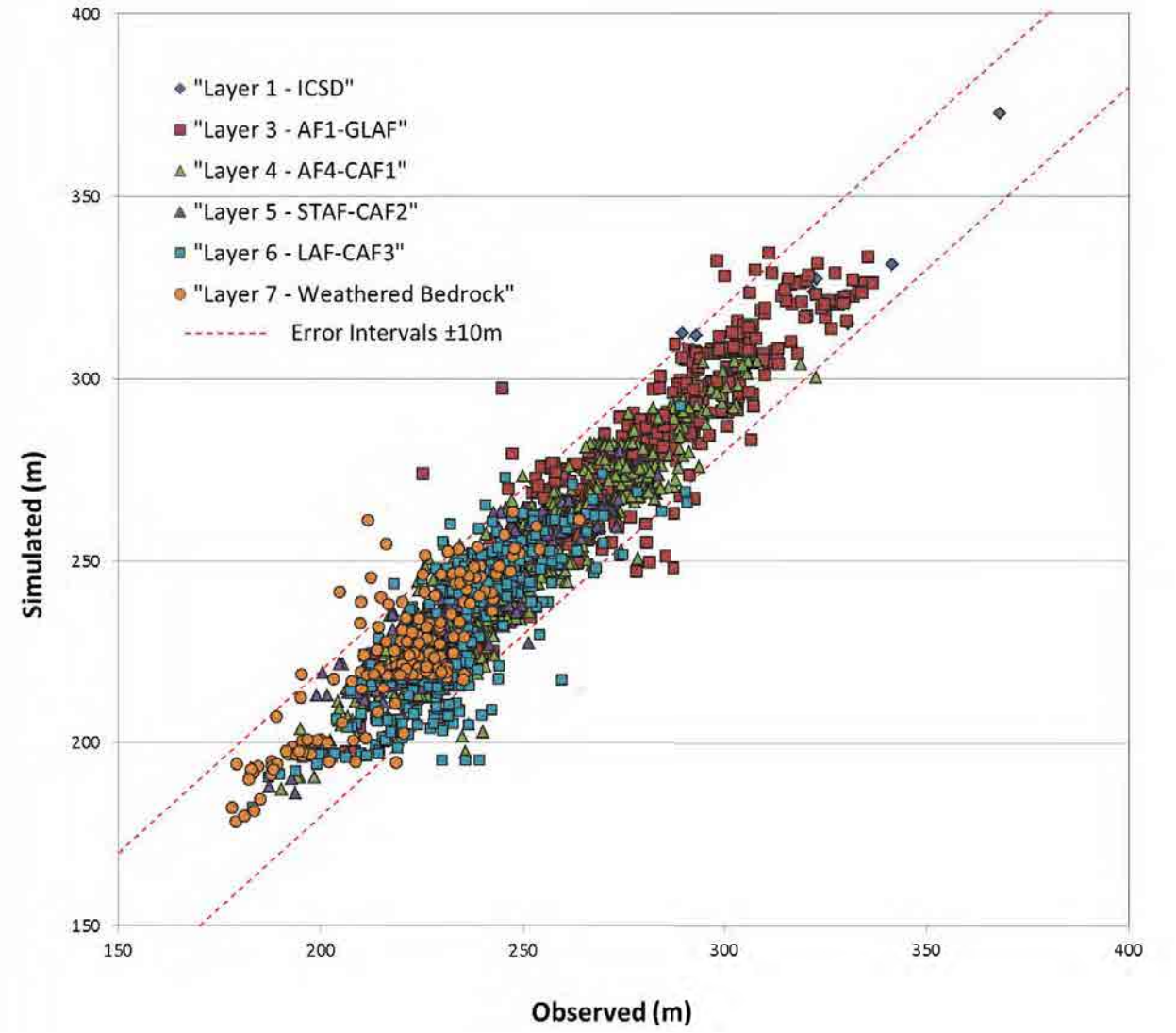

Figure 5.20: Scatter plot of observed versus simulated heads (The Mean Absolute Error (MAE) across the model domain is 5.8m).

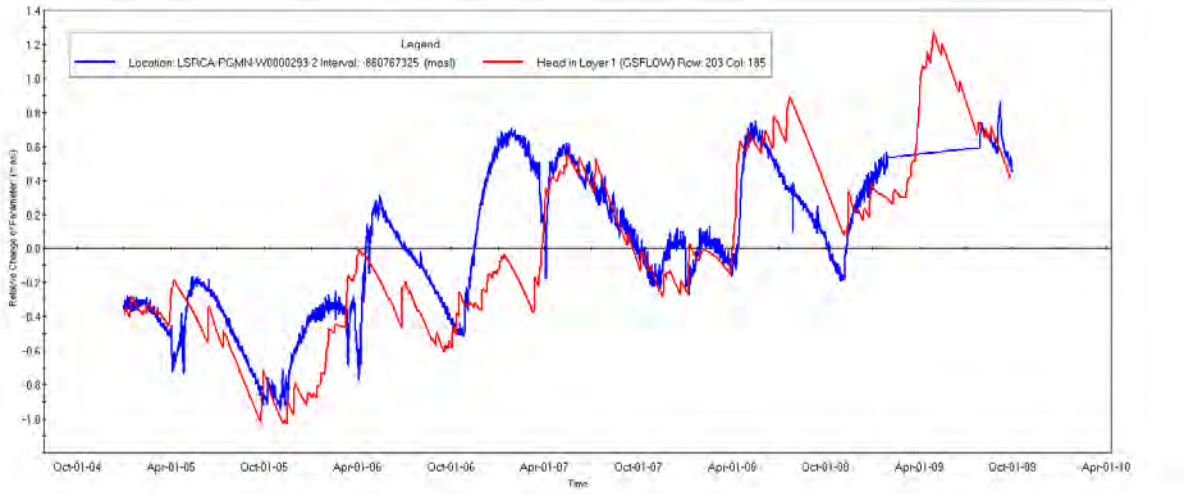

Figure 5.21: Simulated heads in Layer 1 and observed heads at PGMN Well #W0000293-2.

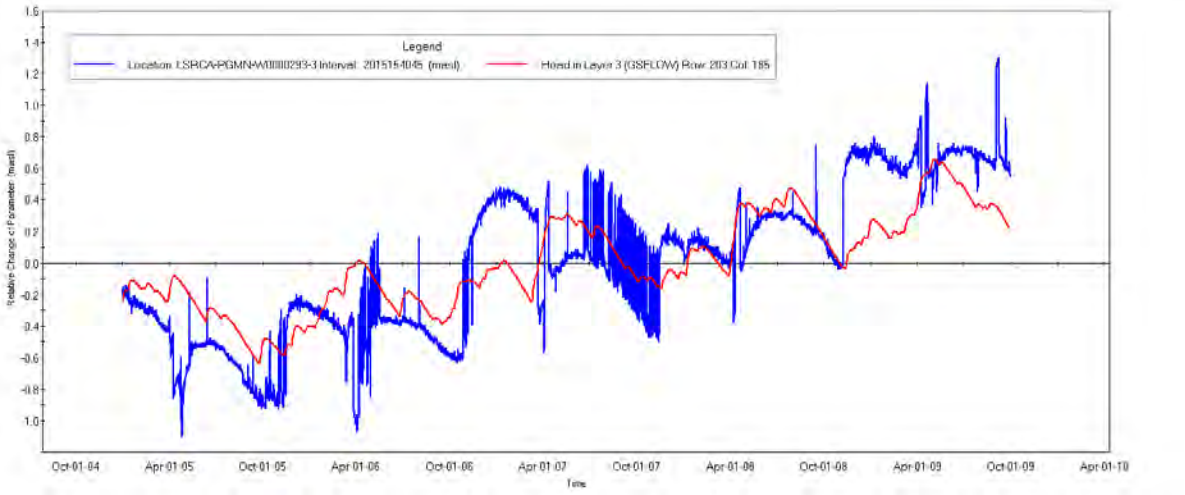

Figure 5.22: Simulated heads in Layer 3 and observed heads at PGMN Well #W0000293-3.

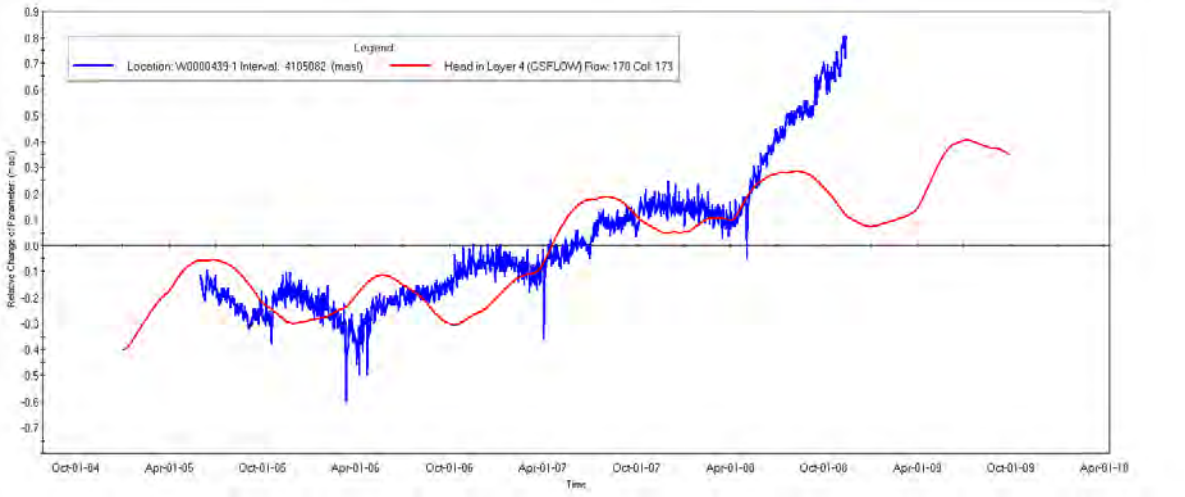

Figure 5.23: Simulated heads in Layer 4 and observed heads at PGMN Well #W0000439.

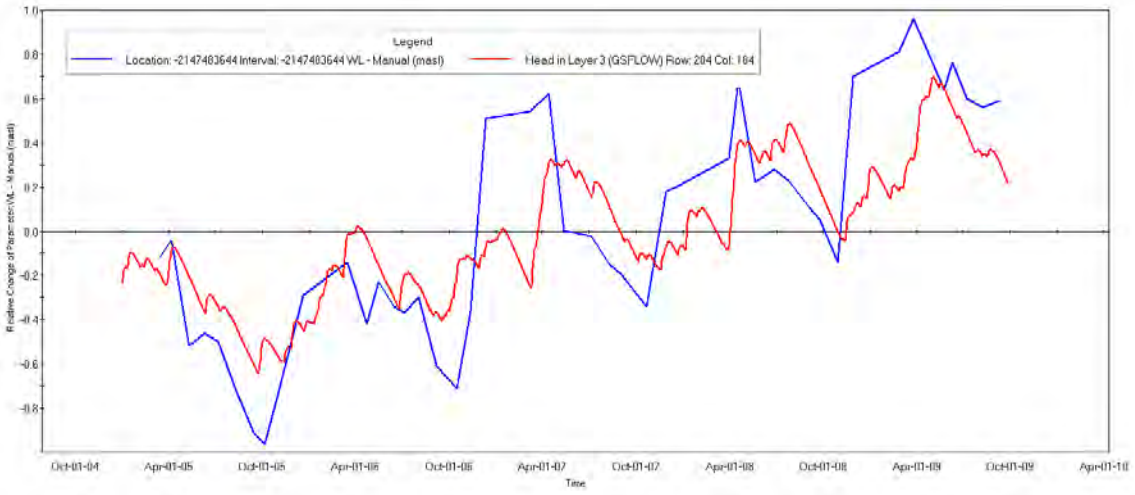

Figure 5.24: Simulated heads in Layer 3 and observed heads at Edgar Pit OW1.

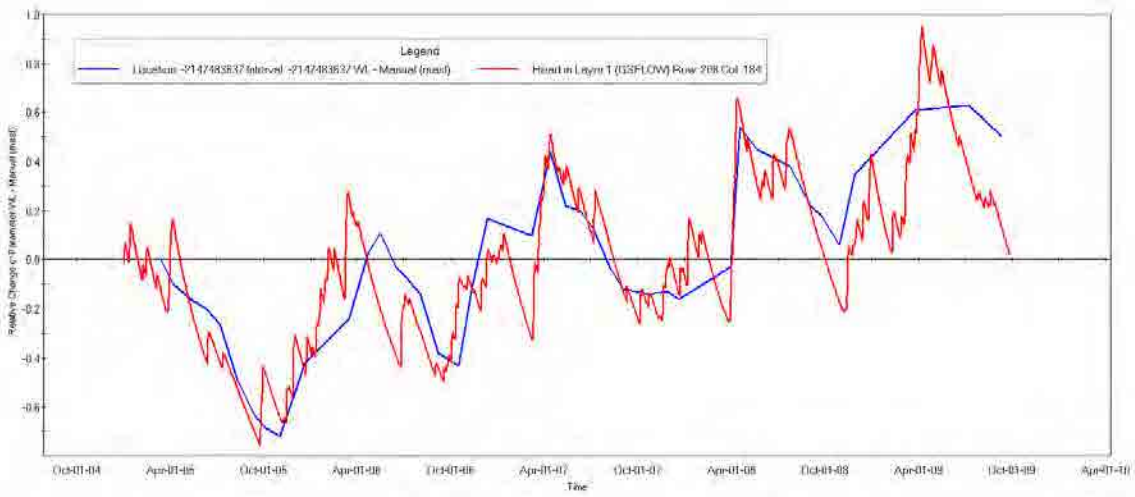

Figure 5.25: Simulated heads in Layer 1 and observed heads at Private Well "M".

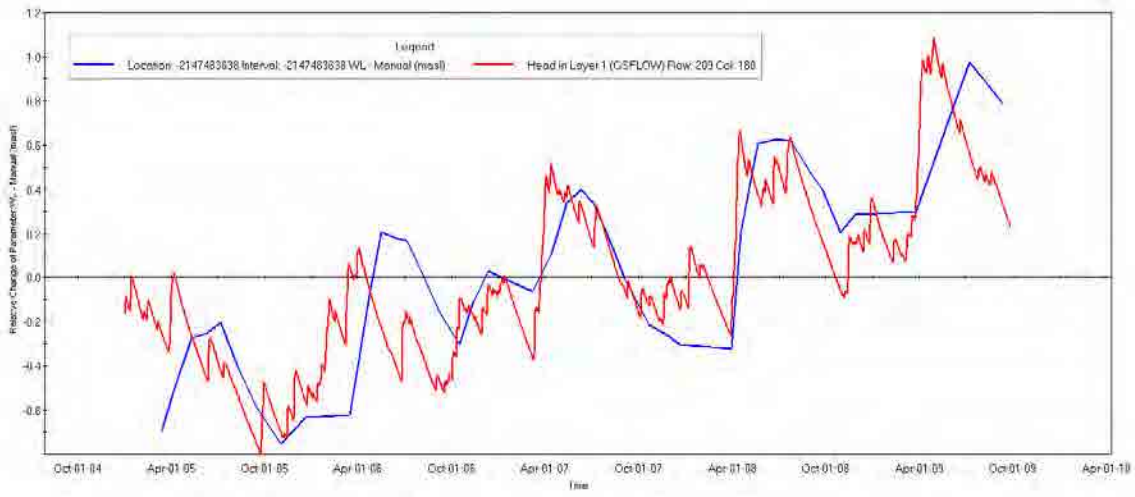

Figure 5.26: Simulated heads in Layer 1 and observed heads at Private Well "R".

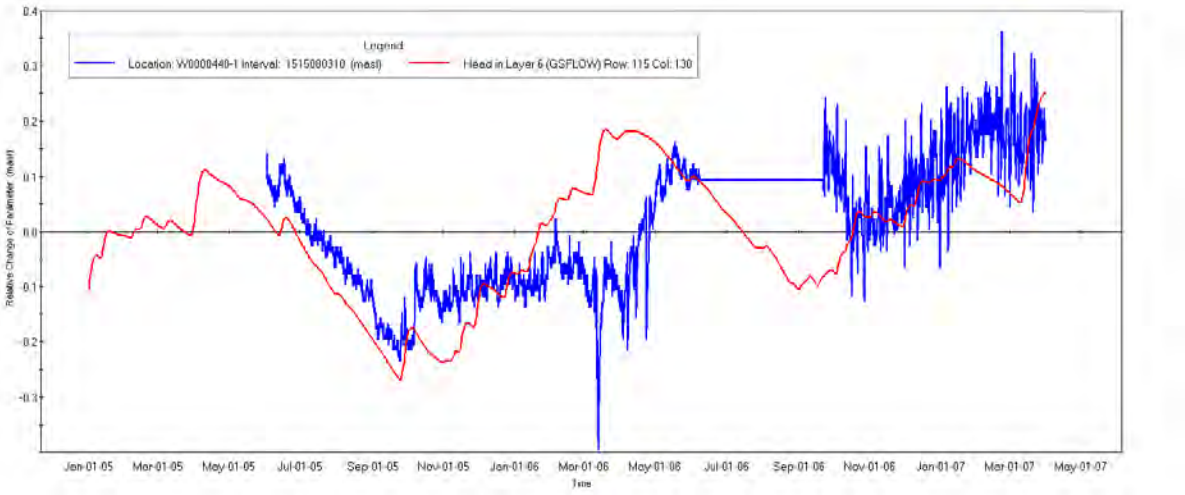

Figure 5.27: Simulated heads in Layer 6 and observed heads at PGMN Well #W0000440.

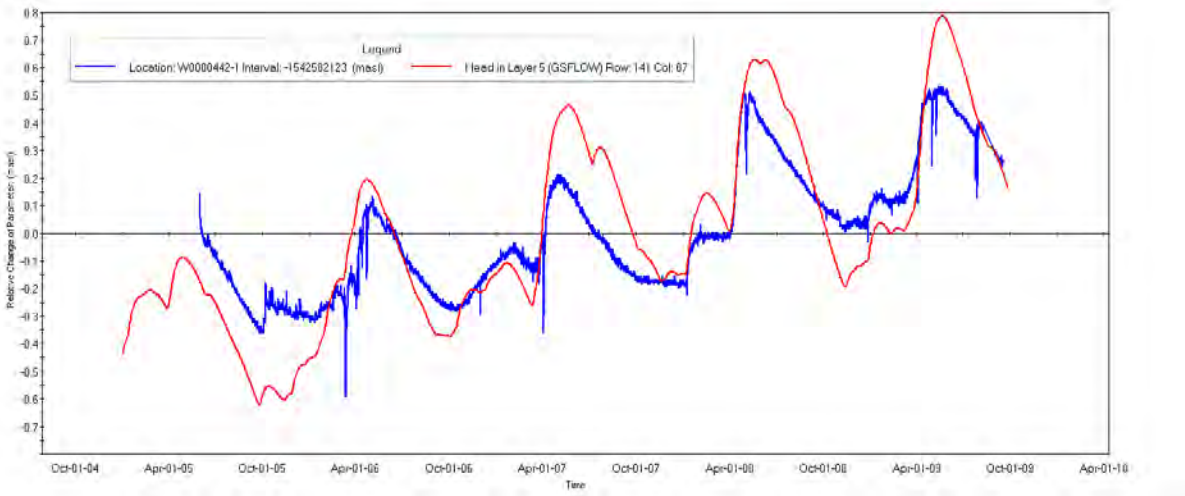

Figure 5.28: Simulated heads in Layer 5 and observed heads at PGMN Well #W0000442.

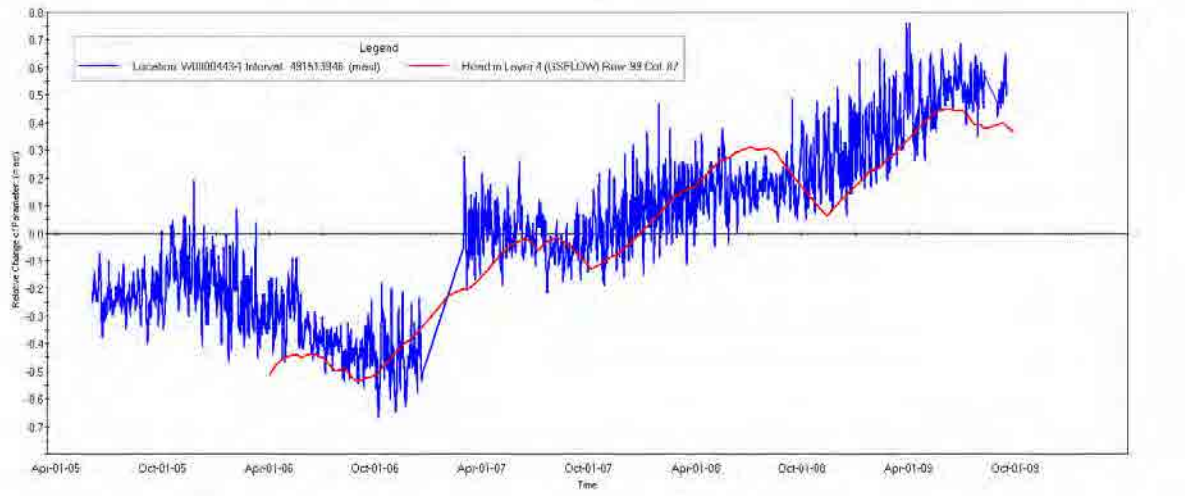

Figure 5.29: Simulated heads in Layer 3 and observed heads at PGMN Well #W0000443.

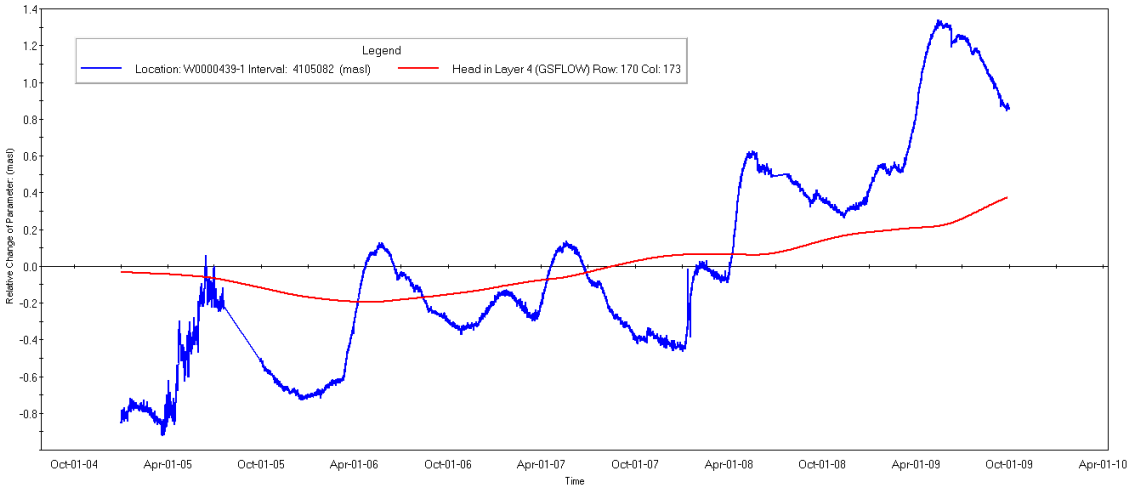

Figure 5.30: Simulated heads in Layer 3 and observed heads at PGMN Well #W0000244.

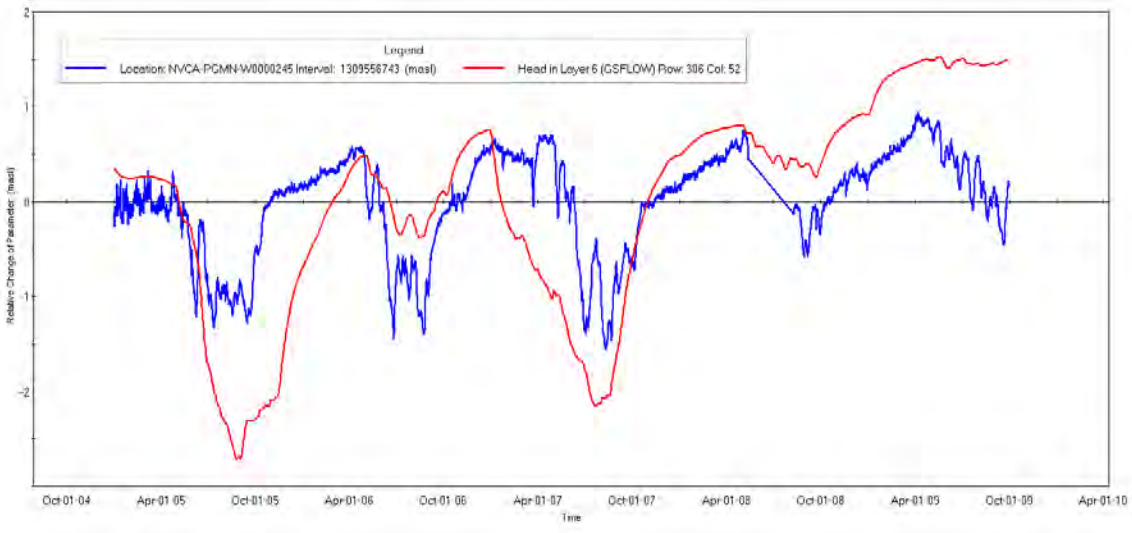

Figure 5.31: Simulated heads in Layer 6 and observed heads at PGMN Well #W0000245.

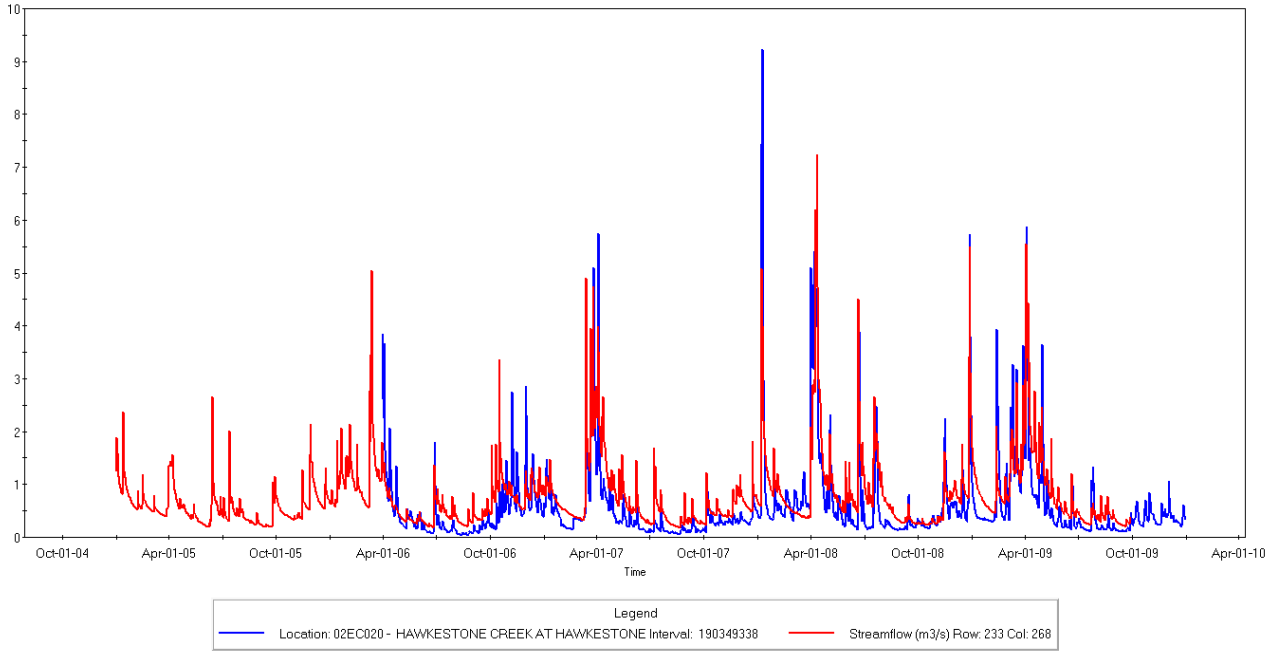

Figure 5.32: Simulated and observed streamflow at Hawkestone Creek at Hawkestone (WSC 02EC020).

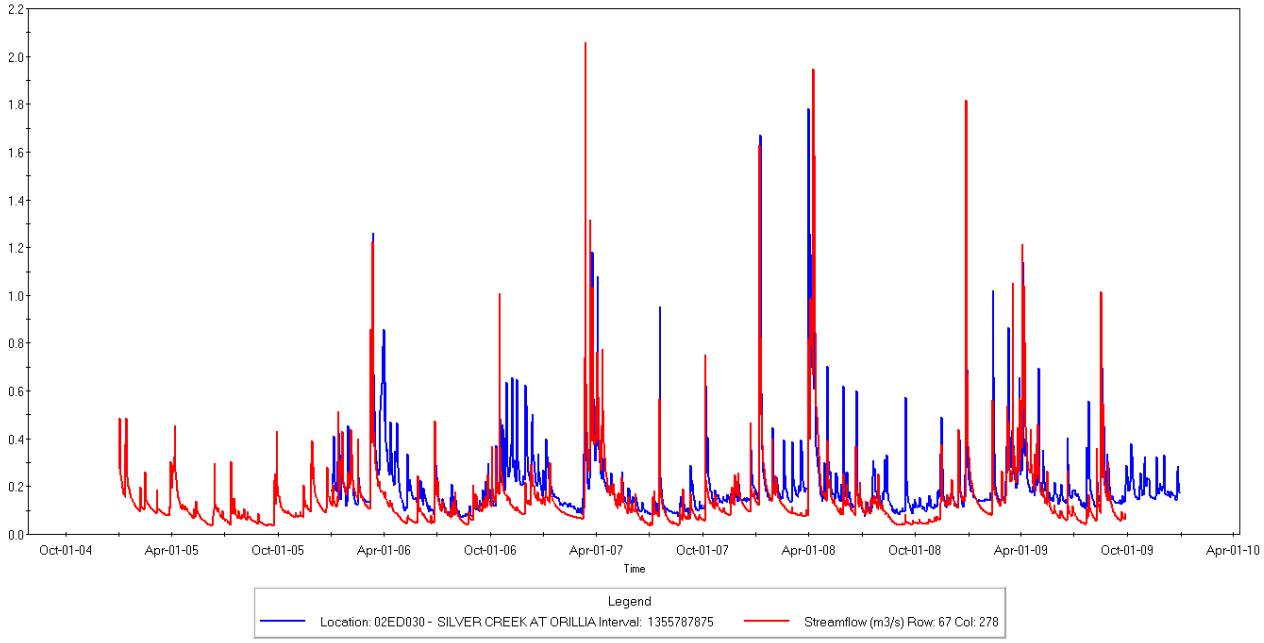

Figure 5.33: Simulated and observed streamflow at Silver Creek at Orillia (WSC 02ED030).

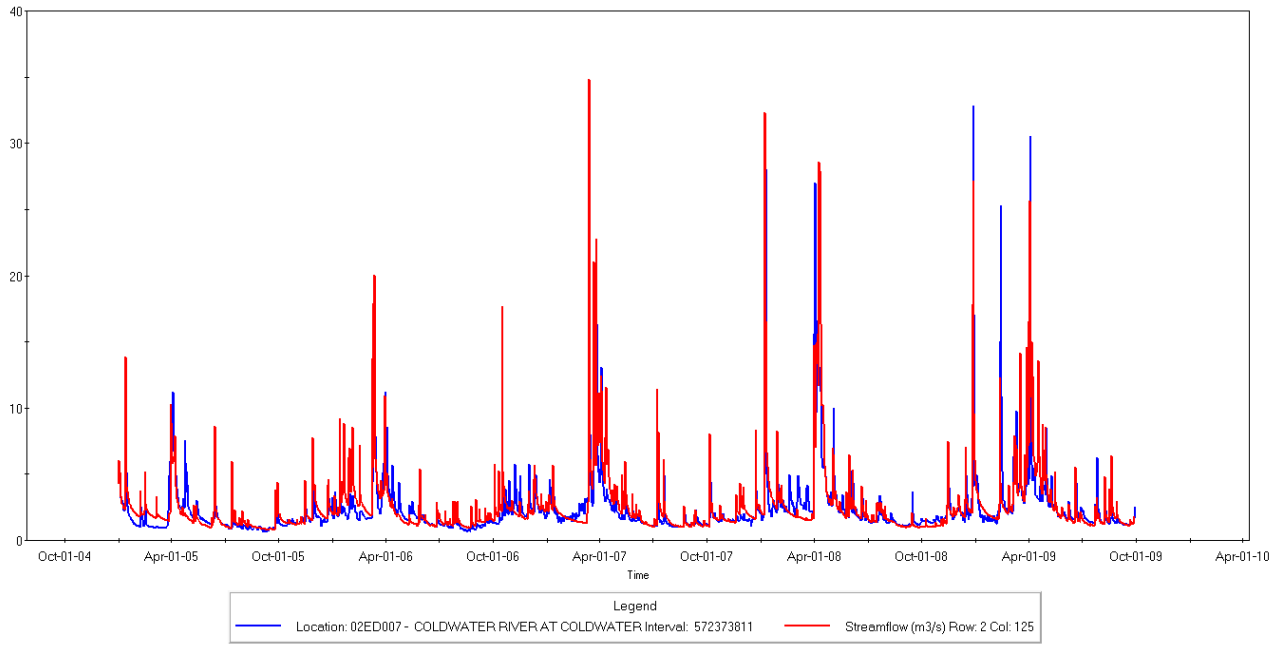

Figure 5.34: Simulated and observed streamflow at Coldwater River at Coldwater (WSC 02ED007).

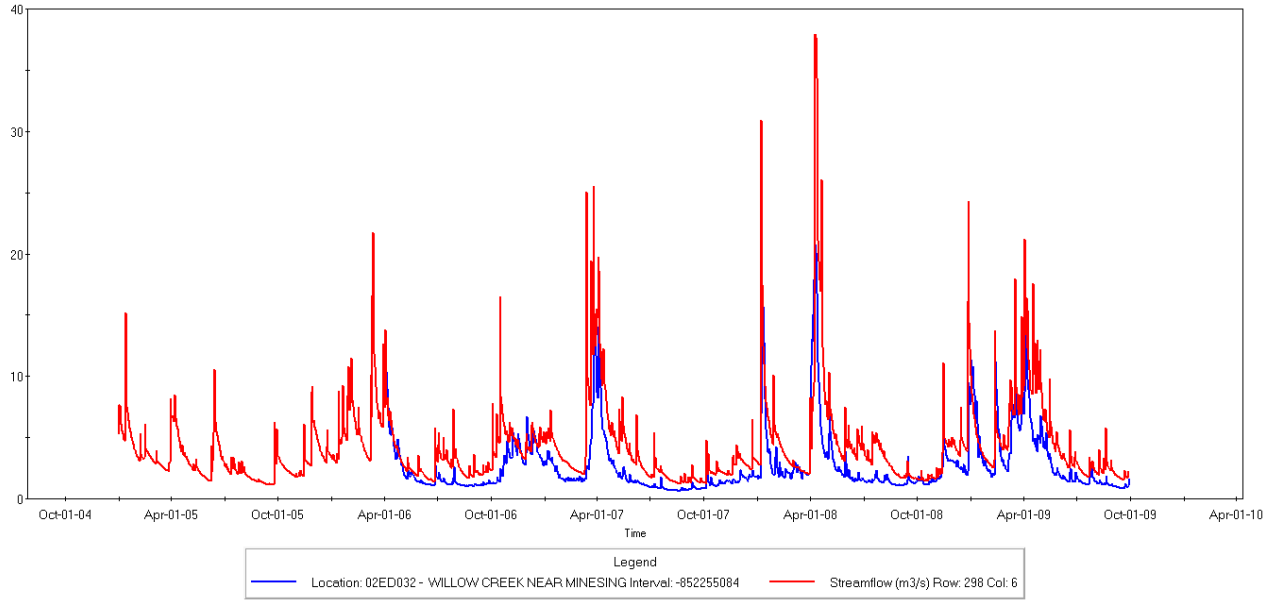

Figure 5.35: Simulated and observed streamflow at Willow Creek near Minesing (WSC 02ED032).

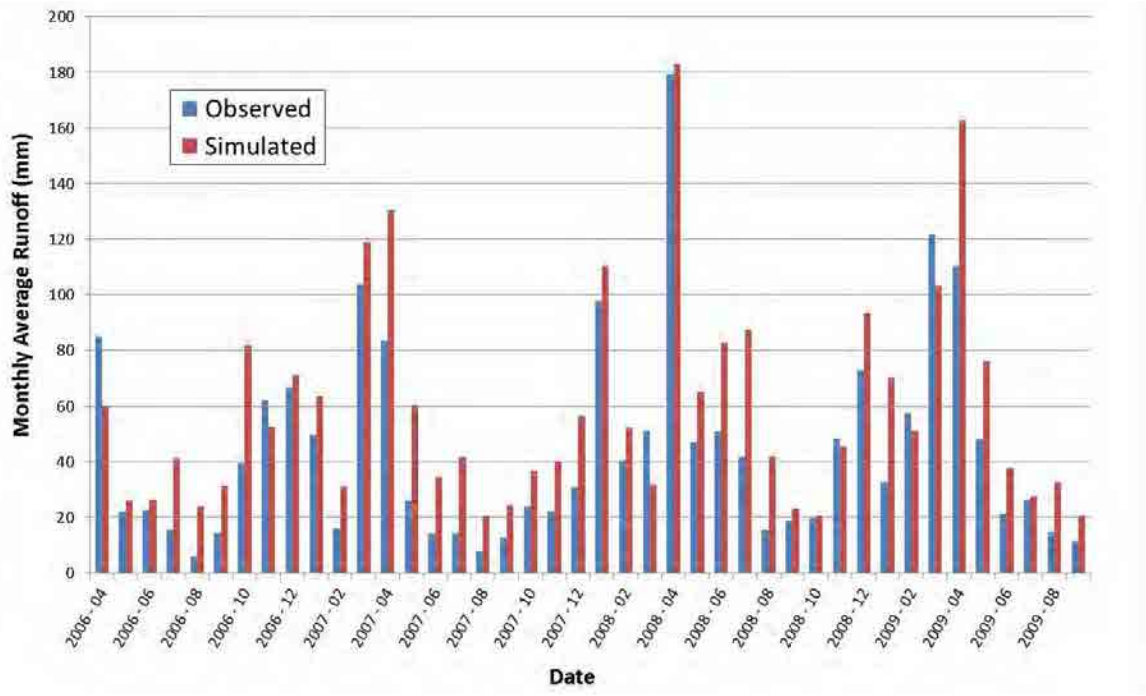

Figure 5.36: Simulated and observed monthly runoff volumes at Hawkestone Creek at Hawkestone (WSC 02EC020).

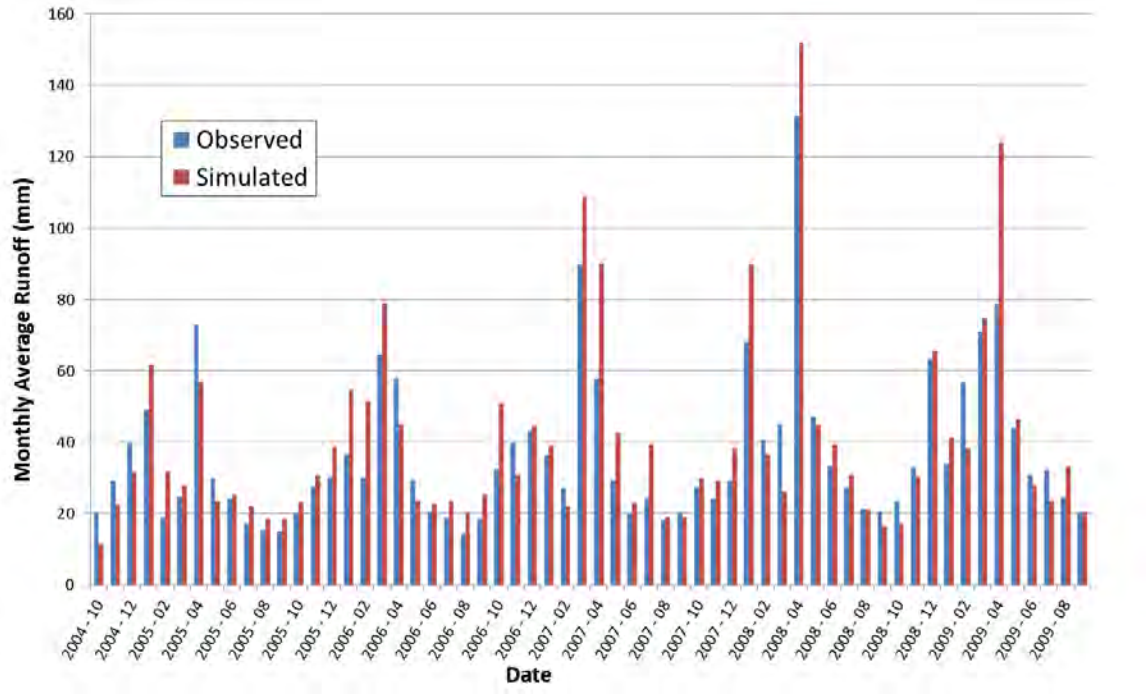

Figure 5.37: Simulated and observed monthly runoff volumes at Coldwater River at Coldwater (WSC 02ED007).

6 Subwatershed Stress Assessment

6.1 Overview

The Tier 2 Water Budget and Water Quantity Stress Assessment is intended to identify subwatersheds that are potentially stressed from a water quantity perspective. Specifically, that stress assessment evaluates the ratio of the consumptive demand for permitted and non-permitted users to the available water supply (i.e., recharge plus lateral inflow minus water reserve), within each subwatershed and determines whether the ratio, referred to as the percent water demand, exceeds threshold values shown below:

Groundwater Quantity Stress Assignment	Average Annual	Monthly Maximum
Significant	> 25%	> 50%
Moderate	> 10%	> 25%
Low	0 – 10%	0 – 25%

Estimates of the major components of the water budget have been discussed in the preceding sections of this report, including water demand, available water supply, and water reserve. The Tier 2 stress assessment integrates and compares these estimates to evaluate the overall level of stress within each catchment. The key difference between a Tier 1 and Tier 2 assessment is in the level of detail involved in the assessment of available supply and water demand. Particular care was taken to properly represent the interaction between the groundwater and surface water systems in the modelling analyses, as required by the Technical Rules for Assessment Reports. The linkage of the groundwater model to the hydrologic analyses and integrated model calibration helped to ensure a balanced assessment of stress levels.

The Tier 2 analysis requires the evaluation of the following scenarios, based on Table 4.9 in the Water Budget and Water Quantity Risk Assessment Guide:

Scenario	Description	Data Restrictions - Demand	Data Restrictions - Supply and Reserve
A	existing system – average	Data related to the study period	Data related to climate and stream flow is the historical data set for climate and streamflow.
B	existing system and future demand	Data related to demand associated with the system within the subwatershed reflects future development in the subwatershed	Data related to climate and stream flow is the historical data set for climate and streamflow. Data related to land cover reflects future development in the subwatershed.
D	existing system and 2-year drought	Data related to the study period	Data related to climate and stream flow reflects the 2-year drought period.
E	existing system and future 2-year drought	Data related to demand associated with an existing system within the subwatershed reflects future development in the subwatershed.	Data related to climate and stream flow reflects the 2-year drought period. Data related to land cover reflects future development in the subwatershed
G	existing system and 10-year drought	Data related to the study period	Data related to climate and stream flow reflects the 10-year drought period.
H	existing system	Data related to demand associated	Data related to climate and stream flow

	and future 10-year drought	with an existing system within the subwatershed reflects future development in the subwatershed.	reflects the 10-year drought period. Data related to land cover reflects the future development in the subwatershed.

Scenarios C and F have been eliminated in the table presented here as there are no new "planned" water supply systems in the study area.

6.2 Water Demand Calculation Methodology

The Technical Rules for Assessment Reports provides the following equation for calculating the percent water demand for groundwater:

$$\textit{Percent Water Demand} = \frac{Q_{DEMAND}}{Q_{SUPPLY} - Q_{RESERVE}} \times 100$$

The Water Budget and Water Quantity Risk Assessment Guide defines the terms of the equation as follows:

Term	Definition	Calculation
Q_{DEMAND}	Groundwater Consumptive Use	The estimated average annual and monthly rate of groundwater takings in a subwatershed.
Q_{SUPPLY}	Groundwater Supply	The estimated annual recharge rate plus the estimated groundwater inflow across the boundaries of a subwatershed.
$Q_{RESERVE}$	Groundwater Reserve	[Component of baseflow discharge reserved for ecological needs or other users] calculated as 10% of the annual average groundwater discharge rate (GD) to streams in a subwatershed (or 10% of the annual groundwater supply if groundwater discharge cannot be estimated).

Q_{DEMAND} was calculated for study area subwatersheds as presented in Section 3. Groundwater supply was calculated as:

$$Q_{SUPPLY} = Q_{RECHARGE} + Q_{IN}$$

Output from the steady-state groundwater model was summarized to produce tables summarizing the groundwater balance under current (Table 6.1) and future conditions (Table 6.4). The groundwater recharge ($Q_{RECHARGE}$) and lateral groundwater inflow (Q_{IN}) terms were summed for use as Q_{SUPPLY}. It should be noted that the simulated recharge actually represents net recharge because unserviced domestic demand and agricultural use have been subtracted, as discussed in Section 3. The recharge term was corrected and unserviced domestic demand and agricultural use was added to Q_{DEMAND} for the stress analysis.

The groundwater discharge to streams term (G_D) was used in estimating $Q_{RESREVE}$. It is important to note that the PRMS submodel simulations of daily water balances indicated that seasonal and year-to-year variation in groundwater recharge is very large, with near zero recharge in the summer months and highly variable recharge throughout the other months of the year, depending on ET processes, snowpack accumulation, and snowmelt events. The annual average values used in the stress assessment were taken as approximation of the long-term average values for these water budget components. The monthly stress assessments also

use the long-term annual average rates, despite the seasonal variations in recharge, as per the Water Budget and Water Quantity Risk Assessment Guide.

This study showed that groundwater inflow across subwatershed boundaries was a significant component of the annual water budget for the Tier 2 study area. Lateral groundwater inflow ranged from 19% (North Oro) to almost 40% (Hawkestone and Oro South) of the total groundwater supply. Lateral outflow (Q_{OUT}) to other subwatersheds is also a significant component of the water balance. Oro South, for example, had a high net lateral inflow (i.e., $Q_{IN} – Q_{OUT}$), while net lateral inflow was small in Hawkestone. Oro North had greater lateral outflows than inflows.

Groundwater discharge to streams and wetlands is the most significant outflow from the Oro North and Hawkestone Creek subwatersheds (77% and 59%, respectively) while it is smaller (30%) in Oro South. Direct discharge to Lake Simcoe, represented in the model as outflow at constant head cells is a small component of discharge in the Oro North and Hawkestone Creek subwatersheds but very significant (59%) in Oro South. Variations in the geology and drainage patterns account for these differences.

6.3 Stress Assessment Criteria

The Technical Rules for Assessment Reports (Rule 35) requires that the average annual and maximum monthly percent water demand for each subwatershed (Scenarios A and B) be compared to the threshold values.

6.4 Tier 2 Stress Assessment Results

6.4.1 Groundwater Stress Assessment: Current Conditions

The detailed components of the groundwater budget for each of the study area watersheds are shown in Table 6.1 for current demand conditions. They are shown schematically in Figure 6.1.

Using the stress assessment equations presented above, the percent water demand for current conditions is shown for each subwatershed in Table 6.2. Under current conditions, all of the watersheds are assessed at the low stress level.

For comparison, in the previous Tier 1 study (LSRCA, 2009) current conditions percent water demand was found to be less than 1% in each of the study watersheds. Some differences exist between the consumptive demand values derived in the Tier 1 and the values provided above. The Tier 1 study was completed before the introduction of the WTRS and some of the municipal takings were estimated using maximum permitted rates. Differences in methods of estimating recharge, discharge to streams, and cross-watershed flows lead to additional variation in the values used in the percent water demand computations between the two studies.

Monthly stress assessments were also conducted. As noted earlier, the monthly stress assessments use the long-term annual average rates for Q_{SUPPLY} and $Q_{RESERVE}$. The monthly water demand term was calculated from the tables of monthly consumptive use presented in Section 3. Unserviced domestic and agricultural takings were assumed to be constant year-round.

Values used in the calculations and the percent water demand are presented in Table 6.3. Values are well below the thresholds for all months. The highest value (3.1%) occurs in the July in Oro South. More realistic assessments of potential stress might be achieved by considering the monthly variation in water supply as well as water demand.

6.4.2 Groundwater Stress Assessment: Future Conditions

The detailed components of the water budget for each of the study area watersheds are shown in Table 6.4 for future demand conditions. They are shown schematically in Figure 6.2.

Using the stress assessment equations presented earlier, the percent water demand for future conditions are shown in Table 6.5. Under future conditions, all of the watersheds are assessed at the low stress level. Because of the small changes in future water demand, the stress levels are close to those for current conditions. These values are consistent with the values derived in the previous Tier 1 study (LSRCA, 2009).

Monthly stress assessments were also conducted for future conditions. As noted earlier, the municipal takings in the subwatersheds were increased by 10%. Values used in the calculations and the percent water demand are presented in Table 6.6. Values did not increase much from the current conditions simulations and are well below the thresholds for all months. The highest values (3.2%) occur in the June-August in Oro South. More realistic assessments of potential stress might be achieved by considering the monthly variation in water supply as well as water demand.

6.5 Drought Scenarios

The Tier 2 Water Budget also evaluated the effects of sustained drought on the water budget in each subwatershed. For Source Water Protection studies, the drought analysis focuses on the predicted response of water levels in the municipal wells. For these analyses, the focus was on the response of groundwater levels, groundwater discharge to streams, total streamflow, and stage in the wetlands across the subwatersheds.

Two drought scenarios were simulated. The first represents an extreme condition assuming that no recharge occurs to the groundwater system for a two-year period. The second scenario considers a historic 10-year period of low rainfall. Annual average rainfall for the study area is provided in Figure 6.3. The selected period for drought simulation extends from 1953 to 1967. Monthly rainfall data from this period is shown in Figure 6.4. As can be seen, the annual rainfall in the period is generally below average with 1958 and 1964 representing extreme lows. The simulation of the extended drought period provides an opportunity to evaluate the influence of storage on drought response. For example, it is useful to know whether dry years at the beginning of the drought have as large an effect as dry years towards the end of the drought. Discussions of the results of the two drought analyses are provided below.

6.5.1 2-year Drought Simulation

A Tier 2 level 2-year drought assessment was completed by setting recharge to zero and running the transient groundwater model (MODFLOW-NWT only) for a two-year period. Under the extreme conditions, the water table is seen to decline and groundwater discharge to streams

is also significantly reduced. Figure 6.5 presents the simulated heads in Layer 3 (GLAF and AF1) at the end of the 2-year drought scenario while Figure 6.6 presents the simulated change in head in this layer as compared to steady-state conditions. Groundwater levels are depressed on the east and west flanks of the Oro Moraine and significant head change is observed adjacent to the Shanty Bay municipal well system however no municipal pumping wells went dry during the 2-year drought assessment.

Groundwater discharge to surface features, which represents a significant component of baseflow, at the start (i.e., at steady-state conditions) and end of the drought scenario are presented in Figure 6.7 and Figure 6.8, respectively. The net change in groundwater discharge was determined by subtracting the simulated flows and is shown in Figure 6.9. Figure 6.10 presents the percent change in surface discharge due to the drought. Model results show that the largest relative impact on streamflow occurs in the headwater tributaries. Many of these tributaries have flow only when the stream bottom intersects the water table and therefore were sensitive to small changes in aquifer heads. Table 6.7 summarizes the change in the groundwater discharge to surface features on a subwatershed basis.

6.5.2 10-year Drought Simulation

The 10-year drought scenario utilized the transient GSFLOW model. A model run spanning from October 1954 to April 1967 was executed using MNR in-filled hourly precipitation data. This run encompassed the drought period (Spring 1957 to Spring 1967) with an additional 3 years for model start-up.

Figure 6.11 presents the simulated heads in Layer 3 at the beginning of the 10-year drought period. For this study, simulated monthly average conditions (i.e., aquifer heads and streamflow) in August 1957 were taken to represent conditions at the start of the drought period. Maximum simulated decrease in head was observed during November 1964. Monthly average conditions during this month (Figure 6.12) were taken to represent the most severe drought conditions. Simulated change in head between these two months is shown in Figure 6.13.

The areas most affected by the drought are similar to those in the two-year drought simulation. As expected, the drawdowns are not as severe as those predicted by the 2-year drought scenario, with a 2.5-m drawdown predicted on the moraine rather than the 6.5 m predicted by the 2-year simulation. As with the previous scenario, no municipal pumping wells went dry during the 10-year drought assessment.

Total streamflow at the start (i.e., August 1957) and at the most severe period of the drought (i.e., November 1964) are presented in Figure 6.14 and Figure 6.15, respectively. Total streamflow, an output from the GSFLOW model, includes contributions from overland runoff and channel precipitation as well as from groundwater inflow. The net change in total streamflow was determined by comparing the August 1957 and November 1964 simulated flows and is shown in Figure 6.16. Figure 6.17 presents the percent change in total streamflow between the two periods. Model results show that the largest relative impact on streamflow occurs in the South Oro Creek watershed. This differs from the two-year drought impacts which were mainly restricted to the headwater tributaries and had more uniform distribution over the study watersheds. Table 6.8 summarizes the change in total streamflow on a subwatershed basis.

Rather than looking at accumulated streamflow, the direct contribution of groundwater to streamflow (as leakage across the streambed) can be assessed from the integrated model output. This value does not account for the total groundwater contribution to streamflow

because it does not include groundwater discharge to wetlands and lakes and does not include discharge of groundwater in riparian areas (surface leakage) that subsequently reaches the stream as Dunnian runoff. However, direct groundwater discharge to streams provided a good parameter to study the sensitivity of channel features to changes in the groundwater system.

The net monthly average groundwater discharge to stream channels is shown in Figure 6.18 for each study catchment. Groundwater seepage to streams is at its minimum in late-summer/early fall in the study catchments and shows a decreasing trend over the drought period. Annual average seepage rates are provided for each study watershed in Figure 6.19. The Oro North Creeks demonstrate the highest net groundwater discharge of the study catchments, followed by Hawkestone Creek and the Oro South Creeks. Groundwater seepage is reduced during 1958 (the driest year on record in the study area). A recovery is observed in 1959 and 1960 however Oro South does not appear to rebound to the same extent as the northern catchments. Precipitation is again reduced from 1961 to 1964, which results in a decrease in groundwater seepage. Seepage is reduced to levels below those of 1958, suggesting the study watersheds are more sensitive to periods of prolonged drought than an extreme yearly event.

Monthly average groundwater discharge to streams is presented for the months of April and August on Figure 6.20 and Figure 6.21 respectively. Groundwater seepage during April was most affected by the extreme 1958 event rather than the prolonged drought. Monthly average seepage during August was consistently low from 1962 to 1966.

In addition to considering groundwater discharge to stream channels lumped by catchment, it is also possible to analyze stream channel seepage on a reach-by-reach basis by examining the GSFLOW model output. Groundwater seepage to the reach immediately upstream of the WSC gauge on Hawkestone Creek is shown on Figure 6.22. Discharge out of the groundwater system to the stream channel is considered a loss by GSFLOW and is negative on this plot. Seepage varies significantly on a daily basis (shown in blue) and monthly average values are used for long term comparisons. Large spikes can be observed on the daily hydrograph which correspond to surface runoff or snowmelt events. When stage in the channel increases during these flows, the gradient across the streambed decreases as well, reducing the volume of groundwater seeping into the stream. During large events, the gradient can reverse, forcing surface water into the aquifer. Water leaks back out after the stage has receded and groundwater heads rise. Several events of this nature can be observed on Figure 6.22. It also follows that groundwater discharge to streams intersecting the water table will typically be maximized during periods of low flow or stage in the early spring before the water table enters its summer recession. Figure 6.23 further illustrates this relationship between stream stage and aquifer head. When the stage in the creek exceeds the head in the groundwater system, seepage is reversed.

To better illustrate the connections between the groundwater system and specific surface features, groundwater seepage can plotted on a reach-by-reach basis. Groundwater seepage along the entire main channel of Hawkestone Creek (Figure 6.24) in August 1957 and November 1964 is plotted on Figure 6.25. Chainage starts at Lake Simcoe and ends at a first-order stream in the Hawkestone Wetland Complex. The leakage on this plot has not been normalized by the length of stream channel per cell; however, the information provides much insight into the interactions between the groundwater system and the surface channel. High rates of seepage are noted where the overlying till thickens and the shallow aquifer appears to thin further downgradient. Similar figures are provided showing groundwater seepage along Bluffs Creek up the west branch in Oro North (Figure 6.26) and along Shellswell's Creek in Oro South (Figure 6.27).

Hawkestone Creek and Bluffs Creek appear well connected to the groundwater system. Groundwater seepage occurs along the entire length of these stream channels. The headwaters of the Hawkestone and Oro North watersheds are well connected to the Oro Moraine aquifers. Seepage to Bluffs Creek (west branch) is not reduced during the 10-year drought suggesting there is sufficient storage in the moraine to support this creek during periods of reduced precipitation. Hawkestone Creek appears more sensitive to drought conditions in its lower reaches, this may suggest a reliance on local recharge to support the features lower in the watershed that are poorly connected to the available storage within the moraine.

Shellswell's Creek is poorly connected to the groundwater system, receiving substantially less groundwater seepage than channels in the northern catchments. Also, the seepage it does receive appears very sensitive to drought conditions. Silt to sandy silt till, correlated with the Newmarket Till (OGS, 2010 and Barnett, 1992), dominates the surficial geology of the area to the south and east of the Oro Moraine (Figure 2.6). These tills at surface likely retard flow from the groundwater system and lower-order streams positioned in the till units would be sensitive to drought conditions

6.6 Tables

Table 6.1: Model water budget details - Current Conditions

Inflows and Outflows (all values in m^3/day)	North Oro	Hawkestone	South Oro
Inflow Components			
Recharge in	56,451	25,716	16,158
Stream leakage in	39	12	20
Lake leakage in	2	16	3
Lateral inflow	8,729	16,859	9,972
Total Groundwater Inflow:	65005	42,484	25,796
Outflow Components			
Lateral outflow	12,423	15200	2,598
Net groundwater discharge to surface features	50,441	24925	7,892
Net outflow in at constant head cells	2,373	2,304	15,602
Wells	206	170	283
Total Groundwater Outflow:	65,443	42,599	26,375

*values subject to round off

Table 6.2: Percent Water Demand Stress Assessment – Current Conditions

Component (all values in m^3/day)		North Oro	Hawkestone	South Oro
Groundwater Supply	Net Recharge In	56,669	25,834	16,516
	Stream Seepage	39	12	20
	Lake Seepage	2	16	3
	Lateral Inflow	8,729	16,859	9,972
	Total:	65,440	42,721	26,510
Groundwater Reserve		5044	2493	789
Consumptive Demand		424	289	640
Percent Water Demand		**0.7%**	**0.7%**	**2.5%**

Table 6.3: Monthly percent groundwater demand by subwatershed – current conditions.

Subwatershed	Month	Recharge In	Stream Seepage	Lake Seepage	Lateral Inflow	Total	Ground water Reserve	Consumptive Groundwater Demand	Percent Ground water Demand
Oro North	Jan	56,669	39	2	8729	65,440	5044	245	0.4%
	Feb	56,669	39	2	8729	65,440	5044	237	0.4%
	Mar	56,669	39	2	8729	65,440	5044	236	0.4%
	Apr	56,669	39	2	8729	65,440	5044	340	0.6%
	May	56,669	39	2	8729	65,440	5044	665	1.1%
	Jun	56,669	39	2	8729	65,440	5044	674	1.1%
	Jul	56,669	39	2	8729	65,440	5044	608	1.0%
	Aug	56,669	39	2	8729	65,440	5044	647	1.1%
	Sep	56,669	39	2	8729	65,440	5044	518	0.9%
	Oct	56,669	39	2	8729	65,440	5044	372	0.6%
	Nov	56,669	39	2	8729	65,440	5044	291	0.5%
	Dec	56,669	39	2	8729	65,440	5044	240	0.4%
Hawkestone	Jan	25,834	12	16	16,859	42,721	2493	133	0.3%
	Feb	25,834	12	16	16,859	42,721	2493	132	0.3%
	Mar	25,834	12	16	16,859	42,721	2493	232	0.6%
	Apr	25,834	12	16	16,859	42,721	2493	257	0.6%
	May	25,834	12	16	16,859	42,721	2493	394	1.0%
	Jun	25,834	12	16	16,859	42,721	2493	374	0.9%
	Jul	25,834	12	16	16,859	42,721	2493	375	0.9%
	Aug	25,834	12	16	16,859	42,721	2493	396	1.0%
	Sep	25,834	12	16	16,859	42,721	2493	371	0.9%
	Oct	25,834	12	16	16,859	42,721	2493	343	0.9%
	Nov	25,834	12	16	16,859	42,721	2493	285	0.7%
	Dec	25,834	12	16	16,859	42,721	2493	162	0.4%
Oro South	Jan	16,516	20	3	9972	26,510	789	564	2.2%
	Feb	16,516	20	3	9972	26,510	789	561	2.2%
	Mar	16,516	20	3	9972	26,510	789	548	2.1%
	Apr	16,516	20	3	9972	26,510	789	573	2.2%
	May	16,516	20	3	9972	26,510	789	695	2.7%
	Jun	16,516	20	3	9972	26,510	789	782	3.0%
	Jul	16,516	20	3	9972	26,510	789	789	3.1%
	Aug	16,516	20	3	9972	26,510	789	782	3.0%
	Sep	16,516	20	3	9972	26,510	789	672	2.6%
	Oct	16,516	20	3	9972	26,510	789	569	2.2%
	Nov	16,516	20	3	9972	26,510	789	559	2.2%
	Dec	16,516	20	3	9972	26,510	789	567	2.3%

Table 6.4: Model water budget details - Future Conditions

Inflows and Outflows (all values in m^3/day)	North Oro	Hawkestone	South Oro
Inflow Components			
Recharge in	56,407	25,696	16,108
Stream leakage in	39	12	20
Lake leakage in	2	14	3
Lateral inflow	8,730	16,858	9,975
Total Groundwater Inflow:	65,178	42,581	26,105
Outflow Components			
Lateral Outflow	12,418	15,198	2,597
Net groundwater discharge to surface features	50,427	24,886	7,868
Net outflow in at constant head cells	2,369	2304	15,569
Wells	209	172	309
Total Groundwater Outflow:	65,423	42,560	26,344

*values subject to round off

Table 6.5: Future groundwater demand.

Component (all values in m^3/day)		North Oro	Hawkestone	South Oro
Groundwater Supply	Net Recharge In	56,695	25,851	16,593
	Stream Seepage	39	12	20
	Lake Seepage	2	14	3
	Lateral Inflow	8,730	16,858	9,975
	Total:	65,466	42,735	26,591
Groundwater Reserve		5043	2,489	787
Consumptive Demand		497	326	795
Percent Water Demand		**0.8%**	**0.8%**	**3.1%**

Table 6.6: Monthly percent groundwater demand by subwatershed – future conditions.

Subwatershed	Month	Recharge In	Stream Seepage	Lake Seepage	Lateral Inflow	Total	Ground water Reserve	Consumptive Groundwater Demand	Percent Ground water Demand
Oro North	Jan	56,695	39	2	8730	65,466	5043	246	0.4%
	Feb	56,695	39	2	8730	65,466	5043	239	0.4%
	Mar	56,695	39	2	8730	65,466	5043	238	0.4%
	Apr	56,695	39	2	8730	65,466	5043	342	0.6%
	May	56,695	39	2	8730	65,466	5043	668	1.1%
	Jun	56,695	39	2	8730	65,466	5043	676	1.1%
	Jul	56,695	39	2	8730	65,466	5043	611	1.0%
	Aug	56,695	39	2	8730	65,466	5043	650	1.1%
	Sep	56,695	39	2	8730	65,466	5043	520	0.9%
	Oct	56,695	39	2	8730	65,466	5043	374	0.6%
	Nov	56,695	39	2	8730	65,466	5043	293	0.5%
	Dec	56,695	39	2	8730	65,466	5043	243	0.4%
Hawkestone	Jan	25,851	12	14	16,858	42,735	2489	134	0.3%
	Feb	25,851	12	14	16,858	42,735	2489	133	0.3%
	Mar	25,851	12	14	16,858	42,735	2489	234	0.6%
	Apr	25,851	12	14	16,858	42,735	2489	258	0.6%
	May	25,851	12	14	16,858	42,735	2489	395	1.0%
	Jun	25,851	12	14	16,858	42,735	2489	376	0.9%
	Jul	25,851	12	14	16,858	42,735	2489	377	0.9%
	Aug	25,851	12	14	16,858	42,735	2489	397	1.0%
	Sep	25,851	12	14	16,858	42,735	2489	372	0.9%
	Oct	25,851	12	14	16,858	42,735	2489	345	0.9%
	Nov	25,851	12	14	16,858	42,735	2489	286	0.7%
	Dec	25,851	12	14	16,858	42,735	2489	163	0.4%
Oro South	Jan	16,593	20	3	9975	26,591	787	584	2.3%
	Feb	16,593	20	3	9975	26,591	787	581	2.3%
	Mar	16,593	20	3	9975	26,591	787	567	2.2%
	Apr	16,593	20	3	9975	26,591	787	595	2.3%
	May	16,593	20	3	9975	26,591	787	725	2.8%
	Jun	16,593	20	3	9975	26,591	787	821	3.2%
	Jul	16,593	20	3	9975	26,591	787	828	3.2%
	Aug	16,593	20	3	9975	26,591	787	820	3.2%
	Sep	16,593	20	3	9975	26,591	787	700	2.7%
	Oct	16,593	20	3	9975	26,591	787	590	2.3%
	Nov	16,593	20	3	9975	26,591	787	580	2.2%
	Dec	16,593	20	3	9975	26,591	787	588	2.3%

Table 6.7: Two year drought assessment – Impact on groundwater discharge to surface features.

Component (all values in m^3/day)	North Oro	Hawkestone	South Oro
Average groundwater discharge (m^3/d)	56,451	25,716	16,158
Groundwater discharge at end of 2-year drought (m^3/d)	16166	9781	1205
Percent Reduction	**71.4%**	**62.0%**	**92.5%**

Table 6.8: Ten year drought assessment – Impact on groundwater discharge to stream channels.

Component (all values in m^3/day)	North Oro	Hawkestone	South Oro
Monthly Groundwater Discharge to streams August 1957 (m^3/d)	7750	4593	2259
Monthly Groundwater Discharge to streams November 1964 (m^3/d)	6945	3242	1278
Percent Reduction	**10%**	**29%**	**43%**

6.7 Figures

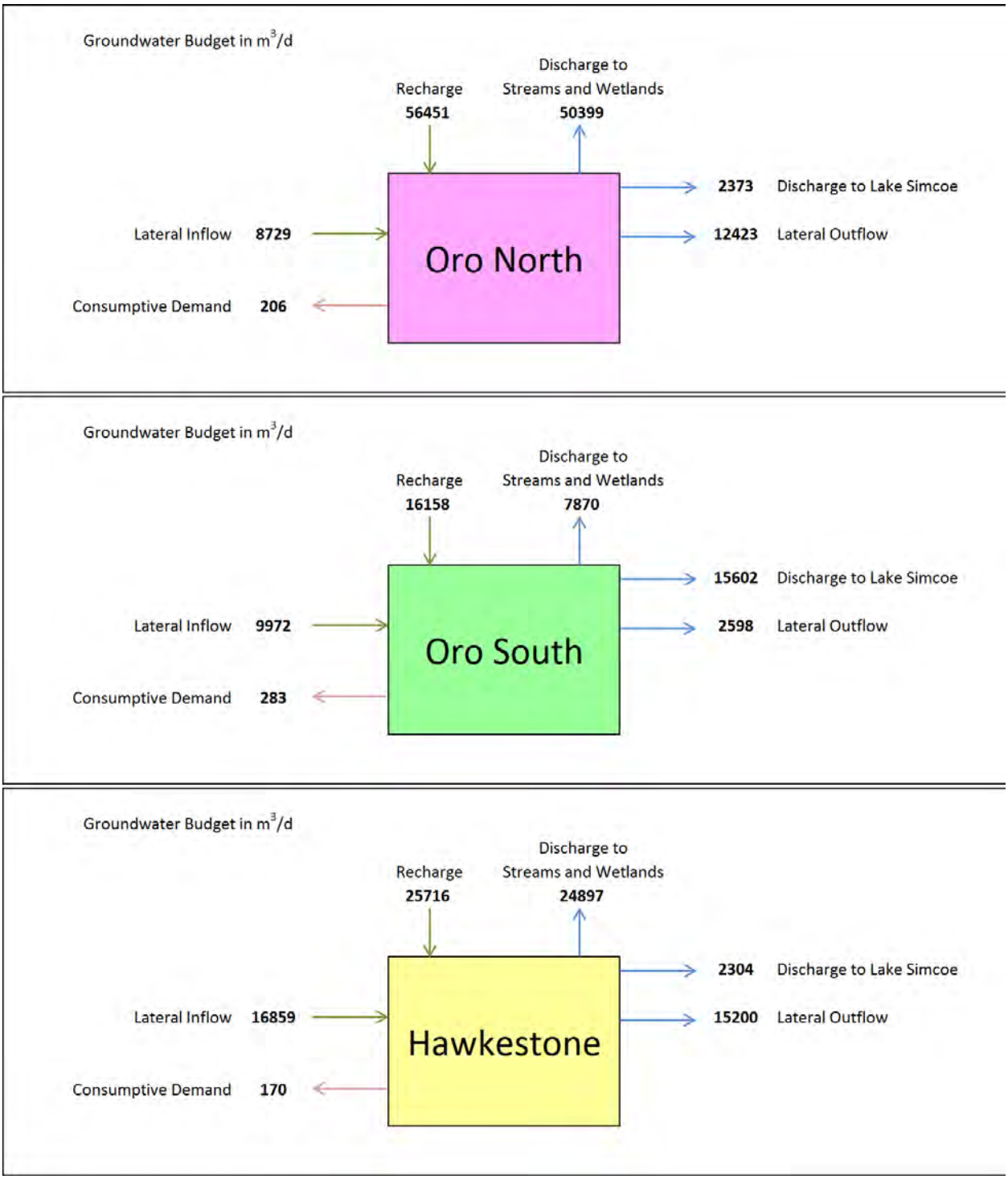

Figure 6.1: Simulated groundwater budget for the study area subwatersheds – current conditions.

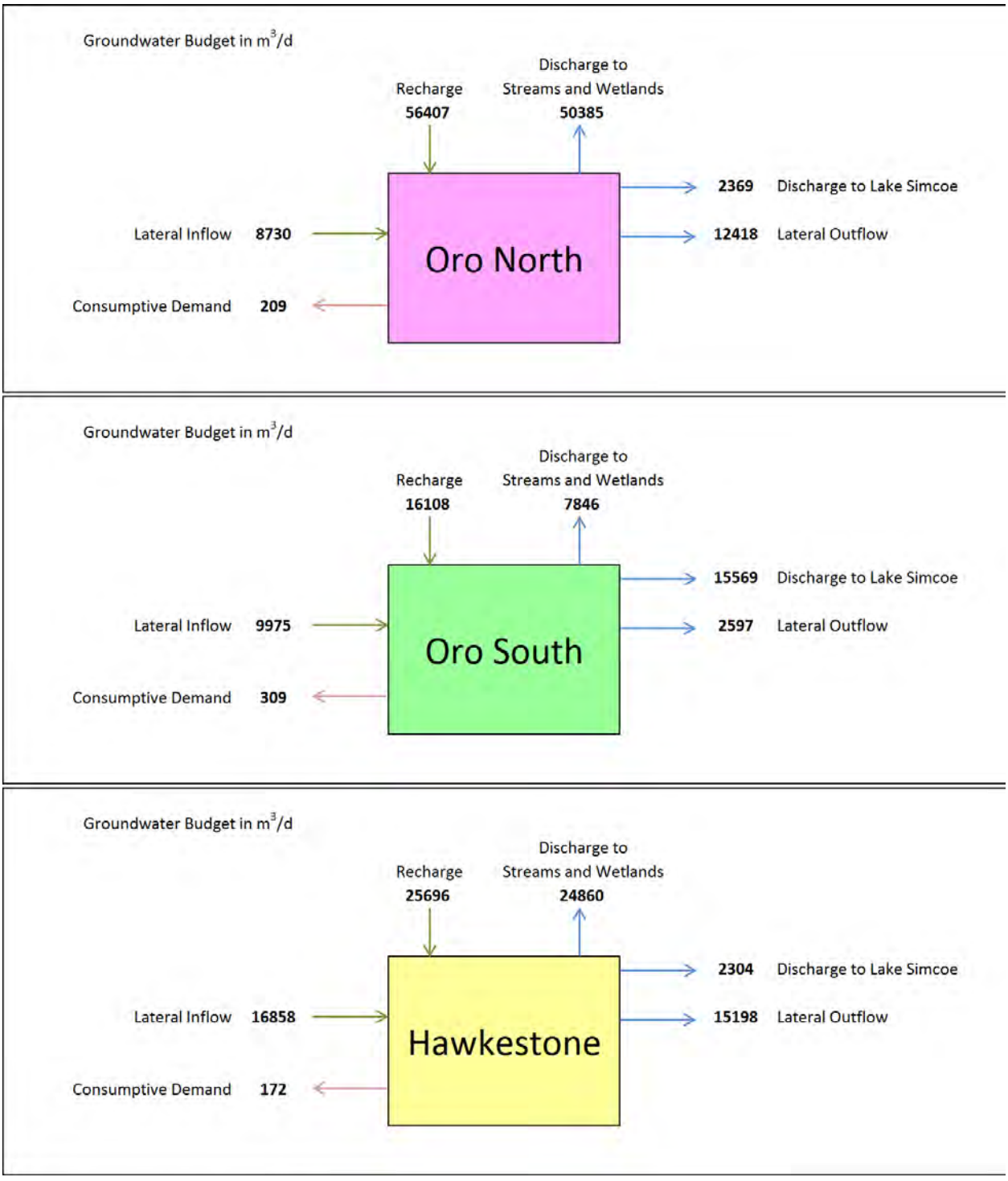

Figure 6.2: Simulated groundwater budget for the study area subwatersheds – future conditions.

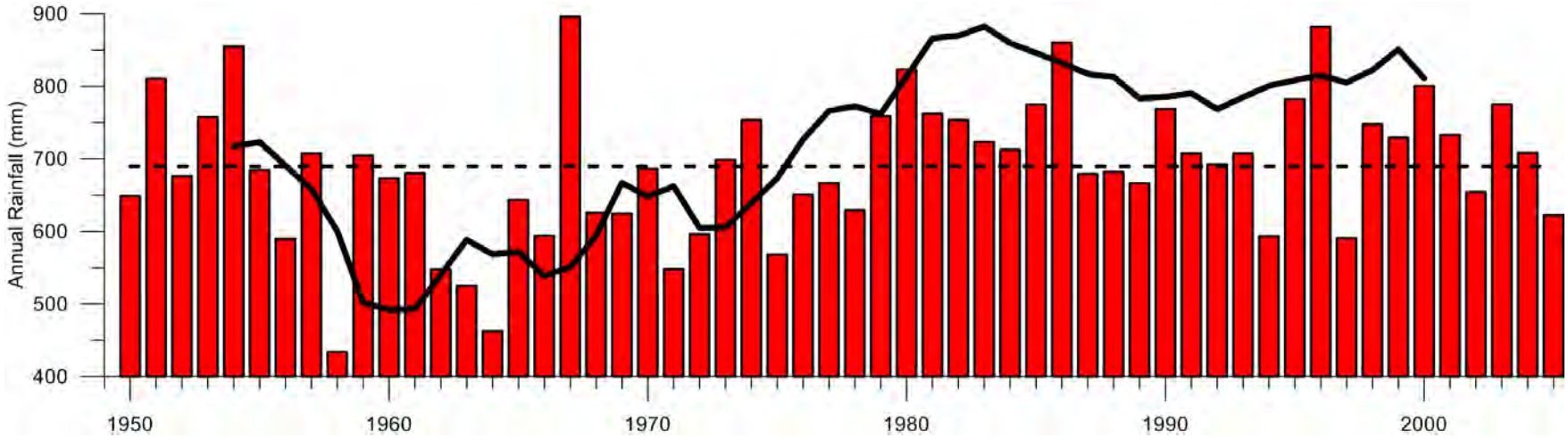

Figure 6.3: Annual average rainfall within the study area (with 10-year moving average).

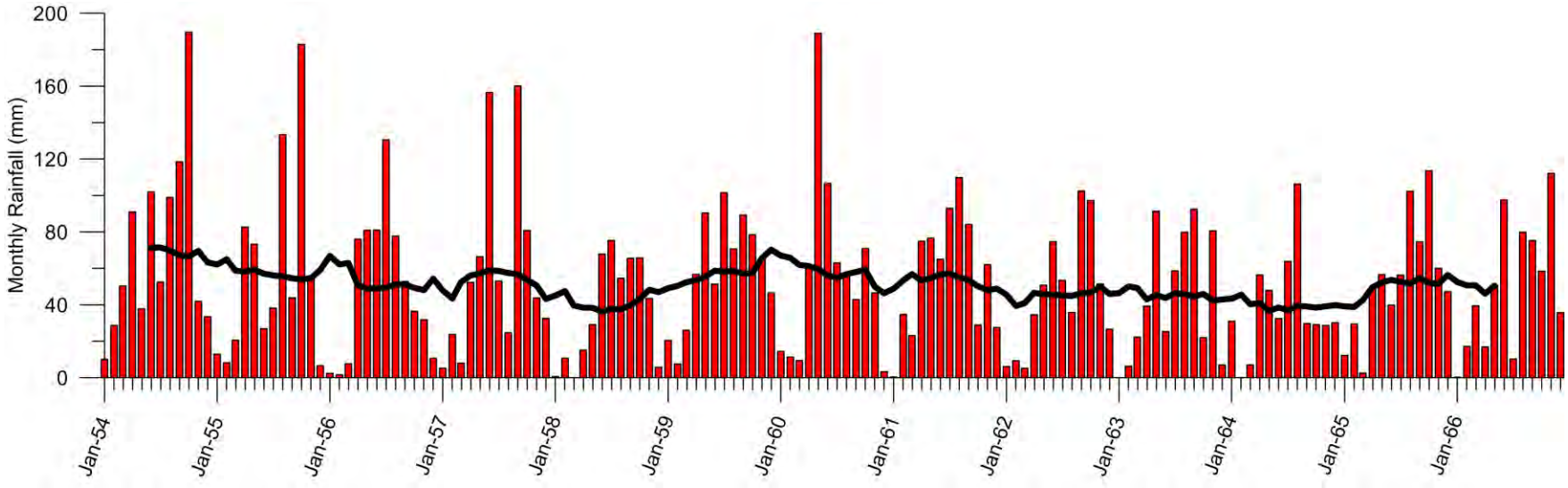

Figure 6.4: Monthly average rainfall within the study area (with 12-month moving average).

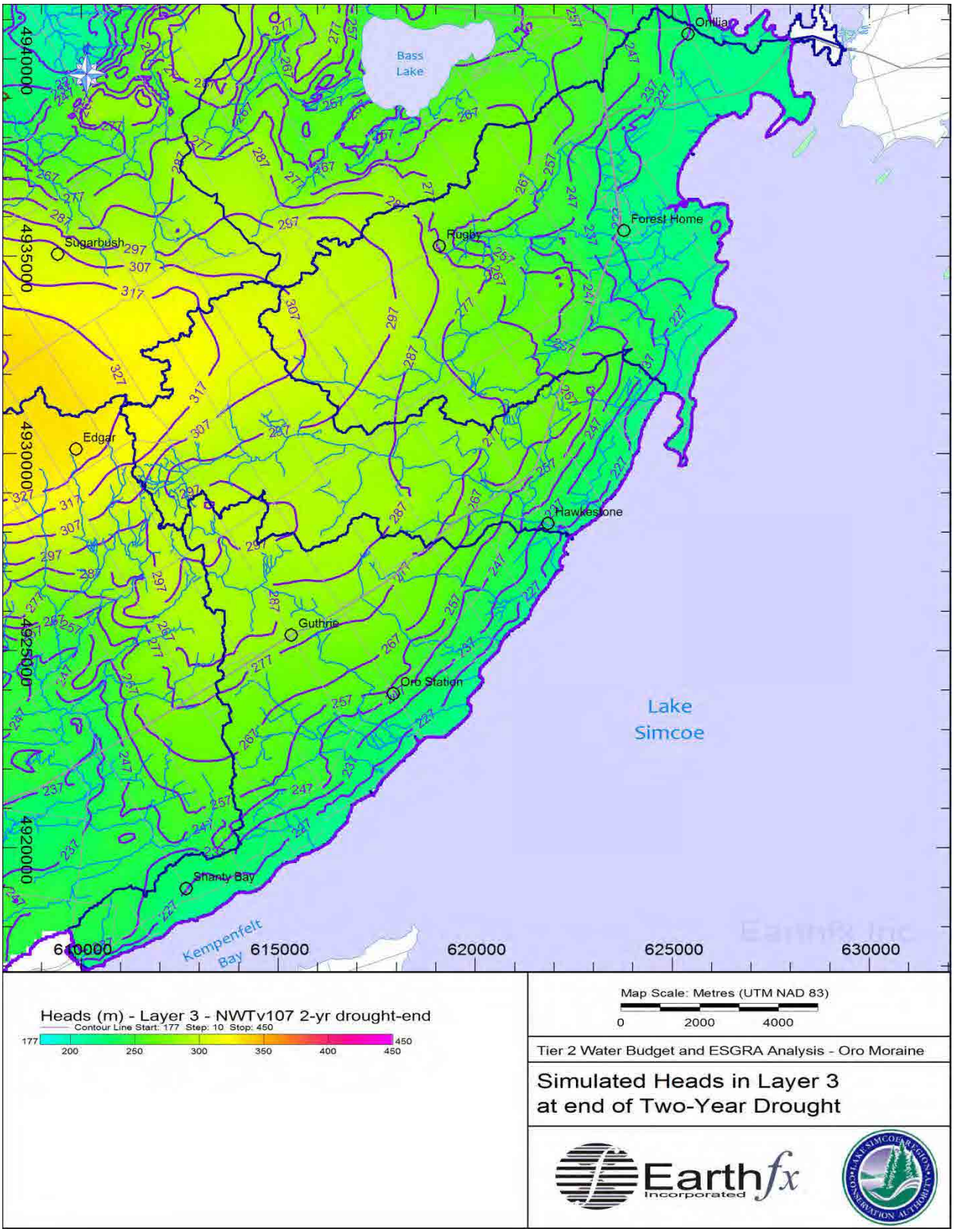

Figure 6.5: Simulated heads in Layer 3 (GLAF-AF1) at the end of the two-year drought simulation.

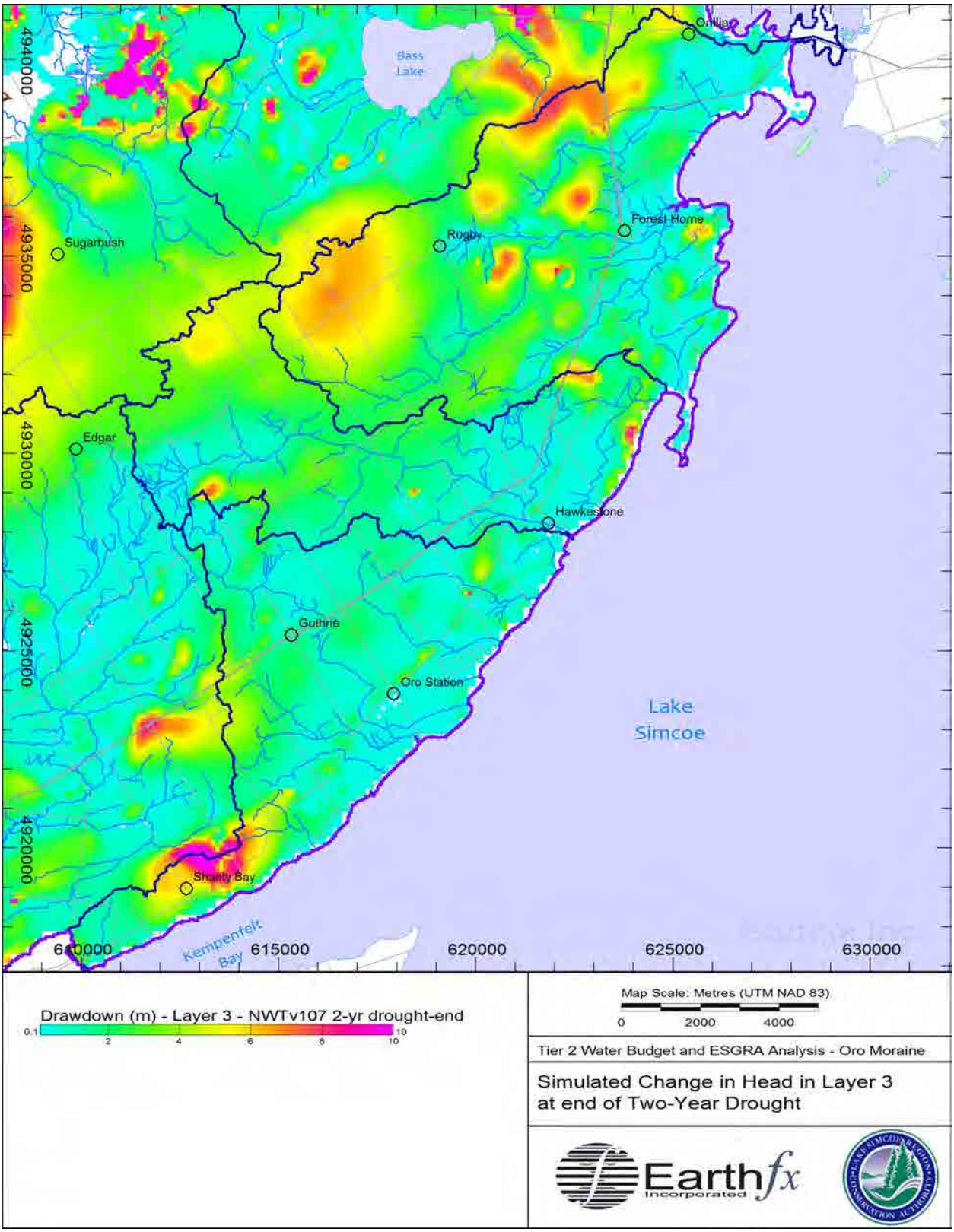

Figure 6.6: Simulated change in head in Layer 3 (GLAF-AF1) at the end of the two-year drought simulation.

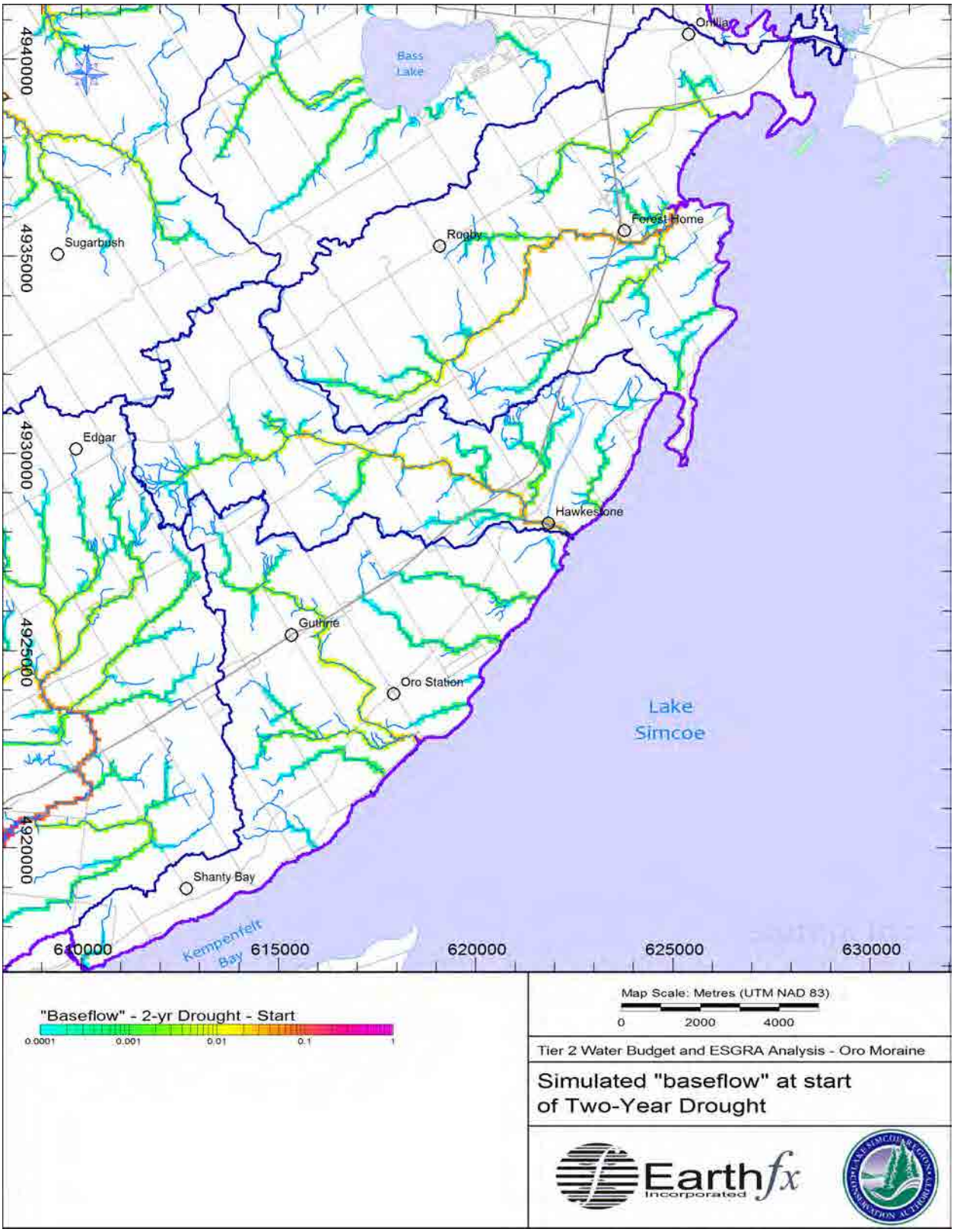

Figure 6.7: Simulated baseflow (m^3/s) at the start of the two-year drought period.

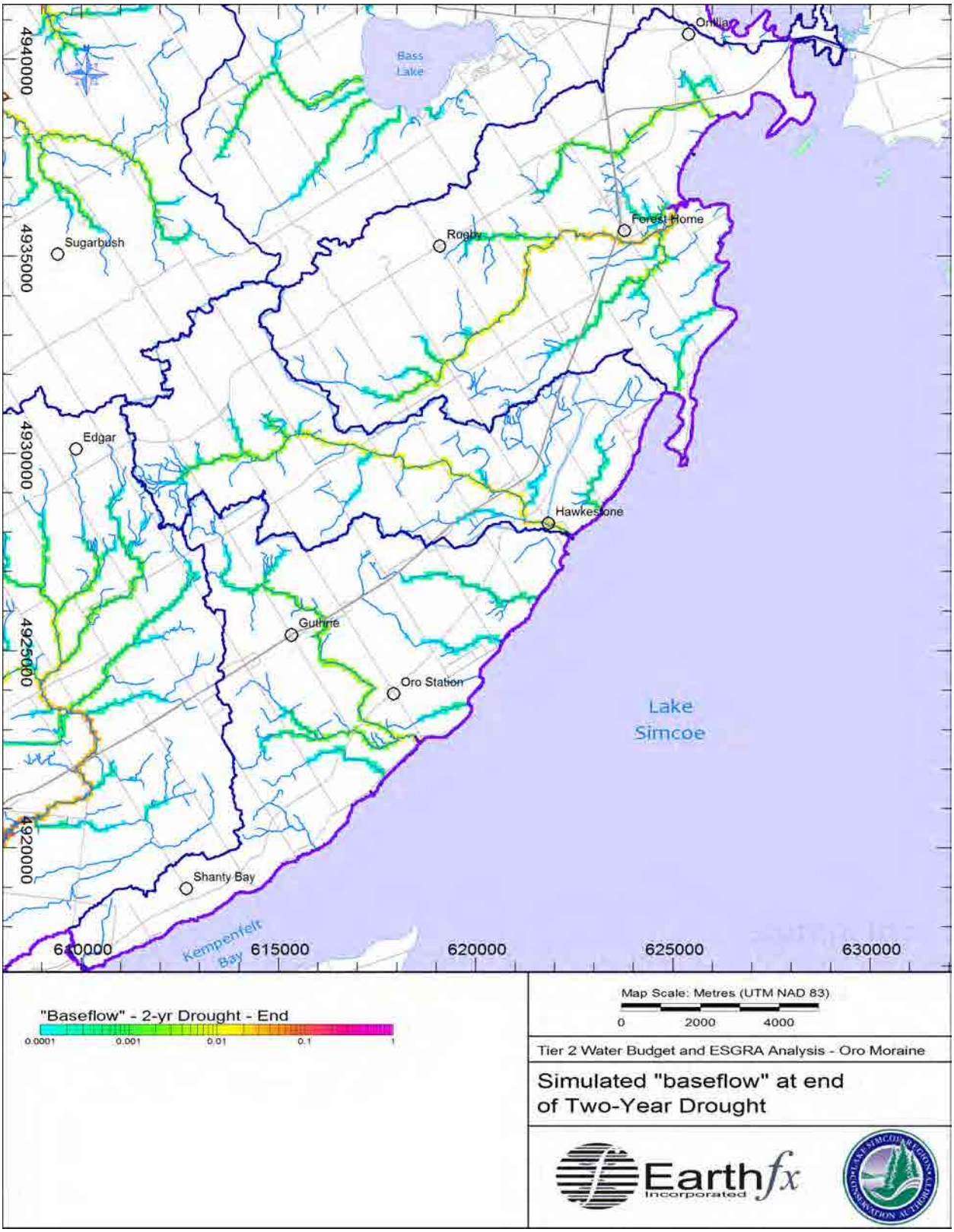

Figure 6.8: Simulated baseflow (m^3/s) at the end of the two-year drought simulation.

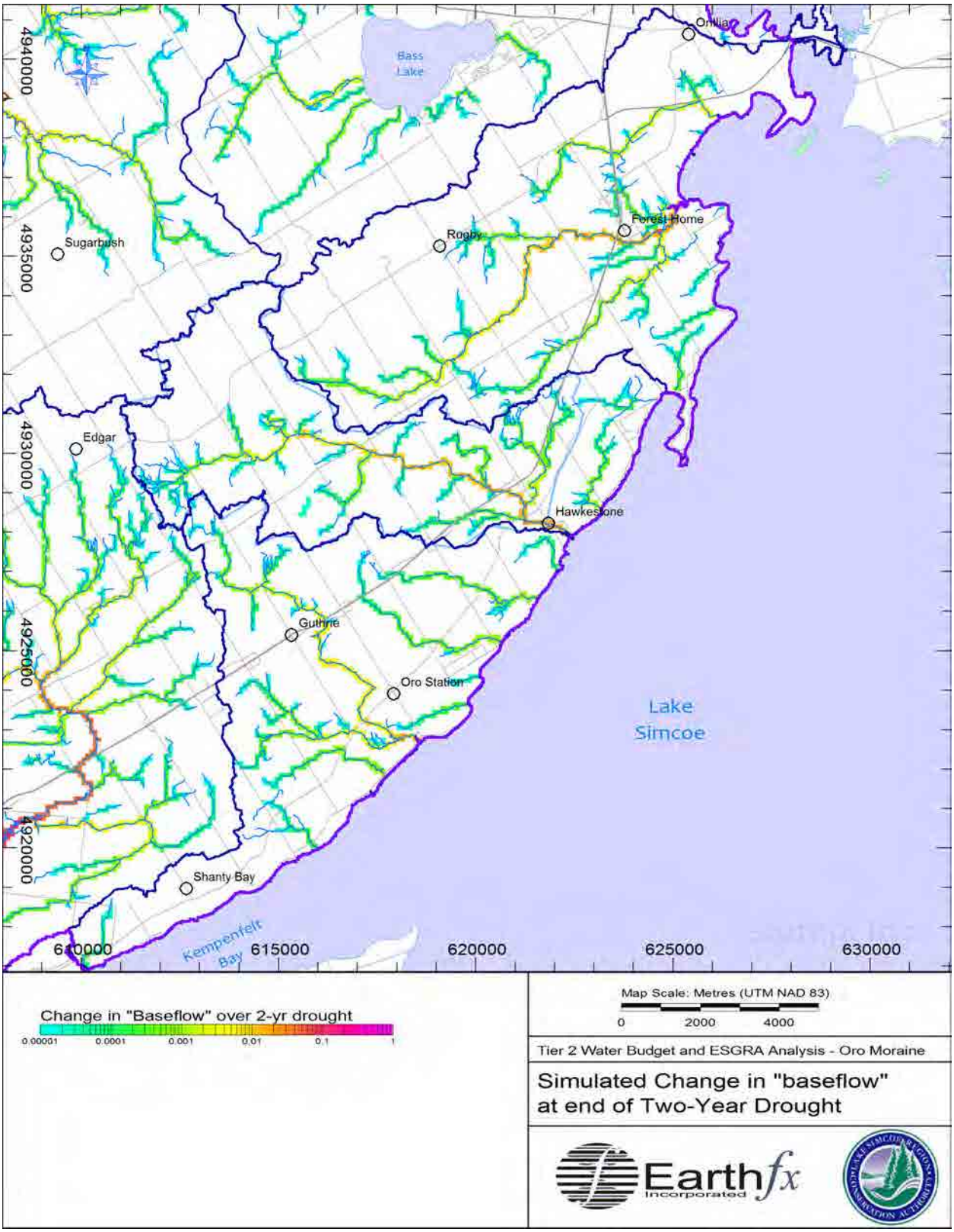

Figure 6.9: Simulated change in baseflow (m^3/s) over the two-year drought simulation.

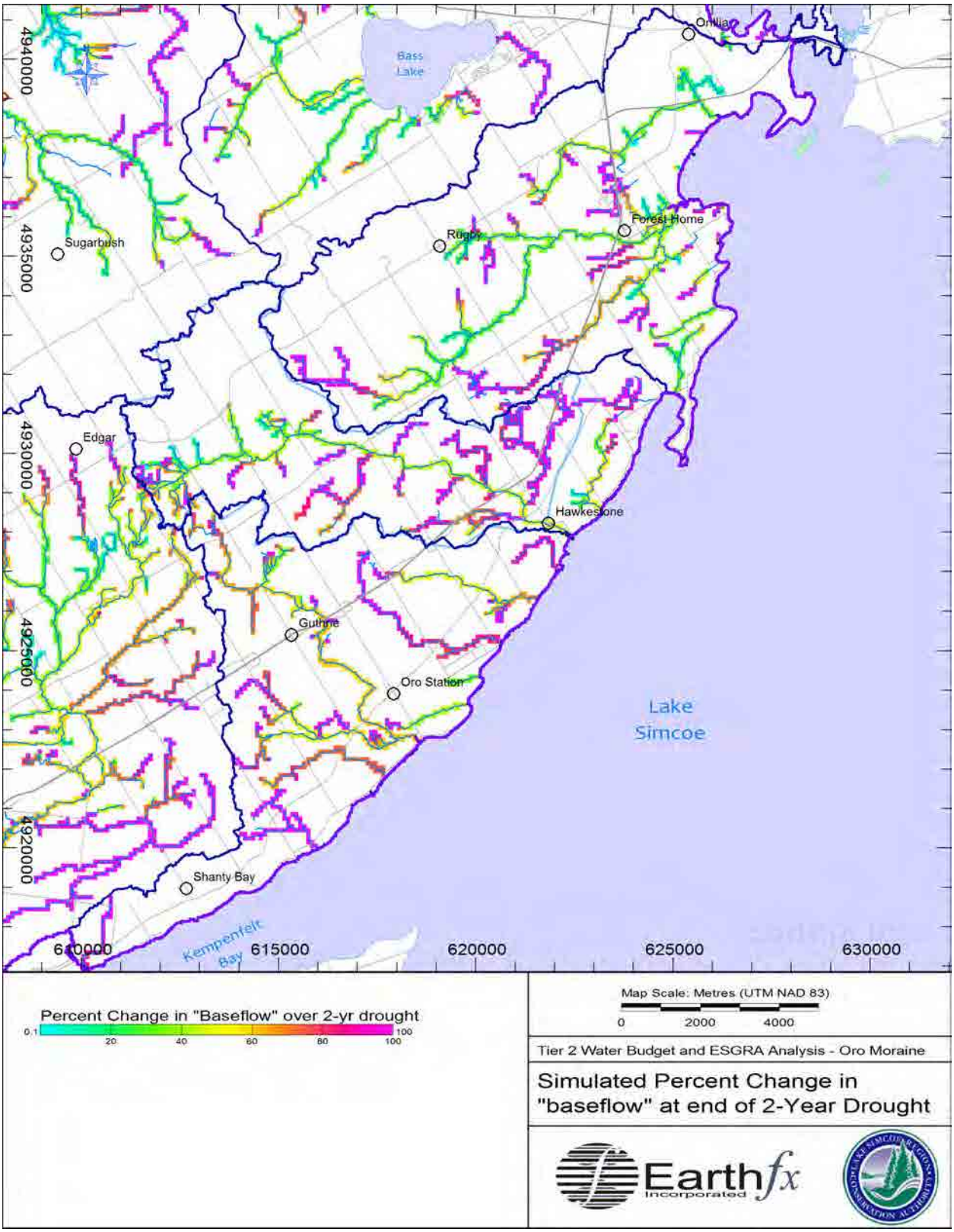

Figure 6.10: Simulated percent change in baseflow over the two-year drought simulation.

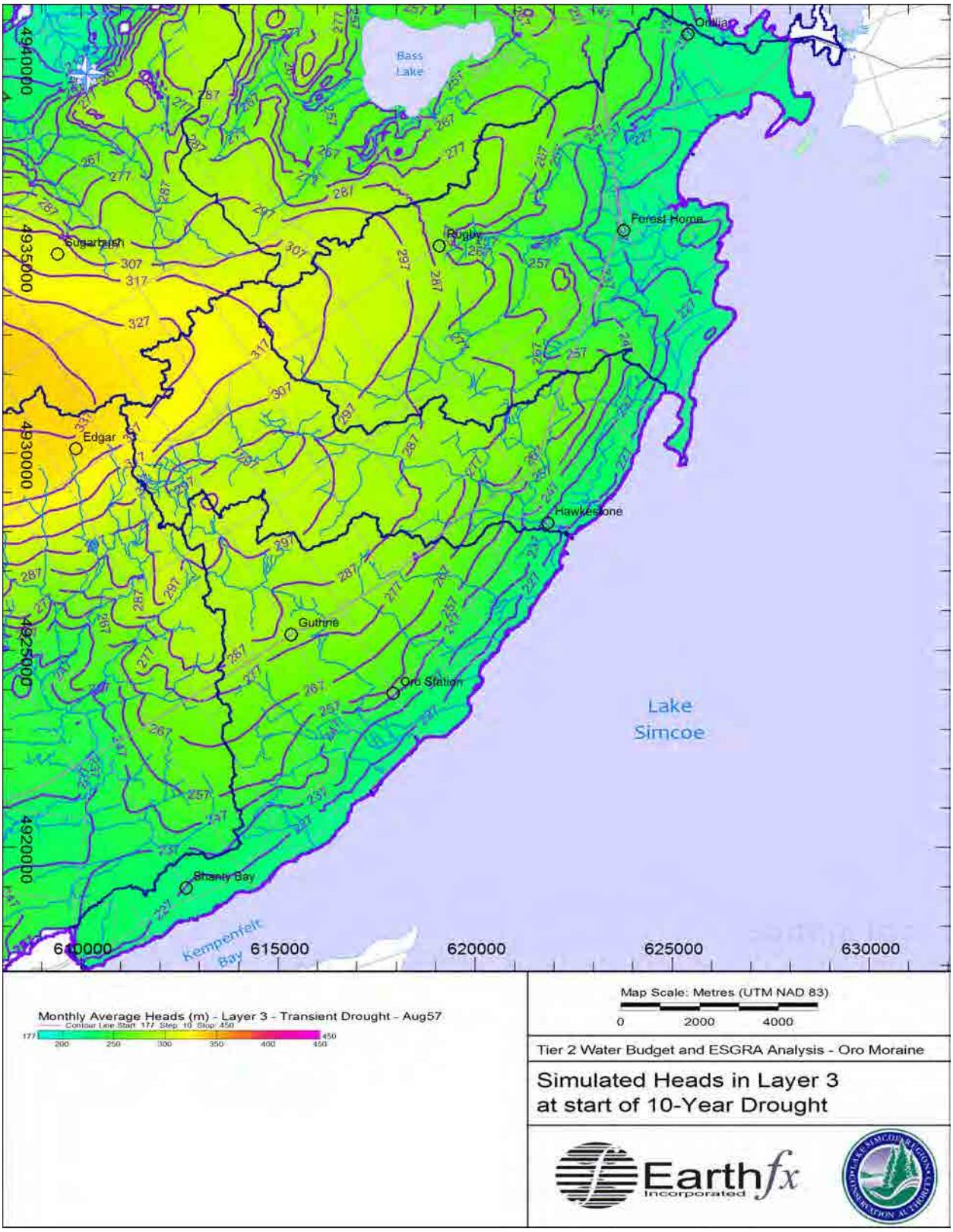

Figure 6.11: Simulated heads in Layer 3 (GLAF-AF1) at the approximate start of the modelled drought period (August 1957).

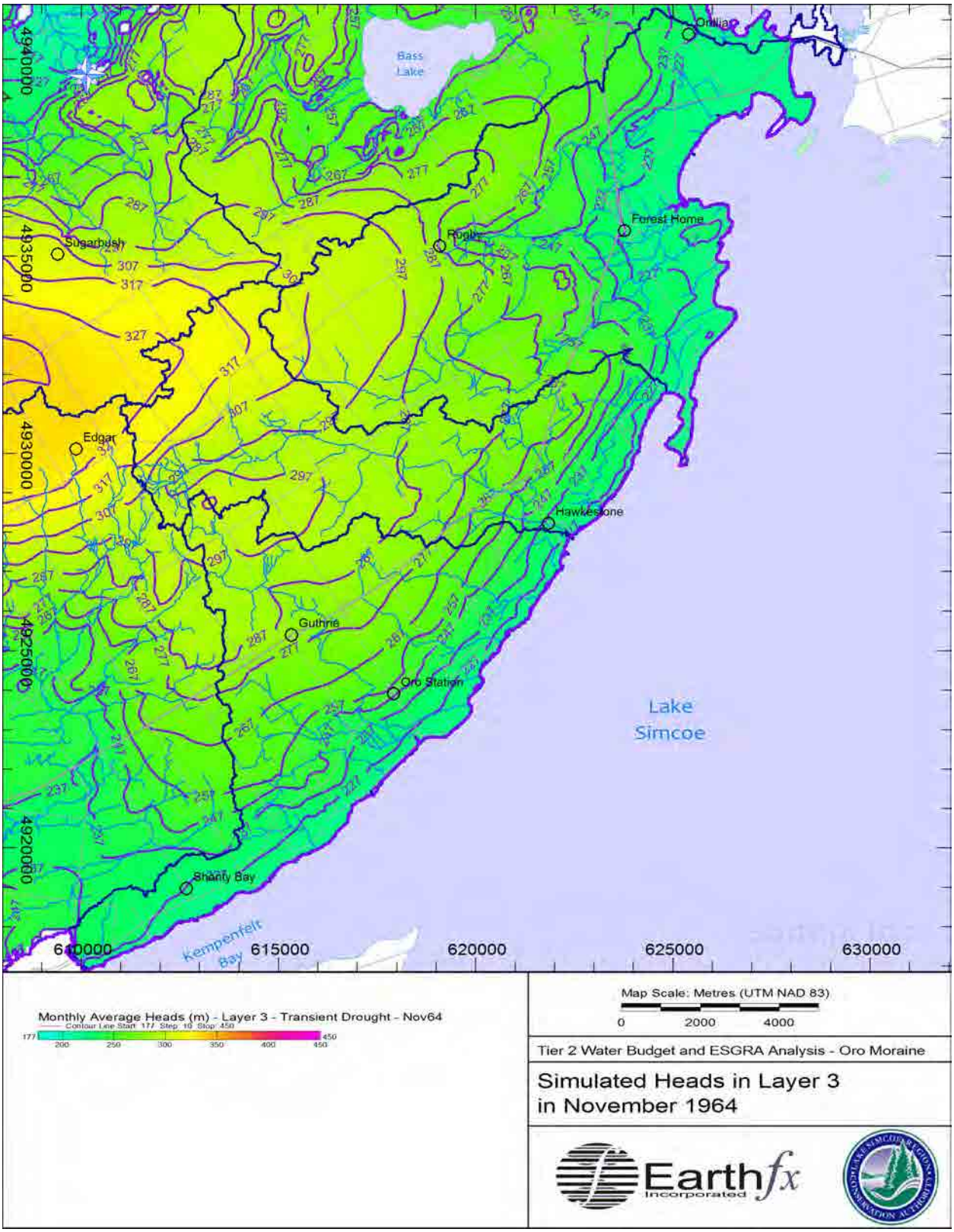

Figure 6.12: Simulated heads in Layer 3 (GLAF-AF1) during worst observed drought conditions (November 1964).

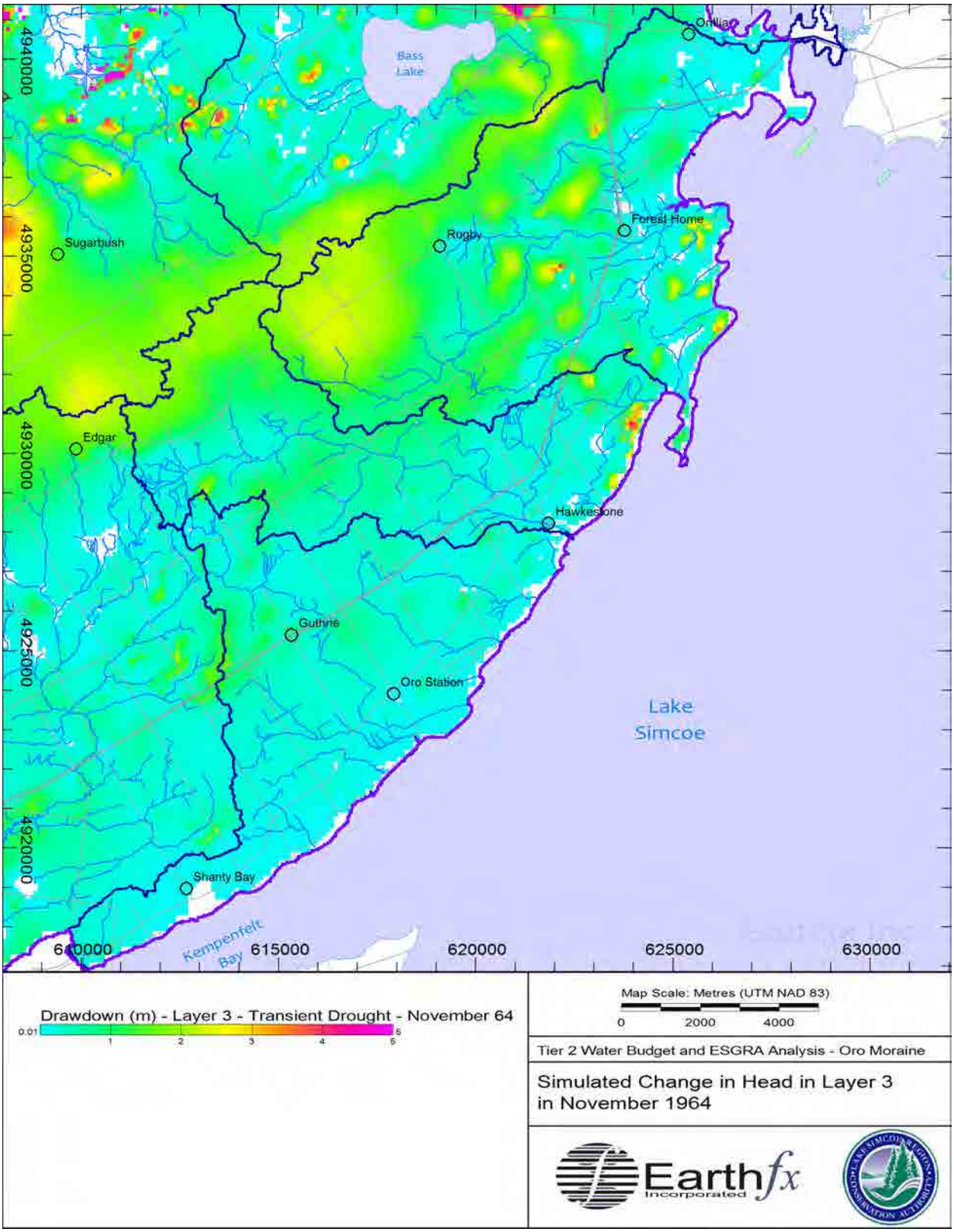

Figure 6.13: Simulated change in head in Layer 3 (GLAF-AF1) during most severe observed drought conditions (November 1964).

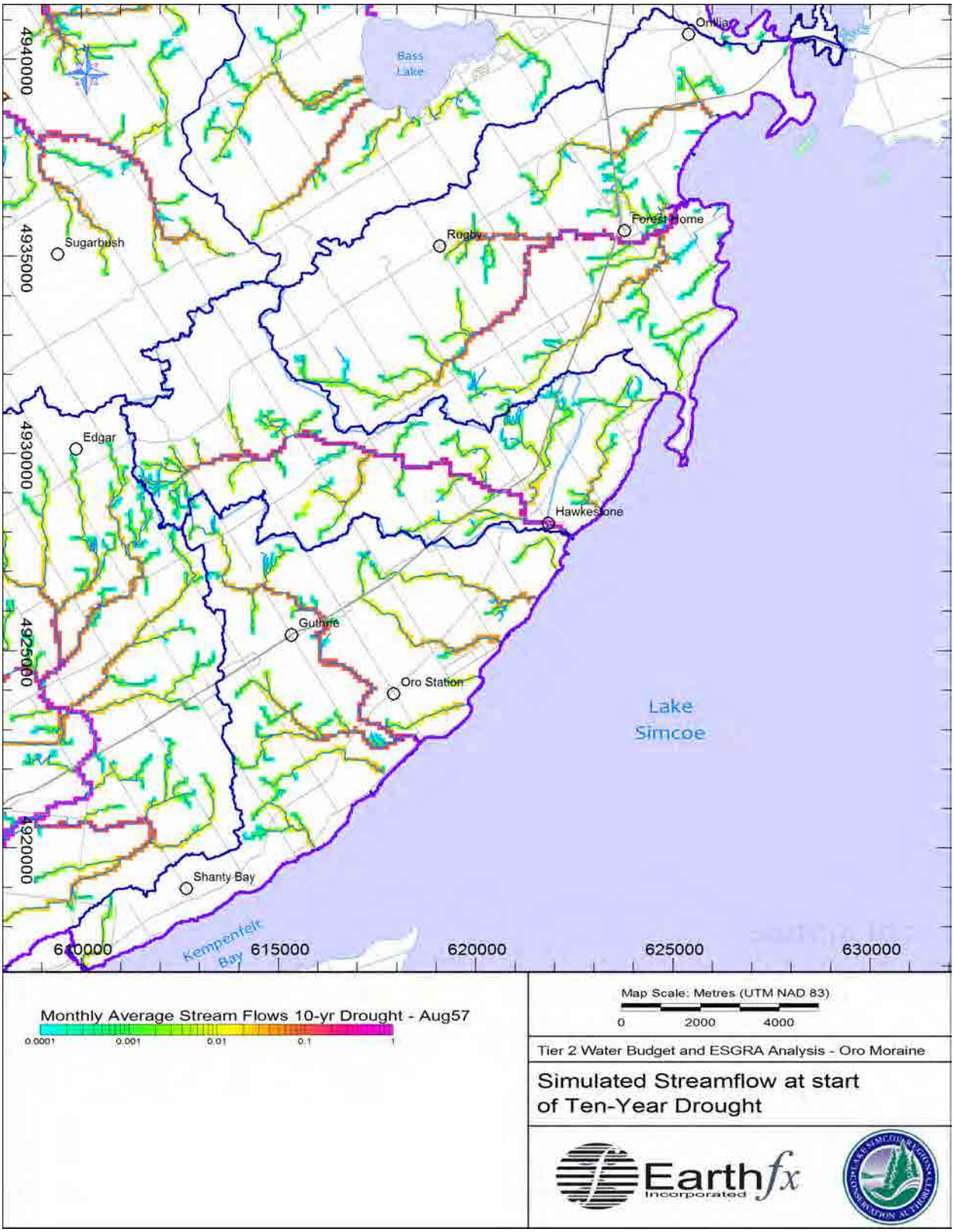

Figure 6.14: Simulated average monthly streamflow (m^3/s) at the approximate start of the modelled drought period (August 1954).

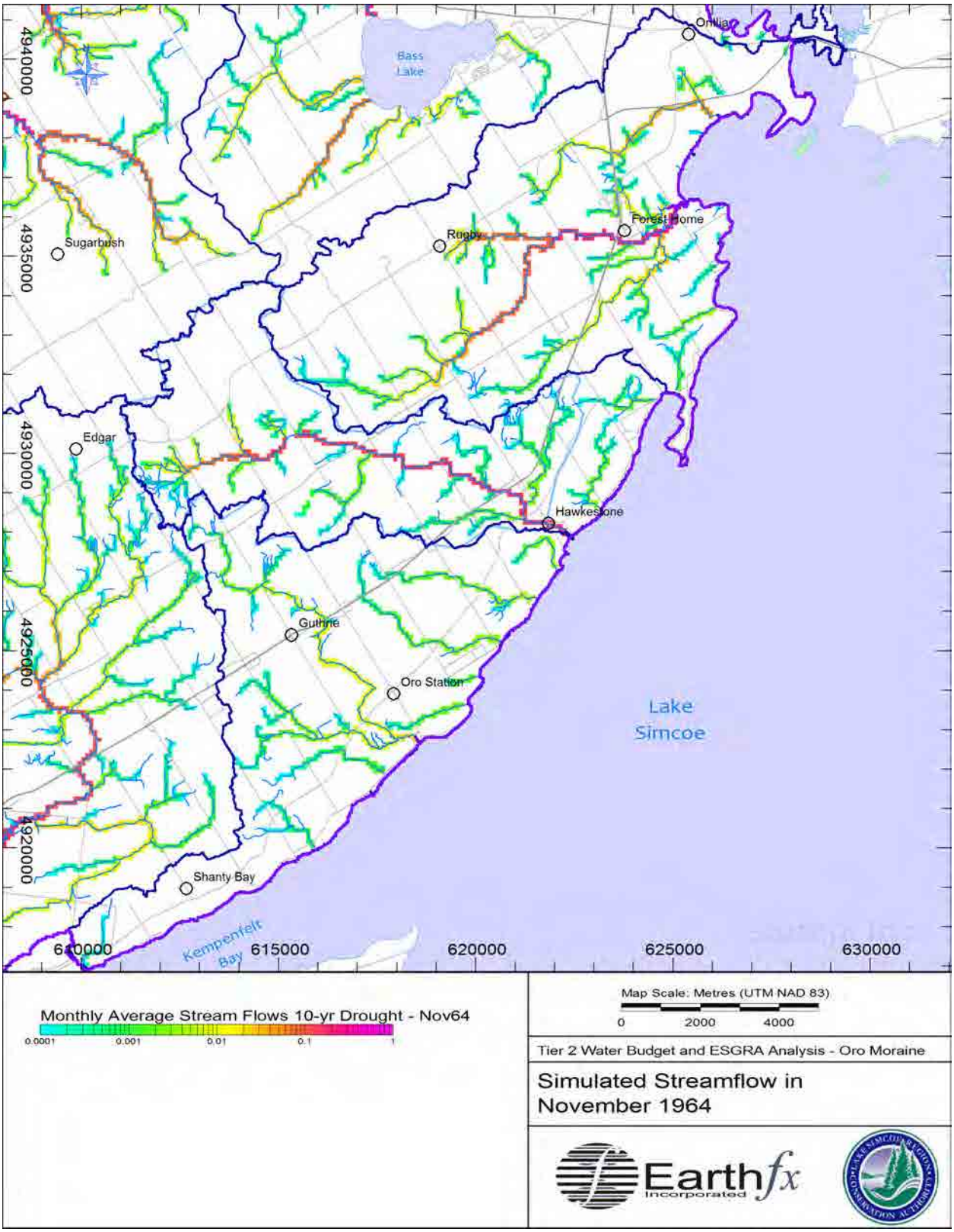

Figure 6.15: Simulated average monthly streamflow during worst observed drought conditions (November 1964).

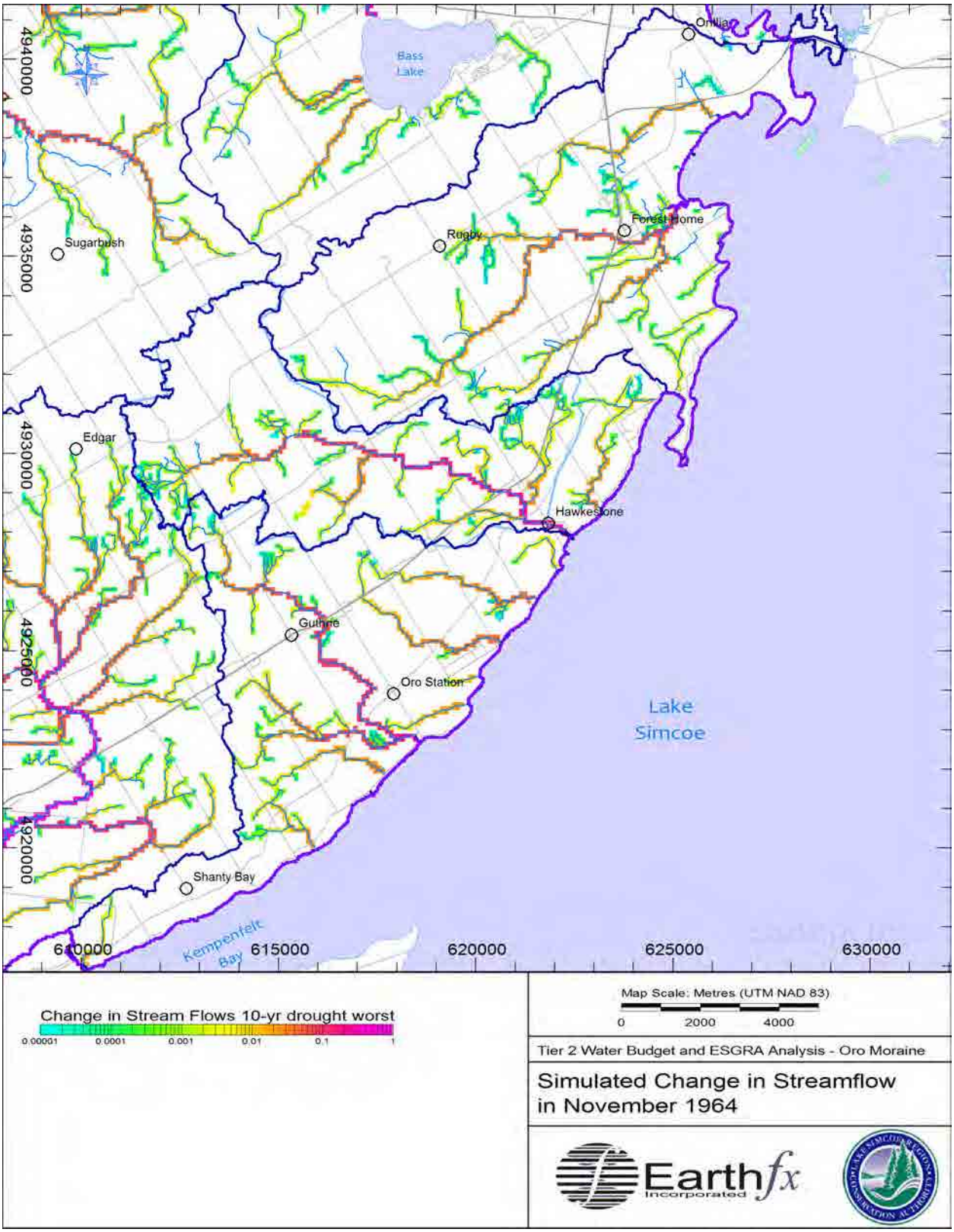

Figure 6.16: Simulated change in average monthly streamflow (m^3/s) over the 10-year drought period.

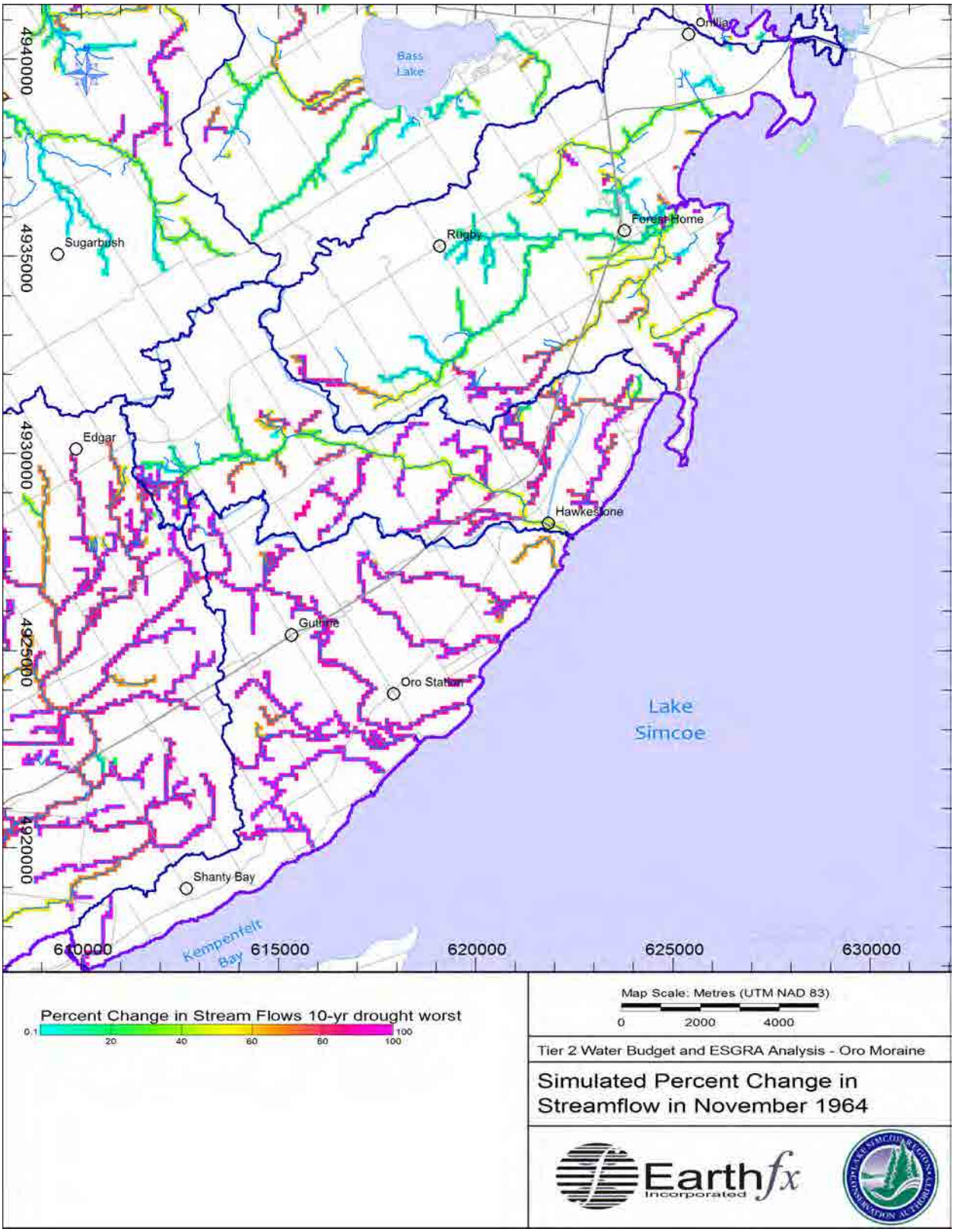

Figure 6.17: Simulated percent change in monthly average streamflow over the 10-year drought period.

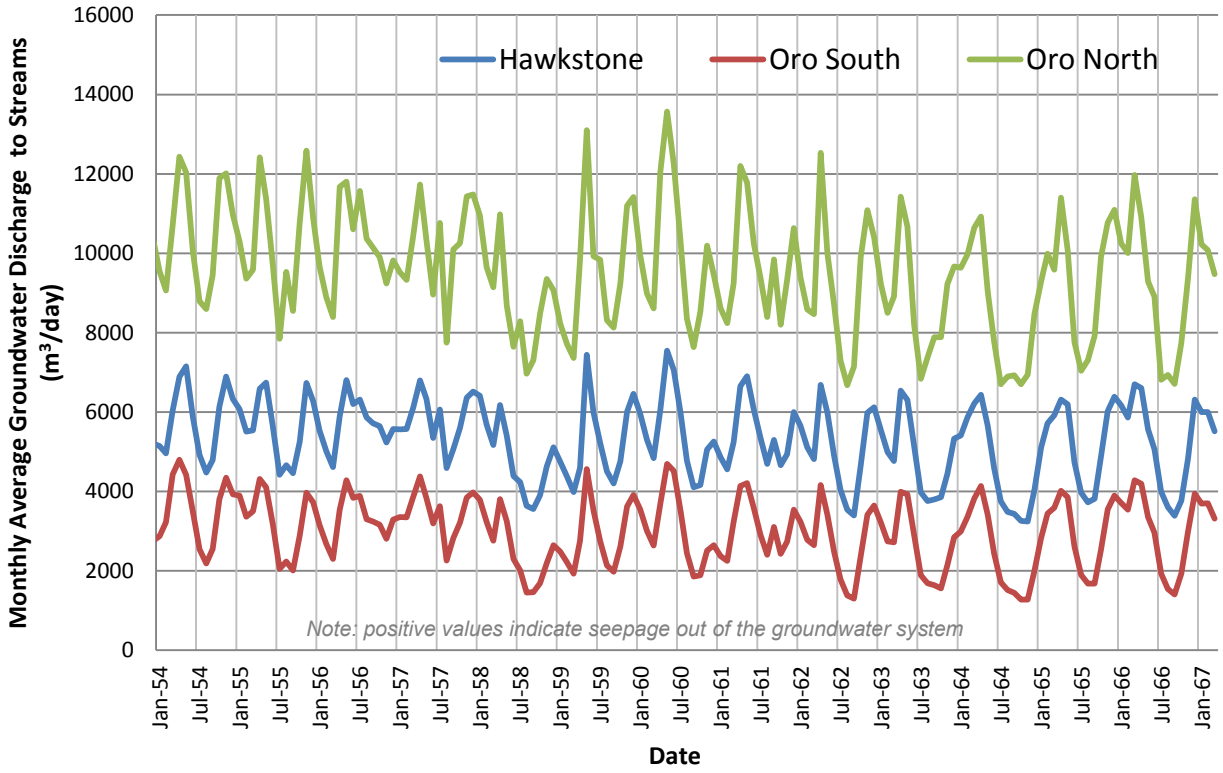

Figure 6.18: Monthly average total groundwater discharge to stream channels (m^3/d) in the study catchments.

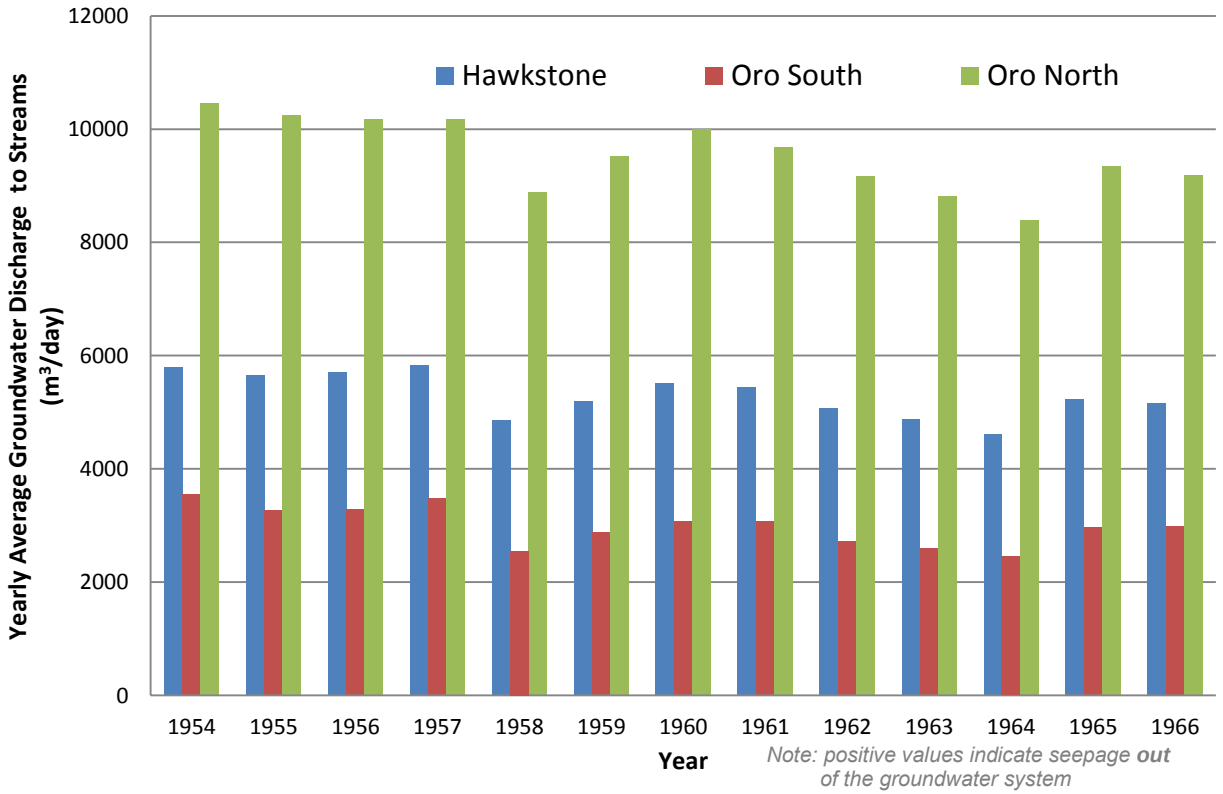

Figure 6.19: Yearly average total groundwater discharge to stream channels (m^3/d) in the study catchments.

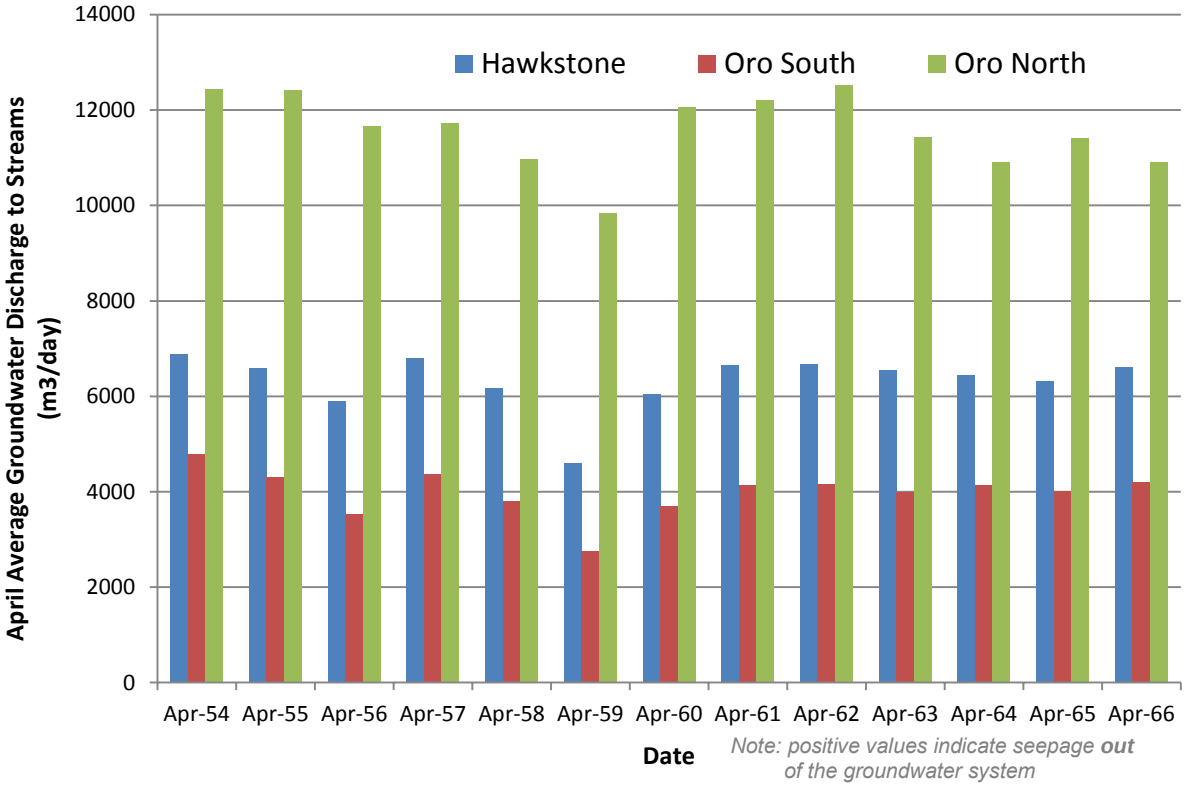

Figure 6.20: Average April total groundwater discharge to stream channels (m^3/d) in the study catchments.

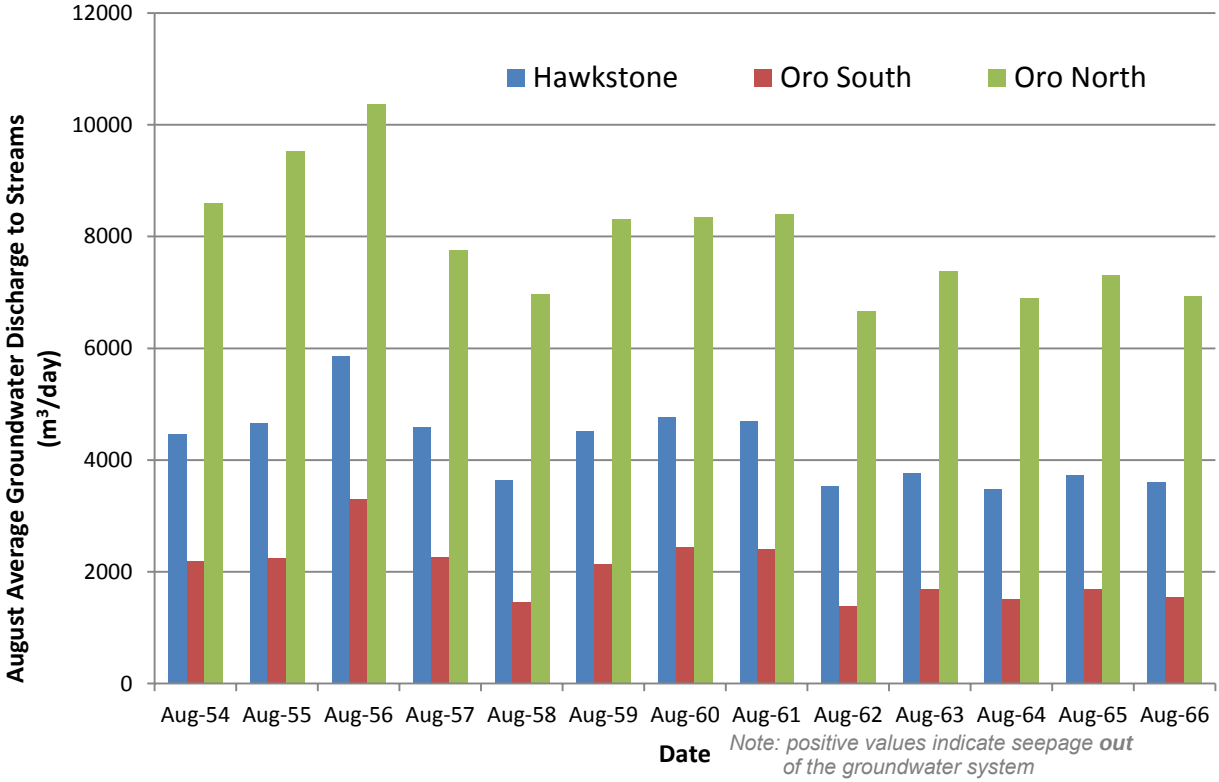

Figure 6.21: Average August total groundwater discharge to stream channels (m^3/d) in the study catchments.

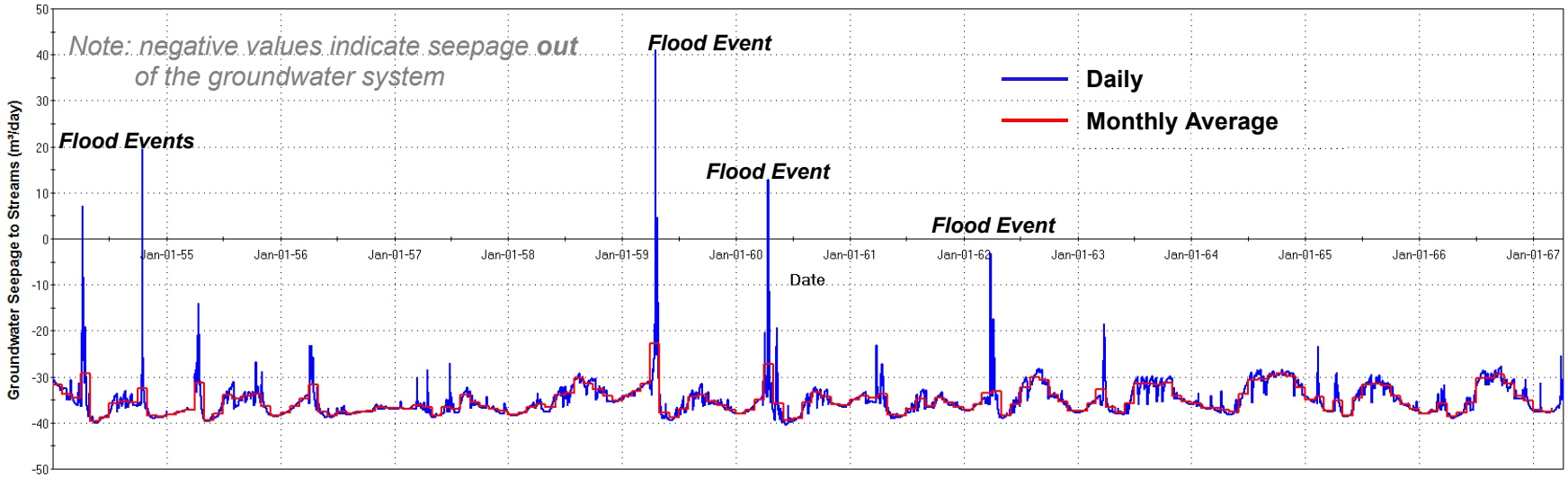

Figure 6.22: Groundwater seepage to Hawkestone Creek from the model cell immediately adjacent to the WSC gauge.

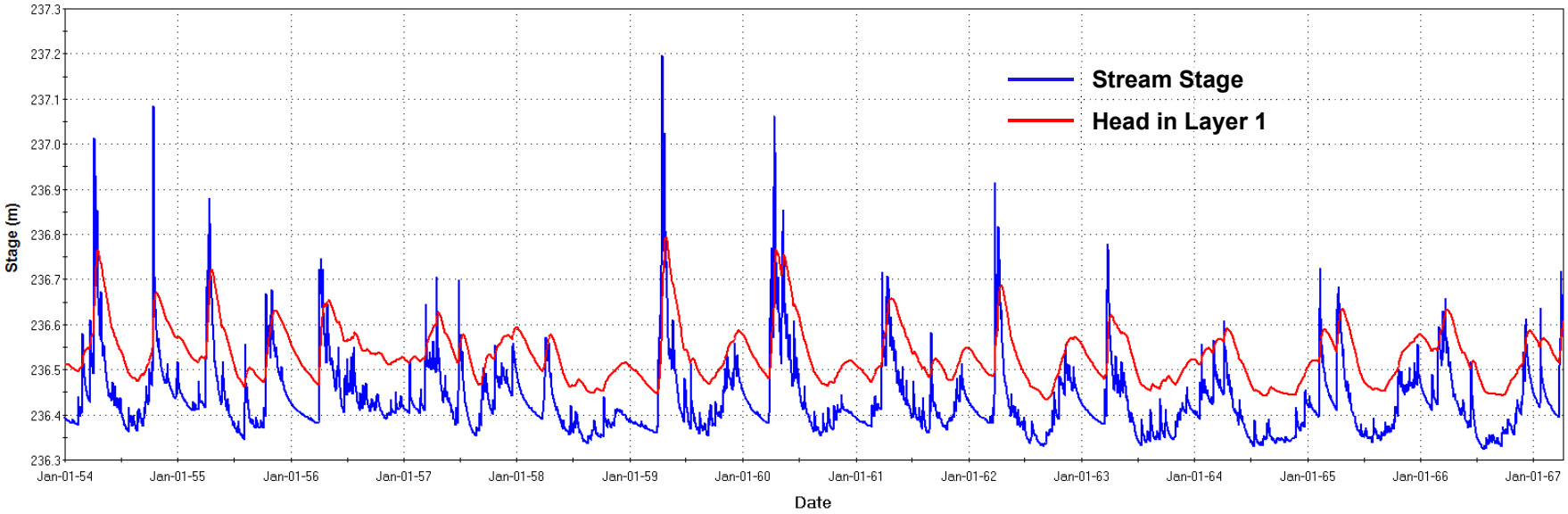

Figure 6.23: Stream stage and groundwater head in Hawkestone Creek from the model cell immediately adjacent to the WSC gauge.

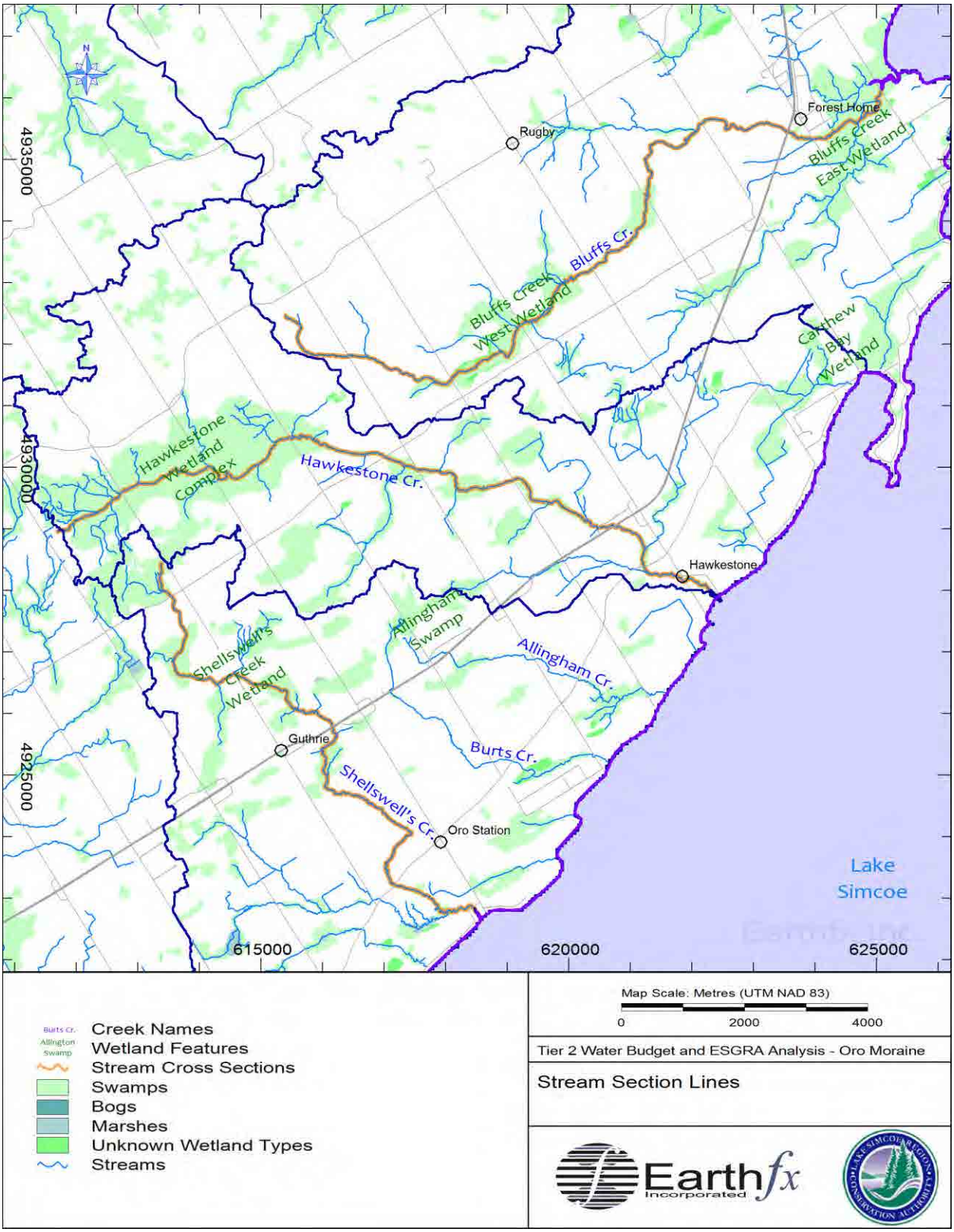

Figure 6.24: Stream seepage sections lines and associated wetland features.

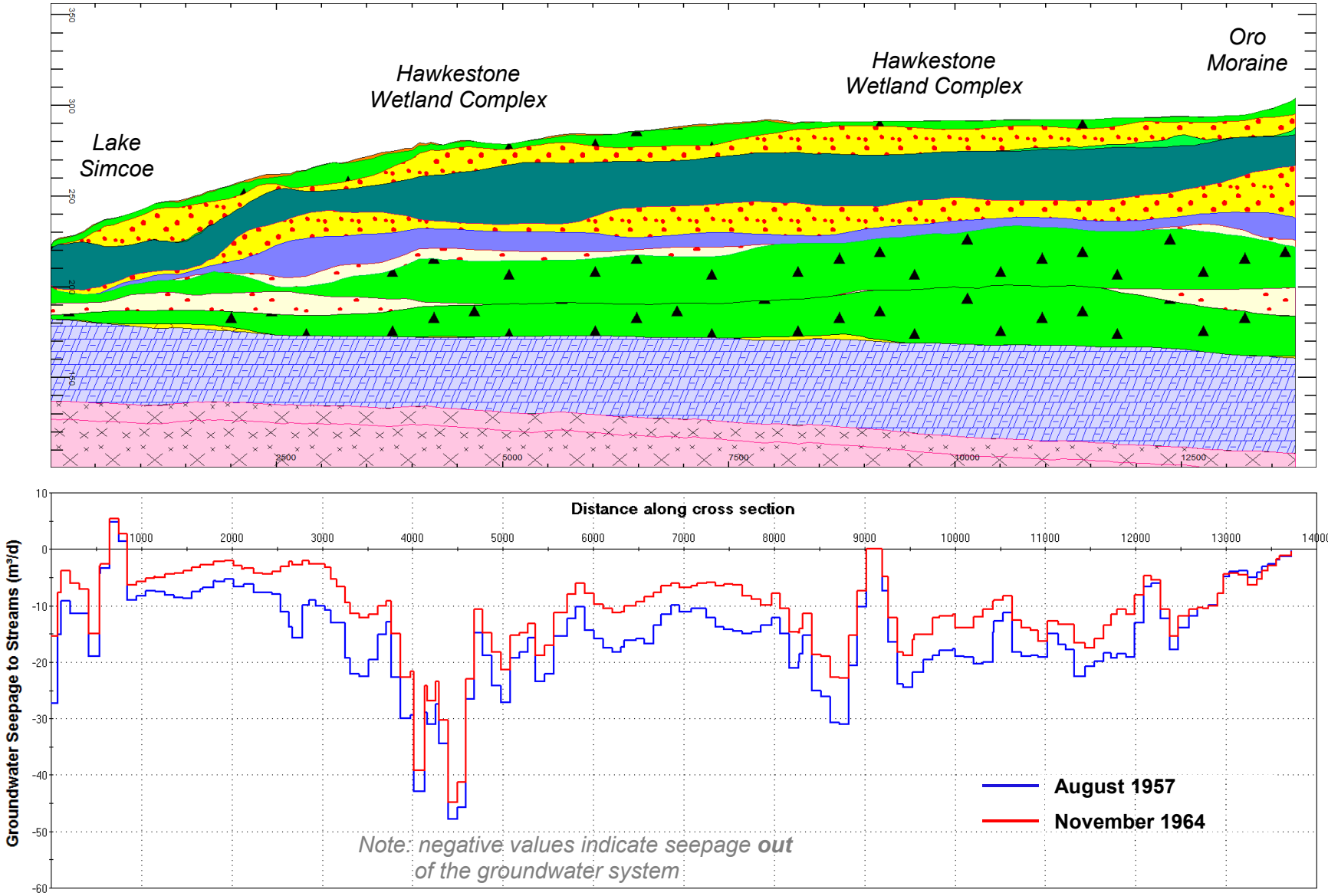

Figure 6.25: Groundwater seepage to the main branch of Hawkestone Creek by chainage (from Lake Simcoe) with geology.

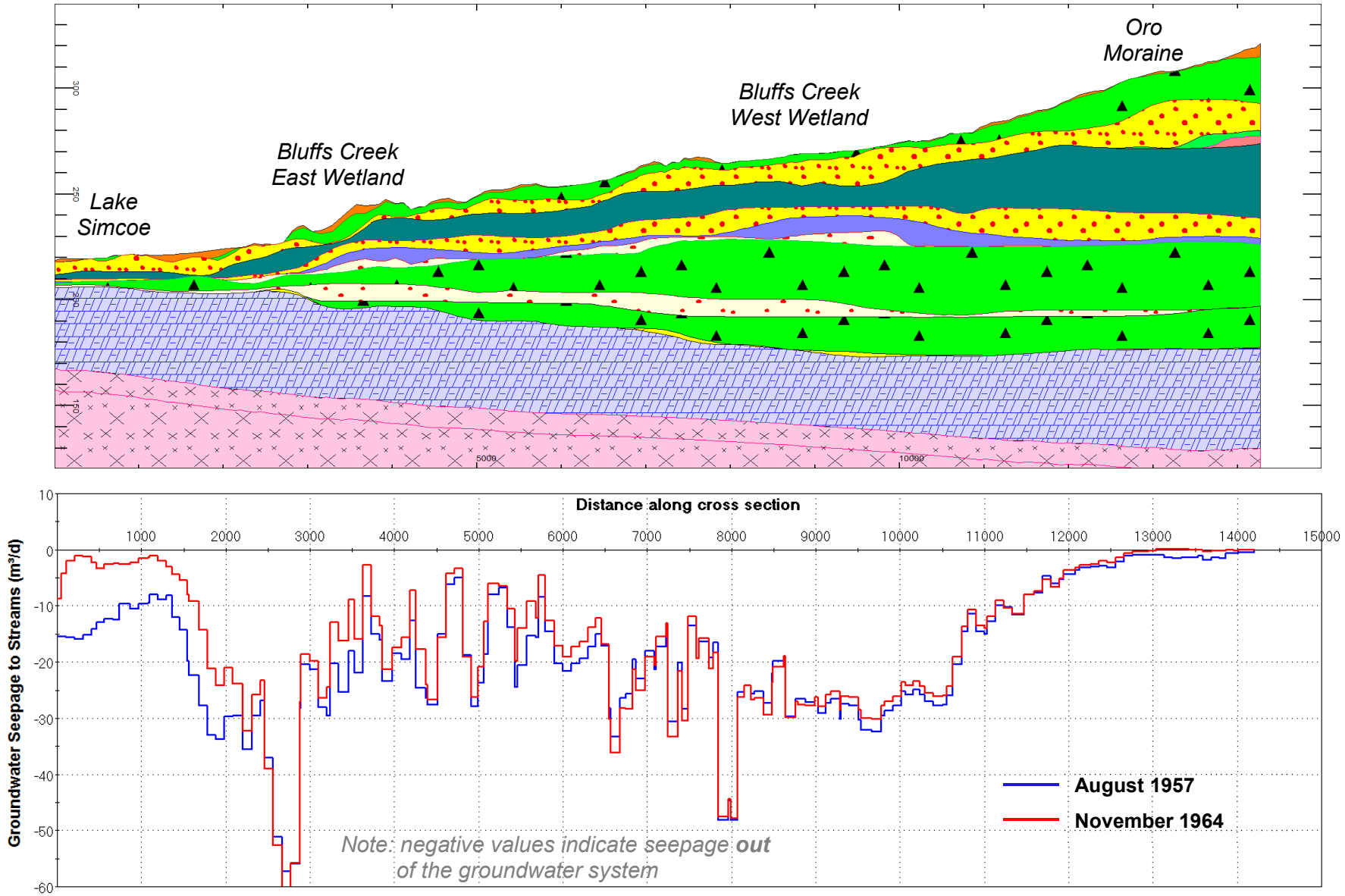

Figure 6.26: Groundwater seepage to Bluffs Creek West Branch (North Oro) by chainage (from Lake Simcoe) with geology.

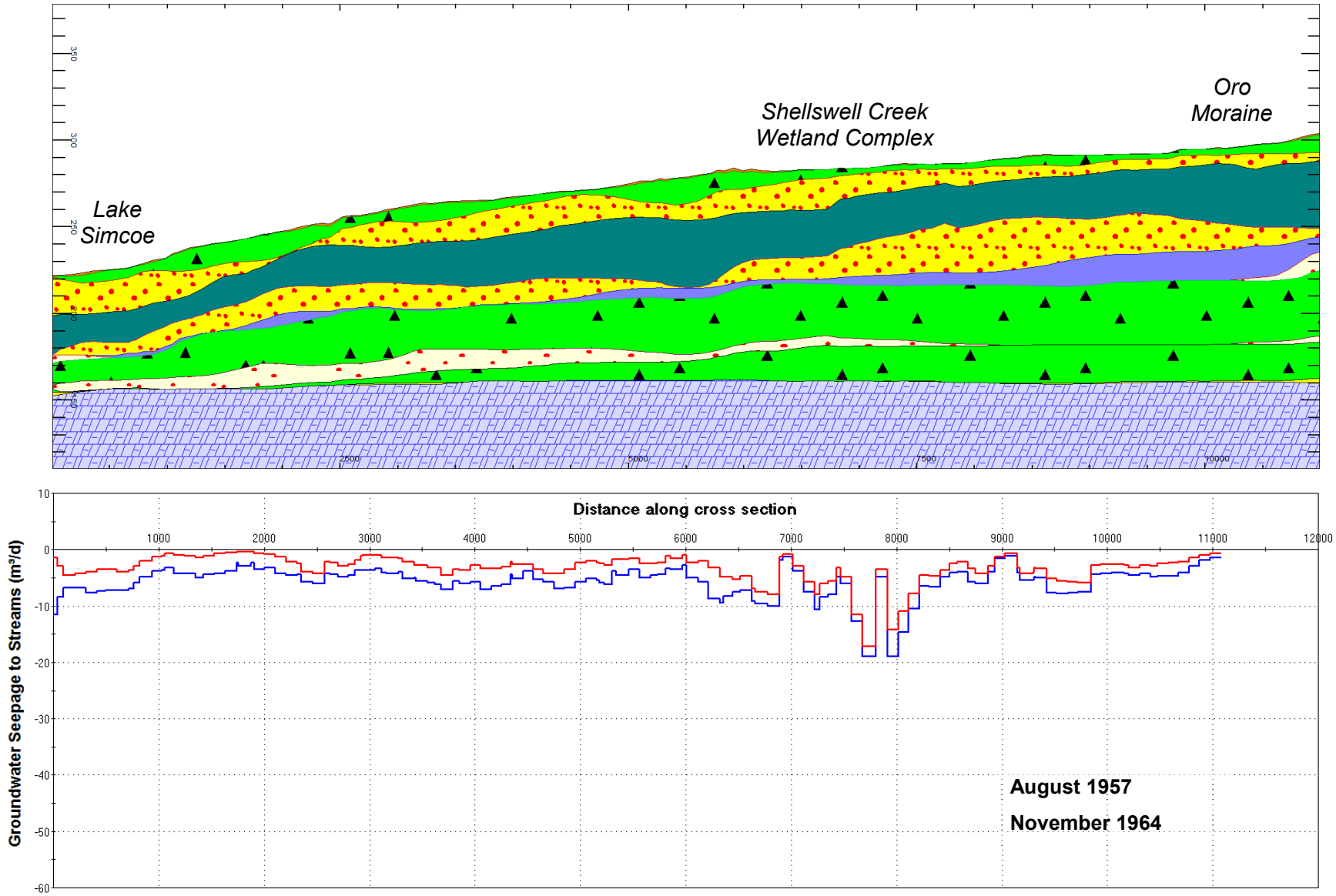

Figure 6.27: Groundwater seepage to Shellswell's Creek (South Oro) by chainage (from Lake Simcoe) with geology.

7 Conclusions

The purpose of this Tier 2 Water Budget and Water Quantity Stress Assessment was to describe the water budget and evaluate potential stress levels within Oro North, South and Hawkestone subwatersheds. A second objective was to analyze how the watershed will likely respond to future conditions such as increase in water demand or drought.

This report summarizes the update of the water use estimate and development of the integrated groundwater/surface water GSFLOW model. The model calibration appears, overall, excellent indicating that the integrated model is able to match gauged streamflow as well as long-term rising trends observed in the PGMN data and short-term seasonal patterns. The updated Tier 2 water budget provided the components, including lateral inflows and groundwater discharge estimates, needed for the subsequent stress assessment.

The updated Tier 2 stress assessment showed that none of the study watersheds are stressed under existing and future water use conditions. Simulations of drought conditions focussed on the effects of drought on groundwater levels and groundwater seepage to streams. Two-year (extreme) and 10-year (historic) drought conditions were analyzed. The Tier 2 analysis showed that the groundwater-fed streams, particularly headwater reaches, are affected by extreme and prolonged drought conditions although streams that are better connected to the Oro Moraine are less sensitive. Further discussion of groundwater linkages to surface features and the effect of drought on ESGRA delineation will be investigated in greater detail in Phase 2 of the project.

8 Limitations

Services performed by Earthfx Incorporated were conducted in a manner consistent with that level of care and skill ordinarily exercised by members of the environmental engineering and consulting profession.

This report presents the results of data compilation and computer simulations of a complex geologic setting. Data errors and data gaps are likely present in the information supplied to Earthfx, and it was beyond the scope of this project to review each data measurement and infill all gaps. Models constructed from these data are limited by the quality and completeness of the information available at the time the work was performed. Computer models represent a simplification of the actual geologic conditions. The applicability of the simplifying assumptions may or may not be applicable to a variety of applications.

This report does not exhaustively cover an investigation of all possible environmental conditions or circumstances that may exist in the study area. If a service is not expressly indicated, it should not be assumed that it was provided. It should be recognized that the passage of time affects the information provided in this report. Environmental conditions and the amount of data available can change. Discussions relating to the conditions are based upon information that existed at the time the conclusions were formulated.

All of which is respectively submitted,

EARTHFX INC.

Report prepared by:

Dirk Kassenaar, M.Sc., P.Eng.
President, Senior Hydrogeologist

E.J. Wexler, M.Sc., M.S.E., P.Eng.
Vice President, Senior Hydrogeologist

Mason Marchildon, M.A.Sc.
Hydrologist

Peter John Thompson, M.A.Sc
Hydrologist

Asoka Kodippili, P.Geol.
Hydrogeologist, Data Analyst

John Ford
Senior Geologist

9 References

American Society for Testing and Materials, 2000, Standard Guide for Subsurface Flow and Transport Modeling (ASTM) D5880-95.

Anderson E.A., 1968, Development and testing of snow pack energy balance equations. Water Resource Research, v. 4, no. 1, 19-37p.

Anderson, M.P. and Woessner, W.W., 1992, Applied groundwater modelling -- Simulation of flow and advective transport: Academic Press, USA.

Armstrong, D.K., 2000, Paleozoic geology of the northern Lake Simcoe area, south-central Ontario; Ontario Geological Survey, Open File Report 6011, 52p.

Armstrong, D.K. and, J.E.P. Dodge, 2007, Paleozoic geology of southern Ontario; Ontario Geological Survey, Miscellaneous Release—Data 219.

Barnett, P.J., 1986, Quaternary geology of the eastern halves of the Barrie and Elmvale areas, Simcoe County; in Summary of Field Work and Other Activities 1986, Ontario Geological Survey, Miscellaneous Paper 132, 193-194p.

——— 1992, Quaternary Geology of Ontario; in Geology of Ontario, Ontario Geological Survey, Special Volume 4, Part 2, 1011-1088p.

——— 1988, Quaternary geology of the eastern half of the Elmvale area, Simcoe County; in Summary of Field Work and Other Activities 1988, Ontario Geological Survey, Miscellaneous Paper 141, 405-406p.

——— 1989, Quaternary geology of the Barrie and Elmvale area; in Summary of Field Work and Other Activities 1989, Ontario Geological Survey, Miscellaneous Paper 146, p.205-206.

——— 1990a, Stratigraphic drilling of Quaternary sediments in the Barrie area, Simcoe County; in Summary of Field Work and Other Activities 1989, Ontario Geological Survey, Miscellaneous Paper 151, p.157-158.

——— 1990b, Tunnel valleys: evidence of catastrophic release of subglacial meltwater, central-southern Ontario, Canada; abstract in Geological Society of America, Northeastern Section, Syracuse, New York, Abstracts with Programs, v.22, p.3.

——— 1991a, Preliminary report on the stratigraphic drilling of Quaternary sediments in the Barrie area, Simcoe County, Ontario; Ontario Geological Survey, Open File Report 5755, 80p.

——— 1991b, Quaternary geology of the Barrie area, Simcoe County, Ontario; in Summary of Field Work and Other Activities 1991, Ontario Geological Survey, Miscellaneous Paper 157, p.135-136.

——— 1992, Quaternary geology of Ontario; in Geology of Ontario, Ontario Geological Survey, Special Volume 4, Part 2, p.1011-1090.

——— 1995, Geology of the Oak Ridges Moraine area, parts of Peterborough and Victoria counties and Durham and York Regional Municipalities, Ontario; in Summary of Field Work and Other Activities 1989, Ontario Geological Survey, Miscellaneous Paper 164, p.177-182.

——— 1997, Quaternary geology, eastern half of the Barrie and Elmvale areas; Ontario Geological Survey, Map 2645, scale 1:50 000.

Barnett, P.J. and D.J. Mate, 1998, Quaternary geology, Beaverton area; Ontario Geological Survey, Map 2560, scale 1:50,000.

Barth, C., 2005, Hydrologic Modelling of a Groundwater Dominated Watershed using a Loosely Coupled Modelling Approach. Friedrich-Schiller-Universitat Jena.

Bear, J., 1979, Hydraulics of Groundwater: McGraw Hill, NY, 567 p.

Beckers, J., Frind, E.O., 2000, Simulating groundwater flow and runoff for the Oro Moraine aquifer system. Part I. Model formulation and conceptual analysis. Journal of Hydrology No. 229 P. 265-280.

——— 2001, Simulating groundwater flow and runoff for the Oro Moraine aquifer system. Part II. Automated calibration and mass balance calculations. Journal of Hydrology, No. 243 P. 73-90.

Burt, A.K. and J.E.P. Dodge, 2011, Three-dimensional modelling of surficial deposits in the Barrie–Oro Moraine area of southern Ontario; Ontario Geological Survey, Groundwater Resources Study 11, 125p. PDF document.

Burt, A.K. and Russell, D.F., 2006, Results of 2004 Oro Moraine drilling program in the Barrie area, central Ontario; Ontario Geological Survey, Miscellaneous Release-Data 198.

Burt, A.K., 2007, Results of 2005 and 2006 Oro moraine drilling program in the Barrie area, central Ontario; Ontario Geological Survey, Miscellaneous Release---Data 227.

Burwasser, G.J. and S.T. Boyd, 1974, Quaternary geology of the Orr Lake area (western half)-Nottawasaga area (eastern half), southern Ontario; Ontario Division of Mines, Preliminary map P.975, scale 1:50 000.

Central Lake Ontario Conservation Authority, 2008, Revised Draft Tier 1 Water Budget: Central Lake Ontario Source Protection Area. 166p.

Chapman, L.J. and Putnam, D.F., 1984, The physiography of southern Ontario; Ontario Geological Survey, Special Volume 2, 270p.

——— 1984, The Physiography of Southern Ontario; Ontario Geological Survey, Special Volume 2, 270p. Accompanied by Map P.2715 (coloured), scale 1:600,000.

Chow, V.T. (ed.), 1964, Handbook of Applied Hydrology: A Compendium of Water-Resources Technology. McGraw-Hill Book Company, New York, 1418p.

Dawdy, D. R., Uchty, R. W., and Bergmann, J. M., 1972, A rainfall-runoff simulation model for estimation of flood peaks for small drainage basins: U.S. Geological Survey Professional Paper 506-B, p. Bl-828

Deane, R.E., 1950a, Pleistocene geology of the Lake Simcoe district, Ontario; Geological Survey of Canada, Memoir 256, 108p.

——— 1950b, Lake Simcoe district, Ontario, Pleistocene and Recent deposits and bedrock outcrops; Geological Survey of Canada, "A" Series Map 993A, scale 1:126,720.

de Loe, R., 2001. Agricultural Water Use: A Methodology and Estimates for Ontario (1991, 1996 and 2001)

——— 2005, Assessment of Agricultural Water Use/Demand Across Canada.

DeWalle, D.R. and A. Rango, 2008, Principles of Snow Hydrology. Cambridge University Press, New York.

Dixon Hydrogeology, 1992, Oro Seventh Line Aggregate Pits Hydrogeological Study.

Earthfx Inc., 2009, Model Calibration Report for the Trent South Slope Model.

——— 2008a, Water budget study of the watersheds in the Central Lake Ontario Conservation Authority (CLOCA) area. 175pp.

——— 2008b, Tier 1 Water budget study of the watersheds in the Central Lake Ontario Conservation Authority Area, Prepared for the Central Lake Ontario Conservation Authority, August 2008.

——— 2008c, Tier 1 Water budget model calculations for watersheds in the Conservation Halton Area. Prepared for the Regional Municipality of Halton.

——— 2010a, Water balance analysis of the Lake Simcoe Basin using the Precipitation-Runoff Modelling System (PRMS). 106pp.

——— 2010b, Tier 1 water budget and water quantity stress assessment of the Black-Severn River watershed: 124pp.

——— 2013, York Region Tier 3 Water Budget – Water Quantity Risk Level Assignment Study; in prep.

Easton, R.M., 1992, The Grenville Province and the Proterozoic history of central and southern Ontario; in Geology of Ontario, Ontario Geological Survey, Special Volume 4, Part 2, 714-904p.

Easton, R.M. and T.R. Carter, 1991, Extension of Grenville basement beneath southwestern Ontario; Ontario Geological Survey, Open File Map, OFM 162, scale 1:1,013,760.

Ely, D.M., 2006, Analysis of sensitivity of simulated recharge to selected parameters for seven watersheds modeled using the precipitation-run-off modeling system. USGS Scientific Investigations Report 2006-5041, 21p.

Eyles, C.H. and N. Eyles, 1983, Sedimentation in a large lake: a reinterpretation of the Late Pleistocene stratigraphy at Scarborough Bluffs, Ontario; Geology, v.11, p.147-152.

Fetter, C.W., 1980, Applied Hydrogeology. Charles E. Merrill Publishing Co. 488p.

Final Report for Sustainable Water Use Brank Water Policy and Coordination Directorate, Environment Canada, Guelph, Ontario: Rob de Loe Consulting.

Finamore, P.F. and A.F. Bajc, 1984, Quaternary geology of the Orillia area, southern Ontario; Ontario Geological Survey, Preliminary map P.2697, scale 1:50,000.

Freeze, R. A. and Cherry, J. A., 1979, Groundwater: Prentice Hall, Inc.

Golder Associates Inc. and AquaResources Inc., 2010, South Georgian Bay West Lake Simcoe Tier Two Water Budget and Stress Assessment, Draft Report.

Golder Associates Inc., 2004, South Georgian Bay West Lake Simcoe Tier Two Water Budget and Stress Assessment, Draft Report.

Golder Associates Inc., 2004, South Simcoe Municipal Groundwater Study.

Green, W. H., and Ampt, G. A., 1911, Studies on soil physics, I--Flow of air and water through soils: Journal of Agricultural Research, v. 4, p. 1-24.

Hall D.K., Riggs, G.A., and Salomonson, V.V., 1995, Development of methods for mapping global snow cover using moderate resolution imaging spectroradiometer data: Remote Sensing of Environment, no. 54, 127-14Op.

Harbaugh, A.W., and McDonald, M.G., 1996, User's documentation for MODFLOW-96, an update to the U.S. Geological Survey modular finite-difference ground-water flow model: U.S. Geological Survey Open-File Report 96-485, 56 p.

Hardy, J.P., Melloh, R., Koenig, G., Marks, D., Winstral, A., Pomeroy, J.W. and Link, T., 2004, Solar Radiation transmission through conifer canopies. Agri. And Forest Metrology, 126, 257-270.

Hicock, S.R. and A. Dreimanis. 1989. Sunnybrook Drift indicates grounded Early Wisconsinan glacier in the Lake Ontario basin.

Johnson M.D., Armstrong, D.K. Sanford, B.V, Telford P.G. and Rutka, M.A., 1992, Paleozoic and Mesozoic Geology of Ontario; in Geology of Ontario, Ontario Geological Survey, Special Volume 4, Part 2, p.907-1010.

Karrow, P.F., 1967, The Pleistocene geology of the Scarborough area; Ontario Department of Mines, Geological Report 46, 108p.

Karrow, P.F., A. Dreimanis, and P.J. Barnett, 2000, A proposed diachronic revision of Late Quaternary time-stratigraphic classification in the eastern and northern Great Lakes area; Quaternary Research, V. 54, no. 1, 1-12p.

Karrow, P.F., J.H. McAndrews, B.B. Miller, A.V. Morgan, K.L. Seymour and O.L. White, 2001, Illinoian to Late Wisconsinan stratigraphy at Woodbridge, Ontario; Canadian Journal of Earth Science, v.38, p.921-942.

Kassenaar, J.D.C. and Wexler, E.J., 2006, Groundwater Modelling of the Oak Ridges Moraine Area: CAMC-YPDT Technical Report #01-06.

Kelly, R.I. and I.P. Martini, 1986, Pleistocene glaciolacustrine deposits of the Scarborough Formation, Ontario, Canada; Sedimentary Geology, v.47, 27-52p.

Kelly, R.I., 1994, Results of a Quaternary geology hollow stem augering program, Woodbridge, Ontario; Ontario Geological Survey, Open File Report 5887, 52p.

Lake Simcoe Region Conservation Authority, 2009, Tier 1 water budget and water quantity assessment for the Lake Simcoe Watershed.

Leavesley, G.H., Litchty, R.W., Troutman, B.M. and Saindon, L.G., 1983, Precipitation-Runoff Modeling System: User's Manual. Water Resources Investigations Report 83-4283. USGS. Denver Colorado.

Liberty, B.A., 1969, The Paleozoic geology of the Lake Simcoe area, Ontario; Geological Survey of Canada, Memoir 335, 201p.

Linsley, R.K., Kohler, M.A., Paulhus, J.L.H., 1975, Hydrology for Engineers. 2nd ed. McGraw-Hill Company. 482p.

Markstrom, S.L., Niswonger, R.G., Regan, R.S., Prudic, D.E., and Barlow, P.M., 2008, GSFLOW: Coupled ground-water and surface-water flow model based on the integration of the Precipitation-Runoff Modeling System (PRMS) and the Modular Ground-Water Flow Model (MODFLOW-2005): U.S. Geological Survey Techniques and Methods 6-D1, 240 p.

McDonald, M.G., and A.W. Harbaugh, 1988, A modular three-dimensional finite-difference groundwater flow model: U.S. Geological Survey Techniques in Water Resources Investigations Book 6, Chapter A1, 586 p.

Mirynech, E., 1962, Pleistocene geology of the Trenton-Campbellford map area, Ontario; Unpublished Ph.D. thesis, University of Toronto, 197p.

Morrison Environmental Ltd., 2004, Municipal Groundwater Study - Paleozoic Area - Volume 1 - Aquifer characterization.

Ontario Geological Survey, 2003, Surficial geology of southern Ontario: Ontario Geological Survey Miscellaneous Release – Data, MRD-128, digital compilation of southern Ontario surficial geological mapping.

——— 2007, Physiography of southern Ontario; Ontario Geological Survey, Miscellaneous Release—Data 228.

——— 2010, Surficial geology of southern Ontario; Ontario Geological Survey, Miscellaneous Release—Data 128–Revised.

Ontario Ministry of Natural Resources, 2008, Southern Ontario Land Resource Information System (SOLRIS) V.1.2.

Ontario Ministry of the Environment, 2007, Assessment Report: Guidance Module 7 Water Budget and Water Quantity Risk Assessment Draft, 178p.

——— 2008, Technical Rules: Assessment Report, Clean Water Act, 2006.

——— 2009, Technical Rules: Assessment Reports, November 16, 2009.

Piggott, A., Moin, S., and Southam, C., 2005, A revised approach to the UKIH method for the calculation of baseflow, Hydrological Sciences, Journal 50(5) October 2005.

Prickett, T. and Lonquist, C., 1971, Selected digital computer techniques for groundwater resource evaluation: Bulletin no. 55, Illinois State Water Survey, Urbana.

Rees, G.W., 2006, Remote sensing of snow and ice: CRC Press - Taylor and Francis Group, Boca Raton, FL, 285 p.

Rosner, B., 1983, Percentage points for a generalized ESD many-outlier procedure: Technometrics, 25:165-172

Russell, D.J. and Telford, P.G., 1983, Revisions to the stratigraphy of the Upper Ordovician Collingwood Beds of Ontario – a potential oil shale; Canadian Journal of Earth Sciences, v.20, o,1780-1790.

Slattery, S.R., 2003, Subsurface mapping of the Barrie area, central Ontario; in Summary of Field Work and Other Activities 2003, Ontario Geological Survey, Open File Report 6120, p.25-1 to 25-8.

Sloto and Crouse, 1996, HYSEP: A Computer Program For Streamflow Hydrograph Separation and Analysis U.S.Geological Survey Water-Resources Investigations Report 96-4040.

South Georgian Bay-Lake Simcoe Source Protection Committee., 2011. Approved Assessment Report: Lakes Simcoe and Couchiching-Black River Source Protection Area Part 1.

Spitz, K., and Moreno,J., 1996, A practical guide to groundwater and solute transport modeling, John Wiley & Sons, Inc., New York, NY.

Tennant, D.L., 1976, Instream flow regimens for fish, wildlife, recreation, and related environmental resources. Fisheries 1(4):6-10.

Tessmann, S.A., 1980, Environmental assessment, technical appendix E in environmental use sector reconnaissance elements of the western Dakotas region of South Dakota study. Brookings, SD: South Dakota State University, Water Resources Research Institute.

Todd, D.K., 1980, Groundwater Hydrology. John Wiley and Sons. New York. 535p.

Toronto and Region Conservation Authority, 2008, Draft Tier 1 Water Budget: Toronto and Region Source Protection Area. 294p.

User Manual: 5 Edition with minor additions to the 2005 version.

Watermark Numerical Computing, 2010, PEST, Model-Independent Parameter Estimation,

White, O.L., 1975, Quaternary geology of the Bolton area, southern Ontario; Ontario Division of Mines, Geological Report 117, 118p.

XCG Consultants Ltd., 2008, Tier 1 Water Budget And Water Quantity Stress Assessment Trent River Basin, Lake Ontario And Bay Of Quinte Tributaries. 229p.

Yeung, C.W., 2005, Rainfall-runoff and water balance models for management of the Fena Valley Reservoir, Guam. USGS Scientific Investigations Report 2004-5287, 52p.